



**HAL**  
open science

# Role of phospho-S27-,S33-Ku70 in the efficiency of DNA double strand break repair

Amélie Schellenbauer

► **To cite this version:**

Amélie Schellenbauer. Role of phospho-S27-,S33-Ku70 in the efficiency of DNA double strand break repair. Cellular Biology. Université Sorbonne Paris Cité, 2017. English. NNT : 2017USPCB146 . tel-04460297

**HAL Id: tel-04460297**

**<https://theses.hal.science/tel-04460297>**

Submitted on 15 Feb 2024

**HAL** is a multi-disciplinary open access archive for the deposit and dissemination of scientific research documents, whether they are published or not. The documents may come from teaching and research institutions in France or abroad, or from public or private research centers.

L'archive ouverte pluridisciplinaire **HAL**, est destinée au dépôt et à la diffusion de documents scientifiques de niveau recherche, publiés ou non, émanant des établissements d'enseignement et de recherche français ou étrangers, des laboratoires publics ou privés.



Ecole Doctorale  
Médicament - Toxicologie  
Chimie - Imageries

UNIVERSITÉ PARIS DESCARTES

École doctorale MTCI

*Institut de Radiobiologie Cellulaire et Moléculaire (IRCM)*

*Laboratoire de Cancérologie expérimentale (LCE)*

# Role of phospho-S27-,S33-Ku70 in the efficiency of DNA double strand break repair

Par Amélie SCHELLENBAUER

Thèse de doctorat de biologie cellulaire et moléculaire

Dirigée par Jozo DELIC

Présentée et soutenue publiquement le 15 novembre 2017

Devant un jury composé de :

Dr. Vincent PENNANEACH	Rapporteur - Institut Curie
Dr. Jean-Baptiste CHARBONNIER	Rapporteur - CEA Saclay
Dr. Janet HALL	Examineur - Université de Lyon I
Prof. Dr. Pierre VERRELLE	Examineur - Institut Curie
Dr. Jozo DELIC	Directeur de thèse - CEA Fontenay-aux-Roses



Except where otherwise noted, this work is licensed under <http://creativecommons.org/licenses/by-nc-nd/3.0/>

# *Abstract*

DNA integrity is permanently challenged by a plethora of endogenous and exogenous threats. Double strand breaks (DSB) are the most toxic lesions when un-or-misrepaired, since they can become a source of mutations and drive carcinogenesis. Two main DNA repair pathways classical non-homologous end joining (cNHEJ) and homologous recombination (HR) have evolved to repair these lesions. Our group previously identified phospho-Ku70 overexpressed in a patient subset of treatment-resistant chronic lymphocytic leukemia (R-CLL). Multiple observations such as apoptosis resistance after genotoxic stress, error-prone repair junctions, genomic instability and a significant resection of telomere ends led to the assumption of a deregulated c-NHEJ in R-CLL. The Ku protein (Ku70/Ku80 heterodimer) is a core component of c-NHEJ with multiple other cellular functions. In this work we characterize the functions of phospho-Ku70 on the DSB site induced by irradiation or enzymatically. We show that phospho-Ku70 provides radioresistance and genomic stability, when compared to a non-phosphorylatable Ku70 mutant. We further demonstrate that phosphorylation of Ku70 is important for DNA repair kinetics and for Ku70 release from the DNA after repair completion. In addition, we employ a site specific I-SCEI reporter assay to monitor efficiency of c-NHEJ and HR, and establish that phospho-Ku70 affects both c-NHEJ and HR repair pathways. Finally, we developed a humanized KI mouse model to study the role of phospho-Ku70 *in vivo*. Preliminary data on mouse embryonic fibroblasts indicate that non-phosphorylatable Ku70 expressing cells have growth defects and increased apoptosis susceptibility.

In summary, we determine that the new form of phospho-Ku70 drives DNA DSB repair, radioresistance and genomic stability. An in-depth knowledge of the molecular processes of phospho-Ku70 in DNA DSB repair may be exploited in specific cancer treatment strategies in the future.

**Keywords:** NHEJ, Ku, DNA, Double strand break repair, genomic stability

# Résumé

L'intégrité de l'ADN est menacée en permanence par de nombreuses agressions endogènes et exogènes. Les cassures double brin (CDB) sont les lésions les plus toxiques lorsqu'elles sont non- ou mal- réparées car elles deviennent une source de mutations susceptible d'entraîner une carcinogenèse. Deux voies principales de réparation de l'ADN ont été développées pour réparer ces lésions : la jonction d'extrémités non-homologue classique (cNHEJ) et la recombinaison homologue (RH). Notre groupe a préalablement identifié phospho-Ku70 sur-exprimé dans une sous-population de patients atteint d'une leucémie lymphocytaire chronique (R-CLL) résistant à tout traitement. Des observations telles que la résistance à l'apoptose induite par le stress génotoxique, la réparation de jonctions sujette à erreur, l'instabilité génomique et une résection des extrémités des télomères ont conduit à l'hypothèse d'un cNHEJ dérégulé dans la R-CLL. La protéine Ku (hétérodimère Ku70 / Ku80) est un facteur central de c-NHEJ avec plusieurs autres fonctions cellulaires. Dans ce travail, nous avons caractérisé les fonctions de phospho-Ku70 sur le site de la CDB induites par irradiation ou activité enzymatique. Nous montrons que phospho-Ku70 assure une radio-résistance et une stabilité génomique par rapport à un mutant Ku70 non phosphorylable. Nous montrons en outre que la phosphorylation de Ku70 influence la cinétique de réparation de l'ADN et la libération de Ku70 de l'ADN après achèvement de la réparation. Nous avons par ailleurs utilisé un test rapporteur I-SCEI pour évaluer l'efficacité de cNHEJ et HR, et nous avons pu montrer que le phospho-Ku70 affecte à la fois les voies de réparation c-NHEJ et HR. Enfin, nous avons développé un modèle de souris KI humanisé pour étudier le rôle de phospho-Ku70 *in vivo*. Les données préliminaires sur les fibroblastes embryonnaires de souris indiquent que les cellules exprimant le Ku70 non-phosphorylable présentent des défauts de croissance et une susceptibilité à l'apoptose.

En résumé, nous montrons que la nouvelle forme de phospho-Ku70 favorise la réparation d'ADN DSB, la radio-résistance et la stabilité génomique. La connaissance fine des processus moléculaires de phospho-Ku70 dans la réparation ADN DSB pourrait ouvrir la voie à des stratégies spécifiques de traitement du cancer à l'avenir.

**Mots-clés:** NHEJ, Ku, ADN, Réparation de cassures double brin, stabilité génomique



# *Acknowledgements*

Je tiens tout d'abord à remercier les rapporteurs le Dr. Vincent Penneneach et le Dr. Jean-Baptiste Charbonnier ainsi que les examinateurs le Dr. Janet Hall et le Prof. Dr. Pierre Verrelle d'avoir accepté de juger ce travail de thèse.

Je remercie le Dr. Sylvie Chevillard. Merci pour ton accueil au sein du laboratoire, tes conseils et ton oreille ouverte aux difficultés que j'ai pu rencontrer durant cette thèse.

Merci au Dr. Jozo Delic. Tu m'as accordé ta confiance et donné l'opportunité de travailler sur ta découverte du phospho-Ku70. Merci pour ton sourire, ta bonne humeur au quotidien et la liberté et l'autonomie que tu m'as laissé.

Je tiens à remercier l'ensemble de l'équipe du LCE que j'ai eu la joie d'apprendre à connaître toutes ces dernières années : Emilie, Kristelle, Yoann, Nicolas, Youenn, Arnaud, Julie K., Eléonore, Maud, Benoît, Kathy, Dan, Ivana, Jérôme, Romain et Sandrine. Merci.

Et plus particulièrement...

... Julie, Caroline et Sam pour les repas de midi toujours très sympas !

... François pour avoir relu l'ensemble de ce manuscrit et pour ton intérêt, tes remarques et ton soutien à ce projet.

... Yidan et Allan pour votre soutien en toute occasion, au laboratoire comme à l'extérieur, votre aide scientifique et vos efforts pour maintenir mon moral.

... Emilie R. pour tes conseils et ta bonne humeur.

... et surtout M-No, un immense merci pour ton aide, ton travail et tes efforts, tes mots... qui m'ont énormément aidé ! (On fête ça, promis !)

Enfin, je tiens à remercier mon père, Claire et Carmen pour notre relation si proche et votre confiance en moi, ma mère pour ton amour que je ressens toujours.

Clément, mon partner in crime, tu m'as encouragé, soutenu, supporté, attendu et su me faire rire à la fin de chaque journée pendant ces 4 longues années. J'ai hâte de démarrer nos prochaines aventures !

# Contents

<b>Abstract</b>	<b>ii</b>
<b>Acknowledgements</b>	<b>iv</b>
<b>Contents</b>	<b>v</b>
<b>List of Figures</b>	<b>xi</b>
<b>List of Tables</b>	<b>xiii</b>
<b>Abbreviations</b>	<b>xv</b>
<b>I Introduction</b>	<b>1</b>
<b>1 General introduction</b>	<b>3</b>
<b>2 The Ku protein: History, protein domains and functional characteristics</b>	<b>5</b>
2.1 The identification of the Ku protein- a historical review . . . . .	5
2.2 The different protein domains of Ku70 and Ku80 and their functions	6
2.3 Functional characterization of Ku as part of the XRCC gene family- links between DSB repair and V(D)J recombination . . . . .	10
<b>3 DNA maintenance and metabolism</b>	<b>13</b>
3.1 DNA repair . . . . .	14
3.1.1 c-NHEJ step-by-step . . . . .	17
3.1.2 Fidelity of c-NHEJ . . . . .	23
3.1.3 Homologous Recombination . . . . .	24
3.1.4 alternative/mutagenic/microhomology mediated NHEJ . . .	26
3.2 Crosstalk of DNA DSB repair pathways . . . . .	29
3.2.1 DNA end resection dictates repair pathway choice between HR and NHEJ during S/G2-phase . . . . .	30
The end resection mechanism . . . . .	31

	Upstream regulation of end resection by 53BP1- RIF and BRCA1- CtIP on the chromatin level . . . . .	31
	Regulation of resection by DNA-PKcs . . . . .	32
	Regulation of resection by Ku at the DSB . . . . .	33
	A resection dependent c-NHEJ was recently revealed . . . . .	34
3.2.2	Other determinants of pathway choice . . . . .	35
3.2.3	Ku outcompetes HR dependent repair pathways and alt-NHEJ . . . . .	35
3.3	DNA damage response (DDR) . . . . .	35
3.3.1	DNA damage signalling by ATM and ATR . . . . .	36
	Ku impacts on ATM/ATR activation . . . . .	38
3.3.2	Cell cycle and its checkpoints . . . . .	39
	Ku impacts on cell cycle regulation . . . . .	43
3.3.3	Senescence . . . . .	43
	Ku in senescence . . . . .	45
3.3.4	Cell death pathways . . . . .	46
	3.3.4.1 Apoptosis . . . . .	46
	Ku's role in apoptosis . . . . .	49
	3.3.4.2 Mitotic catastrophe . . . . .	50
	3.3.5 Autophagy . . . . .	51
3.4	Coordination and cell fate decisions upon the DDR . . . . .	53
<b>4</b>	<b>V(D)J recombination</b>	<b>55</b>
4.1	V(D)J recombination relies on the cNHEJ machinery . . . . .	56
4.2	Deficiencies in core NHEJ factors impair V(D)J recombination and lead to radiosensitive SCID . . . . .	58
<b>5</b>	<b>Other cellular roles of Ku</b>	<b>61</b>
5.1	Enzymatic functions of Ku . . . . .	61
5.2	Ku in transcription . . . . .	62
5.3	Ku in the mobility of genetic elements . . . . .	63
5.4	Ku in DNA replication . . . . .	63
5.5	Ku on telomeres . . . . .	64
<b>6</b>	<b>Ku associated with disease</b>	<b>67</b>
6.1	Ku associated with autoimmune disease . . . . .	67
6.2	Ku associated with cancer . . . . .	67
<b>7</b>	<b>Chronic lymphocytic leukemia (CLL) patients overexpress phospho-S27-S33 Ku70 - Data from the lab</b>	<b>71</b>
7.1	Chronic lymphocytic leukaemia (CLL)- an overview . . . . .	71
	7.1.1 Epidemiology . . . . .	72
	7.1.2 Diagnosis and prognostic factors . . . . .	72
	7.1.3 Staging . . . . .	73

---

7.1.4	Treatment . . . . .	74
	Chemotherapy . . . . .	75
	Chemoimmunotherapy . . . . .	75
	Small molecules . . . . .	75
	Inhibitors of BCR signalling . . . . .	75
	BCL-2 inhibitor . . . . .	76
7.2	Other prognostic markers like apoptosis resistance to irradiation, NHEJ activity and telomere maintenance come into focus and define a novel subpopulations in CLL - data from the lab . . . . .	76
7.3	Identification of phospho-S27-S33 Ku70 . . . . .	82
7.4	Posttranslational modifications (PTM) regulate cellular processes .	85
	7.4.1 Ku70 phosphorylation sites reviewed . . . . .	86
 <b>II Aim of this project</b>		 <b>89</b>
 <b>III Materials and Methods</b>		 <b>93</b>
 <b>1 Materials and Methods</b>		 <b>95</b>
1.1	Cell lines and culture conditions . . . . .	95
	1.1.1 Cell lines . . . . .	95
	1.1.2 Cell culture . . . . .	95
	1.1.3 Splitting cells . . . . .	96
	1.1.4 Thawing cells . . . . .	97
1.2	Stable cell line generation using pEBV vectors . . . . .	97
	1.2.1 Transfection . . . . .	98
1.3	Irradiation . . . . .	99
1.4	Cell growth . . . . .	100
1.5	Clonogenic assay . . . . .	100
1.6	Cell death and apoptosis using DiOC <sub>6</sub> -IP . . . . .	100
1.7	Cell cycle and hyperploidy . . . . .	101
1.8	Cell cycle synchronization . . . . .	101
1.9	$\gamma$ -H2AX-foci detection via immunofluorescence . . . . .	101
1.10	Chromosomal aberrations . . . . .	102
1.11	Chromosomal translocations . . . . .	103
1.12	Whole cell protein extraction . . . . .	103
1.13	Protein extraction for co-immunoprecipitation (Co-IP) . . . . .	104
1.14	Bradford assay for protein quantification . . . . .	105
1.15	Protein extraction for chromatin binding assay . . . . .	105
1.16	SDS PAGE . . . . .	106
1.17	Western Blot . . . . .	106
1.18	Protein Immunodetection . . . . .	107
	1.18.1 Antibodies . . . . .	107
1.19	Shotgun proteomics . . . . .	108

---

1.20	NHEJ-HR efficiency . . . . .	109
1.21	Live cell imaging . . . . .	109
1.22	Software . . . . .	110
1.23	Statistics . . . . .	110
<b>IV</b>	<b>Results</b>	<b>111</b>
<b>1</b>	<b>p-Ku70 in DNA double strand break repair</b>	<b>113</b>
1.1	Establishment of a cell model and induction of phospho-Ku70 by different genotoxic stresses . . . . .	113
1.2	Phenotypic characterization of the phospho-mutants . . . . .	115
1.2.1	Cell growth is impaired in Ku70 phospho-mutant cell lines after irradiation . . . . .	115
1.2.2	Clonogenic survival is impaired in Ku70 phospho-mutant cell lines . . . . .	116
1.2.3	Cell death by apoptosis is enhanced in Ku70 phospho-mutant cell lines . . . . .	117
1.2.4	All Ku70 phospho-mutants and phospho-Ku70 interact similarly with Bax . . . . .	118
1.2.5	Hyperploidy and subsequent mortality in non-phosphorylatable Ku70Ala expressing cells upon irradiation . . . . .	119
1.2.6	Summary of the phenotypic characteristics of Ku70 phospho-mutants . . . . .	123
1.3	Functional dynamics and consequences of Ku70 phosphorylation on the DSB . . . . .	125
1.3.1	Impaired DNA repair kinetics in Ku70Ala expressing cells . . . . .	125
1.3.2	phospho-Ku70 localizes to DNA damage and in the NHEJ-repair complex . . . . .	125
1.3.3	Dissociation kinetics of Ku70Ala from the DNA DSB is decelerated compared to Ku70Ser . . . . .	129
1.3.4	Phosphorylation of Ku70 regulates NHEJ and HR repair activity . . . . .	130
1.3.5	Aberrant DSB repair in Ku70Ala cells is at the origin of chromosomal aberrations and chromosomal translocations . . . . .	132
<b>2</b>	<b>Generation of a humanized knock-in (KI) mouse model to study p-Ku70's role <i>in vivo</i></b>	<b>139</b>

---

<b>V</b>	<b>Discussion</b>	<b>145</b>
<b>VI</b>	<b>Conclusion &amp; Perspectives</b>	<b>161</b>
<b>VII</b>	<b>Appendix A: Article - Bouley et al. Oncotarget, 2015</b>	<b>165</b>
<b>VIII</b>	<b>Appendix B: Supplementary</b>	<b>188</b>
<b>IX</b>	<b>Appendix C: Article - Dynamics of phospho-S27-S33-Ku70 at DNA DSBs : functional link to genome stability</b>	<b>192</b>
	<b>Bibliography</b>	<b>228</b>



# List of Figures

<b>I</b>	<b>Introduction</b>	<b>3</b>
2.1	Ku functional domains and interaction with DNA . . . . .	8
2.2	Functions of Ku70 and Ku80 C-terminal domains . . . . .	9
3.1	DNA repair mechanisms . . . . .	14
3.2	c-NHEJ: 5 steps . . . . .	23
3.3	Homologous Recombination . . . . .	25
3.4	alt-NHEJ: 5 steps . . . . .	27
3.5	DNA DSB repair mechanisms . . . . .	30
3.6	End Resection . . . . .	32
3.7	DNA damage response . . . . .	36
3.8	ATM in the DDR . . . . .	39
3.9	Cell cycle . . . . .	40
3.10	Cell cycle checkpoints . . . . .	42
3.11	Senescence . . . . .	45
3.12	Apoptosis . . . . .	49
3.13	DDR cell fate . . . . .	54
4.1	V(D)J-Recombination . . . . .	57
5.1	Other cellular roles of Ku . . . . .	62
7.1	Radiosensitivity of LLC samples and classification in R-CLL and S-CLL . . . . .	77
7.2	Comparative survival proportion of patients diagnosed with R-CLL and S-CLL . . . . .	78
7.3	R-CLL derived cells have faster DNA repair kinetics and show chromosomal aberrations compared to S-CLL derived cells . . . . .	80
7.4	NHEJ activity in R-CLL and S-CLL derived lymphocytes . . . . .	80
7.5	Telomere dysfunction with telomere loss is higher in R-CLL than in S-CLL . . . . .	81
7.6	Identification of pS27,S33-Ku70 . . . . .	83
7.7	Induction of p-Ku70 by genotoxic stress . . . . .	84
7.8	Identified phosphorylation sites of Ku70 . . . . .	86



---

<b>III</b>	<b>Materials and Methods</b>	<b>95</b>
<b>IV</b>	<b>Results</b>	<b>113</b>
1.1	Establishment of a working model with the U2OS cell line . . . . .	114
1.2	Induction of p-Ku70 by different genotoxic stressors . . . . .	115
1.3	Cell growth . . . . .	116
1.4	Clonogenic Survival . . . . .	117
1.5	Cell death by apoptosis . . . . .	118
1.6	Interaction between (phospho-)Ku70 and Bax . . . . .	119
1.7	Cell Cycle . . . . .	120
1.8	Hyperploidy . . . . .	122
1.9	Phenotypes of Ku70 mutants . . . . .	124
1.10	$\gamma$ -H2AX expression . . . . .	126
1.11	Co-localization of p-Ku70 to damaged DNA . . . . .	127
1.12	Interaction of phospho-Ku70 in the NHEJ-complex . . . . .	128
1.13	Ku70 DNA DSB dissociation kinetics . . . . .	131
1.14	NHEJ and HR efficiency . . . . .	135
1.15	Chromosomal aberrations (U2OS) . . . . .	136
1.16	Chromosomal translocations (HME) . . . . .	137
2.1	Humanized KI mouse strategy . . . . .	141
2.2	Homozygous KI-Ku70Ser and KI-Ku70Ala mice . . . . .	142
2.3	Phenotypic characterization of MEF's generated from KI-Ku70Ser and KI-Ku70Ala mouse lines . . . . .	143
4	Supplementary: U2OS HREJ . . . . .	189
5	Supplementary: GC92 . . . . .	190
6	Supplementary: Synchronization of GC92 cells in G1 . . . . .	191
7	Supplementary: Nuclear localization . . . . .	191
<b>VIII</b>	<b>Appendix B: Supplementary</b>	<b>192</b>

# List of Tables

<b>I</b>	<b>Introduction</b>	<b>3</b>
2.1	X-ray cross complementation (XRCC) genes . . . . .	11
6.1	Ku expression in cancer tissue samples . . . . .	69
7.1	Rai and Binet staging system . . . . .	74
<b>III</b>	<b>Materials and Methods</b>	<b>95</b>
1.1	Cell Culture Conditions . . . . .	96
1.2	pEBV transfection conditions . . . . .	99
1.3	Antibodies . . . . .	107
1.4	Software . . . . .	110
<b>IV</b>	<b>Results</b>	<b>113</b>
<b>VIII</b>	<b>Appendix B: Supplementary</b>	<b>192</b>



# Abbreviations

<b>53BP1</b>	p53-binding protein
<b>aa</b>	Amino acid
<b>Ala</b>	Alanine
<b>ATM</b>	Ataxia telangiectasia mutated
<b>ATR</b>	Ataxia telangiectasia mutated and Rad3 Related
<b>ATRIP</b>	ATR interacting protein
<b>BCL-2</b>	B-cell lymphoma 2
<b>BER</b>	Base excision repair
<b>BRCA1</b>	Breast cancer type 1 susceptibility protein
<b>BRCA2</b>	Breast cancer type 2 susceptibility protein
<b>BTK</b>	Burton's tyrosine kinase
<b>Cdk</b>	Cyclin dependent kinase
<b>Chk1</b>	Checkpointkinase 1
<b>Chk2</b>	Checkpointkinase 2
<b>CHO</b>	Chinese hamster ovary cells
<b>CLL</b>	Chronic lymphocytic leukemia
<b>Co-IP</b>	Co-Immunoprecipitation
<b>CSR</b>	Class switch recombination
<b>CtIP</b>	CtBP-interacting protein
<b>DDR</b>	DNA damage response
<b>DNA</b>	Deoxyribonucleic acid
<b>DSB</b>	Double strand break
<b>dsDNA</b>	Double stranded DNA
<b>Exo1</b>	Exonuclease 1

---

<b>FISH</b>	flourescent in-situ hybridization
<b>Glu</b>	Glutamate
<b>hTert</b>	Human telomerase reverse transcriptase
<b>H2AX</b>	Histone 2AX
<b>HR</b>	Homologous Recombination
<b>IF</b>	Immunoflourescence
<b>IR</b>	Irradiation
<b>KI</b>	Knock-in
<b>KO</b>	Knock-out
<b>MDC1</b>	Mediator of DNA damage checkpoint 1
<b>MEF</b>	Mouse embyronic fibroblasts
<b>MES</b>	Mouse embyronic stem cells
<b>MH</b>	Microhomology
<b>MMR</b>	Mismatch repair
<b>MRN</b>	MRE11-Rad50-NBS1 (in mammals)
<b>MRX</b>	MRN (in yeast)
<b>NBS1</b>	Nijmegen breakage syndrome 1
<b>NEDD8</b>	Neural-precursor-cell-expressed developmentally down-regulated 8
<b>NER</b>	Nucleotide excision repair
<b>NHEJ</b>	Non-homologous end joining
<b>NT</b>	Non-treated
<b>PARP1</b>	Poly [ADP-ribose] polymerase 1
<b>PAXX</b>	Paralog of XRCC4 and XLF
<b>PCC</b>	Post cleavage complex
<b>PFS</b>	Progression free survival
<b>PI3K</b>	Phosphatidyl inositol 3 kinase
<b>POT1</b>	Protection of telomere 1
<b>PTM</b>	Post-translational modification
<b>RAD51</b>	Radiation sensitivity abnormal 51
<b>RAD54</b>	Radiation sensitivity abnormal 54
<b>RAG</b>	Recombination activating gene

---

<b>RAP1</b>	repressor-activator protein 1
<b>RPA</b>	Recombination protein A
<b>RNA</b>	Ribonucleic acid
<b>RSS</b>	Recombination signal sequences
<b>SAHF</b>	Senescence-associated heterochromatic foci
<b>SAP</b>	Scaffold-attachment factor A (SAFA) and SAFB, apoptotic chromatin-condensation inducer in the nucleus (ACINUS) and PIAS
<b>SASP</b>	Senescence associated secretory phenotype
<b>SEC</b>	Signal end complex
<b>Ser</b>	Serine
<b>ssDNA</b>	Single strand DNA
<b>SYK</b>	Spleen tyrosine kinase
<b>TdT</b>	Terminal-deoxynucleotidyl-transferase
<b>TIN2</b>	TRF1-interacting nuclear factor 2
<b>TRF1</b>	Telomere-repeat binding factor 1
<b>TRF2</b>	Telomere-repeat binding factor 2
<b>wt</b>	wild-type
<b>XLF</b>	XRCC4-like factor
<b>XRCC</b>	X-ray cross complementing
<b>xrs</b>	X-ray sensitive

## Chemicals

<b>APS</b>	Ammonium persulfate
<b>BSA</b>	Bovine serum albumine
<b>DIOC<sub>6</sub></b>	3,3'-dihexyloxacarbocyanine iodide
<b>DMSO</b>	Dimethyl sulfoxide
<b>DTT</b>	Dithiothreitol
<b>EDTA</b>	Ethylenediaminetetraacetic
<b>EGTA</b>	Ethylene glycol-bis( $\beta$ -aminoethyl ether)-N,N,N',N'-tetraacetic acid
<b>HCl</b>	Hydrochloric acid
<b>HEPES</b>	4-(2-hydroxyethyl)-1-piperazineethanesulfonic acid

<b>KCl</b>	Potassium chloride
<b>MgCl<sub>2</sub></b>	Magnesium chloride
<b>NaCl</b>	Sodium chloride
<b>PBS</b>	Phosphate buffered saline
<b>PFA</b>	Paraformaldehyde
<b>PI</b>	Propidium iodide
<b>SDS</b>	Sodium dodecyl sulfate

# Part I

## Introduction





# Chapter 1

## General introduction

This manuscript deals with the regulation of DNA double strand break repair and cellular fate after genotoxic stress, such as irradiation. More particularly it considers the role of Ku70 and its modified form phosphorylated at serine 27 and serine 33 within these processes. A proper DNA maintenance and DNA metabolism are central to the prevention of genomic instability and cancer development.

**Mutations are at the origin of the biological variations found in cancer.** Even before the DNA structure was decoded, several observations linked an abnormal chromosome distribution to cancer. It was also recognized that cancer cells have more than the 46 chromosomes that are found in normal cells. Moreover it could be shown that exposure of *D. melanogaster* sperm to X-rays induced transmutation, that was visible as chromosomal aberrations and phenotypic variations in the fruitfly progeny. By the middle of the 20th century, it was thus suggested that exposure to DNA damaging agents can cause mutations, however a causality for cancer was not established, yet [1].

**The link between mutations, DNA and cancer** was mainly made after the breakdown of the DNA structure by Watson and Crick. The knowledge of the structural changes brought to DNA by exposure to chemical compounds, such as alkylating agents or polycyclic aromatic hydrocarbons, provided the first link of a causal relationship between DNA changes and carcinogenesis [1].

At this point DNA repair pathways in bacteria such as the enzymatic photoreactivation and later, the in eukaryotic cells conserved nucleotide excision repair and base excision repair, have been discovered. Through the identification of patients with xeroderma pigmentosum, that had an UV-sensitivity due to impaired DNA repair and a skin cancer predisposition, a **causal link between DNA repair defects and cancer susceptibility** was drawn. In this context, not only defects in the DNA repair machinery, but also in the genes that coordinate the DNA damage response, such as ATM, were found to cause radiosensitivity and malignant transformation [1, 2]. Today the accumulation of mutations, and the caused genomic instability are considered as enabling characteristics in cancer development [3].

The Ku protein is a truly remarkable molecule that fills a long list of DNA maintenance functions and is considered as a tumour suppressor gene. We will therefore outline its general characteristics and history in the first place. Then the DNA repair mechanisms and the coordination of the DNA damage response will be determined, before tackling a particular case of DNA double strand break repair, necessary for immunoglobulin receptor rearrangement. We will acknowledge that Ku has functional and regulatory functions that go beyond DNA repair and will see that deregulated Ku is associated with human disease. The end of the introduction, will pay attention to the discovery of a novel form of Ku70 (phospho-S27,S33-Ku70), which was discovered in a subset of chronic lymphocytic leukaemia patients. These patients suffer from an aggressive form of the disease that needs immediate treatment and is linked to a bad survival prognosis.

## Chapter 2

# The Ku protein: History, protein domains and functional characteristics

### 2.1 The identification of the Ku protein- a historical review

The story of the Ku protein begins in the early 1980's, when two different Japanese research groups detected the presence of Ku- auto antibodies in the sera of patients with connective tissue diseases [4],[5]. Due to this observation, they suggested the presence of auto antibodies against the Ku antigen as a diagnostic marker for polymyositis and scleroderma. Ku was shown to localize to the nucleus in samples of different mammal and rodent cells and Reeves et al. demonstrated Ku binding to deoxyribonucleic acid (DNA) by using murine monoclonal antibodies against the deoxyribonucleoprotein complex [6]. In the following year knowledge of Ku gained substantial advancement when Francoeur et al. [7] demonstrated that the Ku protein, actually consists of a heterodimer formed by two closely related protein partners named Ku86 (further on named Ku80) and Ku66 (further on named Ku70), respectively. Ku70 and Ku80 were shown to be non-covalently

bound to each other, and to be highly conserved in different mammals as well as ubiquitously expressed in several organs. Further characterization on the DNA binding preferences of Ku by Mimori et al. [8] demonstrated that the heterodimer efficiently binds double stranded DNA (dsDNA) in a sequence non-specific manner and that the interaction increased dependent on the number of freely available DNA double strand ends. Taken together these data provide the starting point for thirty years of research to decode Ku's substantial role in DNA double strand break repair (DSB) pathways, V(D)J recombination, telomere maintenance etc. Ku is now known to be present throughout eukaryotic evolution. Furthermore in archae and bacteria homologues of Ku have been identified, underlining its importance in the development in all domains of the phylogenetic tree of life [9].

## **2.2 The different protein domains of Ku70 and Ku80 and their functions**

In the early 1990's molecular cloning techniques make it possible to decode Ku80's and Ku70's amino acid sequence [10, 11] and reveal Ku70 to consist of 609 amino acids (aa) and Ku80 of 732 aa. Primary sequence analysis shows no extensive sequence homology between the subunits in higher eukaryotes. Nevertheless their relationship becomes evident when the primary sequences of yeast and lower eukaryotes is decoded, showing that around 22% of identical aa and 38% of similar aa are found in the C-terminal ends of both subunits [12]. Sequence alignment of Ku70 and Ku80 homologues from yeast to human reveal several sequence motifs, named primary homology regions (PHR). These regions are responsible for a conserved secondary and tertiary protein structure in both subunits and thus constitute the presumption that the Ku heterodimer evolved from a common ancestor gene [9, 12, 13]. Inspired by the sequence similarity between the C-termini, Dynan et al. suggested that the ancestral gene product may have formed a homodimer important for DNA binding, and that if so, Ku70 and Ku80 could form a quasi-symmetrical protein-DNA complex. An assumption proven right by the published

crystal structure of a Ku heterodimer bound to a DNA molecule by Walker et al. [14] in 2001.

Walker et al. reveal that Ku70 and Ku80 share a three-domain topology comprising a N-terminal  $\alpha/\beta$ -domain that lies at the periphery of the heterodimer; a central  $\beta$ -barrel core domain forming a cradle for the DNA-binding groove; and a helical C-terminal arm, containing the DNA-PKcs binding element in Ku80 and a DNA-binding SAP domain in Ku70. The three domain topology of the Ku proteins is depicted in Figure 2.1A.

**The N-terminal  $\alpha/\beta$ -domains (also called von Willebrand-domain (vWA))** (Ku70, residues 34-250; Ku80, residues 6-238) make only small contributions to the dimer interface and DNA binding. They are potential sites of protein-protein interactions, such as repair or stress response factors that are recruited to DNA ends. Ku binds with an orientation preference to DNA meaning that Ku70 binds proximal and Ku80 distal to the DNA end. The N-terminus of Ku70 borders the DNA binding groove and is thought to impose a energetic barrier (more than a third of the 33 aa are negatively charged aspartate or glutamate residues) to the inward movement of the Ku heterodimer, helping Ku to be retained in proximity to the DNA end [14]. Precisely regulated sliding of Ku distal to the DNA break is a critical and well regulated process that activates DNA-PKcs and the DNA DSB-end-ligation process catalysed by the Lig4/XRCC4-complex during DNA repair [15–18].

**The central  $\beta$ -barrel domains** (core domains) of Ku70 and Ku80 form contacts across the dimer interface and are centred around a protein dyad that cradles the DNA break (see Fig. 2.1B). Using information gained by the crystal structure, the high affinity but sequence non specific binding of Ku to DNA ( $K_d$ -values:  $1.5 - 4.0 \times 10^{-10}$  M [19, 20]) is explained by two means: first, polarization of positive electrostatic charge at the inner surface of the Ku heterodimer interacts with the

negatively charged sugar-phosphate backbone of the DNA, and second, the pre-formation of the heterodimeric ring before DNA is bound.

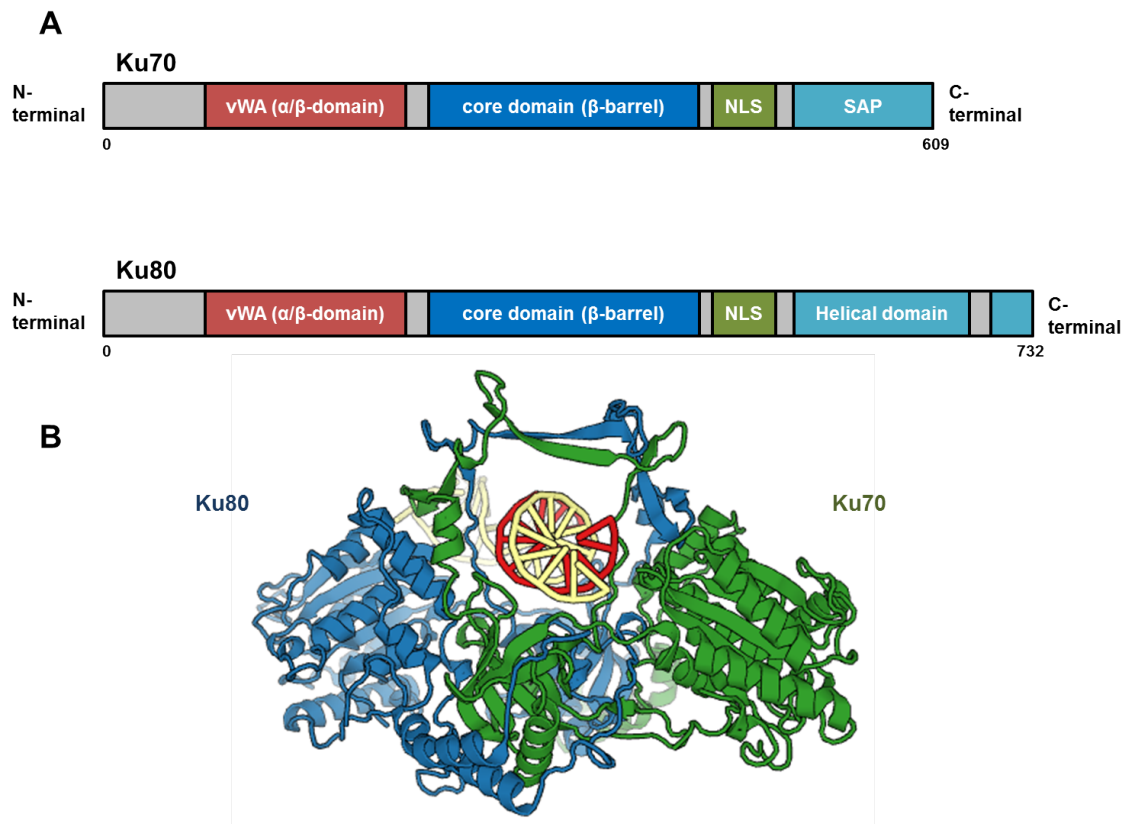


**Figure 2.1: Ku functional domains and interaction with DNA** (A) Schematic view of Ku70 and Ku80 functional domains, showing their three-domain topology. (B) Ribbon diagram of the Ku heterodimer formed around DNA (PDB 1JEQ)

Even though Ku70 and Ku80 show structural similarities concerning their N-terminal and core domains, their **C-terminal regions** are structurally and functionally divergent [21]. The most distal Ku70 C-terminal region (aa 561-609) has similarities with SAP (scaffold-attachment factor A (SAFA) and SAFB, apoptotic chromatin-condensation inducer in the nucleus (ACINUS) and PIAS)-domains, a helix-extended loop-helix motif, shown to bind on non-canonical DNA sequences and important for the organization of chromatin structure [14, 22, 23]. This domain is linked to the heterodimeric main body by a flexible peptide chain (aa 536-560) [21, 23], and lies in proximity to the  $\alpha/\beta$ -domain of Ku80 in absence of DNA. Upon DNA binding the SAP domain moves towards the continuous DNA

strand, distal to the break site, interacts with DNA and thereby stabilizes the Ku complex on the DNA (cf. Figure 2.2A) [24].

The C-terminal region of the Ku80 subunit shows a globular structure and is an important site for protein-protein interaction [25]. Upon DNA binding the C-terminus stays at the Ku core domain but is then displaced towards the arriving DNA-PKcs enzyme, a PI3-kinase (phosphatidylinositol-3-kinase), to favour interaction and trigger its kinase activity [13, 26–28], important for the coordination of DNA DSB repair [24] (see Figure 2.2B). Interestingly the C-terminal Ku80 domain and the DNA-PKcs protein are not conserved throughout evolution. Even though found in vertebrates, they are not found in yeast or worms, thus arguing for a co-evolution of these two components [13, 28]. In fact, this domain is part of a conserved motif shared by other DNA-repair proteins like NBS1 or ATRIP, that are required for recruitment of ATM and ATR, two other family members of the PI3-kinases [29].



**Figure 2.2: Functions of Ku70 and Ku80 C-terminal domains (adapted from [24])** (A) Upon DNA breakage Ku gets recruited to the break site, the movable linker of Ku70 extends the SAP domain to the continuous strand of DNA stabilizing the heterodimeric complex, (B) and upon DNA-PKcs recruitment Ku80 extends its C-terminal domain to interact with DNA-PKcs thereby initiating further steps of the repair process

In summary the Ku proteins Ku70 and Ku80 show structural similarities that form a ring-like heterodimer that cradles DNA after a DNA double strand break. Both subunits are composed of three domains, which are necessary for protein-protein interactions (vWA-domain), formation of a ring structure (core-domain) and the stabilization of the protein-DNA complex (C-terminal of Ku70) and DNA-PKcs



interaction (C-terminal of Ku80), respectively. Both subunits contain a nuclear localization sequence (NLS) between their core and C-terminal domains.

## 2.3 Functional characterization of Ku as part of the XRCC gene family- links between DSB repair and V(D)J recombination

A milestone in the understanding of DNA repair pathways and essential players therein was set by genetic complementation analysis<sup>1</sup> in the 1990's. Different rodent cell lines with DNA repair deficiencies showing sensitivity to different genotoxic agents, ranging from alkylators, cross-linkers, radiomimetics, x-rays,  $\gamma$ -irradiation or others were identified [30–32] and led to the classification of 11 complementation groups (see Table 2.1) [33, 34]. The work performed by Penny Jeggo on the xrs-mutants, isolated from the rodent CHO (chinese hamster ovary) cell line, enable the uncovering of XRCC5 and its role in DNA double strand break repair and chromosome integrity [35–40]. Later Taccioli et al., and Smider et al., prove Ku80 to be the gene product of XRCC5 and establish the knowledge about a direct role for Ku in DNA repair and V(D)J-recombination<sup>2</sup> [41–43]. Indeed, the link between V(D)J recombination and DSB repair becomes more and more evident, when the overlapping phenotypes in cell lines defective for the members of the complementation groups 4 (XRCC4; Ligase IV), 5 (XRCC5; Ku80), 6 (XRCC6; Ku70) and 7 (XRCC7; DNA-PKcs) were uncovered, underlining the action of all these genes in the same pathway during antigen receptor rearrangement and DSB repair [44].

---

<sup>1</sup>Complementation assays investigate whether two parental mutants with the same phenotype (for example IR-sensitivity) have a mutation in the same gene or whether two genes in the same pathway are affected. In the latter case hybrids (F1) of those parental mutants show a wild-type phenotype and the genes are said to be in the same complementation group, as they can complement when crossed; in contrast if the phenotype persists in the hybrids, one concludes that the same gene was affected in the parental mutants.

<sup>2</sup>V(D)J recombination is a mechanism of random gene assembly to generate a unique antigen receptor during the maturation of B- and T-cells (see Chapter 4)

The co-action of these proteins is further demonstrated by the physical interaction and activation of Ku with DNA-PKcs forming the heterotrimeric DNA-PK complex [45–47] and the interaction of DNA-PK with XRCC4/Lig4 in proximity to DSBs [48–50]. Furthermore, functional co-action of Ku80 and DNA-PKcs in V(D)J recombination and DSB repair are demonstrated, when XRCC5 mutants, lacking DNA-PKcs catalytic activity, are complemented with the XRCC5 gene and thus restore kinase activity and radiation resistance [13, 26–28, 45, 46]. Finally, Roth et al., draw parallels between the XRCC genes 4-7 and the DSB repair pathway reactions seen in *Xenopus*, termed non-homologous end joining (NHEJ) [51–54]. We know now that all these factors (and others) are necessary for the DNA repair by NHEJ and that this pathway represents the most commonly used repair pathway in mammals.

**Table 2.1: X-ray cross complementation (XRCC) gene names and DNA repair pathways they are associated with**  
(adapted from [55])

XRCC Nomenclature	Protein name	DNA repair pathway
XRCC1	XRCC1	Base Excision repair
XRCC2	Rad51-family	Homologous Recombination
XRCC3	Rad51-family	Homologous Recombination
XRCC4/Lig4	XRCC4/Ligase 4	Non-homologous end joining
XRCC5	Ku80	Non-homologous end joining
XRCC6	Ku70	Non-homologous end joining
XRCC7	DNA-PKcs	Non-homologous end joining
XRCC8	XRCC8	AT-like phenotype (no specific pathway)
XRCC9	FANCG	Fanconi-pathway
XRCC11	BRCA2/FANCD1	Fanconi-pathway/ Homologous Recombination



## Chapter 3

# DNA maintenance and metabolism

DNA is the essential molecule of life carrying genetic information in all kinds of living organisms. It is transmitted from one generation to another and encodes the essential needs of a cell/organism to develop, live and reproduce. Therefore it is of unconstrained importance that the genetic integrity is preserved. However, the DNA molecule is under constant threat by noxious ravages from endogenous and exogenous origin that can generate genetic alterations and mutations leading to cancer and cell death [56, 57]. It is thus of no surprise, that the cell has established protective mechanisms, like DNA repair and DNA surveillance pathways to maintain genomic integrity to preserve its kind.

In this chapter I will present the cellular toolbox to deal with different kinds of DNA lesions, before detailing the repair mechanisms that specifically assure repair of DNA DSB. As much in front, Ku has a particular role in DNA DSB repair, not only as an active member of the non-homologous end joining (NHEJ) machinery, but also as a coordinator in DNA repair pathway choice, and a mediator of and actor in the DNA damage response (DDR).

### 3.1 DNA repair

DNA repair represents the most direct action of the cell to fix undesired modifications of the DNA. There exists a plethora of different kinds of DNA damages ranging from nucleotide loss, abasic sites, oxidized nucleotides, single strand breaks, interstrand cross-links, bulky adducts, mismatches, replication errors or double strand breaks, that arise daily. To cope with all these lesions different repair pathways specific for every kind of damage have evolved in mammals (see Figure 3.1).

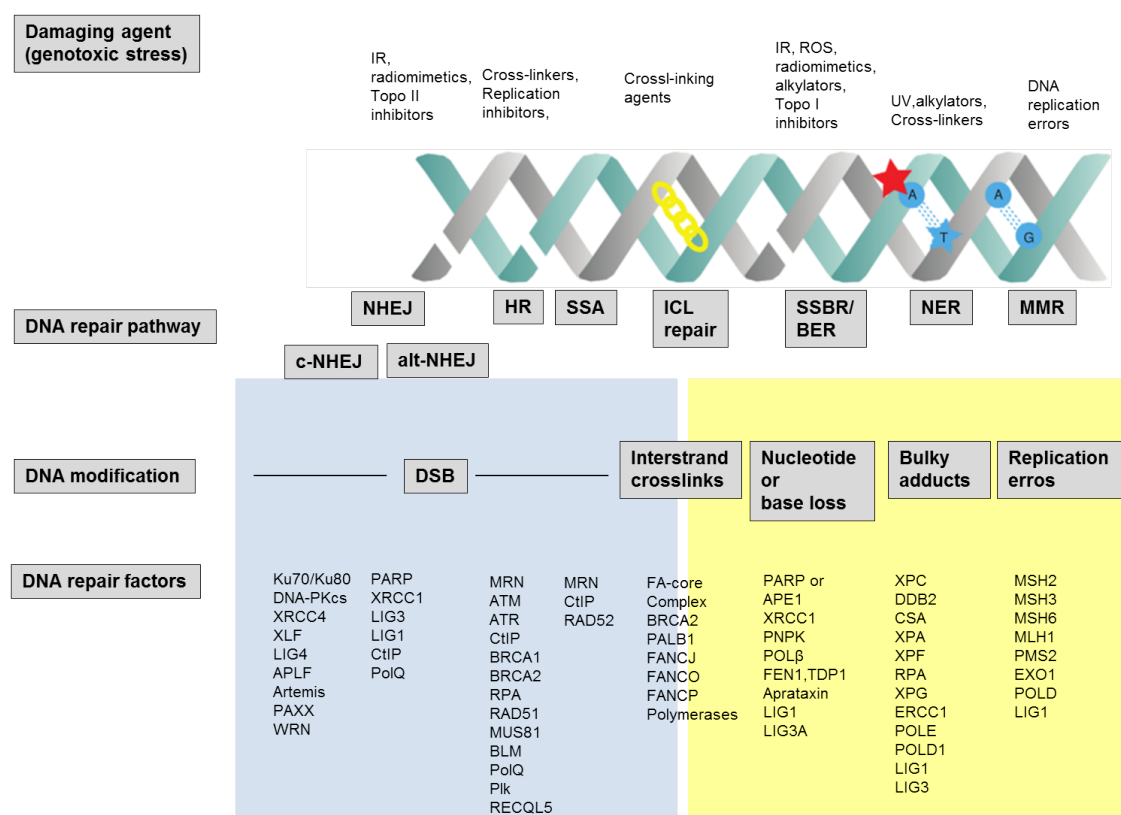


**Figure 3.1: DNA repair mechanisms ( modified from [58])** Different DNA repair mechanisms cope with a plethora of different DNA damages threatening our genome daily. The graph gives a non-exhaustive list of repair factors involved in the particular DNA repair pathways. Highlighted in blue are the so far known double strand break repair pathways. Highlighted in yellow are the single strand damage, repair pathways.

#### Single strand damage

DNA single strand lesions are discontinuities in one strand of the DNA helix and are the most frequently occurring DNA lesions. They can arise due to metabolic attack, like for example reactive oxygen species (ROS), hydrolysis or DNA slippage

during replication. It is estimated that around 10.000 such lesions occur per day and cell [59, 60].

**Single strand break repair (SSBR) and base excision repair (BER)** are closely related processes. The lesions that activate these repair pathways usually do not disturb the DNA structure but are rather the entire loss of a nucleotide (SSBR) or the modification of the nucleobase by purine oxidations, cytosine to uracil deaminations or base methylations (BER) [56–58, 61]. The BER removes the altered nucleobase using different DNA glycolases generating an abasic site (AP-site) which is cleaved by an AP-endonuclease thus creating a SSB. The created SSB, further undergoes end processing, gap filling by the short or long patch repair and is finally ligated by the Lig3 or Lig1 enzymes. The SSBR, acts similar to BER, however the lesion is recognized through PARP-1, which subsequently recruits downstream repair factors [59].

**Nucleotide excision repair (NER)** deals with more bulky lesions, that can distort the DNA structure as a whole and include alterations like pyrimidine dimers (T-T) after UV exposure. The pathway is separated in two sub-pathways, either operating on the whole genome or in transcribed regions. The bulky lesion is excised due to the endonuclease duo XPG and ERCC1/XPF and creates a open stretch of single breaks, which is then filled by DNA replication polymerases [57, 62]

**Mismatch repair (MMR)** deals with base-base mismatches, insertions or deletions of DNA nucleotides that arise during DNA replication or DNA recombination of repetitive sequences. The Mismatch repair homologs MutS and MutL identify the newly synthesized strand to determine the wrong nucleotide, followed by a exonuclease-induced degradation and DNA resynthesis [57].

**Interstrand cross-link (ICL) repair** is a complex repair system that relies on different repair factors, typically found in NER, HR or translesion synthesis (a damage tolerance pathway), as well as the fanconi anemia proteins. During the G1-cell cycle phase, some ICLs are processed by the NER. However some cross-links pass into S-phase where they constitute a replication block, that triggers

replication fork stalling or collapse, generating an one ended DSBs. These are recognized by the Fanconi- anemia proteins, that induce HR mediated replication fork stabilization. Incision on both sides of the ICL by endonucleases unhooks the lesion, and allows strand extension past the damage. Subsequently the unhooked ICL is hydrolysed or excised by NER factors [63].

### **Double strand breaks (DSBs)**

Double strand breaks are far less frequent than single strand breaks but can have severe consequences if non- or misrepaired. Non-repaired the cell can lose parts of entire chromosomes during the next cell cycle, most certainly leading to cell death; and if misrepaired they can become a source of genetic mutations, deletions, inversions or translocations threatening genomic integrity and favouring oncogenic transformation. Double strand breaks are triggered from exogenous sources like irradiation and chemotherapeutics, or endogenously by metabolic ROS and replication fork collapse during DNA replication. However, cells also induce double strand breaks intentionally to maintain genetic variety during meiotic recombination or receptor rearrangement during V(D)J-recombination [60, 64–66].

No matter if a DSB is desired or not, it can be repaired by a multitude of different repair options. The principal repair strategies being classical- non- homologous- end -joining (c-NHEJ) and homologous recombination (HR) [60, 64, 67], we now know that two other pathways can act in DNA DSB repair, alternative-NHEJ (a-NHEJ) and single strand annealing (SSA) [58].

Unlike single-strand damages, where the chemical structure of the damage decides what kind of repair pathway is activated, DSB repair relies on the overall cellular situation in which the DSB occurs e.g. cell cycle, meiosis, V(D)J recombination, genomic localization or the availability of necessary repair factors.

**Homologous Recombination (HR)** Homologous recombination is the most conservative double strand break repair pathway, because it uses a homologous sister chromatid for repair. Upon DNA breakage the DNA is resected on both strands leaving 3' overhangs, which can invade the sister chromatid and replicate the aggrieved area of the DNA. HR is highly dependent on the cell cycle and

acts in S/G2, with highest activity in mid S-phase [65, 68] (more details on this pathway in Chapter 3.1.3).

**Single strand annealing (SSA)** represents another form of mutagenic DSB repair. Like HR, SSA requires long-range end resection, but as opposed to HR does not require a donor sequence, does not entail strand invasion and is independent of RAD51. Instead, SSA uses the resected ends to find sequence homologies and mediates end joining between nucleotide repeats in the genome. In the repair product, one copy of the repeat and the intervening DNA sequence are deleted, thus resulting in loss of genetic information. SSA is considered to be a back-up of HR [65, 69].

**Non-homologous end joining (NHEJ)** Classical non-homologous end joining (**c-NHEJ**) is the predominant pathway for DNA double strand break repair in mammals. It acts throughout the cell cycle but is most active in G0/G1 and G2. Compared to HR it has fast kinetics and repairs double strand breaks via blunt ligation, independent of sequence homology [65, 69–73].

An alternative NHEJ (**a-NHEJ**) pathway has been suggested to act in DSB repair, too. Yet, there is still a lot of debate whether this pathway represents a back-up mechanism or if it is a dedicated pathway. Like the c-NHEJ pathway the a-NHEJ acts throughout the cell cycle, but in contrast is dependent on initial DNA end resection like HR. This kind of repair is mutagenic and favours nucleotide insertions, deletions and chromosome translocations [65, 66, 70, 74] (more details on this pathway in Chapter 3.1.4). It is mostly active when either c-NHEJ and HR fail to repair [65, 75–77].

Ku is part of the c-NHEJ pathway, but is also an important regulator and inhibitor of a-NHEJ and HR (cf Chapter 3.2).

### 3.1.1 c-NHEJ step-by-step

The c-NHEJ pathway appears to be a straightforward mechanism as it "simply" rejoins broken DNA ends, without the necessity of a sister chromatid and homology



search. Still c-NHEJ needs to follow certain steps to realign broken ends in the most accurate way, given the nature of the damage. Blunt ends for example, as generated after endonuclease cleavage can be rejoined directly, whereas IR induced damage causes "dirty" or modified ends that have to be processed prior to joining. The general workflow of c-NHEJ consists of five steps: 1) Recognition of the break by Ku, 2) Synapsis (DNA bridging), 3) Processing of the ends, 4) Ligation of the processed ends and 5) Ku removal from the repaired DNA [66, 70]. A schematic summary of all steps is provided in Figure 3.2).

### 1) Recognition of the break by Ku

The first step in c-NHEJ is the recognition of the DNA DSB by the Ku heterodimer. Ku is considered to be one of the most abundant proteins in the cell (approximately  $400\text{-}500 \times 10^3$  molecules/cell) and is the very first protein recruited to a DSB [20, 78, 79]. The Ku heterodimer slides on DNA with its ring shaped structure, thereby making contacts to a few phosphates of the DNA backbone [14] and then serves as interaction point for the other NHEJ factors like DNA-PK<sub>cs</sub> [45], XRCC4/Ligase4 [49], XLF/Cernunnos (further on called XLF (XRCC4-like factor) in this manuscript) [80] and PAXX (paralog of XRCC4 and XLF) [81–83]. Upon DNA-PK<sub>cs</sub> arrival Ku slides about 10bp distal to the break [16, 18], making place for the kinase and triggering its catalytic activity [28] important for the orchestration of downstream effectors [84, 85]. DNA-bound Ku becomes thus part of the heterotrimeric DNA-PK complex.

It has been a long issue of debate whether there are several Ku proteins binding to a DNA end like "beads on a string" [9, 14, 86] or if one single Ku heterodimer is sufficient per break site [87, 88]. Indeed, Ku does not form distinct DNA repair foci after irradiation, like for example  $\gamma$ -H2Ax or Rad51, suggesting that it does not accumulate in large numbers on DNA DSBs. *In cellulo*, using a particular extraction buffer, Britton et al. visualized Ku foci with a particular extraction buffer and found rarely more than two Ku heterodimers per DNA DSB [88].

### 2) Synapsis

Synapsis describes the tethering of the broken DNA strands and is important to

assure realignment of corresponding ends especially when several DNA DSBs occur in near proximity, thus preventing erroneous joining and translocations. Several factors like Ku, DNA-PKcs and XRCC4/XLF were shown to take part in this process.

Early *in vitro* and atomic force microscopy studies in the late 1990's have already shown that Ku can easily transfer between two strands of DNA, suggesting that DNA molecules are bridged by Ku during DNA repair [89–91]. Later, functional studies affirmed that Ku80 loss in murine fibroblasts leads to higher DNA dynamics of the broken ends. This phenomenon is of particular importance as stresses like  $\gamma$ -irradiation can induce clusters of DNA DSBs, that if not properly aligned, can be the cause of chromosomal translocations *in cellulo* [92]. In this context, Ku is necessary for the recruitment of XLF that assembles into long filaments with its family partner XRCC4, spanning and aligning DNA ends [93, 94]. By using super-resolution microscopy Reid et al. show that after Ku loading onto DNA, XLF/XRCC4/Lig4 filaments are recruited, mediating side-by-side pairing of two filaments until an end-to-end alignment is attained [95]. Interestingly, the mechanism presented by Reid et al. is independent of DNA-PK<sub>cs</sub>.

In contrast, electron microscopy and two photon fluorescence cross-relation spectroscopy, clearly have shown a role for DNA-PK<sub>cs</sub> for juxtaposition of DNA ends and downstream processes like processing and ligation [96, 97]. These observations are in agreement with the two-stage model proposed by Graham et al. [98], which suggests that heterotrimeric DNA-PK on the DNA forms a first long range synaptic complex, which activates DNA-PK catalytic activity and recruits downstream effectors XLF/Lig4/XRCC4 to constitute a short range synaptic complex, which is then ready for ligation.

Discrepancy between the models of Reid et al. and Graham et al. on DNA-PK<sub>cs</sub> dependency might be due to the approaches used, as Reid et al. performed experiments on recombinant proteins and thus eventually revealed the minimal necessary factors in synapsis, whereas Graham et al. used a more physiologic approach, using protein cell extracts including nucleases etc. this may represent a more pragmatic picture of NHEJ in vertebrates.

It seems likely that synapsis is a highly regulated multi-step process with several factors involved such as Ku, DNA-PK<sub>cs</sub> and the XRCC4/XLF filaments, thus stabilizing the DNA ends for proper ligation.

### 3) Processing of the ends

Processing of the DNA ends renders them compatible for ligation by providing a 3'-hydroxyl- and a 5'-phosphate DNA-end. DNA breaks are not always directly connectable and must be processed prior to joining. For instance, IR damaged DNA ends often show 3'-phosphoglycolates, 5'-hydroxyl groups, abasic sites, thymine glycols or ring fragmentations [85]. Several kinases/phosphatases (PNPK), nucleases (Artemis, WRN, APLF, APTX, Mre11) polymerases (DNA polymerase  $\beta$ ,  $\mu$ ,  $\lambda$ , TdT), helicases (RECQ1) or phosphodiesterases (tyrosyl-DNA phosphodiesterase 1) are involved in end processing. They are recruited dependent on the unique chemistry of each break [99, 100].

The most prominent processing enzyme is Artemis, having important roles in V(D)J recombination and NHEJ repair, hence loss of Artemis is associated with increased radiosensitivity and a complete loss of peripheral T- and B-lymphocytes [101, 102]. Artemis has a 5'-exonuclease and 5'-or 3'-endonuclease activity when recruited and is activated by phosphorylated DNA-PK<sub>cs</sub> [85, 99, 100, 103].

Ku has a role in recruiting several factors for the processing step like polymerase  $\mu$  and  $\lambda$  [104, 105], APLF [106], or WRN [107, 108]. Interestingly, Ku itself has been identified to have a processing activity as well, excising 5'-terminal abasic sites that would otherwise block the ligation step [109, 110]. Reid et al. elucidate that the 5'-phosphate group is important for juxtaposition of the ends and a recognition element for Lig4, underlining the importance for proper end processing prior to ligation. They further depict a model in which non-compatible end chemistry can favour the dissociation of the two broken ends, leading to a new round of processing and tethering until compatible ends are generated. They suggest that a certain time window is provided for this "trial and error" process before other repair pathways such as mutagenic alt-NHEJ are favoured to take the job [111].

#### 4) Ligation of the processed ends

Ligation of the broken ends is performed after DNA synapsis and as soon as the processing steps warrant compatible ends. Only one ligase, Lig4, executes ligation during c-NHEJ. Loss of Lig4 is associated with embryonic lethality in mice and hypomorphic mutations lead to radiosensitivity, immunodeficiency, microencephaly and developmental delay in humans [112–116]. Lig4 interacts and is stimulated by the XRCC4 protein, which by itself has no enzymatic activity but still leads to radiosensitivity when lost [48, 117]. XRCC4 is a scaffolding protein and interacts with APLF, Ku70 [79], XLF, PNK and DNA thus stabilizing the Lig4-XRCC4 complex (X4-L4) on the break site [99]. Lig4 stabilization is further provided by DNA-PK dependent phosphorylation [118].

XRCC4 is part of a homologous superfamily and includes the structurally similar proteins XLF and the recently identified protein PAXX. XLF was identified in patients with severe immunodeficiency, radiosensitivity and deficiency in DNA end ligation [93, 94, 119, 120]. Besides its actions together with XRCC4 to align DNA ends, XLF was shown to activate XRCC4/Lig4 for the ligation of mismatched and non-cohesive ends up to 100-fold, probably by stabilizing the XRCC4/Lig4 complex [121, 122]. The other homologue of this family PAXX, has recently been discovered by 3 different laboratories and approaches [81, 123, 124]. Based on the following observations PAXX is sought to be a core protein in c-NHEJ: it co-purifies with Ku and DNA-PKcs, is recruited to DNA damage sites, loss leads to radiosensitivity and its Ku-dependent ligation activating characteristics [81, 123, 124]. Craxton et al. show that PAXX can stimulate the XLF-dependent ligation step by 7.6-fold on DNA substrates with non-cohesive ends, whereas no stimulatory effect was seen for blunt ends [123]. However, Tadi et al. challenges these observations by affirming PAXX only an accessory role in c-NHEJ, stating that PAXX's stimulatory function on DNA ligation is mostly masked by XLF and becomes only noticeable after omitting XLF function [83].

The ligation step is conducted by Lig4 during c-NHEJ, however its activity is highly dependent on the interaction partners XRCC4 and XLF. The role of PAXX in ligation is still an issue of debate.

## 5) Ku removal from the repaired DNA

One of the unresolved mysteries in c-NHEJ is the removal of Ku from ligated double stranded DNA. Unlike other DNA binding proteins like PNCA, which can be released from DNA due to conformational changes separating its two subunits, both Ku subunits encircle DNA and form a protein-protein interdigitation, which gets trapped on the repaired DNA strand [125]. It seems evident that Ku has to be removed after DNA repair to make place for other DNA repair pathways, and to give access to transcriptional and replicative activity [126]. Microirradiation experiments show disappearing Ku signals several hours after DSB induction, but how is it removed, considering the ring shaped structure of both subunits cradling the DNA?

Ubiquitination is a post-translational modification associated with proteasomal degradation and protein regulatory function. In studies using *Xenopus leavis* as a model, Postow et al. discovered that the Skp1-Cul1-F box (SCF) E3 ubiquitin ligase complex accumulates on broken DNA in a Ku dependent manner, where Ku80 becomes highly ubiquitinated (poly K48-ub-chains) leading to its release from the DNA [125, 127]. Interestingly, conjugation of NEDD8 (called neddylation) to the Cullin subunits in the SCF complexes stimulate the SCF ubiquitin-protein ligase activity and Brown et al. show that neddylation is an important step in Ku ubiquitination [126, 128]. However, in contrast to the Postow studies that demonstrate that Ku80 is ubiquitinated independently of accomplished repair, Brown et al. report ubiquitination sites on both subunits of Ku and insist on the release of Ku only after successful DNA repair [125, 127, 128]. Moreover the study of Brown et al. uncovers downregulation of Ku70 specific protein interactors after inhibition of neddylation. One of these interactors is the AAA+-type ATPase VCP/p97, shown to extract trapped Ku from DNA [128, 129].

Another E3-ligase, RNF8, ubiquitinates Ku80 to regulate its release from DNA and successful repair by NHEJ, however Brown et al. could not reproduce retention times of Ku80 on DNA breaks after RNF8 depletion [128, 130].

The above mentioned studies give first insights of the removal of the Ku protein from DNA, but need to be further explored, as it is not clear what mechanism

activates ubiquitination activity on Ku. It has been proposed that Ku changes conformation upon binding to the DNA and that these might unravel Lysine sites for ubiquitination [131], another possibility could be other posttranslational modifications such as phosphorylation [132] that enhance ubiquitination of Ku.

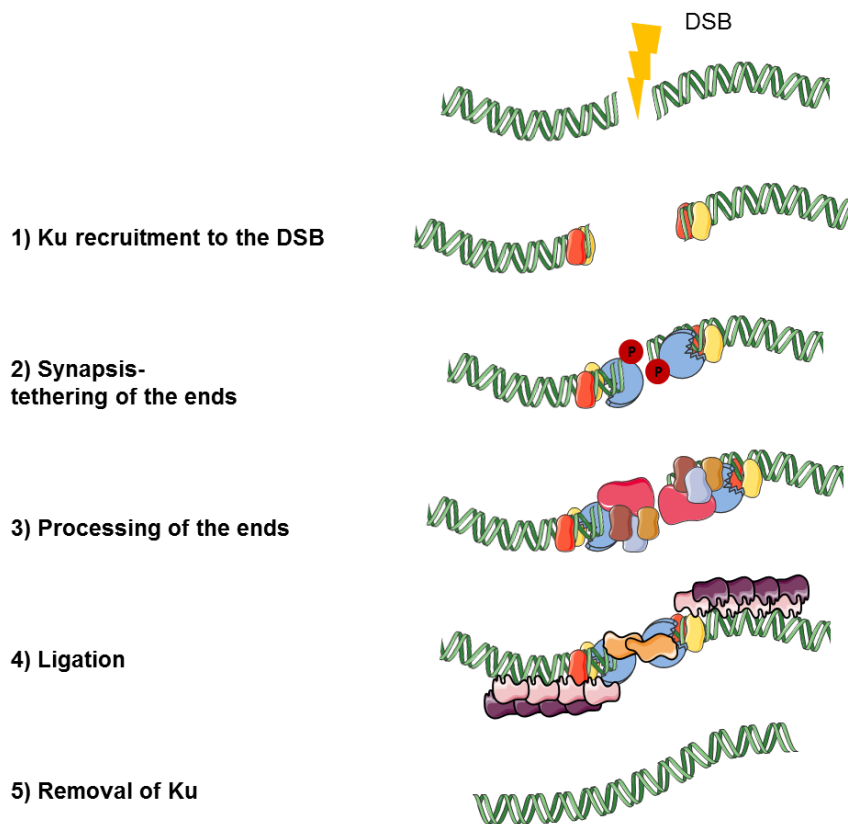


**Figure 3.2: c-NHEJ:** Scheme of the five steps necessary for c-NHEJ

### 3.1.2 Fidelity of c-NHEJ

c-NHEJ has been long time considered to be an error-prone repair pathway, as processing of the ends prior to ligation can lead to the deletion/insertion of nucleotides. However, studies using the endonuclease I-SceI show that complementary DNA ends are joined accurate in up to 75% of cases and that inhibition of Ku80 or XRCC4 abolishes accuracy, underlining the importance of c-NHEJ in error-free DSB repair [67, 133–135]. Additionally, using inverted cleavage sites for

I-SceI, generating non-cohesive ends, c-NHEJ has been shown to adapt to imperfect complementary ends by aligning the maximum of possible correspondent base pairs. The importance of Ku in NHEJ is exemplified in Ku deficient cells that harbour erroneous end-joining using microhomologies or large deletions for repair that generate genomic alterations [67, 92, 136–138].

These data show that c-NHEJ is not an error-prone process per se, but rather adapts to the nature of the broken DNA. Thereby c-NHEJ maximizes the annealing of complementary nucleotides, thus diminishing a maximum of genetic alterations [67].

### 3.1.3 Homologous Recombination

Homologous Recombination is a cellular key pathway, which acts in meiosis when homologous chromosome sequences are exchanged to guarantee genetic variation in offspring. In mitosis homologous recombination assures proper DNA double strand break repair during replication or in S/G2 cell cycle phase.

In contrast to NHEJ the DNA ends are not "simply" rejoined, but are resected to license subsequent strand invasion of a homologous DNA sequence. The process of DSB-induced homologous recombination can be divided into three steps: pre-synapsis, synapsis and postsynapsis (cf Figure 3.3).

**Pre-synapsis** describes the generation of long 3' ssDNA stretches on both sides of the DSB, which are covered by Rad51 filaments. Initial 5' to 3' end resection is performed by endo- and exonucleases such as MRN (MRE11-NBS1-Rad50)/ CtIP. A more extensive resection is assured due to helicases such as BLM (Bloom) and exonucleases such as Exo1 (Exonuclease 1). The free 3'overhangs are recognized and covered by RPA-filaments, preventing secondary DNA structure generation. Later RPA is displaced by RAD51. Several mediators are known to support RPA exchange by RAD51 such as RAD51B, RAD51C, RAD51D, XRCC3, XRCC2 and BRCA2. Especially BRCA2 with its ssDNA and dsDNA binding motifs and RAD51 binding sites has a prominent role in RAD51 filament nucleation to the 3' overhang.

The RAD51-filament covered 3' overhang performs invasion and homology search, called **synapsis**, on the sister chromatid. RAD51 forms a displacement loop (D-loop) stabilized by RAD54, which then displaces RAD51 from the heteroduplex DNA to prime DNA synthesis by the invading strand.

The **postsynaptic phase** summarizes several sub-pathways of HR based on their D-loop resolution and recombination outcomes via either (non-) or cross-over mechanisms. These include BIR (Break induced repair), SDSA (synthesis-dependent strand annealing) or double Holliday Junction (dHJ) resolution [139, 140]. Organisms control the appropriate outcome based on the cellular context, in meiosis for example a cross-over mechanism will be favoured to obtain gene conversion outcomes, whereas in mitosis such mechanisms can lead to loss of heterozygosity (LOH) [141].

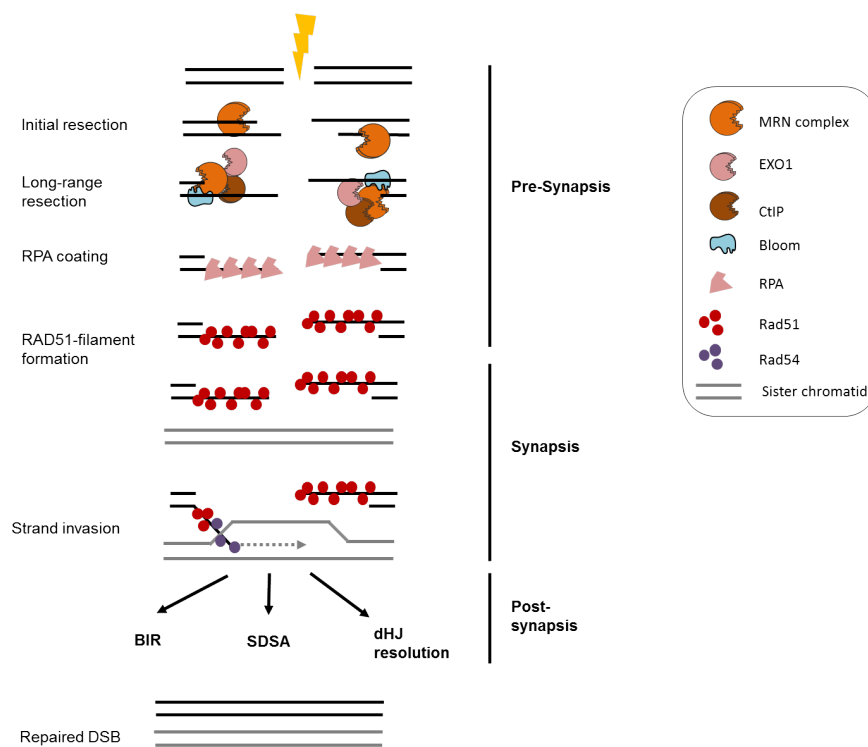


**Figure 3.3: Homologous recombination** The three main phases and the main actors of HR are depicted [140, 142]



### 3.1.4 alternative/mutagenic/microhomology mediated NHEJ

A new "alternative" non-homologous end joining pathway is the most recently discovered double strand break repair pathway and is known under a variety of names: a-NHEJ, alt-NHEJ, backup-NHEJ or MMEJ (microhomology mediated end joining). A main characteristic of a-NHEJ is the alignment of microhomologies (MH) distal from the DNA break, associated with deletions directed by end resection. This pathway represents a mutagenic, error-prone pathway and is associated with chromosomal translocations and oncogenesis [143–145]. It is called alt-NHEJ according to its discovery in yeast and mammalian cells, where c-NHEJ was inhibited through deletion of its core factors, XRCC4 or Ku [133, 146, 147]. The general model for a-NHEJ involves 5 steps: (1) initial 5'-3' end resection of the DNA ends, (2) MH annealing, (3) removal of the resulting flaps, (4) gap filling and (5) ligation (see Figure 3.4).

a-NHEJ shares the **initial end resection** with HR [148–150]. Short-range resection, executed by MRN/CtIP, thus can reveal distal homology sites of two adjacent ssDNA polymers that share complementarity.

Mammalian cells can **anneal** as few as 1 nt homologies [145], but mismatches and low GC content in the MH can result in unstable pairing [74]. Tethering factors have thus been discussed and PARP1 (Poly [ADP-ribose] polymerase 1) was shown to play a role in a-NHEJ synapsis [151] [152]. For example during class-switch recombination (CSR) PARP1 competes with Ku to bind DNA ends [76], therefore a-NHEJ is also often referred as PARP1-dependent NHEJ.

Following annealing **3' flaps removal** distal from the DNA ends is important prior to DNA polymerase dependent fill-in synthesis. In yeast 3'flaps are removed by the endonuclease Rad1-Rad10 [153]. In vertebrates Rad1-Rad10 corresponds to XPF/ERCC1, but ERCC1<sup>-/-</sup> mice revealed only a minor dependence on this flap endonuclease [154]. Further analysis has to elucidate flap removal in vertebrates.

**Fill-in synthesis** of the MH-flanking single stranded regions is carried out by polymerases. Genetic studies reveal a key role for Pol $\theta$  in this process in *Drosophila*

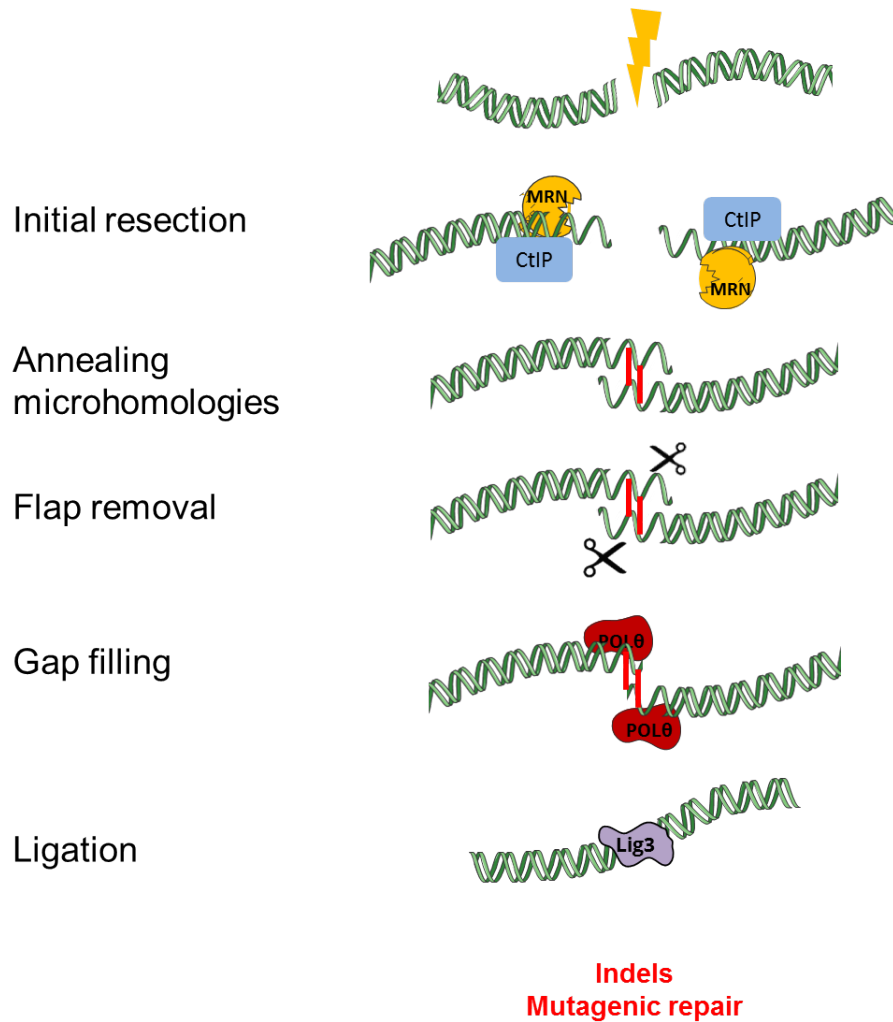


**Figure 3.4: alt-NHEJ** Schematic overview of the 5 steps in alt-NHEJ

*melanogaster* [155, 156], which later on was confirmed to be evolutionary conserved in mice [77] and in HR-deficient tumours [75]. The C-terminal domain of Pol $\theta$  encodes a proofreading-deficient polymerase that copies DNA in a template dependent manner and unlike other polymerases promotes extension and lesion bypass synthesis of ssDNA, increasing the probability to form base pairing by MH. Pol $\theta$ 's N-terminal helicase-ATPase domain is important for MH pairing events, and might be important to displace DNA bound RPA, considered as an inhibitor of alt-NHEJ and a promoter of HR [74, 155, 157]. The central domain of Pol $\theta$  contains a Rad51-interaction domain, which blocks Rad51-mediated recombination together with the N-terminal ATPase domain [75], preventing HR. Pol $\theta$  thus has a central role in driving microhomology mediated alt-NHEJ by its erroneous

polymerase functions and inhibition of HR. Pol $\theta$  has tethering and annealing activities and is recruited to DNA breaks in a PARP1 dependent manner [77, 158]. **Ligation** of the DNA ends is the last step of alt-NHEJ. Lig3 and to a lesser extent Lig1 drive alt-NHEJ mediated sealing of DNA ends in biochemical assays and *in vivo* [144, 151, 159].

It is a long matter of debate whether alt-NHEJ represents a back-up mechanism or if it is a dedicated pathway. This is first, because it became evident in cells that were deficient for c-NHEJ core factors [133, 146, 147] and second because no alt-NHEJ specific key factors have been identified so far. In fact all a-NHEJ factors appear to have overlapping functions with other known repair pathways including HR (MRN/CtIP), interstrand cross-link repair (Pol $\theta$ ), nucleotide excision repair (Lig 1) and base excision repair (PARP1, Lig 3) [74, 157].

However, it seems more and more likely that alt-NHEJ represents a distinct pathway that can coexist with c-NHEJ and HR. Several lines of evidence are in favour of such a function, such as 1) studies in C-terminal RAG2 mutants that show active alt-NHEJ in c-NHEJ proficient cells [160], 2) two papers released in 2011 [149, 161], that show a prominent role for CtIP to drive alt-NHEJ mediated chromosomal translocation and impaired class switch recombination (CSR) in c-NHEJ proficient murine systems, 3) Truong et al. that provide an alt-NHEJ - HR competition assay and find alt-NHEJ to coexist with HR independent of c-NHEJ [148], at levels around 10-20% of HR in human cell models and 4) Shamanna et al. [162] who provide insight into the inhibitory effect of WRN on alt-NHEJ, by impairing recruitment of MRN and CtIP to the break. They also state that WRN mutations in patient fibroblast show multiple, variable chromosomal aberrations and an increase in cancer incidence, however no direct link to alt-NHEJ is drawn by the authors.

Most of the early studies in alt-NHEJ were performed in murine systems [144, 145, 163]. However, there might be some striking species dependent differences concerning chromosomal translocations by alt-NHEJ in murine *vs.* human model systems [164]. Thus, Ghezroaoui et al. surprisingly find that the translocation rate is significantly decreased when core c-NHEJ factor like XRCC4 or Lig4 are

inhibited in human cell models after chromosomal breaks induction. Loss of components of the alt-NHEJ however does not reduce chromosomal translocations, underlining the role of c-NHEJ in chromosomal aberrations in humans compared to mice. Findings in murine and human cell systems thus stand in direct opposition to each other, perhaps due to the higher c-NHEJ activity in human compared to murine systems [164]. But wasn't c-NHEJ considered as an error-free mechanism? So, how could the first choice repair pathway in humans account for such a dangerous outcome like chromosomal aberrations? Biehs et al. [165] provide evidence for a resection dependent (slow) c-NHEJ and a resection independent (fast) c-NHEJ. They argue that Polo-like-kinase3 (Plk3) activated CtIP and Artemis are important factors in resection dependent slow c-NHEJ in G1 and that this type of repair induces MH-mediated repair and chromosomal translocations by c-NHEJ instead of a-NHEJ in human models.

In summary, there exist two types of NHEJ: error-free and error-prone. The error prone a-NHEJ is now recognized as a unique pathway that drives chromosomal translocations in a murine background; however its impact in the human DNA repair processes still remains elusive and needs further clarification. There is evidence for a second type of c-NHEJ in humans that accounts for mutagenic end-joining that has slow kinetics, active in the G1-cell cycle phase.

## 3.2 Crosstalk of DNA DSB repair pathways

Given the ability of a cell to deploy different DNA double strand break repair pathways it is of big interest how pathway choice is regulated. Generally c-NHEJ and HR represent the two major repair pathways that restore DNA integrity after DNA DSBs. Only if those two pathways fail to repair, the more mutagenic pathways like alt-NHEJ or single-strand annealing fill in the task, accepting errors only to avert most severe consequences associated with a complete loss of repair [69] (see Figure 3.5). Special interest has been attributed to the choice between HR and NHEJ. Tight regulation and cooperation of both pathways seem inalienable

to prevent errors and genomic alterations. A central role in DNA repair pathway choice is the cell cycle phase, regulating the availability/activity of HR-factors and the sister chromatid during S/G<sub>2</sub>, as well as Cdk- (cyclin dependent kinase) dependent regulation of end resection, the crossroad between NHEJ and HR [69]. We will see that multiple factors fine tune end resection and that Ku has an important role within.

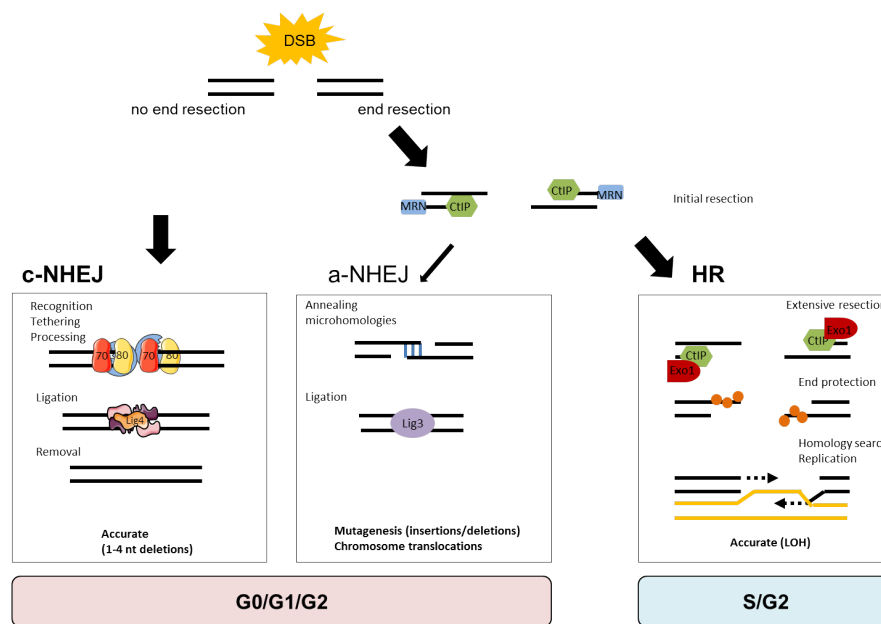


**Figure 3.5: DNA DSB repair mechanisms and end resection as a central decision point(modified from [65])** Available DNA DSB repair mechanisms in the cell. The main repair strategies consist of c-NHEJ and HR which operate during different cell cycle stages, both are considered as accurate. a-NHEJ represents the most recently discovered repair pathway. It is highly mutagenic and it's role as a dedicated repair pathway is still under debate. End resection stands at the crossroads of these repair pathways.

### 3.2.1 DNA end resection dictates repair pathway choice between HR and NHEJ during S/G<sub>2</sub>-phase

The repair-concepts of c-NHEJ and HR repair diverge already at an early time point. During the S/G<sub>2</sub>- phase HR is dependent on a resection step, whereas c-NHEJ is not. In fact, resection inhibits c-NHEJ and *vice versa* Ku/DNA-PKcs block resection [72, 166–168].

**The end resection mechanism** The core machinery and the resection mechanism are preserved throughout evolution, so that the majority of studies concerning end resection have pioneered in yeast as a model system [169].

Generation of long 3' overhangs is a precondition for HR and is obtained in two steps: initial resection and long range resection [168] that act in a bidirectional manner. Initially resection is executed by the coordinated activities of MRN nucleases (MRE11-NBS1-Rad50) and CtIP (MRX and Sae2 in yeast) [169, 170]. The intrinsic endonuclease activity of MRE11 nicks the DNA backbone approximately 300bp distal from the break, giving access to its exonuclease to proceed in 3'-5' direction (towards the break) [171]. Long range resection depends on the coordinated helicase and exonuclease activities of BLM and Exo1 that proceed in 5'-3' direction (away from the break) creating long stretches of ssDNA important for strand invasion [170–172] (see Fig.3.6).

A special role in resection control is attributed to CtIP, as it stimulates MRE11 activity and fine tunes whether end resection takes place or not [169, 173, 174]. Thereby CtIP integrates signals from the cell cycle and chromatin status by interactions with Cdks and BRCA1, that recruit CtIP to the DSB and activate it in S/G2 [173–176]. During G1 end resection is inhibited by 53BP1 [177].

**Upstream regulation of end resection by 53BP1-RIF and BRCA1- CtIP on the chromatin level** So far, the most upstream mechanism for resection is regulated by 53BP1-RIF and BRCA1-CtIP. 53BP1 is an important block for resection and thus promotes c-NHEJ, whereas its counterpart BRCA1 promotes resection by CtIP and thus HR.

Upon DSB induction the DNA damage response (DDR) protein ATM, phosphorylates the histone H2AX over several megabases which recruits the mediator MDC1. MDC1 has been shown important for ATM and MRN recruitment to the DSB extending region. It also leads to the recruitment of the ubiquitin ligases RNF8 and RNF168, which are considered important for the recruitment of 53BP1 to the chromatin. 53BP1 oligomerizes via interaction with dimethylated histone 4 (H4K20Me2) and ubiquitinated H2K15 surrounding the DSB. Phosphorylation

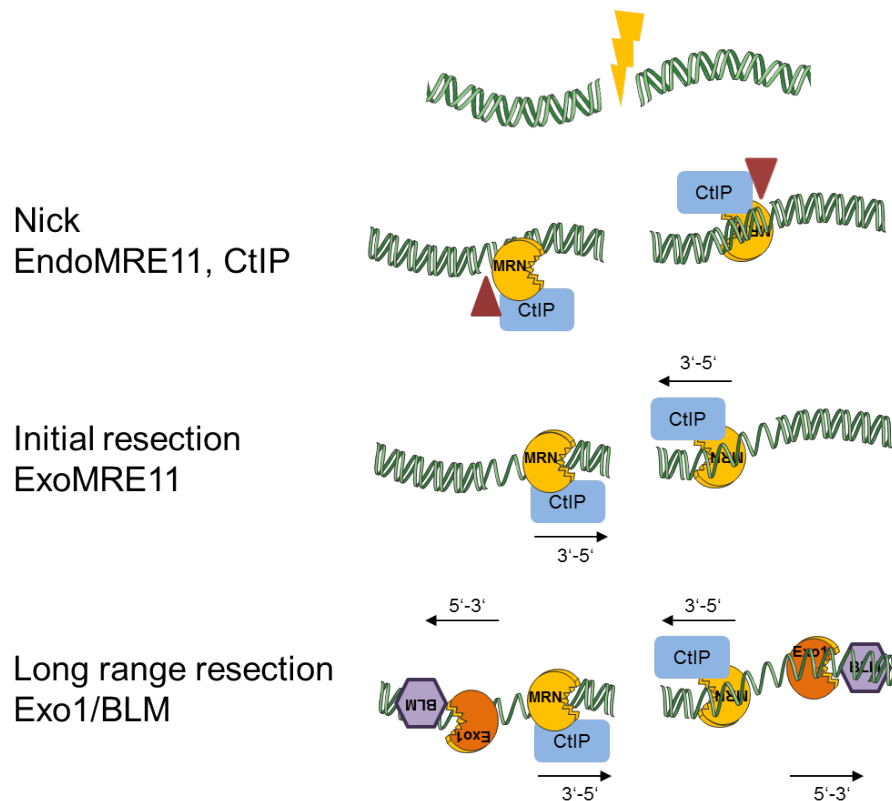


**Figure 3.6: End Resection** Coordination of the short and long range end resection by MRN/CtIP and BLM/Exo1, respectively to create long stretches of ssDNA 3' overhangs to initiate repair by HR.

of 53BP1 by ATM leads to its interaction with RIF1 in G1 promoting c-NHEJ and repressing BRCA1-CtIP mediated resection [178–183]. During S/G2 phase interaction between RIF1 and 53BP1 is disrupted via cell cycle dependent phosphorylation of CtIP (T487) and BRCA1 [179, 181], giving access for nucleases to resect. BRCA1/CtIP and 53BP1/RIF1 are mutually exclusive on the DSB, underlining their reciprocal actions in the decision concerning end resection [182].

**Regulation of resection by DNA-PKcs** As mentioned earlier DNA-PKcs orchestrates NHEJ by phosphorylation events, this also impacts on the DNA pathway choice [184, 185]. DNA-PKcs blocks resection by inhibiting the access of Exo1. This is due to the phosphorylation status of its ABCDE cluster (of DNA-PKcs), partly regulated by ATM [167, 186]. Additionally, DNA-PKcs phosphorylates ATM on multiple sites hence reducing its catalytic activity to promote DNA end

resection [187]. DNA-PKcs and ATM therefore seem to regulate each other in order to fine tune the end resection decision.

**Regulation of resection by Ku at the DSB** Another level of regulation is provided by Ku and MRN (MRX in yeast). In fact Ku and MRN are the first DNA repair proteins that locate to the DNA break [188], activities of either one have to proceed in a regulated manner to assure proper DNA repair.

Studies in yeast show that Ku loss leads to more MRX recruitment, rapid resection and higher levels of HR [189–191]. On the other hand MRX deletion comes along with a 20-fold higher recruitment of Ku [191], blocking the first resection step [192]. Additionally Ku blocks the access for Exo1 to execute long range resection [191, 193, 194]. These observations suggest a competition model between Ku and MRX, so that the choice of a repair pathway resides in which protein complex is faster assembled and activated on the DNA break.

However, in human models the competition model seems not to be adequate due to organism differences concerning pathway dependency (yeast are much more reliant on HR than NHEJ compared to mammals) and cellular protein concentration of Ku (humans have greatly enriched cellular concentrations of Ku, compared to yeast). Additionally, unlike in yeast Ku cannot be pushed away by MRN and its recruitment/release kinetics in S and non-S-phase are similar in human models [194]. Ku therefore seems to be actively released from the DSB, instead of displaced, in human cells [194, 195]. The exact mechanism for Ku removal, (similar to the removal after completion of c-NHEJ) is not fully understood yet. Still, several posttranslational modifications have been suggested including phosphorylation and ubiquitination in a cell cycle dependent manner.

Lee et al. [196] provide evidence that a phosphorylation cluster in the core domain of Ku70 leads to conformational change and release of Ku from the break site, compared to phospho-mutants that are retained on the break. They argue that phosphorylation decreases Ku's affinity for DNA and that partially generated ssDNA on the break (to which Ku has less affinity) might tip the balance towards Ku release.



Ubiquitination already has been shown to play an important role in the release of Ku from DNA after c-NHEJ completion [130]. In agreement, Ismail et al. [197] present a new ubiquitin ligase, RNF138, to be recruited to short stretches of ssDNA after initial MRE11 resection and to ubiquitinate Ku80 for its release. Interestingly RNF138 is also implicated in CtIP activation and its recruitment, strengthening the idea of RNF138 as an important regulator of end resection and pathway choice [198].

Lastly, Chanut et al. [172] have discovered a more radical way to get rid of DNA-bound Ku. A CtIP intrinsic flap-endonuclease activity cleaves off Ku associated to a double stranded DNA-fragment, thus attacking Ku from the flank. This model however was studied on single ended DSB during replication fork collapse, and thus represents a different context of DSB. Still, it might be a valid mechanism during double ended DSB repair, as well. In conclusion, the exact mechanism(s) that regulate the release of Ku and alleviate the resection block are not fully understood, but point to a multistep process.

**A resection dependent c-NHEJ was recently revealed** Surprisingly a report from 2017 shows that DNA end resection is not exclusive to the S/G2-phase and that RPA coated ssDNA can be detected in G1. They show that these resected ends occurring on complex DSB are a substrate for a slow acting, slow fidelity c-NHEJ. The resection process however differs from the resection process described above, as it starts resection not distal but from the DSB end, being independent on MRE11 endonuclease activity. In this case, CtIP is activated by Plk3, allowing its interaction with BRCA1 to promote initiation of resection, a resection eventually completed by Artemis and Mre11 exonuclease activities [165].

In summary, DNA end resection is thought to be one of the major determinants of pathway choice in the S/G2-phase. The process is regulated on several levels and balanced by the presence of factors of both HR and NHEJ which are fine tuned in accordance with the cell cycle, phosphorylation and ubiquitination events. Ku

plays a central role in this dynamic interplay between HR and NHEJ.

### **3.2.2 Other determinants of pathway choice**

Besides the cell cycle and DNA end resection genomic localisation of the DNA break (hetero- or euchromatin) and the complexity of the break have been suggested to guide a switch from NHEJ to HR [69, 72, 199].

### **3.2.3 Ku outcompetes HR dependent repair pathways and alt-NHEJ**

We have seen that Ku plays a central role in regulating end resection and several studies showed that Ku acts in a dominant negative manner inhibiting HR-related and alt-NHEJ repair pathways [200]. The Fanconia Anemia pathway repairs inter-strand cross-links via HR and cell lines deficient in FA genes are sensitive to DNA damaging agents, whereas simultaneous deletion of Ku70 reversed the sensitivity by reactivation of HR [70, 201]. Similarly yeast with impaired MRE11 activity, are shown sensitive to replication stress, due to inhibition of break-induced replication (BIR), and are rescued by Ku70 mutants to restore BIR activity [70, 202]. Besides HR dependent pathways, Ku also blocks alt-NHEJ [200]. Loss of Ku leads to an increase of alt-NHEJ [200]. In accordance, Ku and DNA-PK inhibit PARP1 DNA binding and enzymatic activity impairing alt-NHEJ, respectively [76, 203–205].

## **3.3 DNA damage response (DDR)**

The DNA damage response represents an orchestrated signalling cascade that senses DNA damage, promotes conditions for proper DNA repair and carries out

cell fate decisions to protect the overall health of the organism. In this section we will see that DNA damage sensing and signalling is carried out by large protein complexes, which activate the transducer kinases ATM and ATR that initiate a cascade of posttranslational phosphorylations at the chromatin level and beyond. Further we will see that this mechanism aims to initiate repair, transcriptionally activate cell cycle regulators, or to induce apoptosis and senescence eliminating potentially harmful cells.

Ku as a part of the DDR, having functions in DNA damage signalling, cell cycle, senescence and apoptosis will be evaluated. A graphical outline of the DDR, depicting the central steps and some of its central players is shown in Figure 3.7.

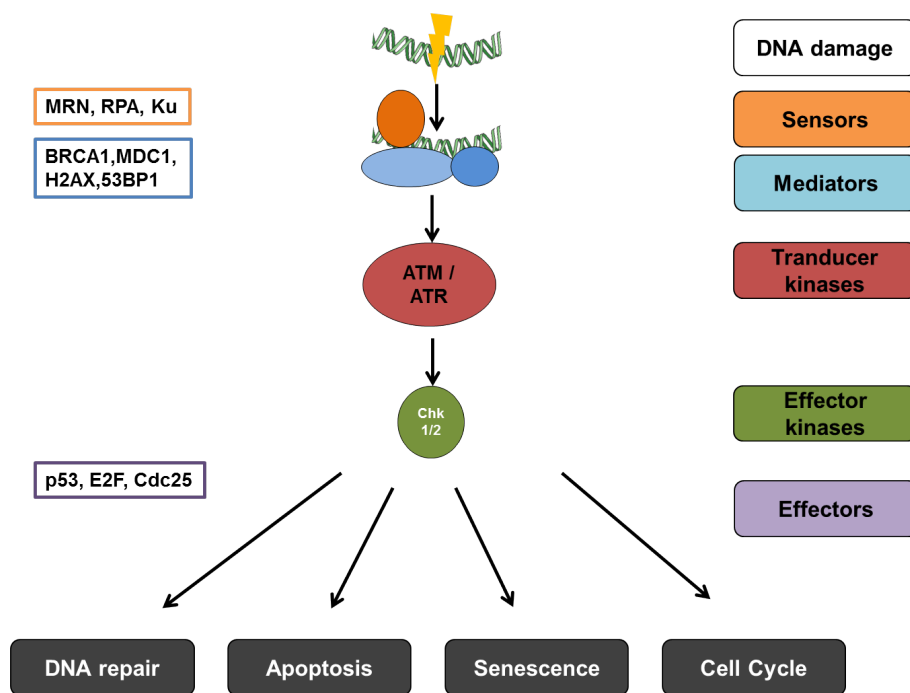


**Figure 3.7: DNA damage response** Scheme of the general outline of the DDR (adapted from [206, 207])

### 3.3.1 DNA damage signalling by ATM and ATR

The DDR is activated by aberrant DNA structures induced by DNA damage or DNA replication stress. Sensors on the damaged DNA activate the most upstream transduction DDR kinases: ATM and ATR. Both are members of the PI3-kinase

family, that also includes DNA-PKcs. ATM (Ataxia-telangiectasia mutated) and ATR (ATM- and Rad3- Related) phosphorylate hundreds of proteins at Ser/Thr-Glu motifs surrounding the DNA damage, as well as the downstream targets, important for cell cycle regulation, or p53, which acts as a transcription factor for several survival and death effector proteins [208, 209].

ATM and ATR thus can be seen as "master" regulators activating and orchestrating a large network of cellular processes to maintain genomic integrity [208].

**ATM** is recruited to the DNA damage by the MRN-complex subunit NBS1, hence its kinase activity is activated [208, 210–212]. The histone variant H2AX is one of the most prominent targets of ATM, and is phosphorylated on S139 at its C-terminal tail (forming  $\gamma$ -H2AX). Phosphorylation of H2AX takes place kilo- to megabases distal the initial DNA damage. It forms distinct foci visible by immunofluorescence microscopy and used as a marker for DSBs [213, 214].  $\gamma$ -H2AX then provides a prominent "docking station" for downstream repair factors like MDC1, 53BP1 or BRCA1, where they can be activated by ATM. Phosphorylated MDC1 in turn tethers ATM to the chromatin, where ATM triggers its own positive feedback loop, by phosphorylating MDC1 and MRN to recruit more ATM molecules, amplifying the DDR signalling cascade. Additionally, ATM undergoes several posttranslational phosphorylation and acetylation modifications itself, like autophosphorylation on S1981 [215–218]. Automodification of ATM has been shown detrimental for the retention of ATM on the break, extending the signalling cascade [210].

**ATR**, in contrast to ATM is activated by long stretches of ssDNA and is thus not restricted to DNA DSB, but also to other types of DNA damages, for example those arising during replication fork progression. Its recruitment to DNA is dependent on the association of its cofactor ATRIP (ATR interacting protein) to RPA coated ssDNA-stretches and the presence of TopBP1 on the junction of ssDNA to dsDNA, which stimulates ATR autophosphorylation and engages its full kinase activity [208].

After recruitment and activation of ATM and ATR on damaged chromatin a

plethora of downstream substrates is activated, coordinating cell fate. Amongst these substrates are the effector kinases Chk2 (Checkpoint kinase 2), phosphorylated by ATM, and Chk1 (Checkpoint kinase 1) phosphorylated by ATR, which are essential for the activation or inhibition of several cell-cycle checkpoint effectors. The stabilization of p53, is another downstream target of ATM/Chk2 and or ATR/Chk1, either by direct phosphorylation of p53 or indirectly by targeting its antagonist, hMDM2 for degradation [219–221]. p53, acts as a transcription factor and is considered, the guardian of the genome, as it activates cell cycle checkpoints and targets excessively damaged cells to apoptosis or senescence, thus preventing any malignant transformation.

Even though DNA-PKcs is part of the same kinase family as ATM and ATR, it has only minor influence in the DDR, playing a role primarily in c-NHEJ. However, it was shown to negatively control ATM function in the DDR [187]. Activation events for ATM and downstream effectors are depicted in Figure 3.8.

**Ku impacts on ATM/ATR activation** First studies on Ku dependent modulation of ATM and ATR activation undertaken by Tomimatsu et al. [222] demonstrate that fibroblasts derived from a murine Ku70<sup>-/-</sup> background, have an altered ATM and ATR activation and thus constant p53 activation. In accordance to this study, an ATM over activation is observed in mouse derived Ku80<sup>-/-</sup> cells, leading to a stronger cell cycle arrest [223]. Lastly, Fell et al. demonstrate that MEF cell lines expressing human Ku70 S155D have a constant ATM activation, measured by phosphorylation on S1981, even in non-damaged cells. In contrast non-phosphorylatable mutant S155A shows no ATM autoactivation even after IR. They furthermore show profound differences for these Ku70 mutants concerning apoptosis and cell cycle arrest [224, 225]. All these studies underline the central role of Ku70/Ku80 in ATM and to a lesser extent ATR activation and the subsequent alterations in cell fate decisions.

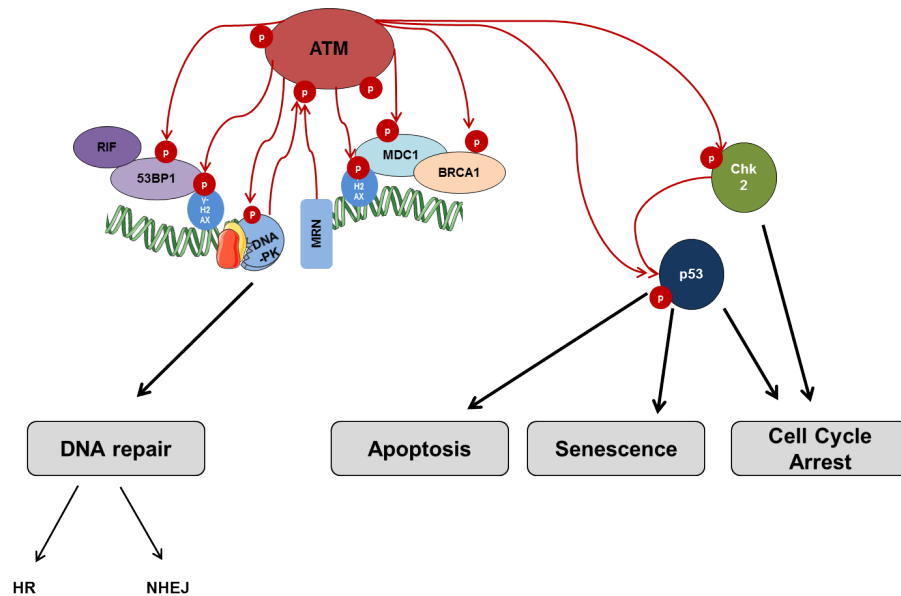


**Figure 3.8: ATM as a central player in the DDR** ATM activation on the DSB and the coordination of downstream effectors during the DNA damage response coordinate cell fate by activating DNA repair, cell cycle senescence or apoptosis

### 3.3.2 Cell cycle and its checkpoints

The cell cycle defines a series of cellular events with the aim of DNA replication and proper cell division to generate two daughter cells. Three periods are distinguished: interphase, mitosis and cytokinesis. Interphase can be further divided into gap 1 (G1)-phase, synthesis (S)-phase and gap 2 (G2)-phase. During G1 the cell activates its metabolism, increases transcription and protein production as well as its organelle content. During S-phase the whole DNA is doubled, so that each chromosome has replicated a sister chromatid. During G2-phase the cell size increases, proteins are produced and the cell prepares for mitosis and cytokinesis, when chromosomes and cytoplasm are divided. After cell cycle completion, two daughter cells emerge and resume a new round of cell cycle. Cells that have stopped dividing (i.e. neurons) are said to be in G0, senescent or quiescent. These cells can re-enter the cell cycle (G0 and quiescent cells) or remain silent until their death (senescence).

The passage through the different cell cycle phases is mediated by the oscillating activity of cyclins, small proteins that activate Cdks in a timely regulated pattern,

so that each cell cycle phase is driven by a particular Cdk/cyclin complex (see Figure 3.9). Cdk's are inhibited by phosphorylation through the kinases Wee1 and Myt1, and activated by the phosphatase-family Cdc25 proteins [226]. The transition between the cell cycle phases is highly controlled and, among others, depends on intact DNA integrity. DNA damage triggers, a transient, reversible block of the cell cycle, termed cell cycle checkpoint, that generates a time window for the repair machinery to fix the broken DNA. Three checkpoints are distinguished, based on the moment between which phases they occur: G1/S-, intra-S- and G2/M-checkpoint.

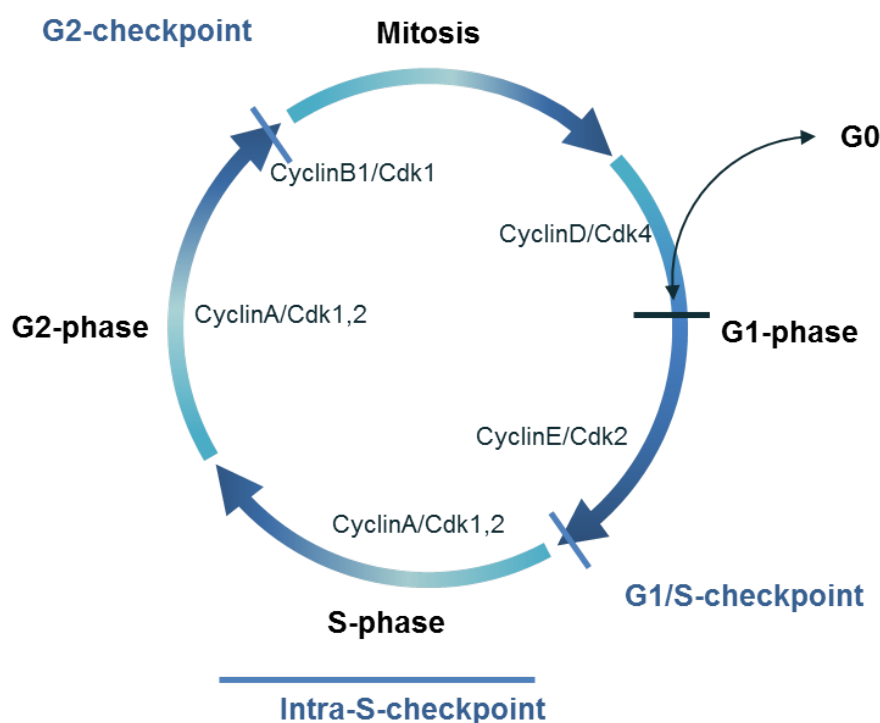


**Figure 3.9: Cell cycle** Oscillating activity of cyclins in complex with Cdks drive the cell cycle (adapted from [227])

Initiation of **G1 to S transition** is driven by the action of Cdk4/CyclinD and Cdk2/CyclinE, that act together to promote S-phase entry. Cdk4/CyclinD inhibits Retinoblastoma(pRb) by phosphorylation, to soften the transcription block on E2F, which in turn leads to transcription of CyclinE. After stripping of the inhibitory phosphorylation on Cdk2 by the phosphatase Cdc25A, the Cdk2/CyclinE

complex can activate the S-phase promoting kinase Cdc45, which ultimately licenses replication origin firing. Cdk2/CyclinE promotes its own positive feedback loop and thus amplifies the signal, by phosphorylation of Rb and increasing E2F-dependent transcription. Additionally the oncogene Myc acts as a transcription factor, further amplifying the system by transcriptional activation of CyclinD1 and D2, CyclinE, Cdc25A and E2F [228].

A delayed entry into S-phase is assured by the **G1/S-checkpoint** and prevents the cell to initiate any DNA synthesis when DNA is damaged. This checkpoint acts via two branches, which are both initiated via the transducer kinases ATM, Chk2 and to a lesser extent ATR and Chk1. The acute response, consists in the phosphorylation of Cdc25 by Chk2, allowing Cdc25 ubiquitination and degradation; thus Cdk2 can not be dephosphorylated and stays locked in an inactive state. The second branch consists in the transcriptional activation of the Cdk inhibitor p21, by p53, which is stabilized and protected from degradation after phosphorylation (S15,S20) by the transducer kinases [226, 228–230]. A schematic overview of this checkpoint is depicted in Figure 3.10 A.

During **S-phase** DNA synthesis for replication takes place and instead of halting the cell cycle at the transition stage from one phase to the next, the **intra-S-phase checkpoint** acts throughout the entire replication-phase. ATM dependent signalling is still engaged during this checkpoint, nevertheless a shift towards ATR signalling is observed with the generation of increasing amounts of ssDNA during DNA synthesis. Similar to the G1-phase checkpoint, inhibition of origin firing is reached by blocking Cdk2/CyclinA/E complex. This however, in contrast to the G1-checkpoint, is independent of p53, and p21. It is instead realized by Chk1/Chk2 dependent degradation of Cdc25A and Wee1 activation. Wee1 kinase is expressed during S-phase and inhibits Cdk2 through phosphorylation [228, 230] (see Figure 3.10 B).

The transition from **G2-phase to mitosis** is essentially due to the activity of the Cdk1/cyclinB complex, which is phosphorylated and inhibited by Wee1 and Myt1, and activated by dephosphorylation dependent on the Cdc25A/C phosphatase. The ATM-Chk2 and ATR-Chk1 axis block Cdc25A/B/C action in several ways



**(G2-checkpoint).** Direct phosphorylation of Cdc25C leads to its sequestration by 14-3-3 in a catalytically less active state, whereas Wee1 is similarly phosphorylated and recognized by 14-3-3, leading to its activation. Additionally the PLK1 (Polo like kinase 1) and PLK3 (Polo like kinase 3), are target of the transducer kinases, leading to the inhibition of PLK1 (an activator of Cdc25) and to the activation of PLK3 (an inhibitor of Cdc25). Similar to the G1/S-checkpoint, p53 activates the transcription of the Cdk inhibitor p21 and inhibits the transcription of Cdk2 and cyclin B, preventing the transition to mitosis [226, 228, 230] (see Figure 3.10 C).

To resume the cell cycle after DNA repair, checkpoint signalling must be turned off, a mechanism called **checkpoint recovery**, best understood for the G2/M-transition [226]. The activity of Plk1 is essential in this process, phosphorylating Chk2, Claspin and Wee, thus reversing their cell cycle blocking functions, as well as promoting nuclear translocation of Cdc25C [231]. Although, Plk1 is essential for cell cycle recovery it is not sufficient. Several phosphatases are important in checkpoint recovery (PP1, PP2A, PP4, PP5, PP6) by dephosphorylating important DDR-factors like ATM, ATR Chk2, Chk1, BRCA1 and  $\gamma$ -H2AX [207, 231]. Among these, Wip1 has a central role as it recognizes specifically p(S/T)Q-motifs, phosphorylated by ATM and ATR, and inhibits p53 expression and activity [231, 232].

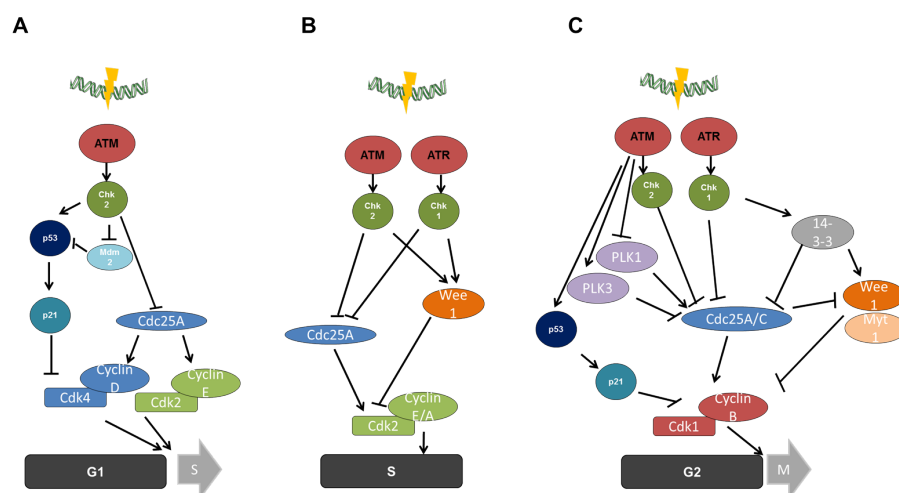


**Figure 3.10: Cell cycle checkpoints** (A) G1/S-checkpoint, (B) intra-S-checkpoint, (C) G2/M- checkpoint (according to [228, 230])

**Ku impacts on cell cycle regulation** Ku80 deficiency drives increased checkpoint activation in S and G2, compared to Ku80 proficiency after irradiation. This is mainly due to deregulated ATM and ATR signalling [223, 233]. Interestingly, Ku80 also impacts on the assembly of replication complexes, necessary to drive DNA synthesis during S-phase and Ku80 deficiency favours accumulation in G1-phase (activated by increased p21 levels, and decreased Cdc25A and Cdk2 levels), independent of DNA damage [234]. Moreover, direct interaction between Ku70 and cyclin A1, A2 and E are observed leading to cell cycle dependent phosphorylation events by Cdk2 that drive proper cell cycle flow [235, 236]. Finally, a specific residue in the vWA domain of Ku70 (S155) can induce cell cycle arrest in G1/S and G2/M phase, driven by the interaction with Aurora B [225]. All of these studies show that Ku can impact on the cell cycle independently of its DNA repair function.

In summary, stalling of the cell cycle is an important means for a damaged cell to provide a "time window" for repair and is a tightly regulated process. Several studies confirm the role of Ku within proper cell cycle progression, but also show that it can, itself, trigger cell cycle checkpoint activation. However, when DNA damage exceeds the cells capacity to repair and hinders the cell cycle to resume, the cells fate is guided through senescence or cell death.

### 3.3.3 Senescence

Cellular senescence is a condition in which cells, despite being alive, are unable to proliferate. This phenotype has first been described by Hayflick and colleagues after they had observed replicative exhaustion in human primary fibroblasts *in vitro* [237].

Senescence is considered as an irreversible stress response, associated with growth arrest of metabolically active cells that can not re-enter DNA replication. These cells thus remain in the G1 phase. Senescence therefore is different from quiescence

or terminal differentiation [238, 239].

Several morphological changes like, enlarged and flattened cells, with increased granularity, a vacuole rich cytoplasm, as well as a reorganisation of the sub-nuclear chromosomes and sometimes multinucleation come along with this cell state [240–242]. Besides these structural markers, several biochemical and molecular biomarkers have been associated to senescence:  $\beta$ -Galactosidase expression, cell cycle inhibitor expression (p21, p53, p15, p27, p16, ARF, hypophosphorylated RB), absence of proliferation, constitutive DNA damage foci in heterochromatic regions (senescence-associated heterochromatic foci enriched in histone 3met-H3K9; SAHF), and the secretion of inflammatory cytokines and chemokines (senescence associated secretion phenotype; SASP) [242].

Triggers of senescence are manifold, and include shortening of the telomeres (replicative senescence, as described by Hayflick), exhaustive amount of DNA lesions (DNA damage induced senescence), overexpression of oncogenes like RAS (oncogene induced senescence) or chronic generation of ROS (stress induced senescence) [239, 242].

Molecularly it is driven and maintained by two pathways, the p53 and the p16-RB pathway. Both interact and finally converge in the activation of cell cycle inhibitors and hypophosphorylation of RB (see Figure 3.11). Stimuli that activate the ATM/ATR (DDR) primarily induce senescence through the p53-p21 pathway, but can also engage the p16-RB pathway dependent on the cell type, species or origin of stress [239, 242]. In humans both, have to be inhibited to prevent the onset of senescence [243, 244].

The biological purpose of senescence is the elimination of damaged cells, which is particularly important in cancer. It is therefore traditionally considered as a tumour suppressor mechanism on a cellular level. Limiting the accumulation of damage, by growth arrest on one hand and the secretion of inflammatory signals (SASP), to attract immune cells for phagocytosis, on the other hand help the organism to prevent malignant transformation and tissue regeneration. Paradoxically senescence is also associated with increased carcinogenesis on an organismal

level, with the accumulation of senescent cells during aging. The constant secretion of inflammatory cytokines, extracellular-matrix degrading proteases and growth factors by senescent cells, disrupts normal tissue structure and stimulates growth and angiogenic activity in potentially premalignant cells in close proximity [241, 242].

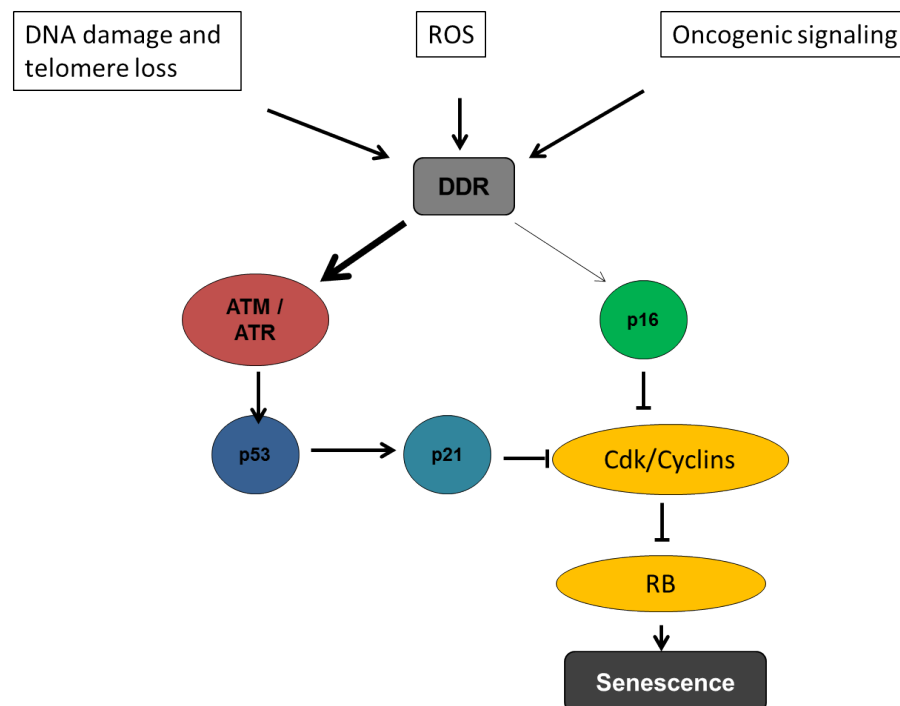


**Figure 3.11: Damage induced senescence** is activated through the DDR and the p53- and p16/RB pathways [241]

**Ku in senescence** Studies in mouse derived knock out cells for Ku70 and Ku80 have revealed a role for Ku in replicative exhaustion, as these cells demonstrate increased premature senescence [245, 246]. Moreover Ku80 deficient mice show signs of premature ageing and senescence, a phenotype that could be reversed by the simultaneous deletion of p53, with the price of an increased B-cell lymphoma incidence in those mice, underlining the close association between senescence and carcinogenic processes [247, 248]. Lastly, the expression of a human phosphomimetic mutant of S155 Ku70 increased the expression of p21 and the  $\beta$ -Galactosidase activity in MEFs and a human cell line, further emphasizing the direct role of

Ku in the onset of senescence [225]. Interestingly, all studies providing evidence for a role of Ku in senescence were performed without exogenous DNA damage, showing that the Ku associated senescence phenotype is independent of its role in DNA DSB repair.

In summary, senescence is a mechanism that is induced upon several cellular stresses, thereunder excessive DNA lesions. As a tumour suppressor mechanism its purpose is the elimination of damaged cells leading to tissue regeneration. Several lines of evidence provide proof for the role of Ku in the onset of senescence, this function however seems to be independent of its repair function.

### **3.3.4 Cell death pathways**

Besides senescence, programmed cell death pathways represent a means to get rid of potentially harmful cells during the DDR. Different cell death programs, such as apoptosis, necrosis, necroptosis, ferroptosis, mitotic catastrophe etc., are distinguished, dependent on their morphological and molecular differences in execution. Special attention should be given to apoptosis in this section, as it represents the principal cell death mechanism triggered upon DNA damage. We will see that Ku has a prominent role within this process independent of its DNA repair function. Additionally mitotic catastrophe is a significant cause of cell death in tumour cell lines after treatment with irradiation [249, 250] and shall be presented at the end of this section.

#### **3.3.4.1 Apoptosis**

Apoptosis was first described in the nematode *C.elegans* where programmed cell death at particular time points was observed during development. It is a mechanism that occurs under physiologic conditions and is a homeostatic mechanism

to maintain constant cell numbers in multicellular organisms. Inappropriate apoptosis is associated with neurodegenerative diseases, ischemic damage, autoimmune disease or different types of cancers [251]. Therefore it is of no surprise that upon an overwhelming amount of DNA damage apoptosis is considered the prevailing defence mechanism to protect the organism from malignant transformation [251, 252].

Morphological changes like chromatin condensation, nuclear fragmentation and collapse of the cytoskeleton, leading to cell blebbing, a phenomenon observable by microscopic examination, accompany apoptosis. During these processes the cell membrane stays intact, but undergoes inner-outer inversion exposing phosphatidylserine to trigger phagocytic clearance by the immune system [253], thus making apoptosis a "silent" death executor.

The molecular drivers of apoptosis are called caspases, as they show a cysteine in their active site and cleave proteins on specific Asp-residues. Functionally caspases can be divided into initiator caspases (caspase 2, 8, 9, 10) and effector caspases (caspase 3, 7). They are synthesized as non-active pro-caspases (zymogens) that are activated upon cleavage by active caspases, amplifying a proteolytic cascade [252, 253].

Two apoptotic pathways are generally distinguished (see Fig 3.12): intrinsic (induced by the depolarisation of the mitochondrial potential) and extrinsic apoptosis (induced by cell death receptors on the cell membrane). Both pathways are activated by DNA damage, they cross communicate and finally lead to the activation of effector caspases that induce cellular decomposition [254].

The **extrinsic pathway** is induced through activation of death receptors (DR) which are part of the tumour necrosis factor receptor (TNFR) super family. The best known death receptors are FASR, TNFR-1, TNF-R2, TRAIL-R1, TRAIL-R2, DR3 and DR6 [252]. All of them contain a cytoplasmic death domain (DD) that upon binding by their cognate/specific ligand initiate the apoptotic cascade. Upon DNA damage, p53 activates the expression of FASR (CD95, DR5) and its ligand FASL (CD95L). Extracellular binding of trimerized FASL clusters FASR

on the cell membrane and their intracellular death domains. Intracellularly this recruits the adaptor protein FADD (Fas-associated death domain), which binds cross-linked CD95-DD, forming the death inducing signalling complex (DISC). This platform serves inactive procaspases 8 or 10 to oligomerize and initiate self-cleavage [254–256]. Subsequently caspase 8 and 10, activate the effector caspases 3 and 7, which cleave and inactivate essential cellular proteins for cell cycle, DNA repair, cell structure or signalling [252].

After irradiation induced DNA damage, it is the **intrinsic apoptosis** that is mostly activated [252, 257]. It is driven by the loss of mitochondrial potential after pore formation and results in the release of apoptotic factors. The status quo of the mitochondrial membrane is dependent on the action of the BCL-2 (B cell lymphoma-2) family members that can have either proapoptotic (BAX, BAK, BOK, BID, BAM, BIM, BIK, BMF, NOXA, PUMA and HRK) or anti-apoptotic (BCL-2, BCL-X<sub>L</sub> and BCL-W) actions. Pro- and antiapoptotic BCL-2 members keep each other in check by mutual sequestration.

After exposure to stress the induction of pro-apoptotic factors, for example due to p53 dependent upregulation, results in pore formation of the mitochondrial outer membrane by BAX and BAK, as they can no longer be neutralized by BCL-2 [251, 252, 258]. Mitochondrial outer membrane permeabilization (MOMP) enables the release of cytochrome c, SMAC/DIABOLO, AIF, endonuclease G and CAD. Cytochrome c and SMAC/DIABOLO, on one hand, help activate caspase 9, which in turn cleaves procaspases 3 and 7; AIF, CAD and endonuclease G, on the other hand, induce nuclear fragmentation [251].

The intrinsic and extrinsic pathways cross-talk through the pro-apoptotic protein BID, which is cleaved to tBID (truncated BID) by caspase 8 and translocates to mitochondria inducing cytochrome c release [259]. Additionally caspase 6 activated downstream of mitochondria, may feed back on the extrinsic pathway by cleavage of procaspase 8 [260]. Caspase 2 is activated through extrinsic and intrinsic signals and is the only caspase that is found in the nucleus in response to DNA damage.

It interacts and gets activated by ATM, ATR and DNA-Pkcs. Beyond its role in apoptosis, caspase 2 is also shown to affect cell cycle checkpoint regulation, NHEJ and genomic stability [261–264].

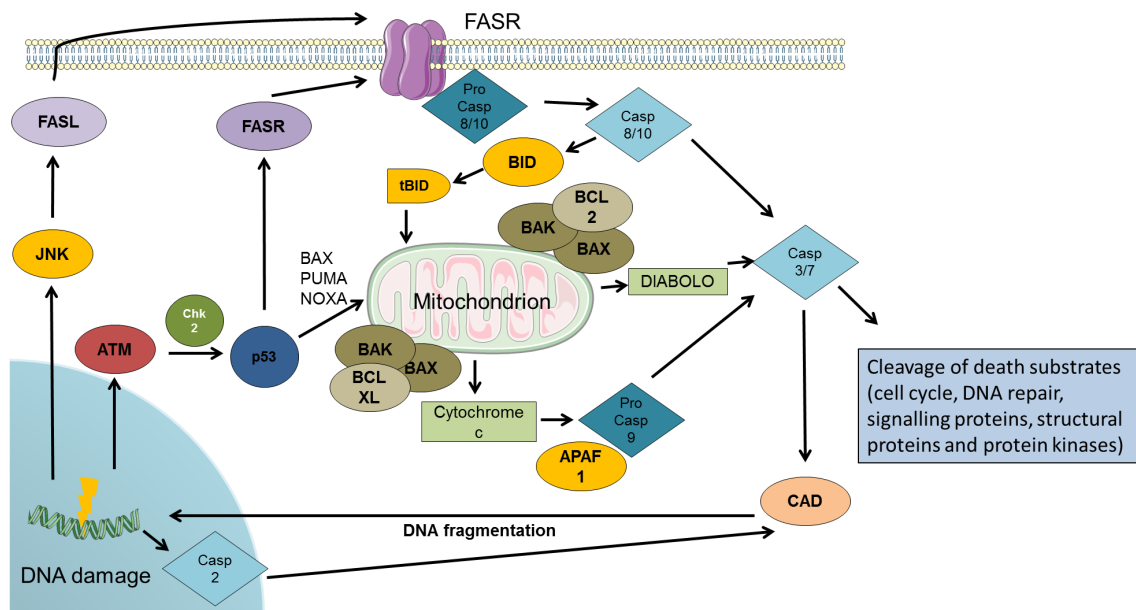


**Figure 3.12: Extrinsic and intrinsic apoptosis pathways and the caspases involved [254]**

**Ku's role in apoptosis** Several lines of evidence point to a significant role of Ku70 in the regulation of apoptosis. The far most studied mechanism concerns the interaction between Ku70 and the pro-apoptotic protein Bax. Ku70 sequesters Bax in the cytosol and prevents its translocation to mitochondria. This is regulated by multiple posttranslational modifications on both proteins. Bax is heavily ubiquitinated in non-stressed cells and becomes bound by Ku70, that possesses deubiquitination (DUB) activity [265, 266]. Upon apoptotic stress several mechanisms are suggested to control, deubiquitinated Bax release from Ku70. First, DNA-PKcs dependent phosphorylation at the aa 6 and 51 of Ku70 is suggested by Liu et al. [267]. Moreover acetylation of Ku70 by CBP and PCAF are shown to free Bax [267–269]. Additionally HDM2, an ubiquitin-ligase, is shown to ubiquitinate cytosolic levels of Ku70 for degradation, thereby releasing Bax [270]. Finally, Mazmunder et al. found that in hematopoietic tumours cells truncated Cyclin E (p18) is needed to release Bax from Ku70 sequestration [271].



Besides the inhibition of intrinsic apoptosis by Bax sequestration, Ku70 is shown to bind the Clu/XIP8 protein, enhancing apoptosis, however the exact mechanism remains elusive [272]. Lastly, a non-phosphorylatable substitution of Ku70 (S155A) represses ATF2-phosphorylation and DNA-damage foci formation, finally preventing apoptosis. The authors suggest that phosphorylation of S155 is a signal for non-completed DNA repair, which ultimately triggers apoptosis induction directly via Ku70 and ATM.

### 3.3.4.2 Mitotic catastrophe

Mitotic catastrophe represents a main event to drive cell death in cancer cell lines exposed to irradiation [250, 273]. It is characterized by a prolonged block of the G2/M-checkpoint, loss of clonogenicity and a delayed death [250, 273]. In contrast to apoptosis, mitotic catastrophe, is a mitosis linked death pathway [273] and is thus associated with the appearance of temporarily viable aneuploid, multi- and micronucleated giant cells [274]. However mitotic catastrophe does not represent a unique cell death pathway. Today it is generally accepted that mitotic catastrophe is a "pre-stage" of cell death, mainly executed by apoptosis [273–275].

As described in chapter 3.10, multiple cell cycle checkpoints guarantee a time window for repair, after DNA damage, and it is only during weakened checkpoint activity, that damage acquired in interphase can be expanded to mitosis. For example, checkpoint adaption describes the entry of mitosis in the presence of persistent DNA damage, when a sustained checkpoint-induced G2/M-arrest can no longer be maintained. Furthermore, these cells can either succumb to mitotic catastrophe in metaphase, or proceed to the next interphase by mitotic slippage, when similar to adaption, the mitotic checkpoints are weakened or an aberrant round of mitosis is conducted without proper segregation of sister chromatids and cytokinesis [273, 275]. Cells that exit mitosis are either tetraploid, due to failed cytokinesis or are highly aneuploid [274]. Most of these cells are non-viable and undergo mitotic catastrophe during the next cycle, however each round can drive the production of new potentially tumourigenic cells with high genetic instability.

Mitotic catastrophe is considered as an onco-suppressive mechanism, that culminates in the clearance of potentially harmful cells [274].

It is thought that inhibition of mitotic catastrophe increases the survival of aneuploid and genetically unstable cells, thereby contributing to carcinogenesis and the karyotypic heterogeneity of cancer cells [274].

### 3.3.5 Autophagy

To provide a full picture of the DNA damage response, autophagy and its role at the intersection of cell death and survival, as well as its genome protection function shall be presented.

The term autophagy translates from the Greek *auto* meaning "oneself" and *phagy* meaning "to eat" and describes the catabolic degradation and recycling of cellular components, to meet with the anabolic and bioenergetic needs of the cell [276, 277]. There exist three different types of autophagy, from which macroautophagy is the best studied. This type of autophagy sequesters cytoplasmic cargo into double membrane vesicles called autophagosomes, which ultimately fuse to lysosomes [277].

Autophagy is a ubiquitous mechanism that is highly conserved in eukaryotic cells with the aim to preserve homeostasis. It is induced upon a variety of stress conditions, such as nutrient deprivation, growth factor withdrawal, energetic stress, oxidative stress or DNA damage. Deregulation of autophagy is involved in a variety of diseases including cancer [278].

The autophagic machinery is a carefully orchestrated process where around 30 members of the Atg-gene family and a plethora of associated proteins take part [277]. The autophagic process can be divided into three steps. First, during **initiation**, an initial double membrane called the phagophore is built up by association of ULK1 with Atg13, FIP200 and Atg101. This step is mainly regulated by an inhibitory phosphorylation of ULK1 by mTORc1, which is the main inhibitor of autophagy. mTORc1 on the other hand is inhibited through phosphorylation by

the AMP-kinase, an activator of autophagy. Second, **nucleation** is driven by different phosphatidylinositol 3-kinases (Vps 34, Vps15/p150, Vps14, and Vps30/Atg6 (Beclin1)), that produce the lipid phosphatidylinositol-3-phosphate, the building unit of the autophagosome. Subsequent, vesicle **elongation** represents the third step and allows the engulfment of cytoplasmic cargo. It is driven by the covalent binding/ decoration of the autophagosome with Atg12, Atg5 and lipidated LC3 (called LC3-II). Following the completion of the autophagic vesicle, it matures through the fusion with lysosomes, leading to the formation of the degradative organelle, called autolysosome [276, 277].

DNA damage initiates autophagy by several molecular pathways that include the activation of AMPK through ATM and PARP1, transcriptional activation of PTEN, DAPK or DRAM by p53 and p63, and the activation of Beclin1 by JNK [276, 277]. When cellular homeostasis is balanced, Beclin-1 is sequestered by the anti-apoptotic protein Bcl-2 and it is only after JNK dependent phosphorylation of Bcl-2, that Beclin-1 is released [278].

The role of autophagy as an independent cell death pathway is highly controversial, and it is rather seen as a survival mechanism, to provide cellular save-energy building blocks during unfavourable environmental conditions [279]. This said, the constitutive activation of autophagy after an overwhelming amount of DNA damage, can however shift the balance to an uncontrolled autophagy, that may be a prerequisite for the activation of cell death pathways [254]. In this context the DNA bound FOXO3 protein triggers transcriptional activation of LC3 and BNIP, both important for autophagy, as well as the sustained activation of the ATM/ATR-Chk1/Chk2-p53-axis, that ultimately activates p53-dependent cell death by necroptosis and apoptosis [254].

Interestingly, besides its role in homeostasis, cell survival and cell death, autophagy protects genomic stability. In first place, this is due to the removal and neutralisation of impaired cellular components like mitochondria, micronuclei or cytoplasmic chromatin fragments, but also the regulation of DNA repair pathways. Autophagy impairs repair by HR by p62-dependent mechanisms that lead to blocked access of HR-proteins to the DNA damage site or the degradation of

RAD51 or filamin A. Additionally the inactivation of autophagy by Atg7 knock out leads to an increased proteasomal degradation of Chk1 and decreased HR activity, making cells hyper-reliant on NHEJ [277].

Despite being a cytoplasmic process placed at the edge of cell survival and cell death, autophagy now gets more and more into focus as a part of DNA repair regulation, and genomic stability as part of the DDR.

### **3.4 Coordination and cell fate decisions upon the DDR**

During this chapter we have seen that a damaged cell has several cell fate alternatives after damage induction, such as irradiation. Still we do not know which parameters are involved in this choice. The decision whether a cell attempts DNA repair, initiates apoptosis or stays in an arrested state are highly dependent on the cell type, cell cycle stage, the environmental conditions, as well as the amount of DNA damage. Apart from lymphocytes that immediately trigger apoptosis after irradiation, and fibroblast that preferentially undergo senescence, most cell types follow a determined hierarchy of decision points. Gudkov et al., proposes that these cells show a cell cycle arrest to allow an attempt of repair by the DNA repair machinery and given successful repair, the cell can restart proliferation. In case of incomplete or erroneous repair, due to repair factor deficiencies or a devastating amount of damage, cells trigger apoptosis or senescence [249]. Importantly, failures in the DDR can reactivate proliferation even in cells where DNA damage persists and thus drive genetic instability [1]. The consequence is on one hand a mutator phenotype, which further drives instability or on the other hand triggers a mitotic catastrophe and cell death [249]. We have also seen in this chapter that the Ku protein is a main regulator of DNA DSB repair and NHEJ, but that it also shows repair-independent activities during the DDR. The decision points described above are summarized in Figure 3.13, additionally Ku is delineated at those points where it has an attributed function.

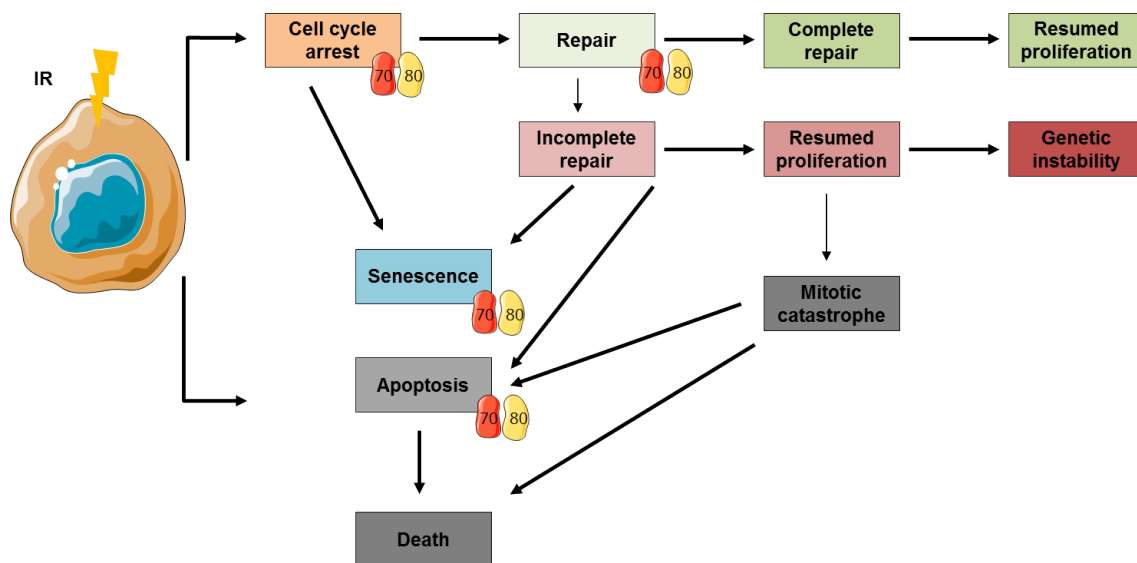


**Figure 3.13: Summary of DDR cell fate decisions after irradiation** The different alternatives of DNA damage response pathways are depicted. Upon DNA damage cells adapt a determined hierarchy of decision points. Successful repair can resume in normal proliferation. If repair was unsuccessful the cell can either succumb to senescence or apoptosis or resume proliferation. If the acquired damage is lethal, cells undergo mitotic catastrophe, however if it is not lethal cell can continue aberrant cycles of proliferation and increase genomic instability and carcinogenesis. Ku was shown to have multiple roles in the control of these decision points, first of all as a repair protein, but also as a factor regulating proper cell cycle, cell cycle arrest, senescence and apoptosis [249].

# Chapter 4

## V(D)J recombination

The adaptive immune-response uses lymphocyte antigen receptors in the form of immunoglobulin (Ig) and T-cell receptors on B- and T-cells, respectively to sense the presence of foreign antigens in an organism. Each lymphocyte possesses several copies of a single antigen receptor, which contains a unique antigen-binding site. The numerous lymphocytes present in an organism thus collectively enable a great variety towards (foreign) antigens. The high variability of the antigen repertoire is attained by varying the aa-sequence within the antigen-binding site, called V(ariable) region, of each receptor. To provide diversification of the V-regions, these are encoded in several gene segments, that can be randomly assembled in the developing lymphocyte by somatic DNA recombination, called gene rearrangement or recombination. A fully assembled V-region is constituted of two-to three gene segments, called V,D and J, and the number of possible rearrangements is  $10^{11}$  (see Figure 4.1A) . Beyond that, further variety is given by the action of endo- and exonuclease activity, as well as by a nucleotide transferase that adds nucleotides in a random manner between the segments [280]. We will see in this chapter, that the cNHEJ factors have crucial functions in V(D)J recombination and that deficiencies can have severe impact on the developing T- and B-lymphocytes.

## 4.1 V(D)J recombination relies on the cNHEJ machinery

In chapter 2.3 we have already mentioned that V(D)J recombination and the NHEJ show similar dependencies on the XRCC- genes. A lack of these genes results in DNA DSB repair deficiency accompanied by weakened V(D)J recombination. Two major discoveries constituted the understanding that these pathways are closely interwoven [281]: first, the observation that mice with a severe combined immunodeficiency (scid) and a defect in circulating B- and T-lymphocytes showed a general radiosensitivity [282, 283], as well as, second the demonstration that CHO XRCC DNA repair mutants showed a severe defect in coding and signal joint formation after RAG 1/2 expression *in vitro* [284].

V(D)J rearrangements do not occur randomly though rather reorganize in a highly controlled manner, accomplished by the existence of recombination signal sequences (RSS), flanking each of the V, D and J gene segments [285] (summarized in Figure 4.1 B)). The whole recombination process can be divided into two steps, the cleavage phase and the cNHEJ dependent joining phase [285]. During the **cleavage phase**, two RSS are brought into close proximity, by the RAG (recombination activating gene) 1/2 protein-complex, forming a multi-subunit synaptic complex, called paired complex. RAG1/2 nicks both RSS to induce DNA-SSB and catalyse the coupled cleavage of the RSS by direct transesterification. This ultimately generates a pair of coding ends that terminate with a covalently sealed hairpin structure and a pair of blunt 5' signal ends, representing an excised part of the genomic DNA. The four DNA ends first remain associated to the RAG1/2 protein in a post-cleavage complex (PCC). At the end of the cleavage phase the coding ends are thought to dissociate first from the RAG protein, leaving the signal ends in a RAG associated signal end complex (SEC). This initiates the **joining phase**, which consists of the DNA DSB recognition, processing and ligation of the rearranged gene fragments. The Ku heterodimer is the first sensor, that recognizes the RAG cleaved DNA structures, thereby displacing the RAG proteins on the signal joint. Ku, also recruits DNA-PKcs and the endonuclease

Artemis that catalyses the opening of the hairpin coding joint. This usually results in a 3' overhang, and Artemis further increases junctional diversity with its exo- and endonuclease activity. Coding end processing is further assured by the TdT (terminal-deoxinucleotidyl-transferase), recruited by Ku80 [286, 287], that catalyses the addition of nucleotides randomly. Finally, the XRCC4/Lig4 complex ligates the coding joint, that codes for the antigen receptor and the excised signal joint, which will be lost in later cell divisions [281, 285].

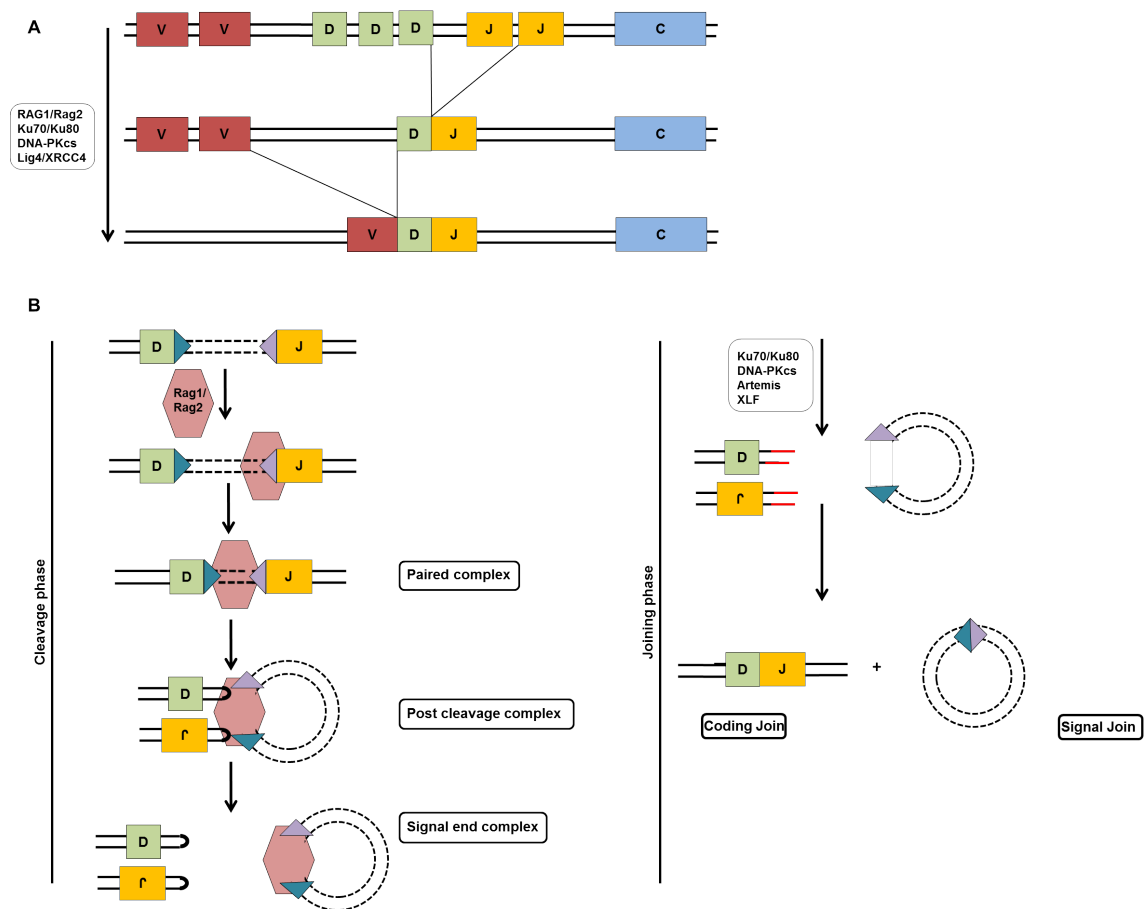


**Figure 4.1: V(D)J- recombination mechanism** (A) General overview of the combination sequence of the different gene segments V, D and J in gene receptor assembly. (B) Detailed overview of the formation of the recognition of the gene segments by RSS sequences by RAG1/2 and the formation of coding and signal joints [281, 285]



## 4.2 Deficiencies in core NHEJ factors impair V(D)J recombination and lead to radiosensitive SCID

In light of the strong dependency of V(D)J recombination on the NHEJ machinery, it comes with no surprise that patients deficient for core NHEJ factors, show DNA DSB sensitivity and parallel immunodeficiency, a disease pattern termed radiosensitive (RS)-SCID. Note that patients with RAG mutations show a radioresistant (RR)-SCID phenotype, underlining its exclusive role to immune-receptor rearrangement [281].

To date mutations in four genes of the cNHEJ have been identified in humans, Lig4, XLF, DNA-PKcs and Artemis. The clinical phenotype of these mutations varies in the severity of immunodeficiency, reaching from Omenn's syndrome to combined immunodeficiency (CID), pancytopenia or progressive immunodeficiency to RS-SCID, being the most severe form, with a complete loss of B- and T-cells [281, 288]. Additional characteristics like microcephaly, dismorphic facial features and growth/developmental delay, are summarized as the Ligase 4 syndrome, primarily observed in Lig4 and XLF mutated backgrounds. Some patients, with Lig4 mutations, but especially those showing Artemis mutations have a predisposition to develop lymphoma [281, 288, 289]. No known mutation or deficiency in the Ku70 or Ku80 has been identified in humans, nevertheless much knowledge on their effects in V(D)J recombination were gained by *in vivo* studies in mice and *in vitro* in CHO cells.

Deficiencies in the core NHEJ factors, Ku80, Ku70, DNA-PKcs, XRCC4 and Lig 4 all show severely impaired lymphogenesis and an arrest in premature cell stages for T- (CD4<sup>-</sup> / CD8<sup>-</sup> / CD25<sup>+</sup>) and B-cells (B220<sup>+</sup> / CD43<sup>+</sup>) assessed in mouse KO models [246, 282, 290–294]. Analysis of the coding and signal joints further reveal large deletions in XRCC4 CHO mutant cells of up to 20bp for coding joints and only 10% of correct signal joints [284]. Incorrect rearrangements were further observed in mice embryonic stem (ES) cells of XRCC4 deficient [290] and MEF's of Lig4 deficient embryos [291]. Similarly a reduction in coding and signal joint formation [41, 43, 246, 284] with an accumulation of hairpin ending coding joints

and blunt-full length signal joints [292] is observed in Ku80 deficient CHO cells and mice. Ku70 deficiency shows comparable characteristics with a reduction of coding joint formation of up to 100-fold compared to Ku70 wt cells and 2-3-fold compared to DNA-PKcs mutated scid mice [293, 294]. Interestingly, DNA-PKcs deficient mice and CHO mutant cells demonstrate aberrant coding joint formation, but unlike XRCC4, Lig4, Ku80 and Ku70, have only few impairment in signal joint formation [282, 295–298]. This phenotype is shared with immuno-deficiencies due to mutations in the Artemis gene [102, 299] and is explained by the structure of blunt signal ends that can be directly ligated, without prior processing by DNA-PKcs mediated Artemis activity [300, 301]. Even though, XLF mutations in humans are associated with profound immunodeficiencies and phenotypes similar to the Ligase 4 syndrome, the targeted mutation of this gene in mice has only a partial effect on lymphocyte numbers and V(D)J recombination [302, 303]. It is thus suggested that XLF function is not necessary for any activation of catalytic processes, but that it might rather stabilize the PCC complex, a function shared with ATM and the RAG complex [302, 303]. A hypothesis, that was confirmed by a strong lymphopenia and defective coding joint formation in double deficient KO mice for XLF/ATM [304] and mice expressing a C-terminal lacking RAG2 ( $RAG2^{c/c}$ ) in a XLF deficient background [305]. The role for the newest member of the cNHEJ family, PAXX, is redundant to XLF, so that single deficiency of PAXX shows no effects in signal and coding joint formation [83, 306] and normal lymphocyte development [82]. However double deficiency of XLF and PAXX triggers a complete block of coding joint formation, similar to the defects seen in XRCC4 or Ku80 and have highly imprecise single joints [82, 306, 307]. Unlike  $XLF^{-/-}$  cells,  $PAXX^{-/-}$  cells are not dependent on ATM and DNA-PKcs kinase or RAG activities [82, 307], suggesting that PAXX has no role in PCC stabilization. However the association of Ku with PAXX is essential for V(D)J recombination in an  $XLF^{-/-}$  background [82, 307]. Liu et al. [82] speculate that PAXX modulates the stability of the DNA-PKcs/Ku-DNA complex, promoting end-synapsis and ligation in an XLF deficient background. This is further supported by the observation that PAXX, stimulates the XRCC4/Lig4 catalytic activity in a Ku-dependent way, when XLF function is

omitted [83]. XLF and PAXX have redundant functions in V(D)J recombination, however these functions are accomplished through different mechanisms.

Finally the study of V(D)J recombination is a elegant model to study the orchestration of cNHEJ factors in the repair of DNA double strand breaks. The knowledge gained by studying this process can certainly, to some extent, be extrapolated to the classical NHEJ reaction during unanticipated DSB induction. Moreover deficiencies and mutations in the core NHEJ factors have clinical importance and have severe consequences for the individual. These patients are predisposed to carcinogenesis, have immunodeficiencies and a high sensitivity to genotoxic agents, which undercuts whatsoever treatment with chemotherapeutics or irradiation. The lifetime expectancy for these patients are generally low, and does often not exceed adolescence.

# Chapter 5

## Other cellular roles of Ku

Given the biochemical characteristic of Ku, to bind DNA in a sequence non specific manner with high affinity, it is certainly of no surprise that the DNA-related functions of Ku go beyond DNA DSB repair. Its function thus reaches from replication, to transcription, over mobile genetic element transposition and telomere maintenance. More unexpected are its roles in the DDR where Ku participates in cell cycle regulation, apoptosis and senescence (discussed in Chapter 3.3.3, 3.3.4.1 and 3.3.2). Additionally several enzymatic activities are attributed to Ku, such as a lyase, deubiquitination and helicase activities. Figure 5.1 summarizes all (so far) known functions for Ku, and we will focus a bit more detailed how Ku acts in these cellular processes.

### 5.1 Enzymatic functions of Ku

Ku possesses a lyase activity associated with NHEJ. Thereby Ku is involved in the excision of abasic sites at the DNA double strand 5' end, to provide proper ends for ligation [109, 110]. The second known enzymatic activity of Ku (Ku70) is its deubiquitination activity on sequestered Bax. Thus, upon apoptotic stimuli Ku70 releases de-ubiquitinated Bax, which can translocate to mitochondria and drive

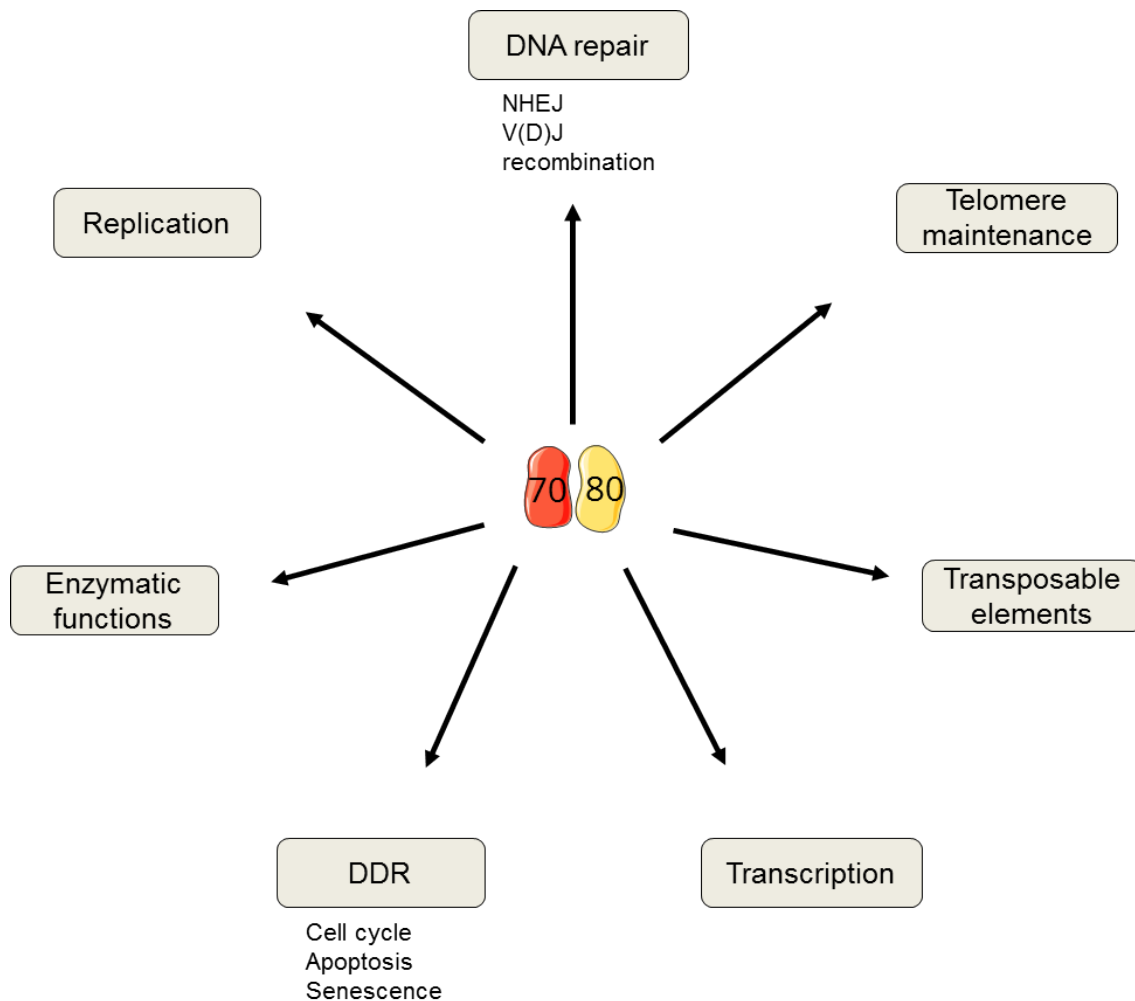


Figure 5.1: The many roles of the Ku protein adapted from [9]

apoptosis [265, 266]. Moreover Ku performs DNA helicase activity to unwind DNA duplexes in 3' to 5' direction, important for its role in DNA replication [308–310].

## 5.2 Ku in transcription

Several lines of evidence point to a role of Ku in transcription, due to protein-protein interactions. For example the C-terminus of Ku80 binds to RNA polymerase II elongation sites, through transcription elongation proteins, and thus regulates global transcription levels in a human cell line [311]. Further the role in transcription regulation is independent of Ku80's function in DNA repair, as a Ku80 mutant lacking C-terminal residues 687-728 and transcription activity had

no effect on DNA end joining *in vitro* [312]. Moreover, associated with DNA-PKcs, Ku80 represses transcriptional activity of RNA Polymerase I, which is further increased when DNA ends are present [313] and might represent a mechanism to repress transcription during DNA repair [9].

### 5.3 Ku in the mobility of genetic elements

Mobile genetic elements are transposons, retrotransposons and retroviruses. All of them exist as linear dsDNA. For instance, retroviruses integrate their genome into a host, after reverse-transcribing their RNA into cDNA with the help of an integrase. By a mechanism similar to V(D)J, a nucleophilic attack of the 3'OH group towards the host genome induces a SSB, to create an insertion site for the cDNA [9]. Ku can potentiate retrotransposon Ty1 integration into the genome of *Saccharomyces cerevisiae* [314], and DNA-PKcs and Ku80 are important factors for retrotransposition of retroviruses in human cells [315, 316].

### 5.4 Ku in DNA replication

DNA replication doubles the genome, generating two identical daughter strains important for cell proliferation. It is initiated at specific locations, called the origins of replication, where the pre-replication complex is formed.

The heterodimer Ku binds to the origins of replication in a cell cycle dependent manner [317], peaking in late G1/S-phase and dissociates after origin firing [318]. It interacts with several origin recognition complex proteins, such as ORC2, ORC3, ORC4 and ORC6 and permits proper loading of the subunits to form the ORC-complex, a prerequisite for the assembly of the pre-replication complex [319]. The association of Ku to the origins of replication is regulated by the periodic phosphorylation of Ku70 by cyclin-Cdk complexes during S,G2 and M-phase. Phosphorylation of Ku70 on Thr residues 401, 428, 455 and perhaps 58 inhibits the association of the heterodimer to origins during these cell cycle phases. With the

decreasing levels of cyclin B at the end of mitosis the inhibitory phosphorylation on Ku70 is released and the heterodimer can de novo participate in the formation of the pre-replication complex [236].

## 5.5 Ku on telomeres

Telomeres are specific DNA-protein complexes localized at the end of chromosomes. Telomeres consist of TTAGGG repeats that range around 10 kb in human cells, to 100 kb in mice. Their end consists of a 3' TTAGGG overhang, that is several hundreds of base pairs long and that can fold back to invade the preceding double stranded region, generating a telomere-loop (t-loop). This structure is recognized and stabilized by the shelterin complex in humans, which consists of 6 protein subunits, notably TRF1 (telomere-repeat binding factor 1), TRF2 (telomere-repeat binding factor 2), TIN2 (TRF1-interacting nuclear factor 2), TPP1, POT1 (protection of telomere 1) and RAP1 (repressor-activator protein 1) [320]. Telomeres are important structures to stabilize chromosome ends that would otherwise be recognized as DNA strand breaks, consequently deficiencies have detrimental consequences. Especially deficiency of TRF2 destabilizes the t-loop and culminates in Ku dependent c-NHEJ mediated chromosomal end-to-end fusions and genetic instability [320, 321]. Paradoxically, Ku70/80 are found to be telomere associated factors [322] and Ku inhibition triggers rapid telomere attrition by intrachromosomal recombination with the formation of t-circles and genomic instability [323–326]. Thus, on one hand, Ku protects telomeres from rapid telomere shortening, but on the other hand can trigger fusion of uncapped telomere ends through c-NHEJ.

Ku on telomeres, similar as on DNA DSB, has a dominant-negative effect on other repair pathways, thus restricting recombination and alt-NHEJ [320, 321, 327]. Moreover a recent paper gives insight onto how Ku's DNA repair function can be suppressed at functional telomeres. Ku70 helix 5 ( $\alpha$  5) interacts with TRF2, which thus inhibits heterotetramerization of two Ku heterodimers on DNA ends. The authors propose an elegant model, where TRF2 forms a physical barrier for

DNA end tethering, thus inhibiting c-NHEJ on functional telomeres [328].

The role of Ku on telomeres represents a double edged sword, as Ku mediated c-NHEJ is the main event for end-to-end fusions promoting genomic instability. However loss of Ku favours telomere shortening and uncapping of telomeres. It thus appears that, in the first place, Ku is an important player in telomere maintenance and protection and that telomere specific factors, mask its c-NHEJ function.





# Chapter 6

## Ku associated with disease

### 6.1 Ku associated with autoimmune disease

In the beginning of this manuscript we have mentioned that Ku has been identified as the target of autoantibodies in connective tissue diseases (CTD), such as systemic lupus erythematosus, systemic sclerosis, polymyositis and Sjogren's syndrome [5, 6, 329, 330]. Additionally Ku is found to be a thyroid autoantigen in Graves disease, an autoimmune disorder that causes hyperthyroidism [331].

It might seem not evident that a nuclear protein could become an antigen for autoantibody development, as it is "hidden" in the nucleus. In fact, different research groups presented data of Ku being associated to the extracellular membrane [332–334].

Finally, the expression of Ku antibodies, in combination with other markers can be used in CTD diagnostics [335, 336].

### 6.2 Ku associated with cancer

Genome instability and mutation is commonly known as a hallmark of cancer, giving cancer cells a selective advantage to outgrow and dominate the local tissue environment [3]. As stated earlier, cellular repair pathways maintain genomic

stability. Therefore deficiencies, especially in DSB repair pathways, predestine genomic translocations or gene amplifications, jeopardizing the cellular homeostasis [70, 337].

Studies in mice clearly show Ku70 and Ku80 to prevent the appearance of chromosomal aberrations, chromosome fusions and aneuploidy [136, 338–340] and thus place them as central caretakers in genome maintenance.

Despite the observed instability, deletion of Ku only leads to a slight increase in cancer incidence, mainly due to B- and T-cell lymphomas in mice [137, 246, 338]. Interestingly however, loss of Ku and another caretaker protein dramatically increases tumours development in mice. For instance, the combined deficiency of Ku80 and the tumour suppressor p53 accelerates the lymphoma onset and rate, underlining their cooperation in the limitation of oncogenic transformation in murine B-cells [136, 247]. Similar to p53/Ku80 loss, haploinsufficiency of Ku80 in a murine PARP1<sup>-/-</sup> background favours hepatocellular cancer formation due to accumulating aneuploidy and chromosomal aberrations [341].

In contrast to mice spontaneous mutation or a complete loss of either of the Ku subunits has not been reported for humans up to date, arguing that it constitutes a lethal condition in humans. However, several studies associate Ku expression to the progression level of different tumour samples (see Table 6.1).

Several therapeutic approaches targeting Ku have been proposed. For example, Ku that translocates to the cell surface in human multiple myeloma cell samples, can be blocked with antibodies, sensitizing these cells towards apoptosis after irradiation and doxorubicin treatment [342]. Additionally, targeting Ku70 with siRNA enhances irradiation and Topoisomerase II inhibitor treatment in cancer cell lines [343]. And finally, histone-deacetylase inhibitors regulate Ku70-Bax interaction and mediate cell death in a neuroblastoma cell line [268].

**Table 6.1:** Ku expression in cancer tissue samples

Phenotype	Cancer type	Ref.
Bcl-XL and Ku80 expression correlate in leukaemia cell samples	B-CLL	[344]
Different DNA-end binding activity of Ku in normal vs. neoplastic tissues, dependent on tumours progression	breast and bladder cancer	[345]
Increased Ku70/Ku80 nuclear protein levels and DNA binding activity compared to normal colonic tissues	colorectal cancer	[346]
Ku70/Ku80 protein expression correlate with tumours proliferation; DNA binding activity is increased in basal cell carcinoma compared to non-cancer tissue	non-melanoma skin cancers	[347]
Ku expression pattern correlates with radiosensitivity and disease free survival	rectal carcinoma	[348]
Downregulated Ku70 and ATM mRNA expression correlate with bad prognosis	colorectal cancer	[349]



## Chapter 7

# Chronic lymphocytic leukemia (CLL) patients overexpress phospho-S27-S33 Ku70 - Data from the lab

### 7.1 Chronic lymphocytic leukaemia (CLL)- an overview

Leukaemia is a type of blood cancer that affects the white blood cells, which accumulate as incompletely matured leukocytes in the bone marrow, lymph nodes and blood stream. Having not passed through the entire maturing process, these white blood cells have restrained ability to defend the organism against pathogens and patients are thus immunodeficient. The accumulation of leukaemia cells furthermore restrains the development of red blood cells and platelets, thus provoking anemia (loss of red blood cells) and thrombocytopenia (loss of platelets). Different types of leukaemia are distinguished based on the involved cell type (lymphoids vs. myeloids) and their aetiopathology (chronic vs. acute). Four major forms

of leukaemia are distinguished: acute myeloid leukaemia (AML), acute lymphocytic leukaemia (ALL), chronic myeloid leukemia (CML) and chronic lymphocytic leukaemia (CLL).

### 7.1.1 Epidemiology

Chronic lymphocytic leukemia is the most common form of leukaemia occurring in the western world [350] (22-30% of leukaemia being diagnosed as CLL [351]) and the incidence-rate is between 1-5.5 per 100.000 people worldwide [351]. CLL is a disease that affects mostly the elderly with a median age at diagnosis of approximately 64-70 years [351]. A gender and race specific shift is observed, with males being more often affected than women, and whites more often affected than blacks or Asians [351–353]. Based on statistics of the National Cancer Intelligence Network 5-year survival rates are approximately 70% for males and 75% for females [354].

### 7.1.2 Diagnosis and prognostic factors

The diagnosis of CLL includes the evaluation of a B-cell blood count ( $> 5 \times 10^9$  B-cells/L called lymphocytosis), blood smear (small, mature-appearing lymphocytes with a narrow border of cytoplasm and dense nucleus without discernible nucleoli) and the assessment of the immunophenotype ( $CD5^{high}$ ,  $CD19^{high}$ ,  $CD23^{high}$ ,  $CD20^{low}$ ,  $CD79b^{low}$ ) of the circulating B-cells [353, 355].

The clinical disease course can be highly variable in CLL patients, ranging from an almost indolent form with patients being free of symptoms and fully active for decades, to patients that rapidly develop high-risk disease with the requirement for treatment shortly after diagnosis and a rapid therapy- or disease related mortality [353]. Several prognostic markers have been associated with the disease course and help to identify those patients that need therapy relatively shortly after diagnosis

[353, 355]. These include genetic, molecular and biochemical characteristics of the CLL cell, such as: molecular cytogenetics, mutation status of the Ig heavy chain locus (IgV<sub>h</sub>), several serum markers and bone marrow infiltration [355].

- **Molecular cytogenetics:** Approximately 80% of CLL patients carry at least one of the following chromosomal aberrations: [del(13q)] in 55% of CLL; [del(17p)] in 7%; [del(11q)] in 18% and trisomy 12 in 16% [353]. [del(11q)] or [del(17p)] are frequently associated with the loss of one allele of the tumour suppressor genes ATM or TP53 (encoding p53), respectively and poor medical response to chemotherapeutics [356, 357]. These patients have an inferior prognosis and overall survival compared to [del(13q)] or B-CLL without chromosomal abnormalities [355].
- **Mutation status of the Ig heavy chain locus (IgV<sub>h</sub>):** CLL patients with unmutated IgV<sub>h</sub> have an inferior prognosis than mutated IgV<sub>h</sub>. However usage of the V<sub>h</sub>- gene 3.21 is an unfavourable prognostic marker independent of the IgV<sub>h</sub> mutation status. The expression of the surface markers ZAP70 and CD38 is correlated with an unmutated IgV<sub>h</sub> and thus is associated with unfavourable prognosis[355].
- **Serum markers:** CD23 and thymidine kinase may predict survival or progression-free survival [355].  $\beta_2$ -microglobulin expression (> 3.5 mg/L blood) is associated with poor prognosis [353].
- **Bone marrow infiltration:** The tumour burden is associated with the type of bone marrow infiltration (diffuse vs. non-diffuse). A diffuse pattern is often associated with advanced disease [353]. Moreover bone marrow aspirates can help evaluate cytopenias of red blood cells or thrombocytes [355].

### 7.1.3 Staging

Two clinical staging systems are used to distinguish low and high risk disease patients into 3 prognostic groups. The Rai staging system is used in the US,



**Table 7.1:** Rai and Binet staging system

System	Risk group	Clinical features	Median life expectancy
Rai	Low risk (Rai stage 0/I)	Lymphocytosis without cytopenia and without lymphadenopathy and/or splenomegaly	13 years
	Intermediate risk (Rai stage II)	Lymphocytosis without cytopenia, but with lymphadenopathy and/or splenomegaly and/or hepatomegaly	8 years
	High risk (Rai stage III/IV)	Lymphocytosis and cytopenia (Hb level of $\leq 11$ g/dL and/ or a platelet count of $\leq 10 \times 10^5$ cells/ $\mu\text{L}$ )	2 years
Binet	Low risk (Binet stage A)	Less than three palpably enlarged sites <sup>1</sup> without cytopenia	13 years
	Intermediate risk (Binet stage B)	Three or more palpably enlarged sites without cytopenia	8 years
	High risk (Binet stage C)	Cytopenia (Hb level of $\leq 10$ g/dL and/ or a platelet count of $\leq 10 \times 10^5$ cells/ $\mu\text{L}$ )	2 years

\* Five zones are examined on the presence of palpable, enlarged lymph nodes of  $> 1$  cm (cervical (head and neck), axillary, inguinal nodes (including superficial femorals), spleen, liver )

whereas the Binet classification is often used in Europe. Both tests rely on a physical examination of the patient and a standard laboratory blood test. High risk patients are identified through the assessment of advanced cytopenias in both staging systems. The different clinical features that identify CLL risk groups, as well as their life expectancy according to the Rai and Binet staging system are depicted in Table 7.1 [353].

### 7.1.4 Treatment

The initiation of treatment is highly dependent on the disease status. Generally asymptomatic patients which have been assessed in the low or intermediate risk category based on the Rai and Binet staging are generally not drug treated. As soon as evidence for disease progression is given by a lymphocyte doubling time

less than one year or progressive palpable lymphadenopathy and/ or splenomegaly, treatment should be considered.

Treatment options include chemotherapy, a combination of immuno- and chemotherapy and small molecules that target B-cell receptor or BCL-2 signalling pathways, which promote growth and survival of malignant B-CLL cells [353].

**Chemotherapy** The traditional treatment relies on the use of chemotherapeutics that target the DNA, such as the purine analogs (fludarabine, pentostatin or cladribine), as well as DNA alkylators including chlorambucil, cyclophosphamide or bendamustine. Common side effects of these therapies are immunodepression and an increased risk of infections.

**Chemoimmunotherapy** Several clinical trials highlight the benefit of a combination therapy using chemotherapeutics in combination with the anti-CD20 monoclonal antibodies rituximab, obinutuzumab or ofatumumab. These trials show higher response rates and progression free survival (PFS) with a combinational therapy than a stand-alone chemotherapy. Subsequently the US FDA (united states federal drug administration) has approved the chemotherapeutic combination therapy with those three antibodies as a first-line treatment for CLL patients. Ofatumumab is additionally approved as a single agent for relapsed or refractory disease. Other clinical trials evaluating the combination of bendamustine and rituximab or obinutuzumab are currently under way.

## **Small molecules**

**Inhibitors of BCR signalling** The BCR signalling pathway is a prominent target site, as it is considered to play a crucial role in CLL pathogenesis [353]. Three different classes of inhibitors are distinguished: BTK- (Burton's Tyrosine kinase), PI3K- (Phosphatidylinositol-3-kinase) and SYK- (spleen tyrosine kinase) inhibitors.

The inhibitors ibrutinib (BTK inhibitor) and idelalisib (PI3K inhibitor) are approved by the FDA as front line treatment (ibrutinib) and in relapsed disease (idelalisib) in combination with ofatumumab or rituximab, respectively. Moreover ibrutinib shows significant improvements of PFS and overall survival in patients with > 65 years of age and del[17p] compared to a treatment with chlorambucil. For the moment SYK-inhibitors show considerable toxicities in phase I and II studies. Side effects for ibrutinib include fatigue, diarrhoea, bleeding ecchymoses, rash, arthralgia, myalgia, increased blood pressure and atrial fibrillation. Adverse effects for idelalisib include transaminitis, pneumonitis and colitis.

**BCL-2 inhibitor** The BH3-mimetic venetoclax inhibits the antiapoptotic BCL-2 protein and thus triggers apoptosis in CLL cells. Its efficiency is proved in patients with relapsed or refractory disease and del[17p] and authorized by the FDA. Ongoing studies now examine the combined therapy with or without anti-CD20 antibodies and with or without ibrutinib to enhance clinical outcomes. Adverse effects of venetoclax are gastrointestinal disturbances, neutropenia, and the tumour lysis syndrome.

## **7.2 Other prognostic markers like apoptosis resistance to irradiation, NHEJ activity and telomere maintenance come into focus and define a novel subpopulations in CLL - data from the lab**

Research by Jozo Delic concerning the impact of the ubiquitin-proteasome system on apoptosis after irradiation in healthy lymphocytes [358] and later lymphocytes derived from CLL patients [359, 360] led to the discovery of two specific subsets of CLL B-cells. These subpopulations are either radioresistant to cell death

(around 20% of cell death) at 24h and after up to 10 Gy post- $\gamma$ -irradiation or are radiosensitive (up to 80-90% of cell death) *in vitro* [359, 360] (Figure 7.1).

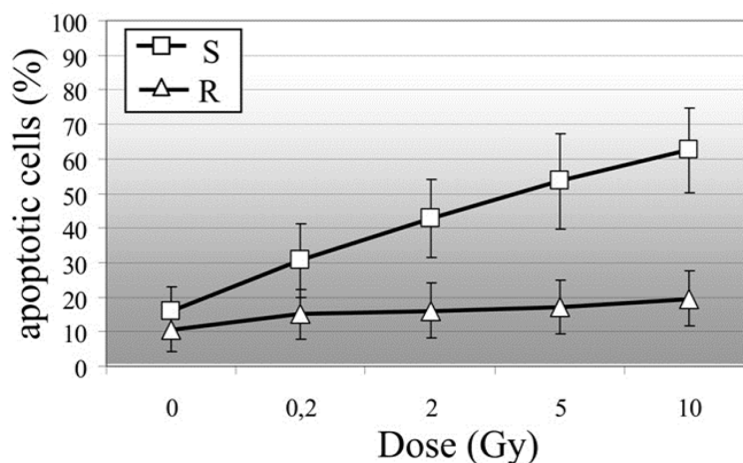


**Figure 7.1:** LLC samples can be classified based on their response to  $\gamma$ -IR in resistant (R) and sensitive (S). The graph represents data from n=79 samples and n=13 for S- and R-CLL, respectively. (Graph taken from [361])

Until today, 308 CLL patient samples over a period of 25 years have been evaluated, and show around 18% to be radioresistant (R-CLL) and 82% to be radiosensitive (S-CLL). Men are proportionally higher represented (20%) in the R-CLL group than women (around 16.8%) [362].

Importantly patients in the R-CLL group have an aggressive course of disease, making front-line treatment inevitable and do nevertheless rapidly succumb to death (oral communication, Jozo Delic). In accordance, the median survival for R-CLL patients is significantly shorter than for S-CLL patients ( $10.593 \pm 1.611$  and  $15.946 \pm 1.014$ ,  $p < 0.0001$  Log-rank, Wilcoxon and Tarone-ware-tests), underlining the prognostic relevance of this marker (see Figure 7.2).

As mentioned earlier chromosomal aberrations in CLL can lead to the loss of the ATM and p53 genes (see Chapter 7.1.2). Accordingly 20-30% of CLL patients with del[11q] have an inactive ATM. p53 deficiency exists in 4% of CLL cases, but rises with aggravation of disease to 10-12% after first line treatment and up to 40% in refractory CLL [363]. Both ATM and p53 are important mediators of the DNA damage response and apoptosis upon irradiation (see Chapter 3.3.1 and Figure 3.8). However, no strict correlation between the R-CLL phenotype and

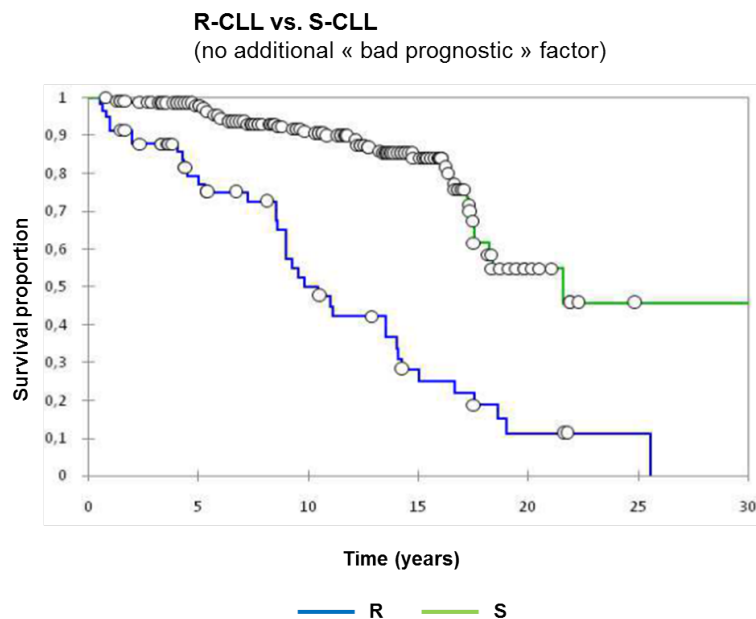


**Figure 7.2: Comparative survival proportion of patients diagnosed with R-CLL and S-CLL** The graph represents data from  $n=11$  samples and  $n=39$  for S- and R-CLL, respectively. Bad prognostic markers are defined as: ZAP70, CD38 or sCD23 positivity, unmutated  $IgV_h$ , cytogenetic abnormalities, aberrant karyotype and ATM or p53 mutations (Graph taken from [362])

the mutation or loss of ATM and p53 can be attested. Examination of the p53-mutation status in 12 R-CLL patients and 10 S-CLL, show 0/10 S-CLL and only 4/12 R-CLL patients to be p53-mutated [364]. Evaluation of 10 R-CLL patients with p53-wt show no loss of heterozygosity for the ATM gene [365]. In summary, the radioresistance observed in the R-CLL subset can't be explained, solely by the presence of mutations in these tumour suppressor genes.

The use of  $\gamma$ -irradiation induces SSB and DSB, as well as base modifications on the DNA molecule which activate the cell's DNA repair mechanisms (see Chapter 3.1). Aberrant DNA repair can cause radiosensitivity (as mentioned for the XRCC mutants in Chapter 2.3) and constitutes the presumption, that different DNA repair kinetics contribute to the variations observed between R-CLL and S-CLL. Using the alkaline comet assay, that measures the residual DNA damage (SSB and DSB), Blaise et al. [366], elegantly show that cells derived from the R-CLL subset have very fast repair kinetics compared to S-CLL derived cells and

normal lymphocytes. All samples show a biphasic DNA repair, however 60% of the damage are repaired at 15 min. post-IR in R-CLL cells, compared to 28% in S-CLL cells (see Figure 7.3 A and B). Even though the comet assay is a highly indicative marker for the repair capacity of DNA strand breaks, it gives no information on the quality and fidelity of DNA repair. Chromosomal aberration that develop, through the misrepair of DNA DSB, can be assessed in metaphase spreads at the first mitosis after irradiation (see Figure 7.3 C). Data presented in Figure 7.3 D clearly depict an increased proportion of chromosome lesions in the R-CLL compared to the S-CLL subpopulation.

Subsequently, the molecular background of this deregulation is found in the overactivation of the NHEJ pathway (see Chapter 3.1.1), with a 2-to 4-fold higher DNA-PKcs activity and a 2-to 3-fold higher DNA end binding activity of Ku in R-CLL samples than S-CLL samples [361]. Moreover the NHEJ pathway used in the R-CLL cells has highly mutagenic characteristics with associated extended deletions when tested in an *in vitro* assay [367].

Likewise a significant resection of the 3' telomere ends and an increased telomere dysfunction with telomere loss and telomere duplication are associated with the R-CLL phenotype compared to the S-CLL phenotype. Overresected telomeres constitute a danger for genomic stability, as soon as they have lost the ability to fold back into a t-loop, protecting them from erroneous DNA repair activities. In R-CLL samples increased numbers of telomere-induced foci containing  $\gamma$ -H2AX and 53BP1, the association of activated DNA-PKcs and Ku70 on telomere repeats as well as increased dysfunctional telomeres are observed. These findings strongly suggest an uncapping of chromosome ends and loss of protection in R-CLL, activating DNA-repair and a damage response at telomeres in R-CLL lymphocytes. The presence of 53BP1, which is normally excluded from functional telomeres, and the colocalization of DNA-PKcs and Ku70, strongly point to an activation of NHEJ, that was previously shown to be deregulated in R-CLL cells [368].

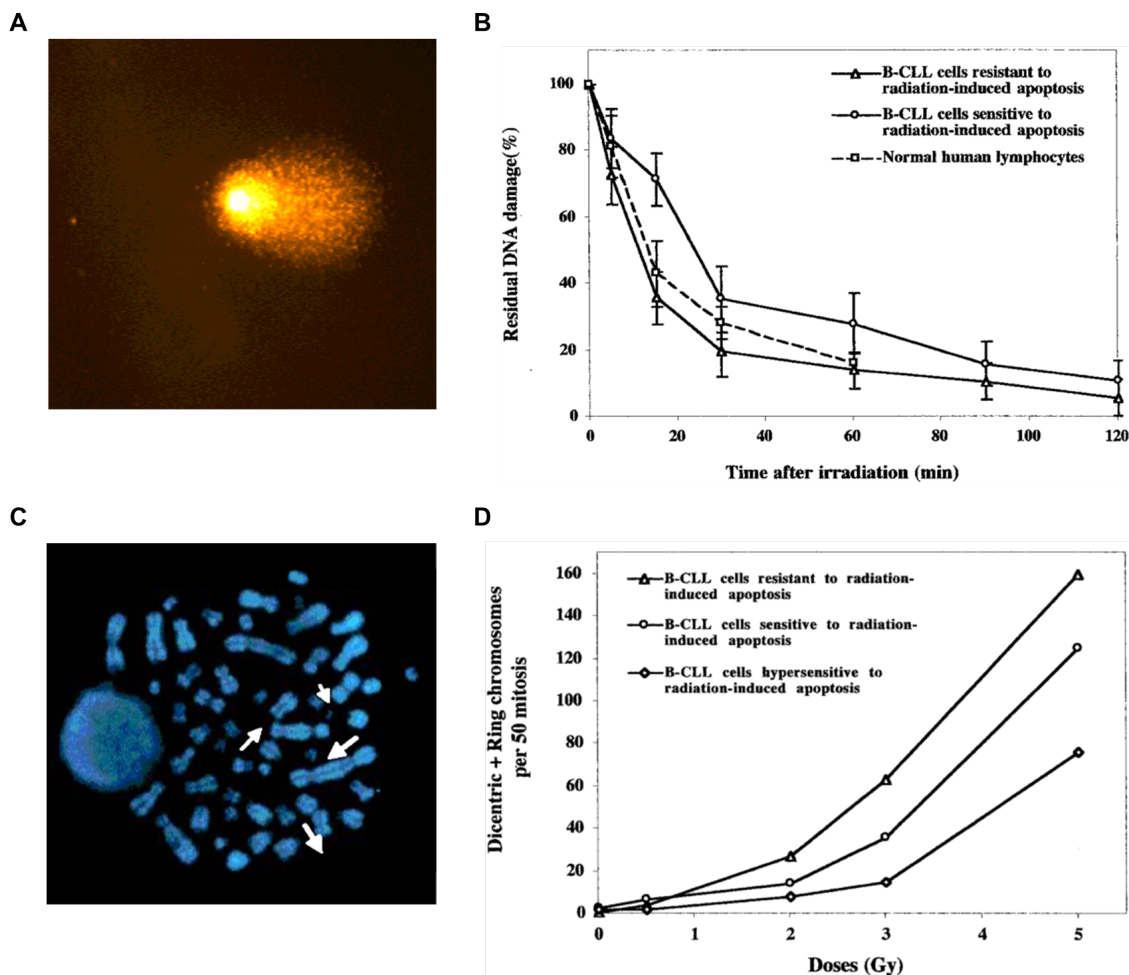


**Figure 7.3: R-CLL derived cells have faster DNA repair kinetics and show chromosomal aberrations compared to S-CLL derived cells** (A) An example of a comet, with an elongated tail, representing non-repaired SSB and DSB; (B) DNA repair kinetics after irradiation of 5Gy (24h) expressed as the residual damage measured by comet assay; (C) An example of a metaphase spread (D) Number of chromosomal aberrations per 50 metaphase spreads at 48h post-irradiation (Graph taken from [366])

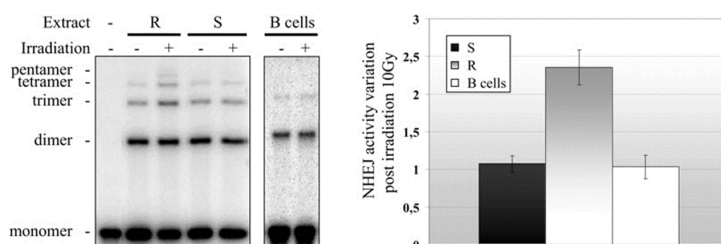


**Figure 7.4: NHEJ activity in R-CLL and S-CLL derived lymphocytes** (Graph taken from [361])

In summary, research in the lab over several years has characterized a novel sub-population of CLL patients, that has radioresistant lymphocytes, with the activation of a rapid and error prone NHEJ and the accumulation of chromosomal

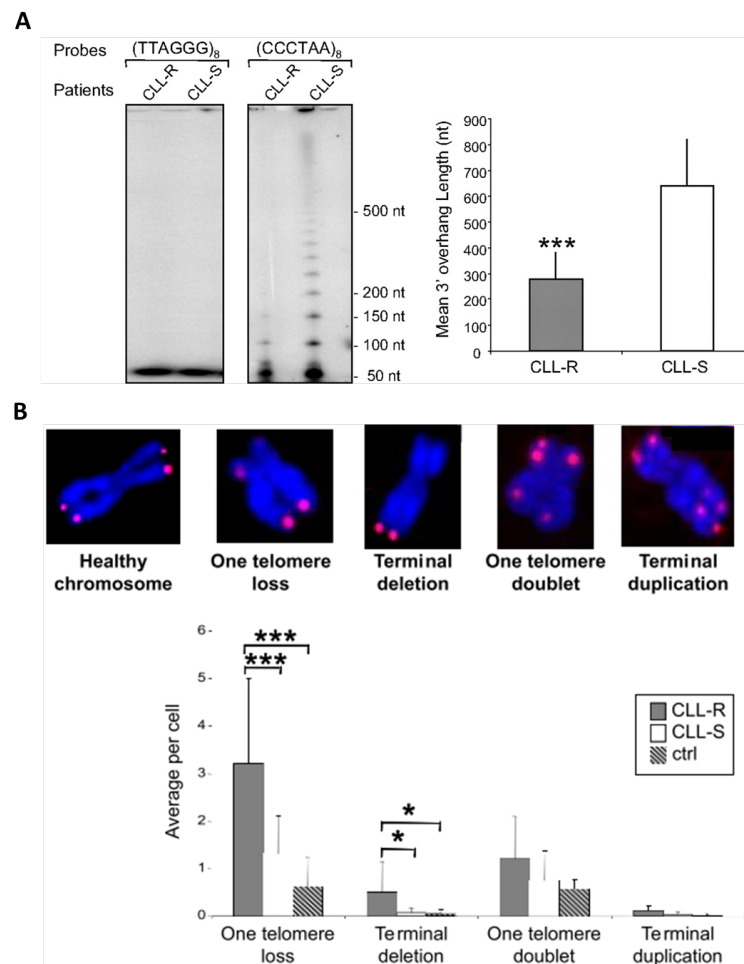


**Figure 7.5: Telomere dysfunction with telomere loss is higher in R-CLL than in S-CLL (A)** (Graph taken from [368])

aberrations. Moreover these patients have uncapped telomeres, linked with a DNA damage response and colocalization of NHEJ-factors on the resected telomere ends. Interestingly, Ku has taken a particular role in all of these studies, as it is found to bind DNA end structures with higher affinity in R-CLL extracts compared to S-CLL extracts. Given the key role of Ku in DNA maintenance and metabolism, a causal relationship between those observations is supposed.



### 7.3 Identification of phospho-S27-S33 Ku70

The studies conducted on the R-CLL and S-CLL subsets reveal several differences in the NHEJ process due to an overactivation of DNA-PKcs and an increased Ku binding. However no differences in the expression level of DNA-PKcs, Ku70 or Ku80 between R-CLL and S-CLL patients are found [361]. Therefore potential posttranslational modifications in the Ku protein are assessed. Using 2-dimensional gel electrophoresis the molecular weight and isoelectric properties of proteins are exploited to separate them on 2 dimensions on an electropherogram. The proteins are first isolated by electrophoresis based on their electric charge, using a pH-gradient, which shifts them up to their isoelectric point (their charge becomes 0). Subsequently, the proteins are denatured and further separated based on their molecular mass on the same gel but in an  $90^\circ$  angle in a classical SDS-PAGE (sodium dodecyl sulfate polyacrylamide gel electrophoresis) (an example for a 2-D electropherogram is given in Figure 7.6A). This method enabled the identification of different kinds of posttranslational modifications in the Ku70 protein between R-CLL and S-CLL subsets. As depicted in Figure 7.6B, 6 spots relate to the Ku70 protein. Spot 2, 6 and 5 in R-CLL are higher expressed than in S-CLL (cf Figure 7.6C.) These spots correspond to phosphorylated Ku70, based on experiments using pretreatment with phosphatase  $\lambda$ . Evaluation of spot 2 by mass spectrometry MALDI-TOF reveals a phosphorylation site at serine 27. Another phosphorylation site on serine 33 has been predicted, corresponding to spot 5. Spot 6 most probably corresponds to phosphorylation of both sites.

Interestingly, research assessing the kinetics of this phosphorylation reveals it to be inducible after genotoxic stress, such as  $\gamma$ -irradiation or treatment with the radiomimetic neocarzinostatin in cancer patients and healthy donors *in vitro* (cf Figure 7.7A,B). Additionally, phosphorylation is enhanced *in vivo* after classical chemotherapy with fludarabine (cf Figure 7.7C).

The induction of a phosphorylation event always raises the question, which kinases are involved. Co-immunoprecipitation studies and the functional inhibition of the

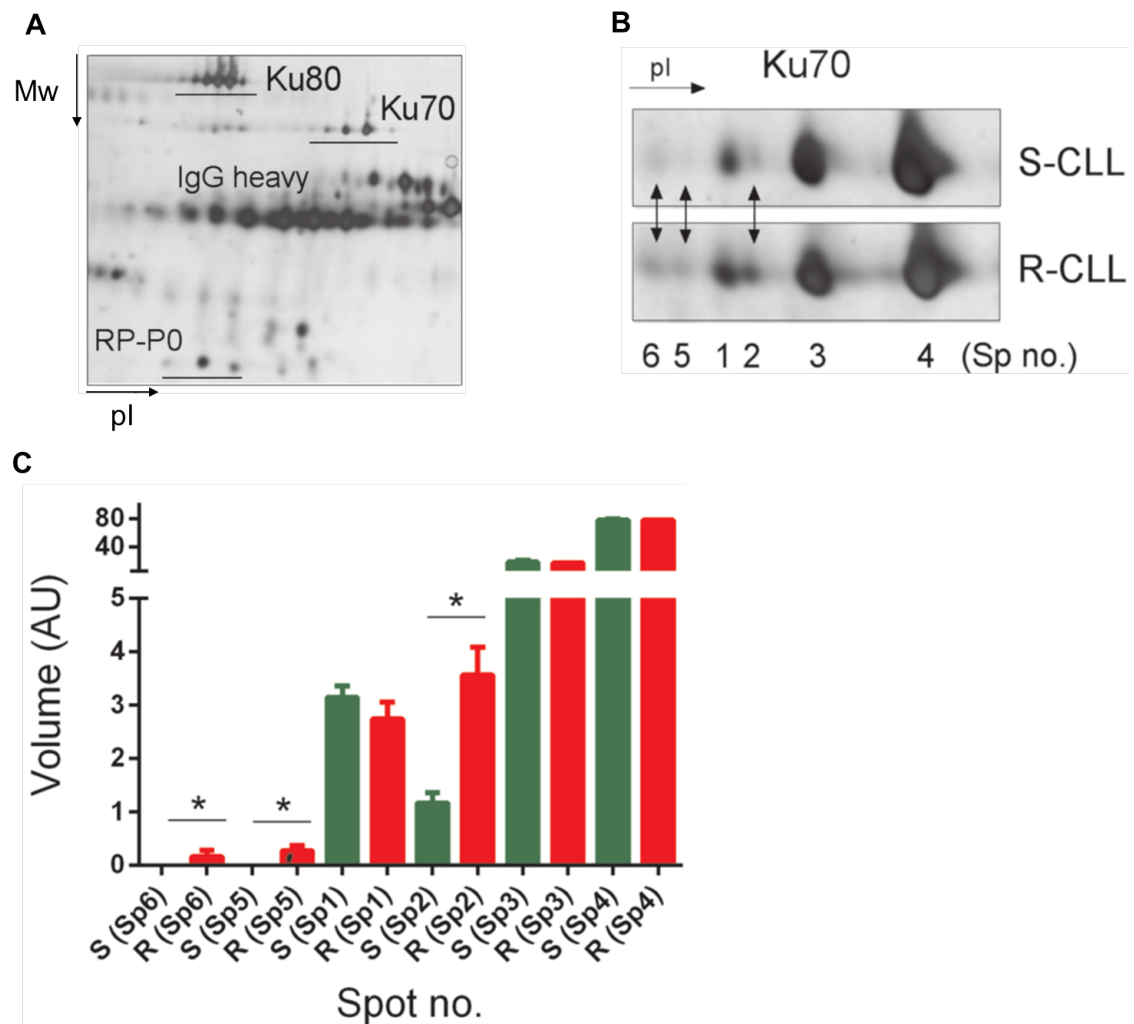


**Figure 7.6: Identification of pS27,S33-Ku70** (A) 2-dimensional gel electrophoresis. The proteins are first separated horizontally based on their electric charge (pI). Afterwards they are denatured and are separated dependent on their molecular weight (Mw) (B) Higher expression of spot 2, spot 5 and spot 6 in R-CLL compared to S-CLL. The spots correspond to Ku70 with different posttranslational phosphorylation. (C) Quantification of the different spots depicted in (B). 6 R-CLL and S-CLL samples have been evaluated. (Graph taken from [369])

PI3-kinases with wortmannin or DNA-PKcs and ATM specific inhibitors, show them to be redundant in the phosphorylation of p-Ku70 [369].

The biochemical characterization of p-Ku70 is further completed by functional assays on DNA repair and cell cycle kinetics. For this a special vector system that represses endogenous Ku70 by shRNA expression, with a simultaneous expression of an exogenous Ku70 gene either in its wild type-transfected (S27,S33), phospho-mutant (A27,A33) or phospho-mimetic form (E27,S33) is expressed in a p53wt

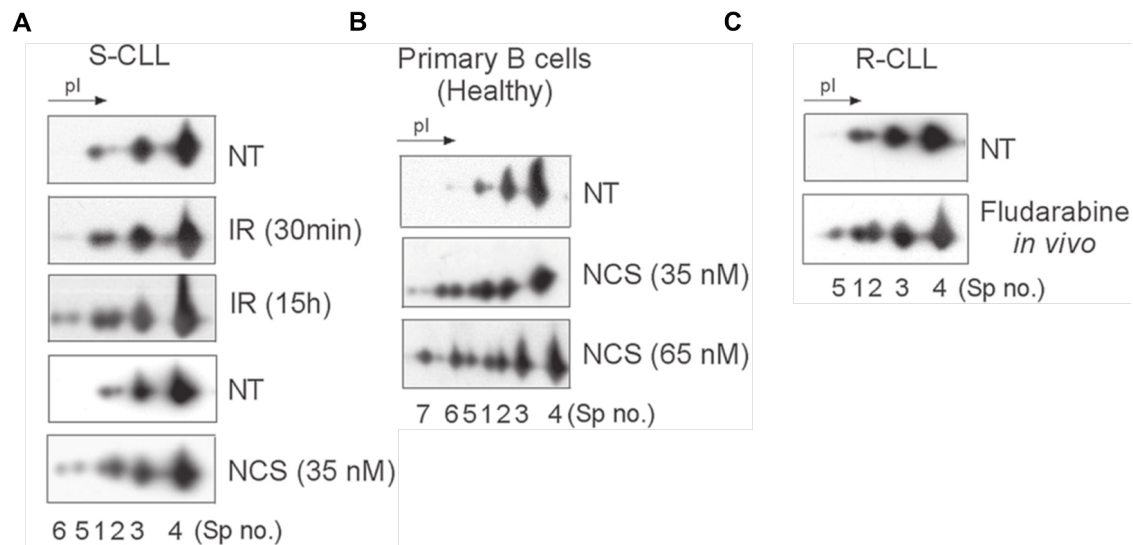


**Figure 7.7: Induction of phospho-Ku70 by genotoxic stress** (A) The phosphorylation of Ku is enhanced after irradiation and NCS treatment as soon as after 30min and persists several hours in S-CLL cells. Spots in the non-treated (NT) cells are less strong, indicating less phosphorylation events. (B) Induction of p-Ku70 in healthy B-cells (C) A R-CLL sample before and after treatment with the chemotherapeutic fludarabine, shows induction of p-Ku70 *in vivo* (Graph taken from [369])

breast cancer cell line. Comparative studies in these cell lines reveal longer DNA repair kinetics in the phospho-mutant than the wt cells, with longer persisting DNA damage. Accordingly, a persisting cell cycle block in G2 is attested for the phosphomutant cells, as well as an accumulation in late S-phase after 12h of irradiation [369].

p-Ku70 is a newly identified phosphorylated form of Ku70, that has first been observed in R-CLL patients. However it is expressed ubiquitously after genotoxic stress, is phosphorylated by the damage activated kinases ATM and DNA-PKcs and has functions in DNA repair kinetics. The article describing the identification of p-Ku70 is attached in Appendix VII.

## 7.4 Posttranslational modifications (PTM) regulate cellular processes

The posttranslational modification (PTM) of proteins is an important mechanism to control cellular processes without the need of *de novo* protein synthesis. These modifications are thus an elegant means for the cell to rapidly and reversibly change protein characteristics, adapting to the current cellular state. For instance, during the cell cycle (as described in Chapter 3.9), the oscillating activity of CDk's, phosphorylating their target proteins, drives a cell through the different phases. Similarly DNA repair is greatly regulated by these modifications. Different post-translational protein modifications are distinguished, ranging from small chemical groups, like a phospho-group, an acetyl-group or a methyl-group to small proteins, like ubiquitin, SUMO or NEDD8. All these modifications have a preferred protein target sites, for example phosphorylation occurs on hydroxy (OH)-containing aa like tyrosine, threonine or serine, whereas acetylation is found on lysine residues and methylation targets lysine or arginine residues. All these modifications are accomplished by the actions of two kinds of enzymes, working oppositely. For example, kinases phosphorylate proteins, phosphatases dephosphorylate them. Similarly, acetyl- or methyl-transferases add acetyl- or methyl-groups to proteins and are antagonized by deacetyl- or demethylases [370].

Furthermore ubiquitination is a ubiquitous process to regulate protein functions and degradation. Ubiquitin is a 76-aa containing protein, that can be attached individually (monoubiquitination) or multiply forming ubiquitin chains (multi- or polyubiquitination) on proteins. Addition of ubiquitin is conducted by a conserved family of ubiquitin ligases, and deubiquitinating enzymes (DUB) remove these protein modifications. Similarly, SUMOylation and NEDDylation are conducted [370].

All of these different PTMs have been mentioned throughout this manuscript and have far-reaching importance in the control of DNA repair and metabolism.

### 7.4.1 Ku70 phosphorylation sites reviewed

Several publications demonstrate Ku associated post-translational-modifications. For instance, ubiquitination processes extract the heterodimer from DNA ends and acetylation controls Bax release for apoptosis induction. Overall, 117 PTMs have currently been described for Ku70 [371]. Phosphorylation is an important regulator of DNA repair and the orchestration of a DDR, particularly induced by the PI3-kinases ATM/ATR and DNA-PKcs.

Early studies have already shown that the Ku heterodimer is phosphorylated on serine residues *in vivo* [372] and that phosphorylation events are catalysed by DNA-PKcs [373]. Today, 35 phosphorylation sites are identified for Ku70, from which 6 (S6, S27, S33, S51, S155, Y530) have been studied more closely [371]. The hitherto identified phosphorylation sites of Ku70 are shown in Figure 7.8. Additionally potential phosphorylation sites in the Ku core region are described (see below), but are not listed by PhosphoSite.

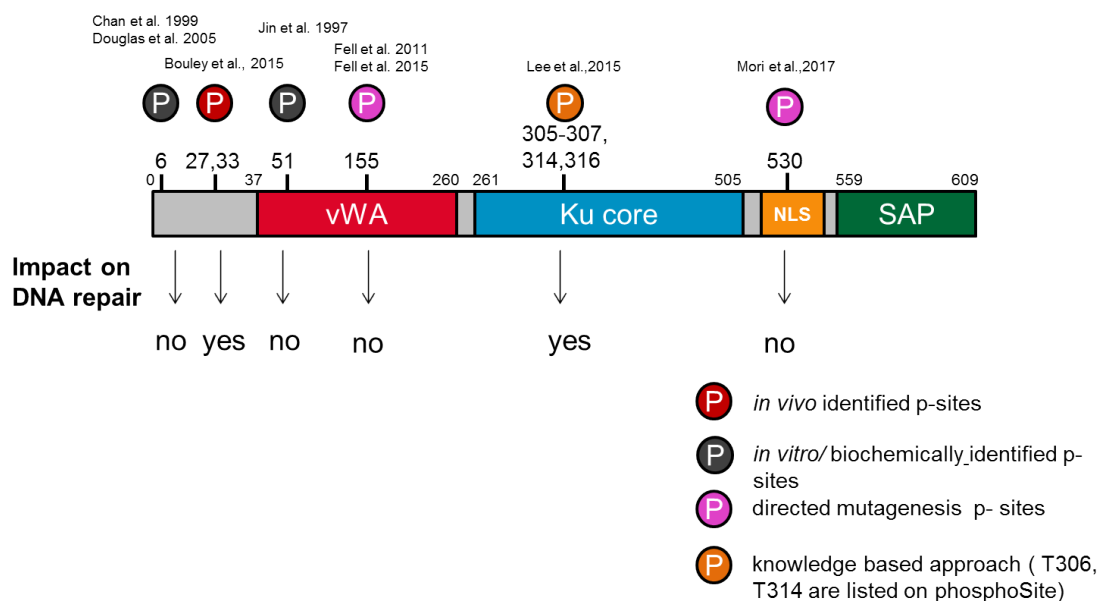


**Figure 7.8: Identified phosphorylation sites of Ku70** Five phosphorylation sites on serine residues of the Ku70 protein have been identified and confirmed by site specific methods.

Phosphorylation on S6 and S51, are the first sites that have been described in the literature but are not necessary for DNA repair, DNA end binding or V(D)J recombination, even though they are target sites for DNA-PKcs dependent phosphorylation *in vitro* [374, 375]. These residues have later been found to be critical regulators in DNA-PKcs and Bax dependent cytotoxic cell death in neurons [267]. More recently the site specific mutation of the S155 residue to a phosphomutant (A155) or phosphomimetic (D155) shows severe cellular consequences. Whereas the cells expressing the phosphomutant have a survival advantage after irradiation, the phosphomimetic expressing cells are highly radiosensitive. Moreover the phosphomimetic is severely impaired in growth, has a pronounced cell cycle arrest, a senescence phenotype and a highly active DNA damage response even without damage induction. Interestingly, although this study reveals a severely impaired DDR, in these phosphorylation-mutants, no defects in DNA repair efficiency and kinetics are established by comet assay or a plasmid repair luciferase assay [224, 225].

Another residue that has no impact on DNA repair, but has a regulatory function on apoptosis is Y530, that is phosphorylated by Src-kinases. Phosphorylation blocks subsequent acetylation of Ku70, thus preventing Bax release and apoptosis [376].

Using a knowledge based approach, Lee et al. [196] target the pillar and bridge region, that form the ring structure of Ku70 for the introduction of site specific mutations at sites T307, T306, T305, T316 and T314 (termed 5A mutant). This mutant has an increased DNA end binding associated with the inhibition of DNA end resection, and an decreased commitment to HR, compared to its phosphomimetic counterpart 5D and the wt protein. However the sites, mutated in this study have not been confirmed to be veritable or inducible phosphorylation sites *in vitro* or *in vivo*.

Finally, our group has discovered the phosphorylation sites at serine 27 and 33 and demonstrates for the first time an impact on the DNA repair kinetics by these sites, which are found to be phosphorylated *in vivo* in a dose dependent manner by irradiation [369].



## Part II

### Aim of this project





## Aim of this project

During the last decade the laboratory has intensively studied the cellular characteristics of lymphocytes derived from CLL patients. The extensive research on their apoptosis resistance guided the way towards the discovery that CLL derived lymphocytes can be divided into two subsets, either resistant (R-CLL) or sensitive (S-CLL) towards IR induced apoptosis. Interestingly, several observations made in the laboratory suggest an imbalance of the NHEJ pathway in the R-CLL compared to the S-CLL derived lymphocytes. First, the R-CLL subsets are shown to upregulate their NHEJ pathway to the cost of repair quality, accumulating repair junctions with extended deletions compared to S-CLL cell samples or healthy lymphocytes. Secondly, a profound dysfunction in telomere maintenance is determined in the R-CLL subset compared to S-CLL. In this context a significant resection of the 3' telomeric overhang and the accumulation of NHEJ factors, like 53BP1 or Ku70, are manifested on the chromosome ends of R-CLL cell samples, arguing for an activation of the NHEJ pathway. Lastly, the identification of two phosphorylation sites (S27, S33) of Ku70, that are found overexpressed in R-CLL compared to S-CLL derived lymphocytes, is the first identified molecular differentiator between R-CLL and S-CLL subsets. Furthermore using a cellular *in vitro* system longer persisting DNA damage and a persisting G2-arrest in phosphomutant (A27,33) were observed, compared to the wild-type transfected (S27,33) cells. In this study we want to further characterize the cellular role of phospho-Ku and more particularly its role in DNA DSB repair. The central questions underlying this study are thus:

- **Is the phosphorylation of Ku70 specific to IR or is it a general response to genotoxic stress?**
- **How does the phosphorylation of Ku influence on the cellular phenotype?**
- **What impact has the phosphorylation of Ku on the DNA DSB repair?**

More precisely, at the molecular level, our questions are as follow:

- Is phospho-Ku70 found on the DNA after stress induction?
- Does phospho-Ku70 have an impact on DNA repair by NHEJ and HR?
- Does the phosphorylation of Ku impact on Ku release from the DNA after damage induction?

These questions are approached by a cellular *in vitro* model in which expression of phospho-Ku70 is inhibited or mimicked.

To better understand the role of phospho-Ku70 in lymphocyte development, V(D)J recombination and its potential role in cancer development it is however imperative to study its function *in vivo*. Therefore, a humanized knock-in mouse model is created and some primary studies on extracted mouse embryonic fibroblast (MEFs) are conducted.

Given the central role of DNA repair in cancer development, the study of factors like phospho-Ku70 can potentially identify new targeting strategies for a more personalized medical approach.

# **Part III**

## **Materials and Methods**



# Chapter 1

## Materials and Methods

### 1.1 Cell lines and culture conditions

#### 1.1.1 Cell lines

The cancer cell lines U2OS (osteosarcoma) and ZR75.1 (mammary duct) have been purchased at the ATCC platform. The U2OS HREJ cell line contains two reporter systems to measure NHEJ and HR efficiency (U2OS HREJ) and were a kind gift by Bernard Lopez (CNRS UMR 8200, Institut de Cancérologie Gustave-Roussy, Villejuif). The human fibroblast cell line GC92 contains a reporter system to measure NHEJ efficiency and was a kind gift from Pascale Bertrand (LREV Team, CEA Fontenay-aux Roses) and Bernard Lopez [377]. The non cancerous mammary epithelium derived HME (hTert immortalized) cell line was a kind gift from RA Weinberg [378].

#### 1.1.2 Cell culture

All cell lines used were passed twice a week at around  $1 - 1.5 \cdot 10^6$  cells in 75cm<sup>2</sup> flasks. Cells were counted at each passage to assure stable growth conditions. Every 6-8 weeks the cell lines were changed to prevent cell line derivation. Culture

conditions and composition of media are summarized in Table 1.1.

All cell lines were kept in culture media (10566016 or 10565018 Thermo Scientific, GIBCO) supplemented with fetal bovine serum (12657029, Thermo Scientific, GIBCO) and Antibiotic-Antimycotic (100x) (15240062, Thermo Scientific, GIBCO). The HME cell line was additionally supplemented with insulin (I9278, Sigma), EGF (E9644, Sigma) and hydrocortisone (H0888, Sigma).

**Table 1.1:** Cell Culture Conditions

Cell line	Culture Media	Culture Conditions
U2OS	DMEM Glutamax, 10 % Fetal bovine serum, 1x Antibiotic-Antimycotic	37 °, 5 % CO <sub>2</sub>
U2OS HREJ	DMEM Glutamax, 10 % Fetal bovine serum, 1x Antibiotic-Antimycotic	37 °, 5 % CO <sub>2</sub>
GC92	DMEM Glutamax, 10 % Fetal bovine serum, 1x Antibiotic-Antimycotic	37 °, 5 % CO <sub>2</sub>
ZR75.1	DMEM, 5 % Fetal bovine Serum, 1x Antibiotic-Antimycotic	37 °, 5 % CO <sub>2</sub>
HME	DMEM/F12+ Glutamax, 5 % Fetal bovine serum, 1x Antibiotic-Antimycotic, Insulin 10 $\mu$ g, Hydrocortisone 0.5 $\mu$ g/mL, EGF 10 ng/mL,	37 °, 5 % CO <sub>2</sub>

### 1.1.3 Splitting cells

To passage adherently growing cells, medium was aspirated and cells were washed two times with PBS<sup>-/-</sup> (14190250, Thermo Scientific, GIBCO), before adding 2mL Tryple Express (12604013, Thermo Scientific, GIBCO) to loosen cell-cell interaction. Cells were incubated at 37 °C for several minutes, until they began to detach from the bottom of the flask. Trypsinized cell suspension was taken up in 5mL medium in a centrifugation tube and centrifuged (1200rpm, 5min) (5804R, Eppendorf).

Supernatant was aspirated and 10 mL fresh medium were added.

Cell counting was performed using approx. 10  $\mu$ L of cell suspension diluted 1:1 with trypan blue, which were added to a counting chamber and counted automatically by a cell counter machine (TC20, Bio-Rad). Cells were split in a late exponentially growing state.

#### **1.1.4 Thawing cells**

Cell lines were stored in a mixture of 10 % DMSO, 50% fetal bovine serum and 40% culture medium in  $-196^{\circ}\text{C}$  nitrogen stocks.

Cells were quickly thawed in a  $37^{\circ}\text{C}$  water bath and added to 5mL culture medium before centrifugation at 1200rpm for 5min (5804R, Eppendorf). Cells were seeded into 75cm<sup>2</sup> flasks containing 10mL medium.

## **1.2 Stable cell line generation using pEBV vectors**

To study the phosphorylation of Ku70 a vector system established and kindly provided by Denis Biard (CEA, Institute of Emerging Diseases and Innovative Therapies (iMETI), Fontenay-aux-Roses, France) was used to generate stable cell lines that either express: S27,S33-Ku70 (phospho-wt), A27,A33-Ku70 (phospho-mutant) or E27,E33-Ku70 (phospho-mimetic). Endogenous Ku70 is repressed using shRNA encoded on the same pEBV-vector. Using this system we generated cell lines that do not express endogenous but rather exogenous Ku70. The vectors replicate in a semi-conservative manner during cellular S-Phase, dependent on the presence of host replication-initiation factors, like Orc2, Orc3, Orc4 and Mcm [379]. The replication is limited to one doubling per cell cycle. During chromosome segregation the vector anchors to a chromosome and therefore assures "one by one" segregation to daughter cells.



### 1.2.1 Transfection

Plasmid purification after bacterial culture was performed using the QIAGEN Plasmid Midi Kit (12143,QIAGEN), following manufacturer's instructions.

Cell transfection for all mutants was performed the same day, using the same transfection (114-15, Polyplus) and antibiotic selection conditions. In general, cells were seeded in a 12-well plate, to attain approx. 70% confluence the following day. The transfection reagent was prepared as follows: 75 $\mu$ L of JetPrime transfection buffer, 0,75 $\mu$ g of plasmid-DNA and 1,5 $\mu$ L of JetPrime reagent were mixed, vortexed and left at RT for approx. 15 min. During the incubation time the culture medium was changed. After incubation the transfection reagent was quickly vortexed and 75 $\mu$ L of the solution were added dropwise to the cells. As a transfection control a GFP-pEBV vector was used. Transfection efficacy was monitored by GFP fluorescence (Zeiss Axiovert 200) and generally reached 40% after 48h. Cells were then trypsinized and 50% re-seeded into a 6-well plate containing medium and appropriate concentration of antibiotics (Puromycine, A1113802, Thermo Scientific, GIBCO or Hygromycine B, 10687010, Thermo Scientific, invitrogen). As a control for antibiotic selection, non-transfected cells and the pEBV-GFP transfected cells were set under antibiotic selection and cell death was monitored over time by light microscopy (Zeiss, Axiovert A1). Generally after several days under antibiotic selection, control cells died, and the antibiotic concentration was decreased to the final concentration in the target cell lines. Successful transfection for the different Ku70 mutants was monitored using SDS PAGE and Western Blot. All stably transfected cell lines were frozen and stocked in liquid nitrogen. GFP-Ku70 expressing cells were freshly transfected before each live cell acquisition. All cell lines were kept under constant antibiotic selection pressure. Table 1.2 summarizes the transfection conditions for each cell line.

**Table 1.2:** pEBV transfection conditions

Cell line	Vector (Vector No.)	Antibiotic	Selection concentration	Final concentration
U2OS	Ku70Ser (2103)	Hygromycine	125 $\mu$ g/mL	125 $\mu$ g/mL
U2OS	Ku70Ala (2104)	Hygromycine	125 $\mu$ g/mL	125 $\mu$ g/mL
U2OS	Ku70Glu (2106)	Hygromycine	125 $\mu$ g/mL	125 $\mu$ g/mL
U2OS	GFP-Ku70Ser(3452)	Hygromycine	125 $\mu$ g/mL	125 $\mu$ g/mL
U2OS	GFP-Ku70Ala (3453)	Hygromycine	125 $\mu$ g/mL	125 $\mu$ g/mL
U2OS	GFP-Ku70Glu (3455)	Hygromycine	125 $\mu$ g/mL	125 $\mu$ g/mL
U2OS HREJ	Ku70Ser (2103)	Hygromycine	200 $\mu$ g/mL	125 $\mu$ g/mL
U2OS HREJ	Ku70Ala (2104)	Hygromycine	200 $\mu$ g/mL	125 $\mu$ g/mL
U2OS HREJ	Ku70Glu (2106)	Hygromycine	200 $\mu$ g/mL	125 $\mu$ g/mL
GC92	Ku70Ser (2464)	Puromycine	0.4 $\mu$ g/mL	0.4 $\mu$ g/mL
GC92	Ku70Ala (2467)	Puromycine	0.4 $\mu$ g/mL	0.4 $\mu$ g/mL
GC92	Ku70Glu (2468)	Puromycine	0.4 $\mu$ g/mL	0.4 $\mu$ g/mL
ZR75.1	Ku70Ser (2103)	Hygromycine	200 $\mu$ g/mL	125 $\mu$ g/mL
ZR75.1	Ku70Ala (2104)	Hygromycine	200 $\mu$ g/mL	125 $\mu$ g/mL
ZR75.1	Ku70Glu (2106)	Hygromycine	200 $\mu$ g/mL	125 $\mu$ g/mL
HME	Ku70Ser (2464)	Puromycine	0.4 $\mu$ g/mL	0.2 $\mu$ g/mL
HME	Ku70Ala (2467)	Puromycine	0.4 $\mu$ g/mL	0.2 $\mu$ g/mL
HME	Ku70Glu (2468)	Puromycine	0.4 $\mu$ g/mL	0.2 $\mu$ g/mL
Control	GFP-control (1486)	Blasticidine		
Control	GFP-control (1675)	Hygromycine		

### 1.3 Irradiation

Irradiation was performed using the  $\gamma$ -irradiator IBL-637 (Cs137). Dose rate used was 4.96 Gy/min for all experiments.

## 1.4 Cell growth

Cell growth was assessed for transfected U2OS cells. The cells were grown to 70-80% confluence, trypsinized, counted in a Malassez chamber and seeded in duplicate for non-treated (NT) and irradiated (IR) conditions into 25cm<sup>2</sup> flasks at 0.2\*10<sup>6</sup> density. Approximately 4-6h after seeding, cells were irradiated at 2Gy or 4Gy. Cells were left to grow over 7 days. From day 1 to day 7 cell numbers were counted with a Malassez chamber under the light microscope (Leitz, Dialux 20EB).

## 1.5 Clonogenic assay

Cells grown to 70-80% confluence were trypsinized, counted in a Malassez chamber and suspended at cell concentrations of 5\*10<sup>3</sup> cells/mL (NT), 10\*10<sup>3</sup> cells/mL (2Gy), 20\*10<sup>3</sup> cells/mL (4Gy) and 40\*10<sup>3</sup> cells/mL (6Gy). Cell suspensions were either non irradiated (0Gy) or irradiated at 2, 4 or 6 Gy. Cells were seeded in duplicates into 10cm<sup>2</sup> cell dishes. Cells were left to grow 14 days.

## 1.6 Cell death and apoptosis using DiOC<sub>6</sub>-IP

Cells were grown to 70-80% confluence, trypsinized and counted in a Malassez chamber and seeded in duplicate to 24-well plates at 0.03\*10<sup>6</sup> (IR) and 0.02\*10<sup>6</sup> (NT) cell density. Approximately 4-6h after seeding, cells were irradiated at 2Gy, 4Gy or treated 1h with 100 μM phleomycine (ant-ph-2p, invivoGen). Cell medium was changed immediately after treatment and cells left to grow. At day 3 and 4 cells were trypsinized and cell suspension added to FACS-tubes. After centrifugation (1200rpm, 5min)(Jouan GR422), supernatant was aspirated and the cell pellet resuspended in medium containing propidium iodide (1:1000) (P 4170, Thermo Scientific) and DiOC<sub>6</sub> (3,3'-Dihexyloxycarbocyanine Iodide) (1:2000) (D 273, Thermo

Scientific). Data were acquired using a cytometer (FACScalibur, BD Biosciences). Analysis was performed using R (Script, Allan Sauvat).

## 1.7 Cell cycle and hyperploidy

Cell cycle analysis was performed at several time points after irradiation. Cells were seeded the day before irradiation into 6-well plates at the following densities:  $0.6 \times 10^6$  cells (NT, 6h, 11h),  $0.3 \times 10^6$  (15h,24h) and  $0.2 \times 10^6$  (48h,72h). Cells were irradiated and collected after the indicated time points. Cell pellets were resuspended in 1 mL cold 5% FCS /PBS<sup>-/-</sup> and 3mL of ice-cold 75% ethanol where added dropwise during vortexing the cell suspension. Collected samples were stored at -20°C. The day before analysis cell samples were washed 2x with PBS<sup>-/-</sup> and centrifuged at 1200rpm, 5 min. Cell pellets were than taken up in 400 $\mu$ L of PBS<sup>-/-</sup> containing 25  $\mu$ g/mL propidium iodide (P 4170, Sigma Aldrich) and 50  $\mu$ g/mL RNase A (Boehringer). Cell suspension was kept in the dark at 4°C, ON. Data were acquired on a cytometer (FACScalibur, BD Biosciences). Analysis of the fcs-files was performed with the FlowJo software, version 7.6.5 and VX.

## 1.8 Cell cycle synchronization

Cells were synchronized with 300 $\mu$ M mimosine (Sigma Aldrich, M0253),ON. Mimosine containing medium was substituted with normal cell medium 1h before irradiation.

## 1.9 $\gamma$ -H2AX-foci detection via immunofluorescence

Cells were grown on 8-well cover slides (PEZGS0816, Millicell EZ Slides) for 2 days until 70-80% confluence was reached. Slides were irradiated at 4Gy and left in the

incubator for the indicated time points (0.5h, 4h or 24h). Cells were then washed 2x with PBS<sup>-/-</sup> and fixed with paraformaldehyde (PFA) 4% during 15min. After a washing step (2x) with PBS<sup>-/-</sup>, 0,1% Triton X-100 (X100, Sigma Aldrich) was added for 10min. to permeabilize the cells. Saturation of the cells was done with 10% goat's serum in PBS<sup>-/-</sup> at RT. After 1h, saturation solution was substituted with H2AX (phospho-S139) antibody (05-636, Merck Millipore) diluted 1:500 in 10% goat's serum in PBS<sup>-/-</sup>. After 1h of incubation cells were washed with Triton X-100 0,025% in PBS<sup>-/-</sup> (3x). An Alexa Flour488-coupled secondary antibody (A-11094, Thermo Scientific) was added during 1h at RT, slides were kept in the dark. After 3 washes with Triton X-100 0,025% in PBS<sup>-/-</sup>, Hoechst 33342 (1 $\mu$ g/mL) was added to the slides and incubated at 37 °C for 20min. Slides were washed with 0,025% in PBS<sup>-/-</sup> (3x) and mounted with Flouromount-G (0100-01, Southern Biotech). Data acquisition was performed using a microscope (Zeiss, Imager Z2) and a Plan Apochromat 63x (numerical aperture 1.4) oil objective. Data analysis was performed using CellProfiler (Script Vincent Paget).

## 1.10 Chromosomal aberrations

Cells were seeded at day (D)-5 at a concentration of  $0.5 \times 10^6$  cells. At D-3 cells were irradiated at 2Gy. To block cells in mitosis colcemid (0.03  $\mu$ g/mL) was added for 2h at D-0. Cells were then washed with PBS<sup>-/-</sup> (2x). Cells were then trypsinized and  $1.5 \times 10^6$  cells centrifuged (1200rpm, 5min). Cells were taken up in 300 $\mu$ L PBS<sup>-/-</sup>, before adding 1mL of KCl (0.06 M, 37 °C) for 25min. at 37 °C. Subsequently a fixative (acidic acid : methanol (1:3), 4 °C) was added. Cells were centrifuged and supernatant was aspirated until approx. 500 $\mu$ L remained, before adding 5mL of fixative. Cells were stored ON at -20 °C. Centrifugation and fixation steps were repeated 2 times the next day. Subsequently cells were pipetted up and down to burst them and spread onto a glass slide.

For chromosome staining of telomeric and centromeric regions specific probes (Panagene) were used. DNA was stained with Dapi. Metaphases were mounted with Flouromount-G aqueous (F4680, Signal Aldrich). Data were acquired using

the Zeiss Imager Z2 microscope. Data analysis was performed with ISIS software (Metasystem).

## 1.11 Chromosomal translocations

Preparation of metaphases was performed as described above (Section 1.10). HME cells were irradiated at 4Gy and metaphases prepared after 24h.

Slides were pre-treated with RNase A (120 $\mu$ L per slide in 2xSSC buffer (AM9763, Thermo Scientific)) during 45min, 37°C to eliminate RNA that could interfere with the hybridization. To remove remaining cytoplasm a pretreatment with pepsine (P6887, Sigma Aldrich) was performed. Slides were incubated for 30sec-1min, 37°C in 0.01M HCl, pH 2; 2 $\mu$ g/mL pepsin. Slides were washed with PBS<sup>-/-</sup> (2x), then with PBS<sup>+/+</sup> for 5min. To fix pepsin treated metaphases, slides were incubated in 1% formaldehyde/ PBS<sup>+/+</sup> for 10min. at RT. Slides were washed with PBS<sup>-/-</sup>, 5min. Dehydration was performed in 3 steps, at 70%, 90% and 100% ethanol at RT for 3min. and left to dry for 2-3min.

mFISH probe denaturation and hybridization were performed according to the manufacturer's protocol (24XCyte, D-0125-120-DI, MetaSystems). Metaphases were mounted with Flouromount-G aqueous (F4680, Sigmal Aldrich). Data were acquired using the Zeiss Imager Z2 microscope. Data analysis was performed with ISIS software (Metasystem).

## 1.12 Whole cell protein extraction

For whole cell protein extraction (WCE) cell pellets stocked at -80 °, were thawed on ice for 5-10 min. before adding WCE lysis buffer (HEPES 10mM, KCl 5mM, MgCl 1.5mM, EDTA 2.5mM, DTT 0.5mM, Iodoacetamine 5mM, cOmplete Protease Cocktail 1x (11836145001, Roche), H<sub>2</sub>O). Per 1\*10<sup>6</sup> cells 80 $\mu$ L lysis buffer were added, disrupting the cell pellet by pipetting up and down vigorously. Cell suspension was left on ice a few minutes and then sonicated at 50% amplitude for

10sec. (2x) (Digital sonifier, Branson).

## 1.13 Protein extraction for co-immunoprecipitation (Co-IP)

The protein extraction for Co-IP is divided in 3 parts, each after which cell lysates can be stored at  $-30^{\circ}$ . Part 1: Cell pellets of at least  $15 \times 10^6$  cells were thawed on ice for approx. 10 min., vortexed, extraction buffer added (NaF 50mM, NaCl 450mM, HEPES 20mM, EDTA 0.2mM, DTT 0.5mM, Iodoacetamine 5mM, Complete Phosphatase Cocktail 1x, H<sub>2</sub>O) (100 $\mu$ L extraction buffer per  $10^7$  cells) and vortexed again. Lysates were left on ice for 1h, for lysis by osmotic shock. Cell lysates were then centrifuged at 67.000rpm for 1h,  $4^{\circ}\text{C}$ , to segregate cell debris and DNA from the protein lysates in the supernatant. 10% Glycerol and  $\beta$ -Mercaptoethanol (1:1250) were added to the supernatant. Part 2: To equilibrate salt content, equilibration buffer (EQ-buffer) (KCl 10mM, MgCl 10mM, HEPES 20mM, EDTA 2.5mM, DTT 0.5mM, Iodoactamine 5mM, Complete Phosphatase Cocktail 1x, Glycerol 10%, H<sub>2</sub>O) was added in a ratio of 1:3 and protein dosage was performed (see section 1.14). Part 3: Dynabeads (BE-M01/03, EMD Millipore) (1 $\mu$ L per 10 $\mu$ g total protein) were washed with PBS<sup>-/-</sup> (2x) and cell lysate added to the beads. EQ-buffer was added to obtain a total volume of 500 $\mu$ L. Antibodies for Ku70 and p-Ku70 were added to the lysate-dynabead mixture at a concentration of 1% of the total protein amount. Samples were put into a heatblock (Thermomixer, eppendorf) set at  $4^{\circ}$ , 1150rpm and left overnight at  $4^{\circ}\text{C}$ . Supernatant was discarded and beads washed 3x in PBS<sup>-/-</sup>, before adding EQ-buffer, Laemmli-buffer (5x) (0.255M Tris HCl (pH 6.8), 50% Glycerol, 5% SDS, 0.05% bromophenol blue, 0.1 M DTT, H<sub>2</sub>O) and boiling the sample at  $95^{\circ}\text{C}$  (Thermomixer, eppendorf).

## 1.14 Bradford assay for protein quantification

Protein cell extracts were quantified using the Pierce Coomassie (Bradford) protein assay kit (23200, Thermo Scientific). 10 $\mu$ L of standards and samples were added to a 96-well plate and 150 $\mu$ L of assay reagent added. After 5 min. on a vertical shaker, samples and standards were analyzed as duplicates by measuring the light absorbance at 660nm with a plate reader (Magellan, Tecan). Data were exported and analyzed using Microsoft Excel 2010.

## 1.15 Protein extraction for chromatin binding assay

Cells were seeded at 0,5\*10<sup>6</sup> cells in 10cm<sup>2</sup> cell dishes until approx. 70% of confluence were reached. For protein extraction the pre-extraction (PEB) buffer (PIPES 10mM (pH 7.0), NaCl 100mM, Sucrose 300mM, MgCl 3mM, Triton X-100 0.7%, H<sub>2</sub>O) was prepared and left on ice. Petri dishes were washed with PBS<sup>-/-</sup> (3x), then 500 $\mu$ L PEB-R buffer (PEB buffer, RNase A 7%) were added per cell dish and left incubate for 3 min., meanwhile agitating the plates 2-3x/minute. The supernatant was collected, corresponding to fraction 1 (F1). The same procedure was repeated once again, to obtain fraction 2 (F2). After, the cell dish was washed twice with PBS<sup>-/-</sup> and 300 $\mu$ L Laemmli- buffer (2x) (100mM Tris HCl (pH 6.8), 10% SDS, 20% Glycerol, 100mM DTT, 1% bromophenol blue, H<sub>2</sub>O) were added. Fraction 3 (F3; chromatin fraction) was collected using a cell scraper. To digest DNA in fraction 3, 4 $\mu$ L of Benzonase (Z0746-10KUN, Merck Millipore) were added. To prepare samples for SDS-PAGE, Laemmli 2x were added to fraction 1 and 2 and all samples were heated for 5min. at 95°C.



## 1.16 SDS PAGE

The principle of a SDS PAGE is the separation of proteins based on their molecular weight due to an electric current. Small proteins wander faster and more distant than bigger proteins, creating a separation, proportional to their molecular weight. Polyacrylamid gels (4561091, BioRad) were inserted into the electrophoresis chamber and filled up with SDS running buffer (0.025M tris-base, 0.05M glycine, 2% SDS, H<sub>2</sub>O, pH 8.3). Generally 10 $\mu$ g protein were loaded per lane. SDS PAGE was performed at 100V.

After the run, gels were rinsed 5 min. in transfer buffer (0.025M tris-base, 0.05M glycine, 2% SDS, 20% ethanol, H<sub>2</sub>O, pH 8.1-8.4) at RT, before proceeding with the Western Blot.

For Shotgun Proteomics the polyacrylamide gels were incubated in 10mL Coomassie Blue for approx.2h and destained ON. The Coomassie gel was sent to the Proteomics Center in Rotterdam for Orbitrap mass spectrometric analysis.

## 1.17 Western Blot

The aim of a Western Blot is to transfer and immobilize the separated protein fractions gained by the SDS-PAGE to a membrane by adding an electric current. For these experiments we used a wet blotting device of Biorad.

Two sponges, 2 Whatman Paper were incubated for 2 min with ice-cold freshly prepared transfer buffer. At the same time a 0.45 $\mu$ m PVDF-membrane (Immobilion-P,IPVH00010, EMD Millipore) was activated in ethanol and rinsed with water, before incubation in transfer buffer for another 2 min.

To assemble the blot the gel was covered by a PVDF membrane, placed in between two Whatman Papers and sponges and inserted into the blotter. The transfer was performed at 300mA, in a tranfer chamber kept at 4 °C

## 1.18 Protein Immunodetection

After western blotting the membrane was removed from the blotter and blocked ON at 4 °C or for 1h, RT in TBST/5 %BSA.

Primary antibodies were prepared using the dilutions depicted in Table 1.3.

After incubation primary antibody is rinsed for 5 min with H<sub>2</sub>O (3x) and incubated for 1h with the secondary antibody.

After the rinsed 1x for second incubation membranes were rinsed 10 min. with TBST and 2x with H<sub>2</sub>O.

The detection was carried out using the ECL Prime Protein Detection Reagent (RPN2232, GE Healthcare) in accordance to the manufacturer's protocol. Western Blots were revealed on chemiluminescence films (Amersham Hyperfilms ECL,28906837, GE Healthcare) in a dark chamber.

### 1.18.1 Antibodies

All antibodies used for Western Blotting are listed in Table 1.3.

**Table 1.3:** Antibodies

Type	Target (clone)	Species	Dilution	Supplier (Reference)
Primary Antibodies	phospho- Ku70 (p-Ku70)	mouse	1:1000 (5%BSA /TBS-T)	BioGenes GmbH
	Ku70 (N3H10)	mouse	1:1000 (5%BSA /TBS-T)	Thermo Scientific (MA5-13110)
	Ku80	mouse	1:1000 (5%BSA /TBS-T)	Thermo Scientific (MS-285)
	Ligase 4	rabbit	1:1000 (5%BSA /TBS-T)	Proteintech (12695-1- AP)
	Bax	rabbit	1:1000 (5% milk /TBS-T)	Millipore (06-499)

**Table 1.3:** Antibodies

Type	Target (clone)	Species	Dilution	Supplier (Reference)
	PAXX		1:2000 (5% milk /TBS-T)	abcam (ab126353)
	$\gamma$ - H2Ax (Ser139) (20E3)	rabbit	1:1000 (5% milk /TBS-T)	Cell Signalling (9718)
	anti-HA- Tag (clone 16B12)	mouse	1:1000 (5% BSA /TBS-T)	Biolegend (901513)
	$\beta$ - Actin	mouse	1:3000 (5% BSA /TBS-T)	Sigma Aldrich (A2228)
	$\alpha$ - Tubulin	mouse	1:2000 (5% BSA /TBS-T)	Sigma Aldrich (T6199)
Secondary Antibodies	anti-rabbit	goat	1:30000	Thermo Scientific (A- 11001)
	anti-mouse	goat	1:30000	Thermo Scientific (A- 11034)

## 1.19 Shotgun proteomics

Data were acquired in collaboration with the Proteomics Center Rotterdam (Dr. J. Demmers). A Label-free quantification method was chosen, meaning that samples had not to be labelled before analysis. Data analysis was performed with Perseus.

## 1.20 NHEJ-HR efficiency

The NHEJ-HR efficiency was performed using transfected (Ku70Ser, Ku70Ala, Ku70Glu) U2OS HREJ and GC92 cells. These cells contain a single copy of a HR and NHEJ reporter to measure the efficacy of DNA break repair after I-SCE1 endonuclease expression, respectively. Cells were washed with PBS<sup>+/+</sup> (2x), trypsinized and counted with a Malassez chamber.  $0.25 \times 10^6$  were seeded into 6-well plates and transfected using JetPEI either with a plasmid coding for the endonuclease I-SCEI or a control. After 72h, cells were detached with sterile-filtered EDTA-PBS<sup>-/-</sup> (20mM). Cell pellets were centrifuged (1600rpm, 5min) (5415R, eppendorf), before fixing with PBS<sup>-/-</sup>/PFA 2%. Cells were then washed with PBS<sup>-/-</sup>, before blocking with PBS<sup>-/-</sup>/BSA 2% during 5min. After centrifugation (1600rpm, 5min) (5415R, eppendorf) cells were taken up in PBS<sup>-/-</sup>/BSA 0.5% containing either 0.5 $\mu$ g CD4-Alexa Flour 647 (557681, BD Pharmigen), 0.5 $\mu$ g H2Kd-PE (553566, BD Pharmigen) or no antibody. Cells were incubated during 45min at RT, protected from the light. After centrifugation (1600rpm, 5min) (5415R, eppendorf), cells were washed and taken up in 300 $\mu$ L PBS<sup>-/-</sup> for FACS analysis. Data were acquired using the cytometer (FACScalibur, BD Biosciences). Analysis was performed using FlowJo 7.6.5. NHEJ and HR efficiency was obtained by subtracting the signal of the control plasmid expressing samples from the I-SCEI expressing samples. H2Kd was used as a control for reporter expression in the GC92 cells. Control and I-SCEI expressing plasmids were prepared using QIAGEN Maxi Plus Kit (12963, QIAGEN).

## 1.21 Live cell imaging

Live cell imaging experiments were performed using U2OS cells expressing GFP-Ku70-mutants (Ku70Ser, Ku70Ala) transfected freshly before each experiment. To stain the nucleus, 1 $\mu$ g/mL Hoescht33342 (14533, Sigma Aldrich) was added 30min before laser irradiation. Background GFP-fluorescence intensity was measured before irradiation for each cell before irradiation with a 405nm diode laser

beam. Cells were followed up to 240 min after irradiation, in intervals of 10min. Data were acquired using the video-confocal inverted microscope Nikon A1 and a Plan Apochromat 60x (numerical aperture 1.3) oil objective. Data analysis was conducted using the NIS Elements software (Nikon).

## 1.22 Software

**Table 1.4:** Software

Application	Name, Version	Company
Western blot quantification	imageJ, Version 1.45 S	freeware
DNA quantification	Nanodrop2000	Thermo Scientific
Plasmid digestion	Sequencher 5.1 Demo	Gene Codes Cooperation
Live microscopy quantification	NIS Elements, Version 4.30	Nikon
Flow cytometry	FlowJo, Version 7.6.5	FlowJo, LLC
Cell death assay (DiOC <sub>6</sub> -IP)	R, Version 3.3.1	freeware, script: Allan Sauvat
Shotgun Proteomics	Perseus, Version 1.5.6.0	Max-Planck Institute of Biochemistry, freeware, script: H.W.J Rijkers
Metaphase analysis, multi-FISH	ISIS, Version 5.7.1	MetaSystems
$\gamma$ -H2AX foci count	CellProfiler, Version 2.2.0	Carpenter Lab, freeware, script: Vincent Paget

## 1.23 Statistics

Statistical analysis was performed with GraphPad Prism Software. Statistical tests are specified underneath each Figure.

# Part IV

## Results



# Chapter 1

## p-Ku70 in DNA double strand break repair

### 1.1 Establishment of a cell model and induction of phospho-Ku70 by different genotoxic stresses

To study the role of the Ku70 phosphorylation on S27, and S33, we generated a working model in the osteosarcoma derived U2OS cell line. Therefore a specific vector plasmid (pEBV) is transfected, that simultaneously represses endogenous Ku70 and expresses a customized exogenous Ku70 (S27-,S33-Ku70 (Ku70Ser); A27-,A33-Ku70 (Ku70Ala); E27-,E33-Ku70 (Ku70Glu) (Figure 1.1 A). Phosphorylation of Ku70 is detected using a specifically raised antibody against the phosphorylation containing epitope. As expected the antibody recognizes the phosphorylated form of Ku70 in the U2OS Ku70Ser cell line, whereas no expression is detected in the U2OS Ku70Ala and U2OS Ku70Glu expressing cell lines (Figure 1.1 B). Total Ku70 is however expressed in all of the transfected cell lines. We can conclude that all three cell lines express exogenous Ku70 and that endogenous Ku70 is repressed. Expression of phospho-Ku70 is enhanced after irradiation stress (10Gy) after 24h.



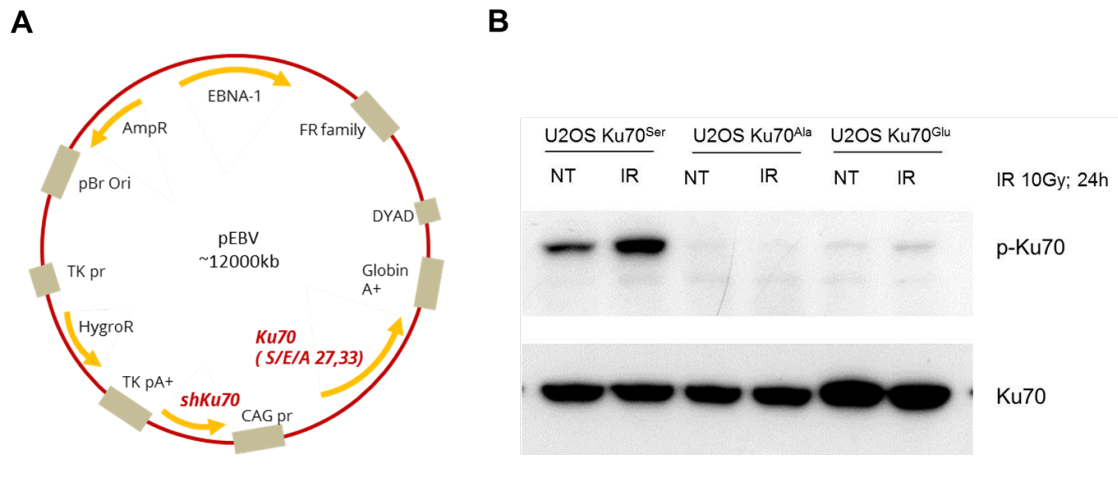


**Figure 1.1: Establishment of a working model with the U2OS cell line (A)** pEBV vector used to transfect the U2OS cell line. This vector contains a shRNA against endogenous Ku70 and expresses exogenous Ku70 protein with either S27-,S33-Ku70 (Ku70<sup>Ser</sup>), phosphomutant A27-,A33-Ku70 (Ku70<sup>Ala</sup>) or phosphomimetic E27-,E33-Ku70 (Ku70<sup>Glu</sup>). (B) Western Blot after transfection with the pEBV vector shows phosphorylated Ku70 in the Ku70<sup>Ser</sup> expressing cell line, but not in the phosphomutant or phosphomimetic cell line. However total Ku70 is expressed in all three cell lines. NT: non-treated; IR: irradiated, 10Gy, 24h

Induction of phospho-Ku70 has extensively been studied after irradiation but not other DNA damaging agents. Therefore we asked whether the induction is specific to irradiation or to the DNA damage. We thus treated the U2OS Ku70<sup>Ser</sup> cell line with different commonly used genotoxic agents, such as camptothecin or etoposide, both respectively topoisomerase-inhibitors I and II, and the radiomimetic phleomycin for 1h at the indicated concentrations. Phospho-Ku70 showed induction after all types of genotoxic stressors. DNA damage was monitored by  $\gamma$ -H2AX expression (see Figure 1.2). This indicates that phosphorylation of Ku70 is a consequence of DNA damage, which is not exclusive to irradiation stress.

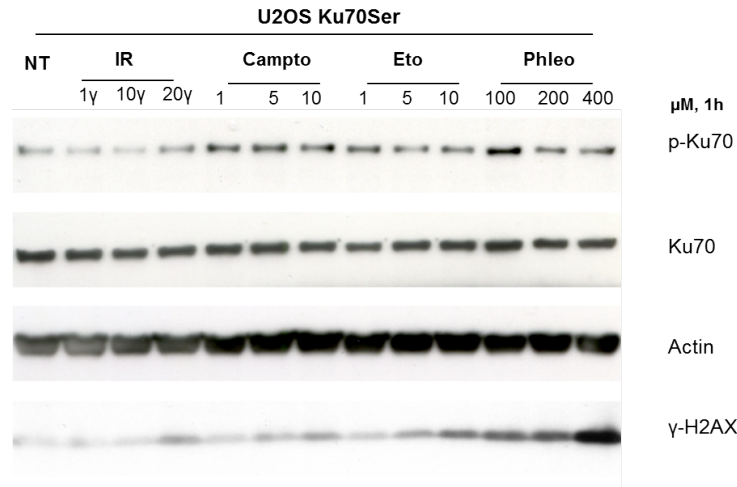


**Figure 1.2: Induction of p-Ku70 by different genotoxic stresses** Western Blot depicting the increase of Ku70 phosphorylation after DNA breakage by IR, camptothecin (Campto), etoposide (Eto) and phleomycin (Phleo). *gamma*-H2AX is used as a marker of DNA damage. Actin and Ku70 are loading controls.

## 1.2 Phenotypic characterization of the phospho-mutants

### 1.2.1 Cell growth is impaired in Ku70 phospho-mutant cell lines after irradiation

Multiple studies have shown that Ku deficiency leads to a growth defect [137, 234, 380]. We evaluated the onset of a growth deficiency over several days in non-treated and irradiated (2 and 4 Gy) cells. In non-treated conditions no significant effect on growth is observed between the different Ku70-mutants (Figure 1.3 A). However after irradiation, by the seventh day of culture, cell numbers of Ku70Ala and Ku70Glu are 37.5% (2Gy), 60% (4Gy) and 25% (2Gy) , 50% (4Gy) less compared to Ku70Ser cells, respectively (Figure 1.3 B,C).

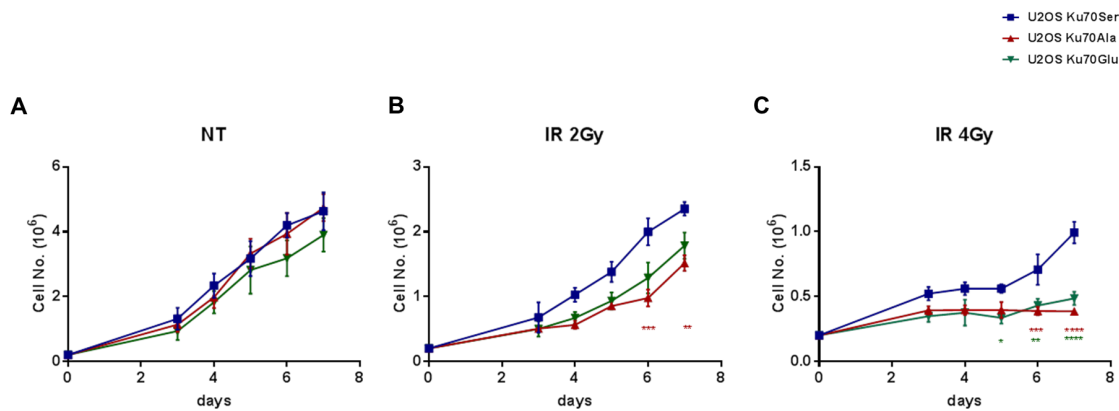


**Figure 1.3: Cell growth** of Ku70-transfected cell lines up to 7 days after irradiation. (A) No growth defects are observed in non-treated cells (B) After 2Gy irradiation a growth defect is noted after 4 days, which propagates until day 7 (C) After 4Gy the growth defect is most pronounced. Whereas Ku70Ala and Ku70Glu expressing cells remain at constant cell numbers between day 3 and 7, Ku70Ser expressing cells resume cell growth after day 5. Data represent total cell numbers. Error bars indicate SEM,  $n=4$ . Two-way ANOVA, Bonferroni-Test;  $p < 0.05 = *$ ;  $p < 0.01 = **$ ;  $p < 0.001 = ***$ .

### 1.2.2 Clonogenic survival is impaired in Ku70 phospho-mutant cell lines

Ku70 deficiency was further shown to induce a profound radiosensitivity [137, 245]. To determine whether the Ku70 mutations interfere with radiosensitivity, clonogenicity of the cell lines was assessed. Unexpectedly the plating efficiency between the Ku70 mutant already differed significantly between Ku70Ser and Ku70Ala or Ku70Glu, respectively. Whereas about 36% of the plated cells formed colonies in the Ku70Ser group, only 24% or 28% of Ku70Ala and Ku70Glu cells did so (see Figure 1.4 A). Nevertheless following irradiation treatment, cell survival decreased further in the Ku70Ala and Ku70Glu expressing cells particularly after 4 and 6 Gy, compared to Ku70Ser (Figure 1.4 B). At 2Gy, 4Gy and 6Gy, approximately 15%, 1% and 0.03% of Ku70Ser transfected cells give clonogenic progeny, compared to 13%, 0.5% and 0.015% of Ku70Ala and 8%, 0.3%, 0.004% of Ku70 Glu cells, respectively. These data suggest that Ku70Ala and Ku70Glu have an initial defect in colony formation and that this deficiency is further enhanced by irradiation.

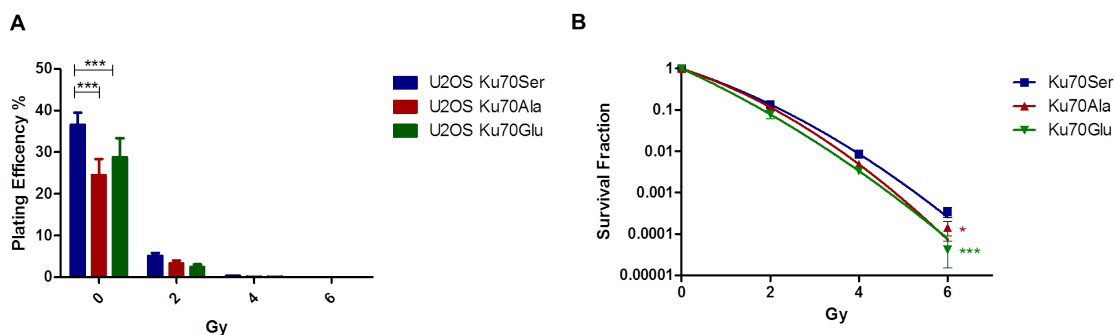


**Figure 1.4: Clonogenic Survival** (A) Plating efficiency (PE) for the Ku70 mutants. Error bars indicate SEM,  $n = 4$ . Two-way ANOVA, Bonferroni-Test;  $p < 0.001 = ***$  (B) Survival fraction of Ku70Ser, Ku70Ala and Ku70Glu cells. PE is standardized to 1 at 0Gy, for each cell line. Data are fit to the linear-quadratic model. Error bars indicate SEM,  $n = 4$ . Two-way ANOVA, Bonferroni-Test;  $p < 0.05 = *$ ;  $p < 0.001 = ***$ .

### 1.2.3 Cell death by apoptosis is enhanced in Ku70 phospho-mutant cell lines

Based on the observations of a slowed cell growth and enhanced radiosensitivity in the mutated Ku70Ala and Ku70Glu cells compared to Ku70Ser after irradiation, we further evaluated the sensitivity to cell death in these cell lines. Total cell death and apoptosis after irradiation and treatment with the radiomimetic were evaluated at day 3 and day 4 with a double staining using DiOC<sub>6</sub> and propidium iodide (PI) (see Figure 1.5 A). Cell death increased with time and dose in all cell lines. Initial cell death under NT conditions fluctuates between 5 to 7% at day 3 and 6 to 7% at day 4 in all cell lines. At day 3 after irradiation, the percentage of cell death is about 7%, 11% and 8.5% (2Gy) and 12%, 18% and 14% (4Gy) in Ku70Ser, Ku70Ala and Ku70Glu expressing cells, respectively (Figure 1.5 B). Similarly after day 4, cell death increases to 12%, 17% and 14% (2Gy) and 19%, 30% and 23% (4Gy) Ku70Ser, Ku70Ala and Ku70Glu expressing cells, respectively (Figure 1.5 D). Similar to the effects seen with irradiation, treatment with phleomycin (100 $\mu$ M, 1h) increases cell death in all cell lines compared to the non-treated conditions. The percentage of cell death is about 15%, 22% and 17% (J3) and 26%, 42% and 31% (J4) for the Ku70Ser, Ku70Ala and Ku70Glu cells, respectively (Figure 1.5 C, E).

Compared to Ku70Ser expressing cells, Ku70Ala cells are about 40% and Ku70Glu

cells are about 20% more sensitive to cell death induced by genotoxic agents. About 2/3 of total cell death are due to apoptosis in all cell lines and treatment conditions.

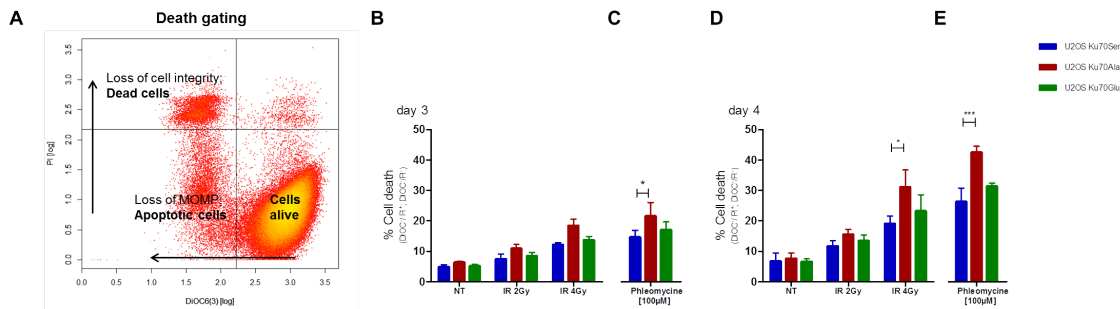


**Figure 1.5: Cell death by apoptosis** (A) A representative plot of cell death and living cells after DiOC<sub>6</sub>-IP staining. The lower right quadrant shows cells that are alive. When losing the mitochondrial outer membrane potential (MOMP) due to apoptosis, cells lose the staining for DiOC<sub>6</sub> (lower left). Dead cells lose their cellular membrane integrity and thus propidium iodide (PI) can accumulate in these cells (upper left). (B) Percent of apoptotic and dead cells on day 3 after NT conditions, 2Gy or 4Gy irradiation. (C) Percent of apoptotic and dead cells on day 3 after Phleomycine treatment (1h). (D) Percent of apoptotic and dead cells on day 4 after NT conditions, 2Gy or 4Gy irradiation. (E) Percent of apoptotic and dead cells on day 4 after Phleomycine treatment (1h). Data represent percent of apoptotic and dead cells. Error bars indicate SEM,  $n \geq 6$ . Two-way ANOVA, Bonferroni-Test;  $p < 0.05 = *$ ;  $p < 0.01 = **$ ;  $p < 0.001 = ***$

### 1.2.4 All Ku70 phospho-mutants and phospho-Ku70 interact similarly with Bax

Ku70 was shown to be a regulator of apoptosis through its interaction with the pro-apoptotic protein Bax [265–268]. Ku70 sequesters Bax, which inhibits its proapoptotic functions. Upon apoptotic stress, posttranslational modifications on Ku70 favour Bax release and translocation to the mitochondria. To verify if the differences in apoptotic cell death observed above are channelled through Ku70-Bax sequestration, we performed co-immunoprecipitation experiments. Interaction between the Ku70-mutants and Bax, as well as phospho-Ku70 and Bax were verified. As depicted in Figure 1.6 phospho-Ku70 interacts with Bax in non-treated conditions and after irradiation (4Gy). However all Ku70 mutants do interact with Bax in non-treated conditions and after irradiation. Therefore Bax sequestration

by phospho-Ku70 or the different Ku70 mutants does not explain the differences seen in apoptosis and cell death.

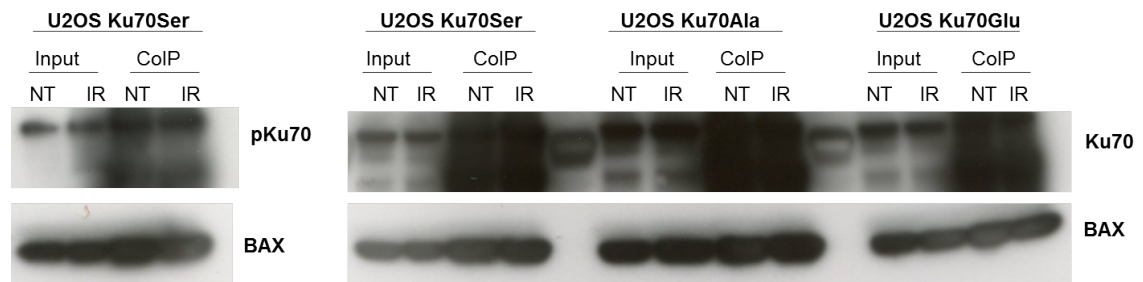
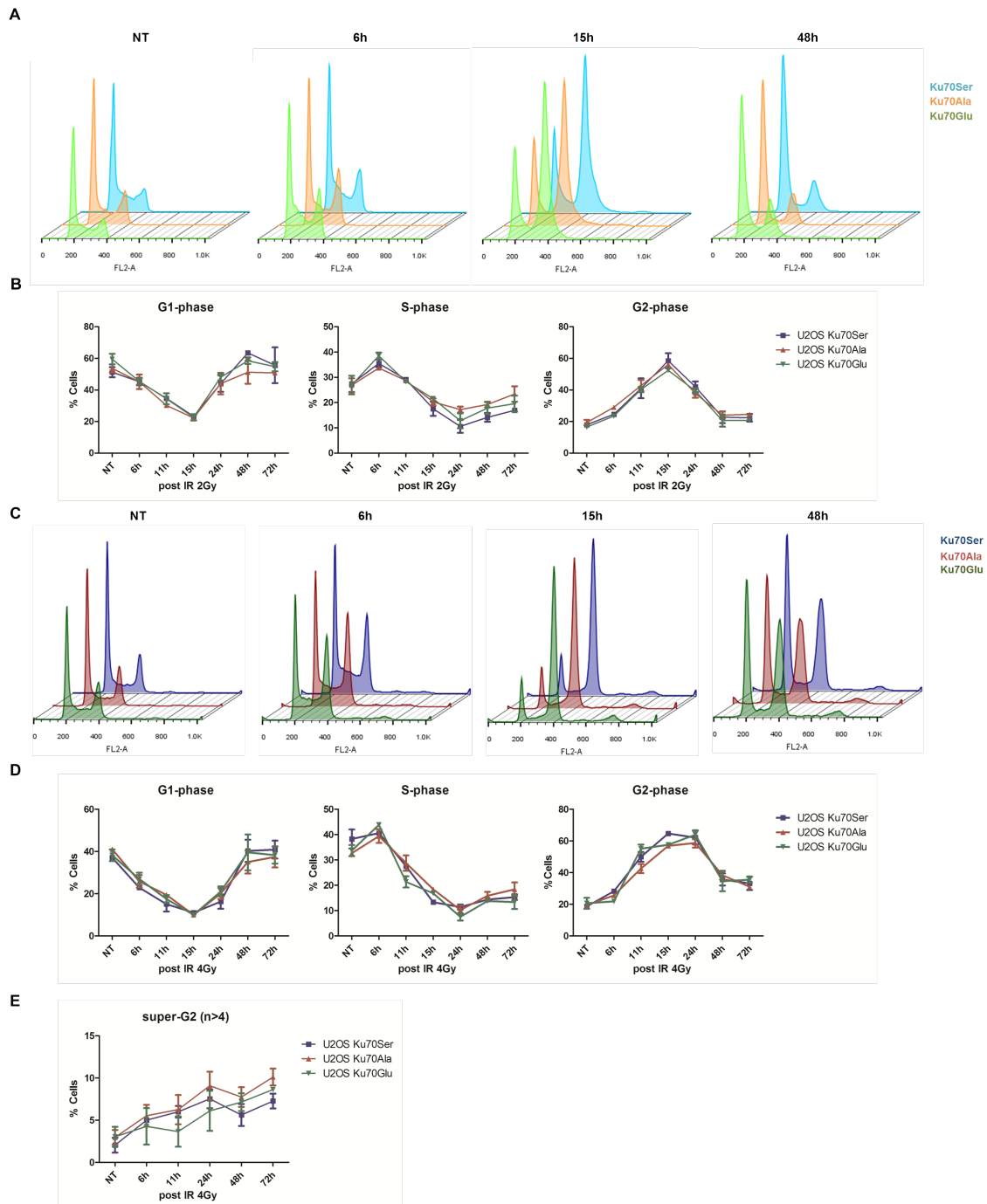


**Figure 1.6: Interaction between (phospho-)Ku70 and Bax** Co-immunoprecipitation with Bax, reveals an interaction of Bax with phospho-Ku70, nevertheless the phosphorylation is not specific for the phospho-Ku70 as all Ku70 mutants do interact with Bax similarly.

### 1.2.5 Hyperploidy and subsequent mortality in non-phosphorylable Ku70Ala expressing cells upon irradiation

The cell cycle was analysed over 72h after  $\gamma$ -irradiation (2Gy and 4Gy). The same cell cycle profile is observed for all cell lines. Indeed, similar block in S- (6h) and G<sub>2</sub>- phase (2Gy; 15h and 4Gy; 15-24h) were observed; the absence of a G<sub>1</sub>/S-block is probably due to an inherent p53-deficiency due to hMDM2 overexpression in U2OS cells (see Figure 1.7 A-D).



We observed a certain amount of hyperploid cells, that accumulate beyond the G2-peak at late time points (48-72h), in all cell lines after 4Gy irradiation. We recognized that the cell line expressing Ku70Ala had approximately 40-60% increased amounts of super-G2 ( $n>4$ ) compared to Ku70Ser. Ku70Glu expressing cells had around 10-30% higher super-G2 content compared to Ku70Ser (see Figure 1.7 E).

After irradiation, cells have a limited time window to repair the acquired damage before resuming the cell cycle. Misrepaired or persistent DSB can be a source of aneuploidy (hyperploidy) and genomic instability during transition from interphase to mitosis [57]. As a consequence, these cells can either develop a mutator phenotype and further drive genomic instability or undergo cell death via mitotic catastrophe [249].

To further pursue this observation, we assessed the cell cycle over 7 days after 4 Gy  $\gamma$ -irradiation and measured the amount of cells that accumulate with  $n>4$  (see Figure 1.8 A). As depicted in Figure 1.8 B the amount of hyperploidy in non-treated cells is stable at 0.5-2%. After  $\gamma$ -irradiation the amount of hyperploid cells increases in all cell lines. Nevertheless the Ku70Ala cells accumulate significantly more (60-80%) hyperploid cells than the Ku70Ser expressing cells (12% vs. 7% at day 7). Ku70Glu expressing cells accumulate approximately 20% more hyperploid cells (9% vs. 7% at day 7). At the same time the mortality in the Ku70Ala expressing cells increases, suggesting that these cells are genomically unstable and undergo mitotic catastrophe (Figure 1.8 C).



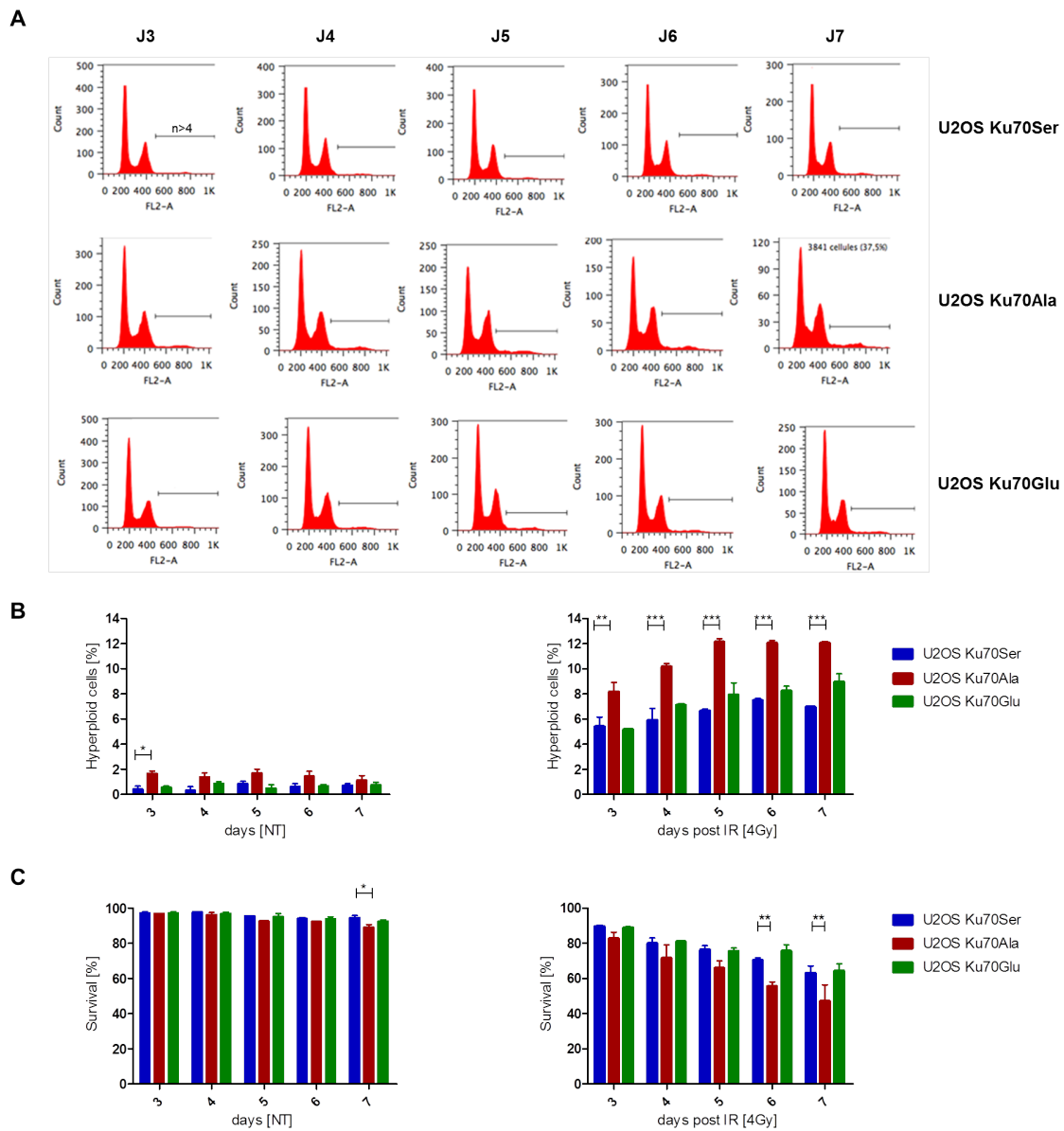


**Figure 1.8: Hyperploidy** (A) Cell cycle profiles that show the accumulation of hyperploidy cells ( $n > 4$ ) from day 3 to 7, after  $\gamma$ -irradiation (4Gy) (B) Percentage of hyperploidy cells before and after irradiation (C) Percentage of cell survival before and after irradiation. Error bars indicate SEM,  $n = 2$ . Two-way ANOVA, Bonferroni-Test;  $p < 0.05 = *$ ;  $p < 0.01 = **$ ;  $p < 0.001 = ***$ .

### 1.2.6 Summary of the phenotypic characteristics of Ku70 phospho-mutants

In this first chapter we established a valid cell model, characterized phospho-Ku70 expression after genotoxic stress and the cellular phenotypes associated with phosphorylation on S27,S33-Ku70. The data obtained in this chapter let us strongly suggest that the phosphorylation of Ku70 has an impact in DNA DSB repair due to several reasons:


First, phosphorylation of Ku70 is induced after different genotoxic stressors that have in common to induce DSB ( $\gamma$ -irradiation, etoposide, camptothecin and phleomycine). Secondly, the evaluation of the phenotypic responses of the established cell model towards irradiated conditions clearly shows that Ku70Ser expressing cells have relative radioresistance (growth curve, clonogenic assay, cell death) when compared to the non-phosphorylated Ku70Ala and in a lesser extent Ku70Glu. Thirdly, a marked increase in hyperploid cells, that are genetically unstable and succumb mitotic catastrophe, manifests after 4Gy irradiation and several days in the Ku70Ala cells compared to the phospho-Ku70 expressing Ku70Ser cells. Fourthly, the phenotypes described above are all enhanced after irradiation and thus let strongly suggest that DNA DSB repair is impaired in Ku70Ala and Ku70Glu mutants compared to the wild-type expressing Ku70Ser cells. Figure 1.9 summarizes the results in this section.

The phenotypic characterization moreover gives the opportunity to draw some conclusions on the functional nature of the phosphorylation site, by comparing the cellular responses between Ku70Ala and Ku70Glu expressing cells. Phosphorylation is a posttranslational modification, which can either result in a conformational change of the protein due to the introduction of a negative charge, or can provide the capacity to interact with cellular factors, that specifically recognize the phosphorylated region [370]. By mimicking the phospho-site (Ku70Glu) we introduce a negative charge and thus mimic the phosphorylated protein conformation, however we can not mimic the phosphate group ( $\text{PO}_4^{3-}$ -group) itself. By introducing a non-charged alanine as amino acid (Ku70Ala) we mimic the non-phosphorylated

state of the protein in its initial confirmation. Given these considerations we can suppose that effects on phospho-Ku70 that are due to its charge and protein confirmation, would have opposing effects between Ku70Ala and Ku70Glu cells, however if the phosphorylated region is important we would rather have similar effects for Ku70Ala and Ku70Glu. The provided data let preferentially suggest, that it is the phosphorylated region rather than the protein confirmation that has an impact on phospho-Ku70 functionality, as no opposing effects are observed between the Ku70Ala and Ku70Glu-mutants. Ku70Glu expressing cells have rather a milder phenotype with less pronounced characteristics than Ku70Ala, when compared to Ku70Ser.

Due to these considerations the further analysis, regarding the repair of DNA DSB mainly concentrates on the Ku70Ser and Ku70Ala expressing cells.

	Ku70Ser	Ku70Glu	Ku70Ala
<b>Cell growth after IR</b>	+++	+	+
<b>Survival after IR</b>	+++	++	+
<b>Clonogenic Survival</b>	++	+	+
<b>Cell Cycle after IR</b>	+++	+++	+++
<b>Genomic stability after IR</b>	+++	++	+



**Figure 1.9: Phenotypes of Ku70 mutants** Summary of the cell line characteristics after irradiation at 2 and 4Gy.

## 1.3 Functional dynamics and consequences of Ku70 phosphorylation on the DSB

### 1.3.1 Impaired DNA repair kinetics in Ku70Ala expressing cells

To characterize the function of phospho-Ku70 on the DSB site, we first analyzed their repair kinetics measuring the  $\gamma$ -H2AX foci by immunofluorescence after irradiation (4Gy) (see Figure 1.10 A). Figure 1.10 B, shows quantification of the obtained foci. In non-treated conditions the amount of  $\gamma$ -H2AX foci is similar in the Ku70Ser and Ku70Ala expressing cell lines (median= 5 foci/cell). After 0.5h the amount of  $\gamma$ -H2AX foci reaches its maximum, both cell lines show a median of 24 foci/ cell. At 4h after irradiation the amount of  $\gamma$ -H2AX foci decreases in both cell lines, however Ku70Ala cells show a slightly higher but significant ( $p < 0.001$ ) amount of remaining  $\gamma$ -H2AX foci (median= 13; 25%-percentile= 8; 75%-percentile= 22), compared to the Ku70Ser expressing cells (median= 11; 25%-percentile= 7; 75% percentile= 19). At 24h,  $\gamma$ -H2AX foci further decrease in both cell lines (median= 9). Similarly, western blot analysis of  $\gamma$ -H2AX shows a stronger signal at 4 and 6h after irradiation for Ku70Ala than Ku70Ser expressing cells (Figure 1.10 C). The strong signal for  $\gamma$ -H2AX in Ku70Ser and Ku70Ala after 24h (Western Blot) might be due to irradiation associated apoptosis.

Altogether these data suggest that phosphorylation of Ku70 accelerates repair capacity between 4 to 6h after irradiation compared to non-phosphorylated Ku70Ala.

### 1.3.2 phospho-Ku70 localizes to DNA damage and in the NHEJ-repair complex

To better understand the differences seen in  $\gamma$ -H2AX foci resolution and the increased genomic instability after irradiation in Ku70Ala expressing cells, we

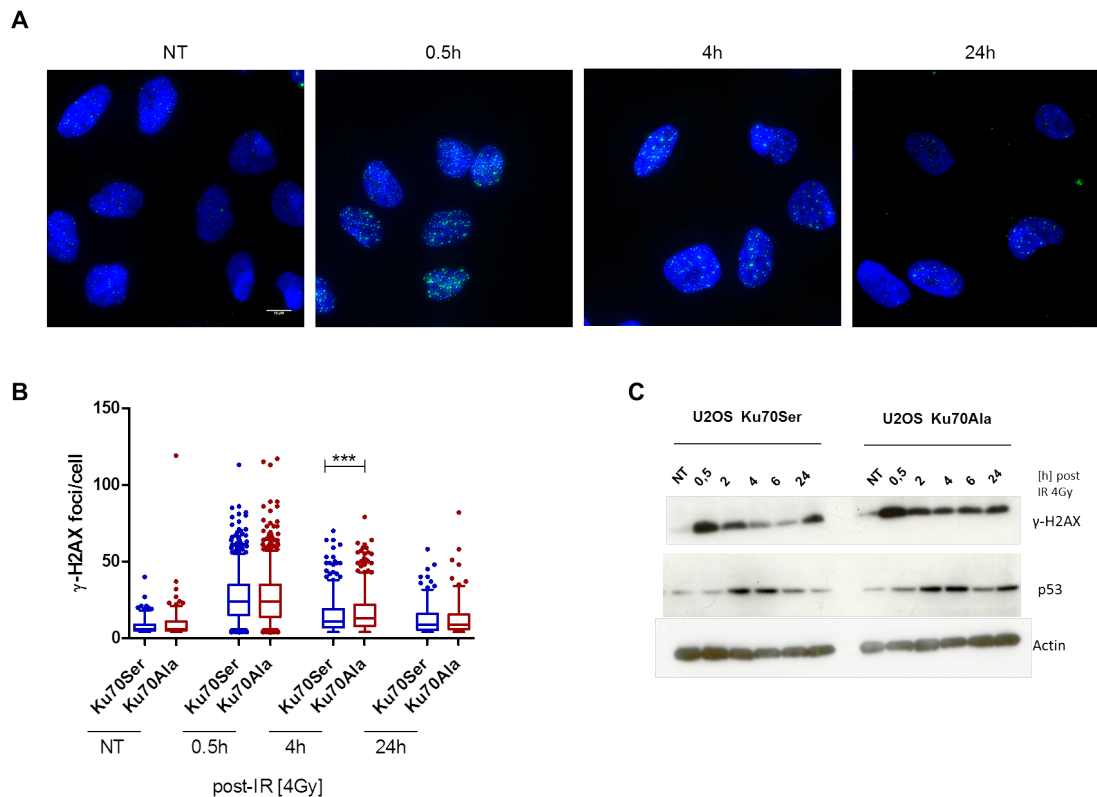


**Figure 1.10:  $\gamma$ -H2AX expression** (A) Representative pictures of  $\gamma$ -H2AX foci in non-treated and irradiated cells (4Gy) at several time points (0.5h, 4h, 24h). Nuclei are stained with Hoechst 33342 (blue),  $\gamma$ -H2AX with AlexaFlour 488 (green). Scale bar:  $10\mu\text{M}$ . (B) Results after automated quantification of  $\gamma$ -H2AX foci. Cells were scored positive, when at least 3 foci were detected. Per cell line at least 800 cells have been evaluated. Graphs represent data as boxplots with median, 1st and 3rd quartile, outliers are shown as dots,  $n=4$ . Unpaired t-test,  $p < 0.001 = ***$ . (C) Western Blot of  $\gamma$ -H2AX after irradiation (4Gy). Actin is used as a loading control. p53 is stabilized in both cell lines after irradiation. One representative western blot is depicted.  $n=2$ .

wanted to check whether phospho-Ku70 localizes to damaged DNA. Two complementary approaches, a chromatin binding assay and evaluation by immunofluorescence were conducted. Indeed, both approaches show a co-localization of phospho-Ku70 to damaged DNA. This happens in a DNA damage-dependent manner when cells were treated with the DSB inducer phleomycin (see Figure 1.11 A,B). Additionally, we could show that after damage induction by microirradiation (405nm), phospho-Ku70 co-localizes with the DNA DSB repair marker  $\gamma$ -H2AX at 30min. (see Figure 1.11 C). Thus phospho-Ku70 localizes to the DSB in a damage-dependent manner.

To further characterize the role of phospho-Ku70 and its functional necessity in

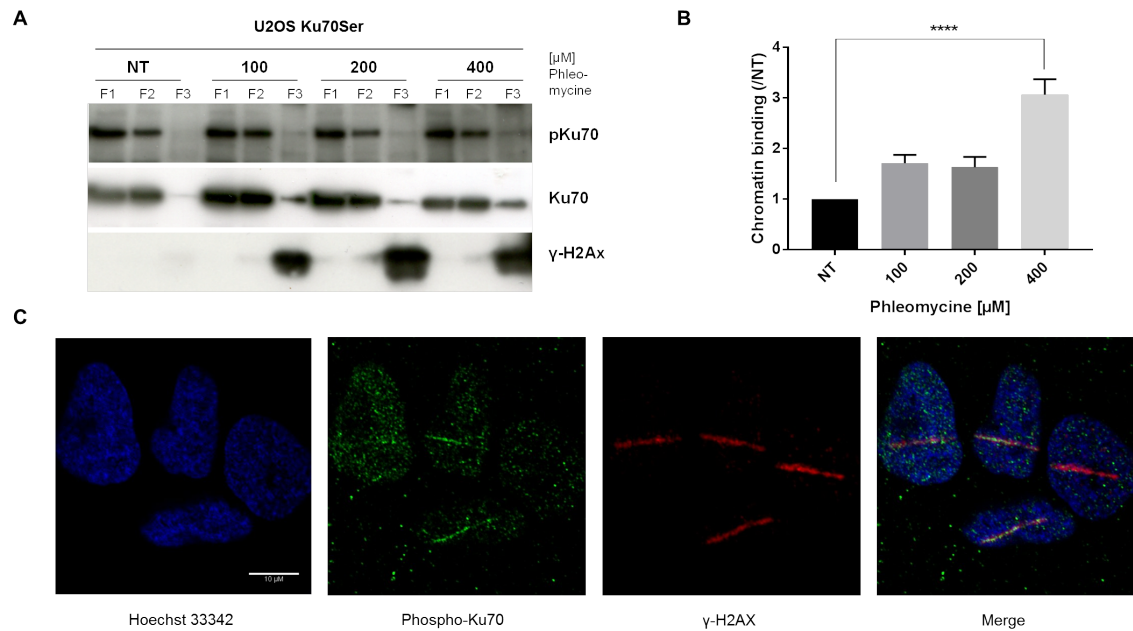


**Figure 1.11: Co-localization of p-Ku70 to damaged DNA** (A) Representative western blot of a chromatin binding assay (B) Quantification of the chromatin binding assay.  $n = 4$ . One-way ANOVA,  $p < 0.0001 = ****$ . (C) Immunofluorescence after microirradiation. Red,  $\gamma$ -H2AX. Green, phospho-Ku70. Blue, Hoechst 33342, scale bar:  $10\mu$ M.

DNA DSB repair, we assessed its co-binding with some of the principle NHEJ factors. Figure 1.12 A demonstrates the interaction of phospho-Ku70 with Ku80, Ligase 4 and PAXX. However Ku70Ala and Ku70Glu interact with Ku80, Ligase 4 and PAXX, too (see Figure 1.12 B). Furthermore a proteomics approach in the Ku70Ser transfected HME cell line, revealed no significant differences between the binding of Ku70 or phospho-Ku70 to the NHEJ core factors XRCC5 (Ku80), PRKDC (DNA-PKcs), Lig4 (Ligase 4) or XRCC4 (see Figure 1.12 C). Altogether these data indicate that phospho-Ku70 is not necessary for the formation and recruitment of NHEJ factors to the break site, but that it is a part of the NHEJ-complex, interacting with key players. It is thus possible that phospho-Ku70 impacts on the DSB repair efficiency and quality.

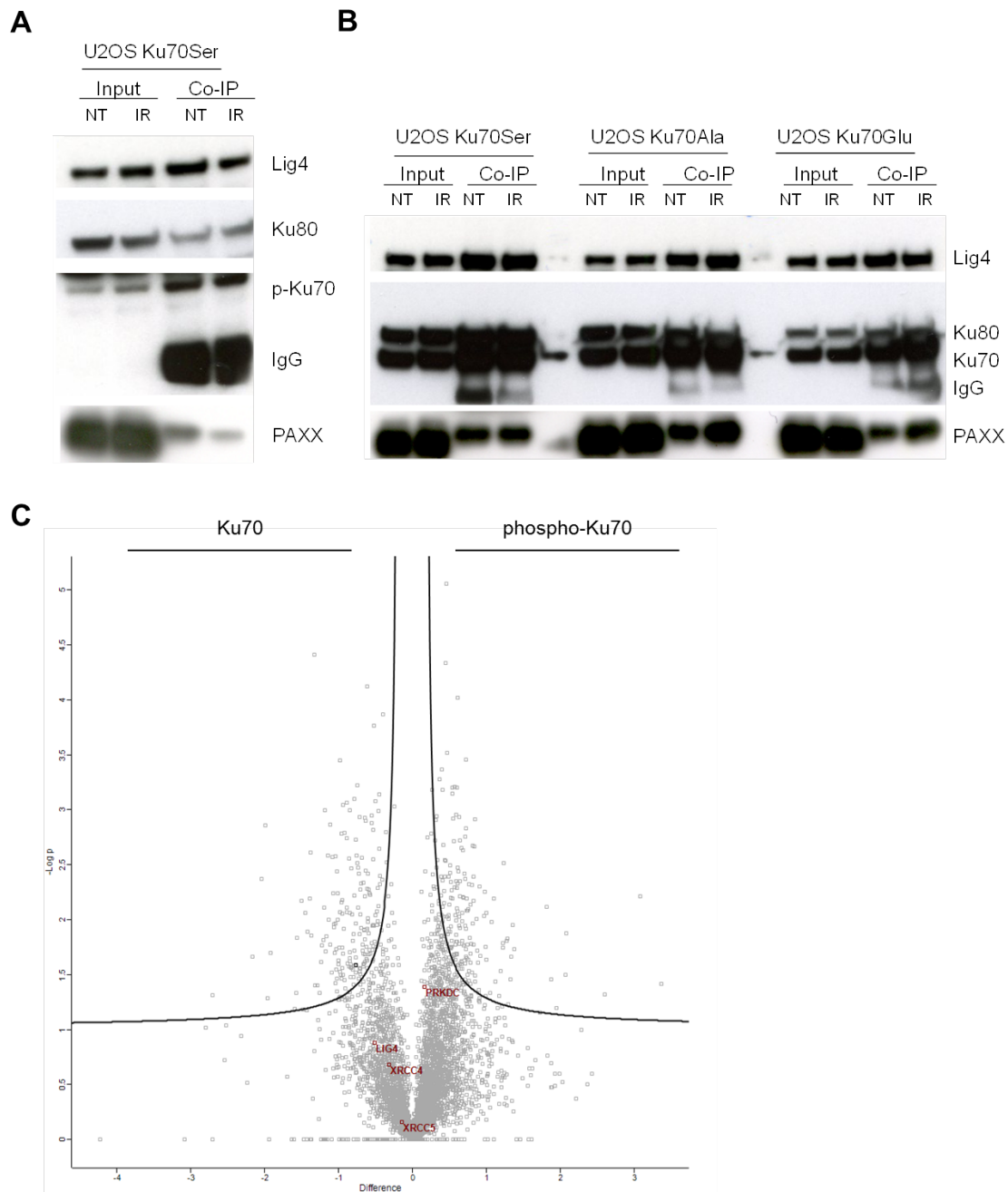


**Figure 1.12: Interaction of phospho-Ku70 in the NHEJ-complex** (A) Co-immunoprecipitation in U2OS cells shows that phospho-Ku70 interacts with Ku80, Ligase 4 and PAXX. (B) Similarly Ku70 mutants show interaction with Ku80, Ligase 4 and PAXX. (C) Whole cell protein extracts of transfected HME Ku70Ser (HME 2464) cells were co-immunoprecipitated, resolved by SDS-PAGE and digested with trypsin. Peptides were analysed through a label-free-quantification (LFQ) - approach using an orbitrap mass analyzer.

### 1.3.3 Dissociation kinetics of Ku70Ala from the DNA DSB is decelerated compared to Ku70Ser

The Ku protein is the very first protein to be recruited to a DSB. It is a major DNA DSB sensor as well as a recruitment factor for core NHEJ proteins to assure proper repair. After the ligation of the break the Ku protein dissociates from the DNA. Proper recruitment and dissociation of the Ku heterodimer is a necessary requirement to provide faithful DNA repair and homeostasis. We measured the recruitment and release kinetics of Ku70Ser and Ku70Ala on DSB sites by using a live cell imaging approach with induced DSBs by microirradiation (UV 405nm). The same conditions as in Figure 1.11 C, that were already shown to induce DSBs were applied. To follow Ku70 kinetics we transfected GFP-coupled Ku70Ser and Ku70Ala into U2OS cells. After microirradiation, cells were followed up to 240min. and pictures were taken every 10min. (see Figure 1.13 A). As shown in Figure 1.13 B, recruitment kinetics are similar in Ku70Ser and Ku70Ala cells, reaching their maximum between 30 and 50min. However the fold induction of Ku70 on the DSB reaches approximately 3.1-fold for Ku70Ala, whereas the maximal recruitment is 2.6-fold for Ku70Ser. Dissociation of Ku70Ser from the DNA is much faster and reaches 50% at 150min. Basal levels for the Ku70Ser expressing cells are reached between 190 and 200min. In contrast, Ku70Ala cells reach 50% only after 220min, and do not reach basal levels within the 240min. These data indicate that phosphorylated-Ku70 is released from the DNA strand break more rapidly than Ku70Ala. Based on the results we obtained on the  $\gamma$ -H2AX kinetics we suppose that Ku70Ala remains on the DSB because of persisting non-repaired DSB and that Ku70Ser is released after the fulfilment of DSB repair by NHEJ.

One of the mechanisms that were described to be required for Ku release is neddylation, a prerequisite for subsequent ubiquitination of the Ku heterodimer [128]. Intrigued by the observation that phosphorylation of Ku70 favours its release, we asked whether inhibition of neddylation with MLN 4924 similarly blocks Ku70Ala and Ku70Ser from their release and if DNA DSB repair is equally impaired after



neddylaton inhibition. Figure 1.13 C depicts Ku70Ser and Ku70Ala dissociation kinetics after treatment with 3  $\mu$ M MLN 4924 (1h). Maximal recruitment of Ku70Ser (6.4-fold) and Ku70Ala (6.1-fold) after MLN 4924 treatment are approximately 2-fold compared to conditions without MLN 4924. Dissociation of Ku70Ser and Ku70Ala is severely hampered in both cell lines, with only 20-25% of Ku70 dissociated at 240min. Inhibition of neddylation dependent ubiquitination thus blocks the release of Ku70Ser and Ku70Ala in a similar manner. Moreover the DNA repair of DNA DSB, measured by  $\gamma$ -H2AX resolution is equally inhibited in Ku70Ser and Ku70Ala cells after inhibition of neddylation (see Figure 1.13 D) compared to non-treated conditions where  $\gamma$ -H2AX disappears faster in Ku70Ser cells (see Figure 1.10 C). Based on these results we suggest that the differences in Ku70 release depicted in Figure 1.13 B are due to persisting DSB in Ku70Ala cells compared to Ku70Ser. We argue that phosphorylation on S27 and S33 Ku70 is necessary for the proper release of Ku70Ser by neddylation dependent ubiquitination from the DNA, as well as DSB repair.

### 1.3.4 Phosphorylation of Ku70 regulates NHEJ and HR repair activity

The Ku protein is an important regulator of DNA DSB repair. It is an invaluable factor for NHEJ, and has a dominant negative effect towards other DNA repair pathways, such as HR [195]. We tested whether phospho-Ku70 promotes quantitatively measurable differences in NHEJ and HR efficacy, compared to non-phosphorylated-Ku70Ala cells. We used two cell systems, GC92 [377] and U2OS HREJ, which have both an integrated reporter construct, to measure the repair after expression of the endonuclease I-SCEI. The activity of NHEJ is measured via the expression of CD4, that is induced upon I-SCEI transfection and after excision of the internal fragment containing the H2Kd and CD8 genes (see Figure 1.14 A). H2Kd expression was monitored before transfection to be about 97-99% in all cell lines (see Appendix B, Figure 5 A) as a control. Equal expression of I-SCEI was verified by western blot (see Appendix B, Figure 5 B). As a negative control an

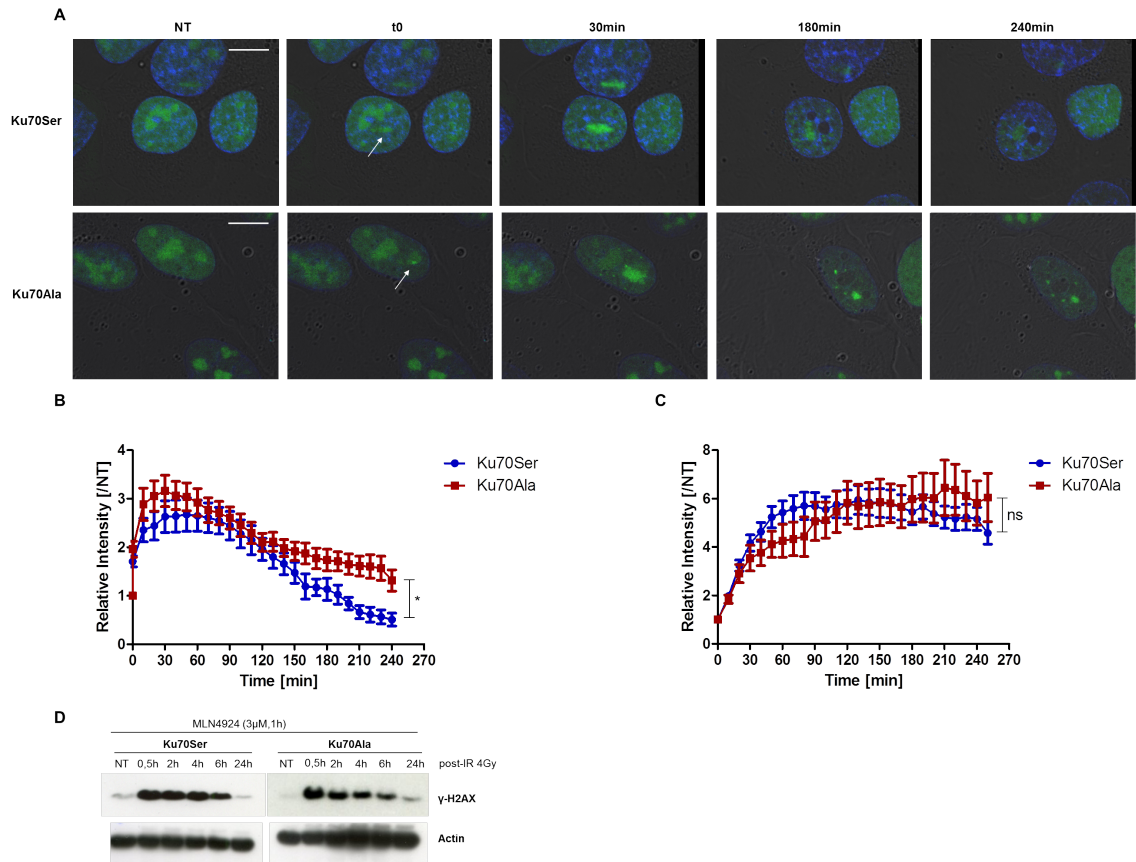


**Figure 1.13: Ku70 DNA DSB dissociation kinetics** (A) Representative pictures of dissociation kinetics in GFP-Ku70Ser and GFP-Ku70Ala cells. Pictures depict cells before (NT), shortly after (t0) and at three time points after microirradiation (405nm). White arrows point to the damage site. (B) Relative intensity fold change based on the initial fluorescence intensity in NT cells. n=20 (Ku70Ser); n=27 (Ku70Ala). Unpaired t-test,  $p < 0.05 = *$ . Scale bar: 10 $\mu$ M. (C) Relative intensity fold change based on the initial fluorescence (NT) after treatment of the cells with the NEDD8 inhibitor MLN 4924 (3 $\mu$ M, 1h before microirradiation). n= 19 (Ku70Ser); n= 11 (Ku70Ala), Unpaired t-test, non-significant. (D) Representative Western Blot depicting  $\gamma$ -H2AX after pre-treatment with neddylation inhibitor MLN4924 (3 $\mu$ M, 1h) and irradiation (4Gy). Actin was used as a loading control.

empty transfection plasmid was used (see Appendix B, Figure 5 A).

The percentage of cells expressing CD4 in Ku70Ser and Ku70Ala cells after I-SCEI induction, depicted in Figure 1.14 A, shows an elevated expression in the Ku70Ala cells compared to Ku70Ser. This suggests that NHEJ activity is increased in Ku70Ala cells compared to Ku70Ser after enzymatic DSB induction. Moreover we tested whether G1-dependent NHEJ in GC92 Ku70Ala cells, had a delayed DNA DSB repair activity compared to GC92 Ku70Ser cells, similar to

what we have previously observed for the non-synchronized U2OS cells after irradiation. For this we synchronized the transfected GC92 cells in the G1 cell cycle phase with mimosine over night and irradiated them 1h after mimosine removal (see Appendix B, Figure 6). As depicted in Figure 1.14 B, the Ku70Ala expressing cells showed a slowed down foci resolution after 2 and 4h, similar to the observations seen in non-synchronized U2OS cells (see Figure 1.10 B). These data thus indicate that even when NHEJ efficiency after enzymatic DSB induction is higher in the Ku70Ala cells, this repair process is aberrant after induction of complex DSBs after irradiation, resulting in persisting DSB when compared to Ku70Ser cells. Ku70Ala cells thus have a DSB repair defect that is specific to NHEJ activity after irradiation.

HR activity was measured through the expression of GFP, after a recombination event. As for the GC92 cells, equal expression of I-SCEI was evaluated via western blot (Appendix B, Figure 4 C) and an empty transfection plasmid was used as negative control (Appendix B, Figure 4 A). To exclude any cell cycle dependent events, cycle distribution was measured before and after transfection. The cell cycle was similar in all cell lines (Appendix B, Figure 4 B). The percentage of cells expressing GFP is slightly, but significantly increased in the Ku70Ser expressing cells compared to the Ku70Ala expressing cells (see Figure 1.14 C). This indicates that Ku70Ser expressing cells have an elevated activity of HR, compared to Ku70Ala cells. This observation is not due to a higher proportion of these cells in S/G2.

To conclude, these data indicate that the phosphorylation of Ku70 can influence the activity of the two main DNA DSB repair pathways, NHEJ and HR.

### **1.3.5 Aberrant DSB repair in Ku70Ala cells is at the origin of chromosomal aberrations and chromosomal translocations**

The observations made on a delayed  $\gamma$ -H2AX foci resolution, an increased amount of hyperploidy, and the persistence of the Ku70Ala mutant on the DSB after

microirradiation, led us to further characterize the quota of genomic instability at the chromosome level. Irradiation can induce chromosomal aberrations like dicentrics, acentrics, ring structures or chromosomal translocations when DSB are left unrepaired and/or rejoined erroneously.

We analysed genomic instability in two different cell lines, U2OS (osteosarcoma) and HME (mammary gland) expressing Ku70Ser and Ku70Ala. Chromosomal aberrations in the U2OS cell lines were measured by counting dicentrics, acentrics and ring structures visible before and after irradiation (2Gy,48h) using DAPI, centromer and telomere staining (see Figure 1.15 A, B) which allowed us to deduce the amount of chromosome breaks. As depicted in Figure 1.15 C and D, similar amounts of chromosomal aberrations/breaks are found under non-treated conditions in Ku70Ser and Ku70Ala expressing cells. After irradiation, the Ku70Ala expressing cells show a greater amount of chromosomal aberrations/breaks than phosphorylated Ku70Ser expressing cells, 160 to 118 DSB, respectively. These observations further underline the increased genomic instability that is severely enhanced in non-phosphorylable Ku70Ala expressing cells and together with the observation of a slowed down repair process ( $\gamma$ -H2AX) argue for a repair defect in the Ku70Ala expressing cells.

To consolidate this result we tested the amount of chromosome translocations in the non-cancerous HME cell line, immortalized by the expression of hTert (Telomerase reverse transcriptase). In contrast to the U2OS cells ( $\simeq$  79 chromosomes), this cell line has a quasi-normal diploid karyotype with 46 chromosomes. This makes it possible to conduct a multi-FISH approach, where each chromosome is "painted" with a unique colour. After transfection with the Ku70-mutants Ku70Ser and Ku70Ala (Figure 1.16 A), the chromosome numbers (46, Ku70Ser; 45-47 Ku70Ala) and karyotype aberrations were similar in both transfected cell lines, except that a proportion of Ku70Ala cells showed an additional translocation der(13)+(5;13;13) (40%) (Figure 1.16 C, NT condition). After irradiation (4Gy, 24h) both cell lines showed an increase in chromosome translocations beyond those identified during non-treated conditions (Figure 1.16 C, IR condition). Ku70Ser cells had a mean of 2.2 translocations/metaphase (45-57

chromosomes/metaphase), compared to the Ku70Ala cells with 3 translocation-s/metaphase (45-51 chromosomes /metaphase) (Figure 1.16 B). However, both cell lines also showed metaphases without additional chromosomal translocations after irradiation, this was the case for 55% (11 metaphases; total of 20 metaphases) in Ku70Ser cells and 23.8% (5 metaphases; total of 21 metaphases). Besides chromosomal translocations we also found aberrations, such as deletions, chromosome fragments, acentric fragments and double minutes, all signs of genomic stability in both cell lines.

In summary these results underline, in two different cell systems, that Ku70Ala cells accumulate a higher proportion of chromosome aberrations and translocations in a majority of irradiated cells compared to Ku70Ser cells. We suggest that this is due to a delayed repair process at the DSB.

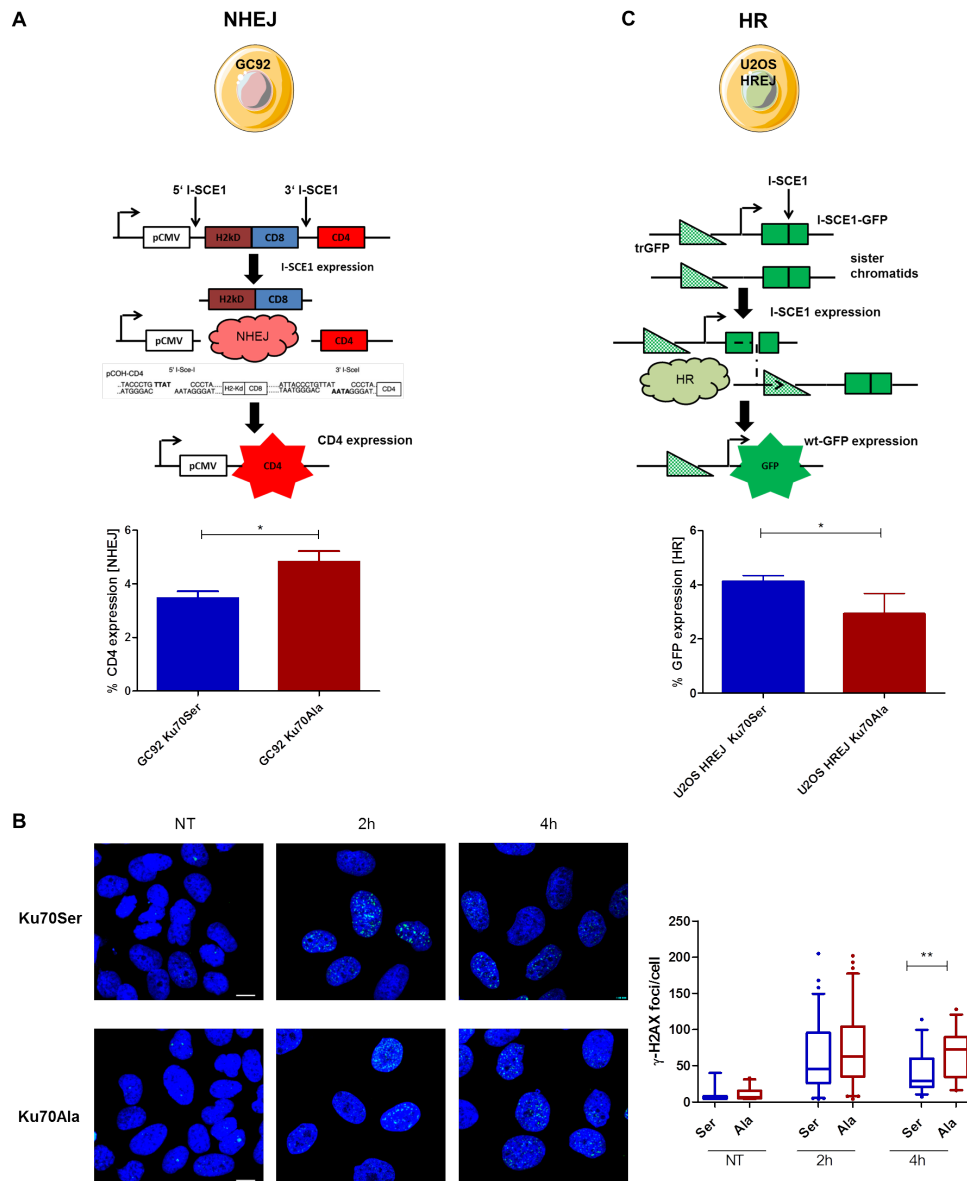


**Figure 1.14: NHEJ and HR efficiency** (A) NHEJ activity was measured using the human fibroblast cell line GC92 (SV40-transformed) that has the pCOH-CD4 (cohesive ends) reporter construct integrated intrachromosomally. Upon cleavage by I-SCEI a fragment containing the H2Kd and CD8 genes is excised. Rejoining of the flanking ends by cNHEJ brings the pCMV promoter closer to the CD4 gene, which promotes its expression. The CD4 expression on the cell surface can be detected via a fluorescence labelled CD4-antibody and flow cytometry. Results represent values that were calculated as: (I-SCEI-transfection events) - (control-transfection events).  $n = 4$ . Unpaired t-test,  $p < 0.01 = *$ . (B) Left: Representative images of  $\gamma$ -H2AX foci in Ku70Ser and Ku70Ala expressing cells after synchronization in G1. Right: Results after automated quantification of  $\gamma$ -H2AX foci. Cells were scored positive, when at least 3 foci were detected. Per cell line at least 50 cells have been evaluated. Graphs represent data as boxplots with median, 1st and 3rd quartile, upper and lower extreme whiskers at 95 and 5 percentiles, outliers are shown as dots,  $n = 2$ . Unpaired t-test,  $p < 0.001 = **$ . Scale bar:  $10 \mu\text{M}$  (C) HR activity was measured using the U2OS HREJ cell line that expresses the integrated reporter construct pDR-GFP. The reporter is composed of two inactive EGFP genes. The upstream GFP gene is truncated, the gene downstream of the promoter has an integrated I-SCEI cleavage site and is therefore inactive. Upon I-SCEI expression the cleaved GFP gene recombines with the truncated GFP gene on the sister chromatid, resulting in the expression of GFP that can be measured via flow cytometry. Results represent values that were calculated as: (I-SCEI-transfection events) - (control-transfection events).  $n = 6$ . Unpaired t-test,  $p < 0.01 = *$ .

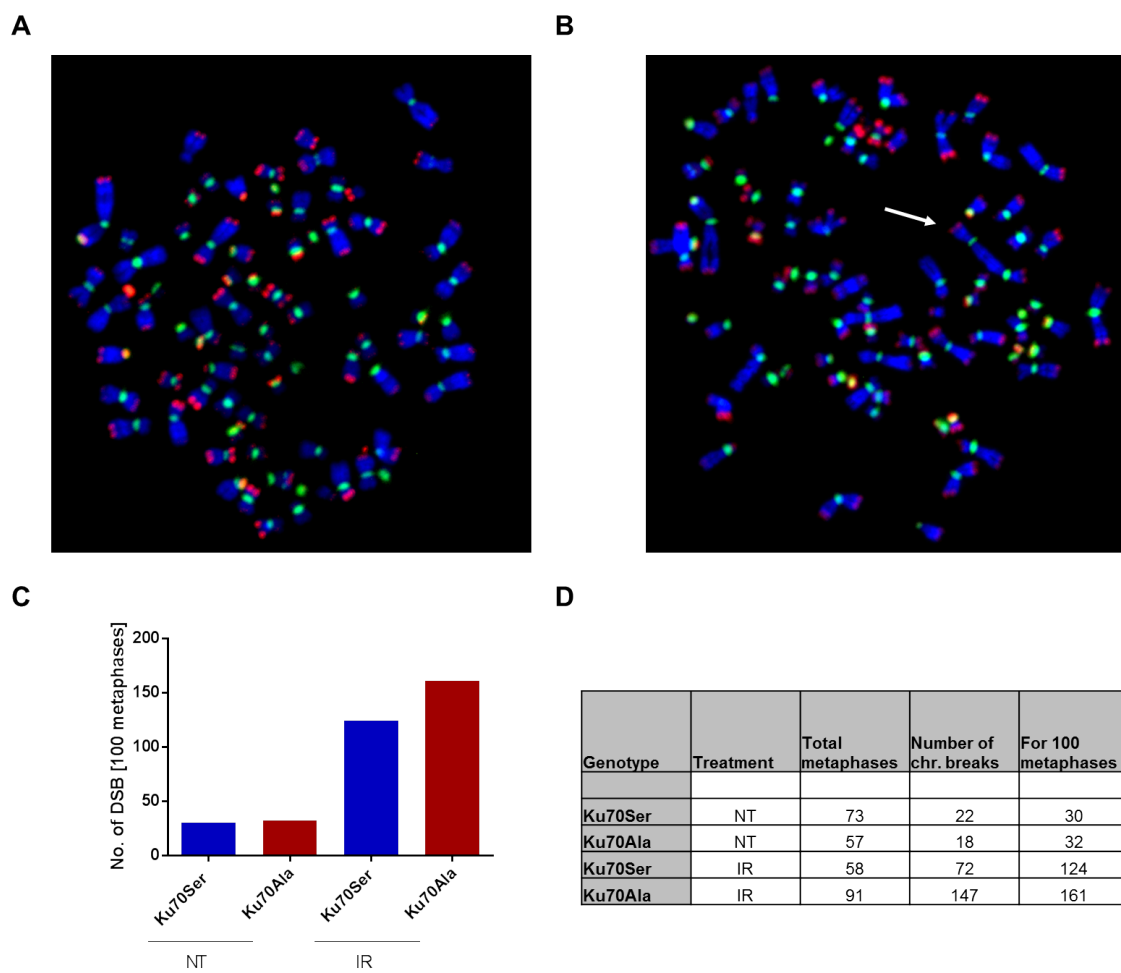


**Figure 1.15: Chromosomal aberrations** (A) Representative picture of a metaphase in non-treated conditions. (B) Representative metaphase of  $\gamma$ -irradiated (2Gy) cells (48h). Arrow indicates a dicentric chromosome. (C) Numbers of unpaired chromosomal DSB during the first metaphase (48h) after irradiation (2Gy). (D) Numbers of counted chromosomal aberrations and extrapolation to 100 metaphases for each cell line.

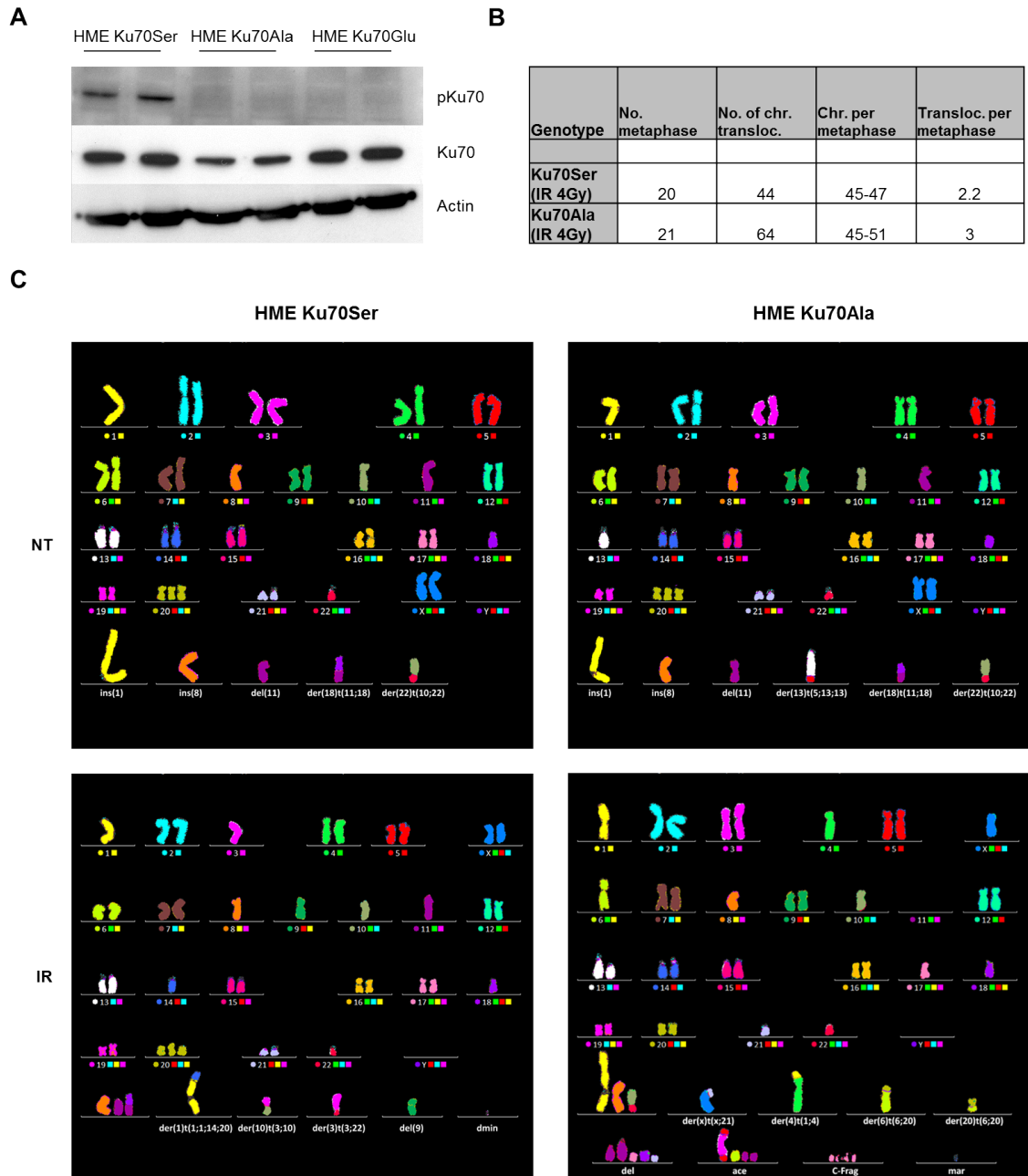


**Figure 1.16: Chromosomal translocations** (A) Western Blot showing the HME cell lines after transfection with pEBV vector, and verification of phospho-Ku70 expression. (B) The number of chromosomal translocations/metaphase is higher in Ku70Ala compared to Ku70Ser cells. (C) Examples of 4 metaphases analyzed. NT Ku70Ser: 46, XX, ins(1), ins(8), -10, del(11), der(18)t(11;18), +20, der(22)t(10;22) [18]; NT Ku70Ala: 46, XX, ins(1), ins(8), -10, del(11), der(18)t(11;18), +20, der(22)t(10;22), der(13)t(5;13;13) [9]; after irradiation only those translocations that are distinct compared to the non-treated condition have been counted. Other markers of genomic instability: dmin, double minute; del, deletion; ace, acentric fragment; C-Frag, chromosomal fragment; mar, marker





## Chapter 2

# Generation of a humanized knock-in (KI) mouse model to study p-Ku70's role *in vivo*

To study the role of Ku70 in the pathophysiology of chronic lymphocytic leukaemia and cancer development more particularly, an *in vivo* model seemed best suited. We therefore collaborated with the Mouse Clinical Institute (Strasbourg, France) for the development of a humanized KI mouse expressing Ku70Ser and Ku70Ala. For the development of such mice the sequence homology, concerning the human residues 27 and 33 were studied in mice. The overall protein sequence homology is about 90% with 83% of aa being identical. Compared to human, mice have a 2 aa shifted sequence of Ku70 (see Figure 2.1 A). The mutation strategy was to humanize the area around aa 21-31 in mice (corresponding to aa 23-33 in human) and to mutate G25,S31 in mice to either S25,S31 (Ku70Ser) or A25,A31 (Ku70Ala). The principal strategy of the KI mouse model generation is depicted in Figure 2.1 B. Briefly, the mouse embryonic stem (MES) cells were obtained from a Bl6/N mouse (wt mouse) background. A gene targeting vector coding for the humanized Ku70Ala and Ku70Ser alleles was added to the MES for homologous recombination. Recombination efficiency of approx. 4%, tested by neomycine resistance

and PCR screening, were obtained. The positive selected MES, were than transferred into blastocysts of a BALB/cN background to obtain chimeric mice. The male chimeras were backcrossed to female wt-mice (expressing the Cre-protein to autoexcise the neomycine resistance) to obtain a first heterozygous generation (F1), expressing a murine wt-Ku70 allele and a humanized KI-Ku70Ala or KI-Ku70Ser allele, respectively. To obtain homozygous mice, expressing humanized KI-Ku70Ala and KI-Ku70Ser, heterozygous F1 mice were crossed, leading to the generation of three possible scenarios for F2 progeny: homozygous wt-Ku70 ( $Ku70^{-/-}$ ), heterozygous wt-Ku70/KI-Ku70Ala ( $KI-Ku70Ala^{KI/-}$ ) or KI-Ku70Ser ( $KI-Ku70Ser^{KI/-}$ ), homozygous KI-Ku70Ala ( $KI-Ku70Ala^{KI/KI}$ ) or KI-Ku70Ser ( $KI-Ku70Ser^{KI/KI}$ ) expressing mice.

The ratios for born viable homozygous  $KI-Ku70Ala^{KI/KI}$  and  $KI-Ku70Ser^{KI/KI}$  mice were equal, without any gender specific differences. Of 48 newborns after 6 crossings, 20 were female (42%) and 28 male (58%) for the KI-Ku70Ser mice. For KI-Ku70Ala mice, out of 40 newborns after 6 crossings, 21 were female (52%) and 19 male (48%).

Previous reports of Ku70 KO mice, showed that these mice have an important growth delay leading to 40-60% smaller littermates, than controls [137]. We thus evaluated growth of newborns over 3 weeks, but did not observe any differences in body ratios between  $KI-Ku70Ser^{KI/KI}$  and  $KI-Ku70Ala^{KI/KI}$  mice (see Figure 2.2 A,B).

To further determine and verify the cellular aspects that we have seen in the human cancer cell line U2OS, we generated mouse embryonic fibroblasts (MEFs) of homozygous  $KI-Ku70Ser^{KI/KI}$  and  $KI-Ku70Ala^{KI/KI}$  embryos. We determined the growth of these cells and their susceptibility to cell death after irradiation. Preliminary results on the cell doubling monitored over 7 days, shows a growth defect in  $KI-Ku70Ala^{KI/KI}$  cells compared to  $KI-Ku70Ser^{KI/KI}$  cells with and without genotoxic stress (irradiation 2Gy). This could argue for a intrinsic genomic instability of these cells, compared to KI-Ku70Ser. In agreement with these

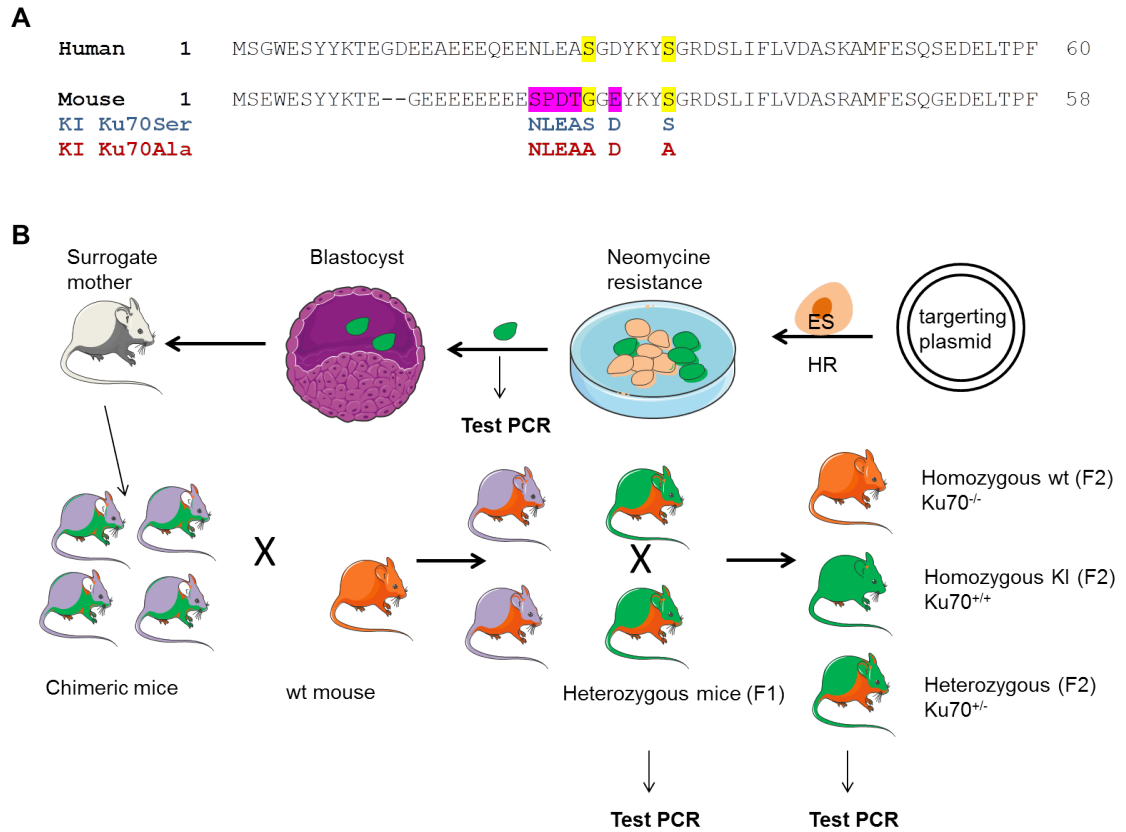


**Figure 2.1: Humanized KI mouse strategy** (A) Comparison of the protein sequences (aa 1-60/58) in human and mice for the Ku70 protein. Yellow underlined aa are the serine residues 27 and 33 in human and the corresponding aa 25 (glycine) and 31 (serine) in mice. The residues underlined in pink are the additionally mutated residues in mice to obtain a humanized protein sequence, surrounding the phosphorylation sites. The sequences in blue (Ku70Ser) and red (Ku70Ala), correspond to the final aa sequence of the Ku70 protein in each of the KI models, respectively. (B) Generation of a KI model. With the help of a targeting vector, containing the nucleotide sequence corresponding to the substituted aa, mouse embryonic stem cells were transfected. Selection with an antibiotic resistance and subsequent PCR analysis revealed successfully recombined ES cells. These could be transferred into an empty donor blastocyst and carried out by a surrogate mother mouse. The born chimeras are composed of cells, from the recombined ES cells and from the donor blastocyst. To select mice that have integrated the KI in their reproductive organs, they were backcrossed with the wt-mouse to give heterozygous progeny (F1). Crossing of the F1 generation can ultimately produce homozygous mice that express KI-Ku70Ser or KI-Ku70Ala on both gene alleles.

findings, is the evaluation of cell death by DIOC/IP, in non-treated and in 2Gy-irradiated cells, cell death is increased in KI-Ku70Ala compared to KI-Ku70Ser cells after non-treated conditions and genotoxic stress with irradiation (2Gy, 4Gy) or phleomycin (100 $\mu$ M, 1h).

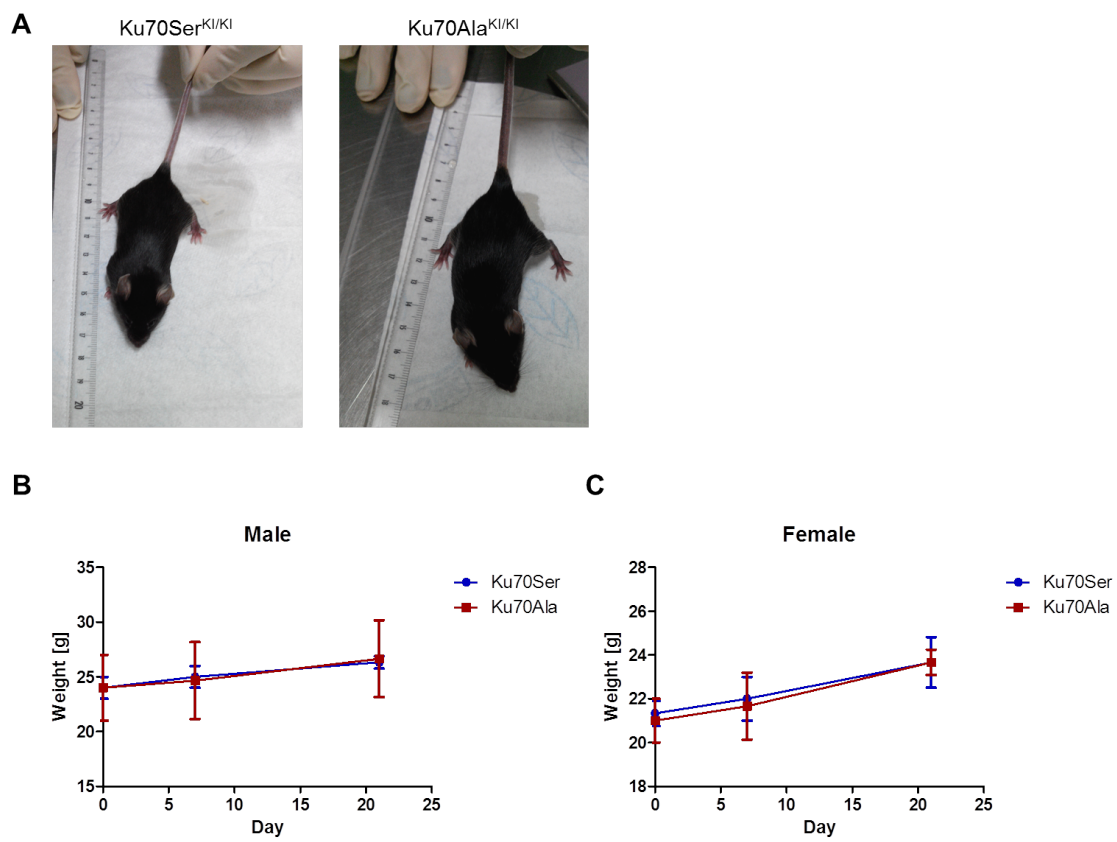


**Figure 2.2: Homozygous KI-Ku70Ser and KI-Ku70Ala mice** (A) Picture of the established humanized KI-Ku70Ser and KI-Ku70Ala KI mouse lines. (B) Comparison of weight [gram] of male and female homozygous KI-Ku70Ser and KI-Ku70Ala mice; n=3.

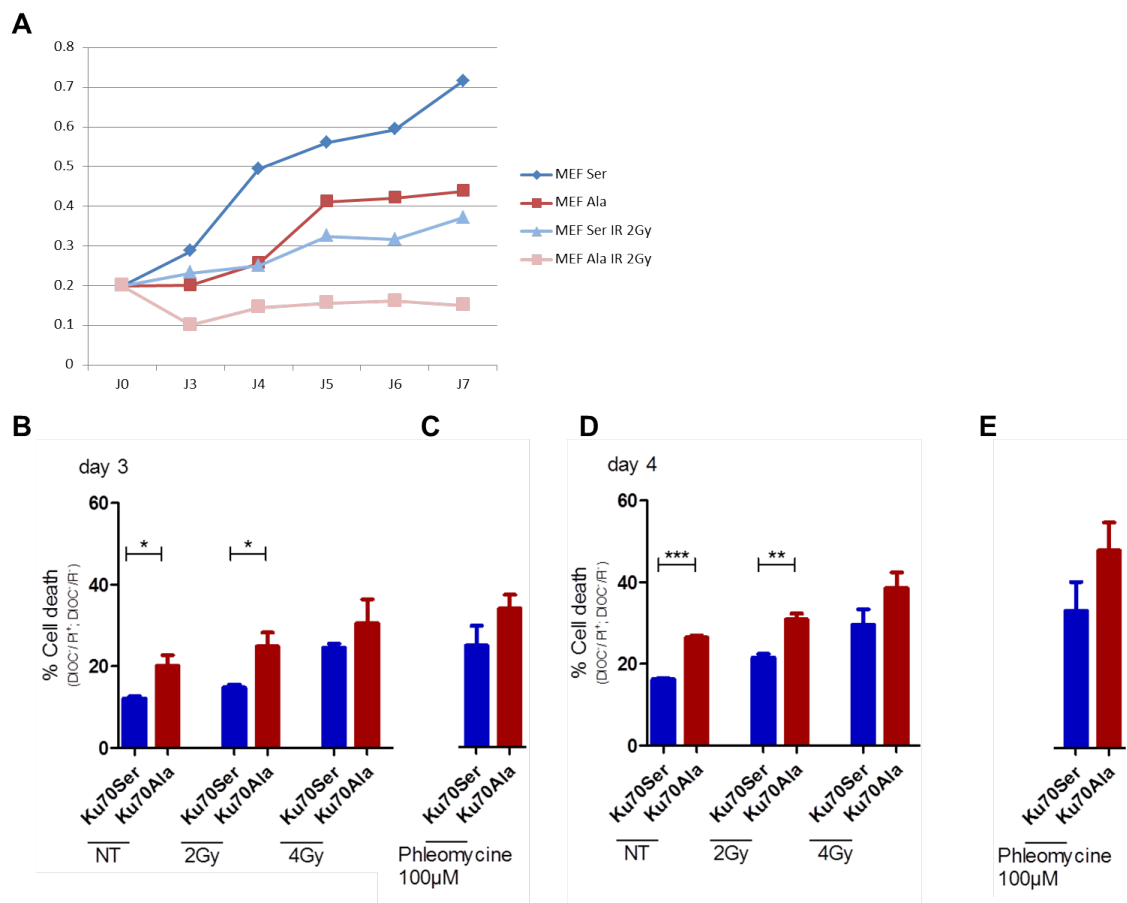


**Figure 2.3: Phenotypic characterization of MEF's generated from KI-Ku70Ser<sup>KI/KI</sup> and KI-Ku70Ala<sup>KI/KI</sup> mouse lines** (A) Cell growth is impaired in KI-Ku70Ala<sup>KI/KI</sup> compared to KI-Ku70Ser<sup>KI/KI</sup> MEFs, independent of genotoxic stress. One representative experiment is depicted. (B) Cell death is impaired for KI-Ku70Ala<sup>KI/KI</sup> compared to KI-Ku70Ser<sup>KI/KI</sup> expressing cells in non-treated conditions and at 2Gy. n=3. Unpaired t-test,  $p < 0.01 = *$ ,  $p < 0.001 = **$ ,  $p < 0.0001 = ***$ .



# Part V

## Discussion





This study was initiated on the basis of a differential apoptosis resistance revealed between R-CLL and S-CLL patient subsets. Intensive research in this field uncovered that resistance to apoptosis may be due to upregulation of an erroneous type of NHEJ, characterized by an increase in the amount of junctional deletions [367] and chromosomal aberrations [366] in R-CLL cells compared to S-CLL. Furthermore a telomeric deregulation characterized by shortened chromosome ends and the presence of Ku70 and 53BP1 at telomeres of R-CLL patients further underlined the potential effects of a deregulated NHEJ in these patient derived samples [368]. Finally, R-CLL cells were shown to overexpress a PTM on Ku70 (phospho-S27-,S33- Ku70) and a first study evaluated the impact of this phosphorylation on DNA repair [369]. This current study aimed to further characterize the impact of phospho-Ku70 on the dynamics on the DSB site. We first established that phospho-Ku70 is an actor in radioresistance and characterized our cellular model on phenotypic aspects. Then we observed that phospho-Ku70 is necessary for proper DNA release after DNA repair, that it impacts on both NHEJ and HR repair pathway efficiency and that it maintains genomic stability compared to non-phosphorylatable Ku70Ala expressing cells. Moreover this study initiated the generation of a KI mouse model with the aim to study the role of phospho-Ku70 *in vivo*.



## *in vitro* study

### Phosphorylation of Ku70 confers radioresistance

In this study we established an *in vitro* system using human cell lines that enabled us to evaluate the biological impact of Ku70 phosphorylation. To overcome Ku-deficiency associated cell death in a human cell system [380], we had to use a system in which we can downregulate endogenous Ku70, while at the same time expressing exogenous Ku70. The exogenously expressed Ku70 mutants contained the desired mutations for wt (Ku70Ser), non-phosphorylatable (Ku70Ala) and phosphomimetic (Ku70Glu).

Even before the Ku protein was identified to be a NHEJ core factor, the impact of radiation on Ku70 and Ku80 defective CHO cells was demonstrated [33, 34, 381]. Since that time multiple studies have evaluated the radioresistance that is conferred by both subunits in different models ranging from mouse [293, 294] to human [382, 383] due to Ku's role in DNA DSB repair. In this present study we establish that the mutation of the serine residues on position 27 and 33 cause a growth defect (Figure 1.3), apoptosis induction (Figure 1.5) and a radioresistance phenotype (Figure 1.4). We suggest that all of these observations are linked through a DNA repair defect present in the mutated Ku70 expressing cell lines, as they are noticed after double strand break induction with  $\gamma$ -irradiation or phleomycine.

Several studies have linked Ku70 to apoptosis-regulation, independent to its DNA repair function. We think that this is not the case for the phospho-Ku70 protein and its mutants. Ku70 dependent apoptosis induction is established through its interaction with the pro-apoptotic protein Bax, regulated by PTM [267–271]. Using

co-immunoprecipitation we do not observe differences in Bax interaction between Ku70Ser, Ku70Ala and Ku70Glu before and after damage induction (Figure 1.6). In contrast to the study by Bouley et al. [369] we cannot establish any extended cell cycle checkpoint response at 2 or 4 Gy irradiation (Figure 1.7). Checkpoint responses are heavily regulated by the protein p53 and whereas ZR75.1 cell lines have a fully functional p53-protein, the U2OS cell line has an upregulated hMDM2 level, the antagonist of p53. Differences in cell cycle dynamics might thus derive from this cell line specific difference.

Finally, we show that expression of a non-phosphorylatable Ku70 protein causes the accumulation of polyploid cells over time after irradiation (Figure 1.8), a characteristic that was already documented for Ku80 haploinsufficient human somatic cells, suggesting that accumulation of genomic instability is a result of defects in DNA repair [380]. The accumulation of hyperploid cells might also point to a checkpoint defect in G2/M-phase in the Ku70Ala cells. This would provide the possibility to drive the cell cycle from G2 to M and interphase in the presence of unrepaired DNA breaks (checkpoint adaption and checkpoint slippage) increasing the amount of aneuploidy and genomic instability, and finally leading to mitotic catastrophe [249]. Interestingly, Shang et al. provide evidence that spindle formation and mitosis are regulated by DNA-PKcs and Ku mediated phosphorylation of Chk2 (T68) [384]. Inhibition of DNA-PK results in aberrant spindle formation during mitosis causing polyploidy and mitotic catastrophe. It might thus be of interest to examine whether spindle formation is affected in Ku70Ala expressing cells.

To summarize, the Ku protein, and its two subunits individually have been associated to the maintenance of radioresistance by their DNA repair function in multiple studies. We show for the first time that phosphorylation on S27 and S33 on Ku70 has significant impact in the maintenance of a radioresistant phenotype.

## **The phosphomimetic (Ku70Glu) fails to reproduce the results of the phosphorylated Ku70Ser**

The results obtained for the phosphomimetic (Ku70Glu) expressing cell line are less pronounced than the phospho-mutant (Ku70Ala) expressing cell line, when compared to the Ku70Ser expressing cells. This is most probably due to the importance of the phosphate group rather than the negative charge in this specific region. The results are in line with the study of Bouley et al. [369]. Moreover, we observed that the phosphomimetic (Ku70Glu) shows different nuclear localization compared to Ku70Ala and Ku70Ser cells, when co-expressed with the fluorescent protein mEOS (see Figure Appendix B, Figure 7) under untreated conditions. This indicates that the phosphomimetic protein has lost key functions to retain normal localization [385]. We strongly believe that the nuclear regions avoided by the phosphomimetic are nucleoli, nuclear regions that are rich in ribosomes and rRNA transcription that now are becoming more and more evident to have an active crosstalk with DNA repair [386]. As a side note, the proteomics approach we performed shows a strong preference for phospho-Ku70 to interact with ribosomal proteins (data not shown).

In summary, the phosphomimetic cell line (Ku70Glu) does not mimic the phosphorylated state of Ku70, most probably due to the importance of the phosphate group in this region. Additionally the phosphomimetic protein did not show similar nuclear localization compared to Ku70Ala and Ku70Ser and its impact in DNA DSB repair was thus no longer pursued.

## **The phosphorylation of Ku70 is part of the NHEJ complex and impacts on DNA DSB repair**

To better situate the phospho-Ku70 protein to the DNA DSB and to underline its function, we ask some easy but yet important questions to localize it to the NHEJ complex and to the DNA DSB. We show that phospho-Ku70 interacts with

core factors of NHEJ (Ku80, DNA-PKcs, Ligase 4, XRCC4 and PAXX) using two different approaches (Figures 1.12 A-C). The phosphorylation however does not seem to be a prerequisite for NHEJ-complex formation, as the phospho-mutated Ku70Ala and Ku70Glu equally interact with Ku80, Ligase 4 and PAXX. Moreover, we show that phospho-Ku70 localizes to the damaged DNA after genotoxic stress by phleomycine or microirradiation and co-localizes with  $\gamma$ -H2AX (Figure 1.11 A-C). Altogether these data strongly suggest that phospho-Ku70 is part of the NHEJ-complex and localizes on the DNA DSB.

We then evaluated the functional impact of the phosphorylation on the DNA repair by assessing the persistence of the  $\gamma$ -H2AX signal by immunofluorescence and western blot techniques. We observe a delayed  $\gamma$ -H2AX foci/signal resolution in the phosphomutant (Ku70Ala) cells compared to the phospho-Ku70 expressing cells (Ku70Ser) by both approaches (Figure 1.10 B,C). This is in agreement with the study of Bouley et al. [369], who show a delayed  $\gamma$ -H2AX foci resolution in the Ku70Ala expressing ZR75.1 cells thus pointing towards an aberrant DNA DSB repair in these cells.

To better understand the DNA DSB repair defect in the phospho-mutant cell line (Ku70Ala) and as there were no differences in the formation of the core NHEJ complex, we thought that the phosphorylation might have a role in the recruitment and/or dissociation kinetics to/from the DSB. Our experiments using microirradiation induced DNA damage, clearly show that there are no substantial differences in Ku70 recruitment to the DNA damage, however release is hindered up to 240min (4h) in the Ku70Ala cells (Figure 1.13 B), likely due to persisting DNA strand breaks (see  $\gamma$ -H2AX resolution kinetics; Figure 1.10 B,C). A mechanism that was recently described to be important for Ku release is neddylation a precondition for Ku ubiquitination and release [128]. We show here that upon inhibition of neddylation both subunits equally stay and accumulate (approx. 2-fold compared to MLN4924 untreated cells) on the DNA strand break (Figure 1.13 C), this is most likely due to persistent DNA damage (see Figure 1.13 D). Indeed, we observe that neddylation inhibition impacts on the repair kinetics of DNA damage (Figure 1.13 D). This is not due to an intrinsic genotoxic activity of the neddylation inhibitor

MLN 4924, as treatment with the inhibitor alone does not induce  $\gamma$ -H2AX (see Figure 1.13 D (NT conditions)). We suppose that phosphorylation is necessary for repair and neddylation dependent ubiquitination as well as release of Ku70 from the repaired DNA. In this context, it is interesting to note that a ubiquitination site is found on aa K31 on Ku70 [371], which lies in direct proximity to the two phosphorylation sites. It would be interesting to study if this site is ubiquitinated dependent on the phosphorylation of Ku70 at S27,S33 and if this ubiquitination affects the release from the DNA. The possibility that the phosphorylation of Ku70 can impact on its release is not surprising, for example autophosphorylation on DNA-PKcs induces its release from the DNA [387].

Besides its key function in NHEJ the Ku protein is also an important regulator of HR [194–197]. Using a cellular system that enabled us to induce DSB via the endonuclease I-SCEI, we determine the efficiency of NHEJ and HR in Ku70Ala and Ku70Ser cells. We were surprised to see an upregulated NHEJ efficiency for Ku70Ala cells compared to Ku70Ser (Figure 1.14 A), as the  $\gamma$ -H2AX foci suggest a less efficient repair in phospho-mutant cells than Ku70Ser cells. We thus used this cell system and evaluated NHEJ efficiency during G1 after  $\gamma$ -irradiation. As for the U2OS cells,  $\gamma$ -H2AX foci persisted longer in the Ku70Ala expressing cells than Ku70Ser cells at 4h (Figure 1.14 B). This points to differences in the function of phospho-Ku70, for the repair of complex (irradiation) vs. enzymatic induced (I-SCEI) DSB and it might be of interest to pursue this hypothesis. On the other hand HR efficiency is increased in phospho-Ku70 expressing cells compared to Ku70Ala cells. This is interesting as Lee et al. described a cluster of potential phosphorylation sites in Ku70, that when mutated to alanine inhibit HR by persisting on the DSB [196]. It would thus be compelling to further study the mechanisms of phospho-Ku70 in HR regulation.

To conclude, we show that phospho-Ku70 is a member of the NHEJ complex that is found on the DSB site upon damage induction. We further demonstrate that phospho-Ku70 participates in DSB resolution and DNA dissociation after DNA



repair. Moreover phospho-Ku70 seems to regulate HR and NHEJ activity, however the exact mechanisms of this observations have still to be determined.

## **Phosphorylation of Ku70 is important to maintain genomic stability**

Whereas it was long thought that mainly alt-NHEJ contributes to chromosomal translocations it now becomes evident that this is the case in murine, rather than in human systems. In their studies Ghezraoui and Biehs et al. [149, 164, 165] provide evidence that it is the classical NHEJ that induces chromosomal aberrations and translocations accompanied by frequent microhomology usage and long deletions on the junctional sites in human cell systems. Especially the study by Biehs et al. presents a model for this phenomenon, raising the possibility of a resection dependent slow-cNHEJ [165]. We evaluated two different cell lines (U2OS, HME) and show an increased amount of genomic aberrations and chromosomal translocations in Ku70Ala cells compared to Ku70Ser cells, after  $\gamma$ -irradiation. Together with the results on the delayed DSB repair in Ku70Ala and its persistence on the DNA breakage site it would thus be interesting to evaluate if the slow-cNHEJ pathway is favoured by this mutant. It will be crucial to evaluate the junctional sites in the GC92 cell system on present deletions and microhomologies, to further consider this hypothesis [388].

By its function in the regulation of DNA repair, phospho-Ku70 limits the accumulation of chromosomal aberrations and genomic instability upon irradiation.

## *in vivo* study

All the studies performed so far on phospho-Ku70 and its role in DNA repair were performed *in vitro*. These cell models are quite different from the CLL samples in which phospho-Ku70 was originally identified. The establishment of an *in vivo* model has the advantage to study phospho-Ku70's role in lymphopoiesis of B-cells, through the study of V(D)J recombination and to approach the original CLL model in the best possible way. That gives the opportunity to evaluate phospho-Ku70's role in the aetiology of R-CLL. Indeed several studies in mice already showed a link between lymphoma development in Ku70<sup>-/-</sup> and Ku80<sup>-/-</sup> mice [137, 245, 247, 389].

Our preliminary studies focussed on the characterization of the homozygous KI mice. The KI-Ku70Ser<sup>KI/KI</sup> and KI-Ku70Ala<sup>KI/KI</sup> mice do not show any growth defects at 3 weeks, a time point at which a growth defect is already visible in Ku70<sup>-/-</sup> [245] and Ku80<sup>-/-</sup> [246] mice. However we do see some cell growth defects in MEF's isolated from KI-Ku70Ala<sup>KI/KI</sup> compared to KI-Ku70Ser<sup>KI/KI</sup> without treatment or after  $\gamma$ -irradiation (2Gy). Additionally, cell death is more pronounced in MEF's from KI-Ku70Ala<sup>KI/KI</sup> than in KI-Ku70Ser<sup>KI/KI</sup> without treatment and after genotoxic stress.

In summary these results support the *in vitro* study using human cell lines. The cells expressing non-phosphorylatable Ku70Ala show a growth defect and accelerated cell death. In contrast to the *in vitro* studies however, KI-Ku70Ala<sup>KI/KI</sup> show cell growth deficiencies and cell death susceptibility compared to KI-Ku70Ser<sup>KI/KI</sup> already at untreated conditions. This might be due to higher levels of spontaneous,

endogenous damage.

# Phosphorylation and their impact on the NHEJ process- impact of phospho-Ku70

Posttranslational modifications such as phosphorylations, are important cellular fine-tuning mechanisms that help the cell to rapidly adapt towards changing environmental or stress conditions, without the need of *de novo* protein synthesis [370]. For instance we have seen that the DDR signalling by ATM and ATR is mainly regulated by coordinated phosphorylation processes.

During DNA repair and more particularly in NHEJ, phosphorylation processes take place. These are mainly due to the PI3-kinases ATM and DNA-PKcs. All members of the core-NHEJ complex have identified phosphorylation sites and even when for some the functional impact still remains elusive, new data on phosphorylation in NHEJ have recently emerged. The most prominent target of phosphorylation during NHEJ is DNA-PKcs with over 40 phosphorylation sites and clusters, from which 16 are autophosphorylation sites [99, 390]. The phosphorylation of DNA-PKcs (for instance in the Thr2609 or Ser2056 clusters) is important for proper DNA repair. Ablation of phosphorylation by alanine mutations induce impaired DNA repair and radiosensitivity [390]. Additionally, autophosphorylation on DNA-PKcs is required for its proper DNA release [391] and impacts on the recruitment of Artemis [392].

Moreover, the members of the ligation complex, Ligase 4, XRCC4 and XLF are

phosphorylated by DNA-PKcs [118, 393–395], the exact role of the phosphorylation of these sites was not clear for a long time. Considerable progress has been made in this field, showing that XRCC4 phosphorylation by CDK2 is implicated in the recruitment of processing factors like PNK, Aprataxin or APLF [396–398] or that XLF phosphorylation on T181 by AKT delocalizes it into the cytoplasm for degradation after DNA repair [399]. Recently, Melo et al. broadened our understanding of the possible roles of DNA-PKcs dependent phosphorylation by mutating clusters of 8 or 4 phosphorylation sites in the C-terminal domains of XRCC4 and XLF, respectively and demonstrate that these phosphorylation sites are necessary for DNA end tethering, error-free DNA repair by NHEJ and dismantling from the repaired DNA site [400].

Finally, the Ku protein has been shown multiple times to contain phosphorylation sites, however none of them was shown to be necessary for DNA repair [224, 374–376, 401]. The phosphorylation sites identified in our lab are thus the very first *in vitro* and *in vivo* confirmed phosphorylation sites identified in Ku70 that are shown to impact directly on Ku release and DNA DSB repair.

The NHEJ pathway is the major DNA repair process in mammals, active in all cell cycle stages and thus carries a major responsibility to repair a large variety of DNA breaks and end configurations in order to provide genomic stability and prevent carcinogenesis. In this regard the understanding of how post-translational modifications such as phosphorylation regulate the NHEJ pathway is an important parameter not only for the mechanistic understanding of the pathway but also for cancer prevention and treatment.

# What impact could phospho-Ku70 have for the clinic?

The identification of phospho-Ku70 is interesting for the clinics in two ways. First, it is a biomarker that distinguishes high risk CLL patients, from patients with an indolent disease progression. The evolution of certain low risk patients towards the high risk group after chemotherapeutic treatment with fludarabine or chlorambucil, point to the development of a resistance phenotype. The measurement of persistent phospho-Ku70 in patients could thus become a potential risk marker to adapt cancer therapy. Second, the mechanistic insights into phospho-Ku70's functions in DNA repair can be important pieces in the characterization of possible drugging strategies. Indeed, the NHEJ pathway and in particular the DNA-PKcs kinase are considered as attractive target for synthetic lethality in HR or ATM deficient tumours [402–404].

However, this study also highlights the complexity of cellular and cancer biology. Whereas in R-CLL-patients the expression of phospho-Ku70 is associated with an accumulation of genomic instability, this seems not the case for the *in vitro* studies we performed in U2OS and HME cell lines. In our *in vitro* studies phospho-Ku70 is an actor in radioresistance that provides less genomic rearrangements compared to the phospho-mutant. This might be due to the different cellular background these studies have been performed in. Lymphocytes are particularly dependent on the NHEJ pathway as they are noncycling cells and thus do mainly use this repair pathway. Additionally these cells are the only to conduct V(D)J recombination and CSR, two molecular pathway that create gene rearrangement and

genomic diversity dependent on the NHEJ pathway. Thus, the NHEJ pathway and eventually the phosphorylation of Ku70 might have a peculiar importance in these cells, responsible for these differences. It will be of crucial interest to study the role of phospho-Ku70 in lymphocytes, in order to understand if there exist cell type specific differences.

## Part VI

# Conclusion & Perspectives





This study characterized the functional role of the newly identified phospho-Ku70 molecule in the dynamics of DNA DSB repair. We show for the first time its importance in radioresistance, characterizing its role in the NHEJ complex and DNA DSB repair. Still, with this work new questions arise.

In direct association to this work it will be of interest to characterize the molecular mechanisms that drive genomic stability in the Ku70Ala cells. We show that the Ku70Ala cells provide a delayed DNA DSB repair, with a longer persistence of Ku70 on the unrepaired DNA end. We speculate that these end extremities ends could become an attractive target for nucleases like CtIP, favouring end resection with revelation of microhomology sites, accounting for genomic rearrangements [149, 165, 388, 405]. A first step to investigate this hypothesis would thus be to study the junctional sites on microhomologies and/or deletions in Ku70Ala versus Ku70Ser expressing cells using the NHEJ reporter construct in the GC92 cells.

We further suggest that neddylation dependent ubiquitination of Ku70 is hampered in Ku70Ala expressing cells. Interestingly the phosphorylation site on S27 and S33, surround a ubiquitination site K31 on Ku70. It would be interesting to mutate this ubiquitination site (R31) and to evaluate, if this mutant has similar release kinetics as Ku70Ala. This would suggest that phosphorylation on S27 and S33 is necessary for ubiquitination on K31 and Ku70 release.

Another intriguing question arises through the differences we observe between the usage of HR and NHEJ between Ku70Ser and Ku70Ala expressing cells. Using the microirradiation approach we could explore whether access of HR factors like BRCA1, MRN, RPA or RAD51 are hindered by Ku70Ala, thus diminishing the access and initiation of this repair process.

Moreover as stated in the introduction, NHEJ factors and in particular the Ku proteins, Ku70 and Ku80 are absolutely required for the maintenance of telomeres. Given the particular role that Ku has on telomeres acting as a double edged sword it would be compelling to shed light on phospho-Ku's role. This is further underlined by the data that R-CLL patients have severely shortened telomeres.

In the second part of this study we introduce the *in vivo* KI mouse model we generated. This model will be of particular interest when studying the role of phospho-Ku70 in V(D)J- recombination and lymphocyte development conducted in a collaboration with L. Deriano (Institut Pasteur). The use of an *in vivo* model gives us the opportunity to investigate phospho-Ku70's role in lymphocytes in a physiological setting and after p53-KO, a condition that was already shown to favour the generation of lymphomas and cancer in Ku-deficient mice [247].

Finally, we started a collaboration with J. Demmers (Proteomics Center Rotterdam) to establish a differential proteomics analysis between R-CLL and S-CLL patient samples based on the interaction with phospho-Ku70 and Ku70. These data should help to establish phospho-Ku70 specific binding partners in R-CLL and S-CLL, thus helping to evaluate critical binding partners and pathways. Additionally we hope that this approach could give further insight into the kinases and phosphatases involved in the (de-)phosphorylation of Ku70.

## Part VII

### Appendix B: Supplementary



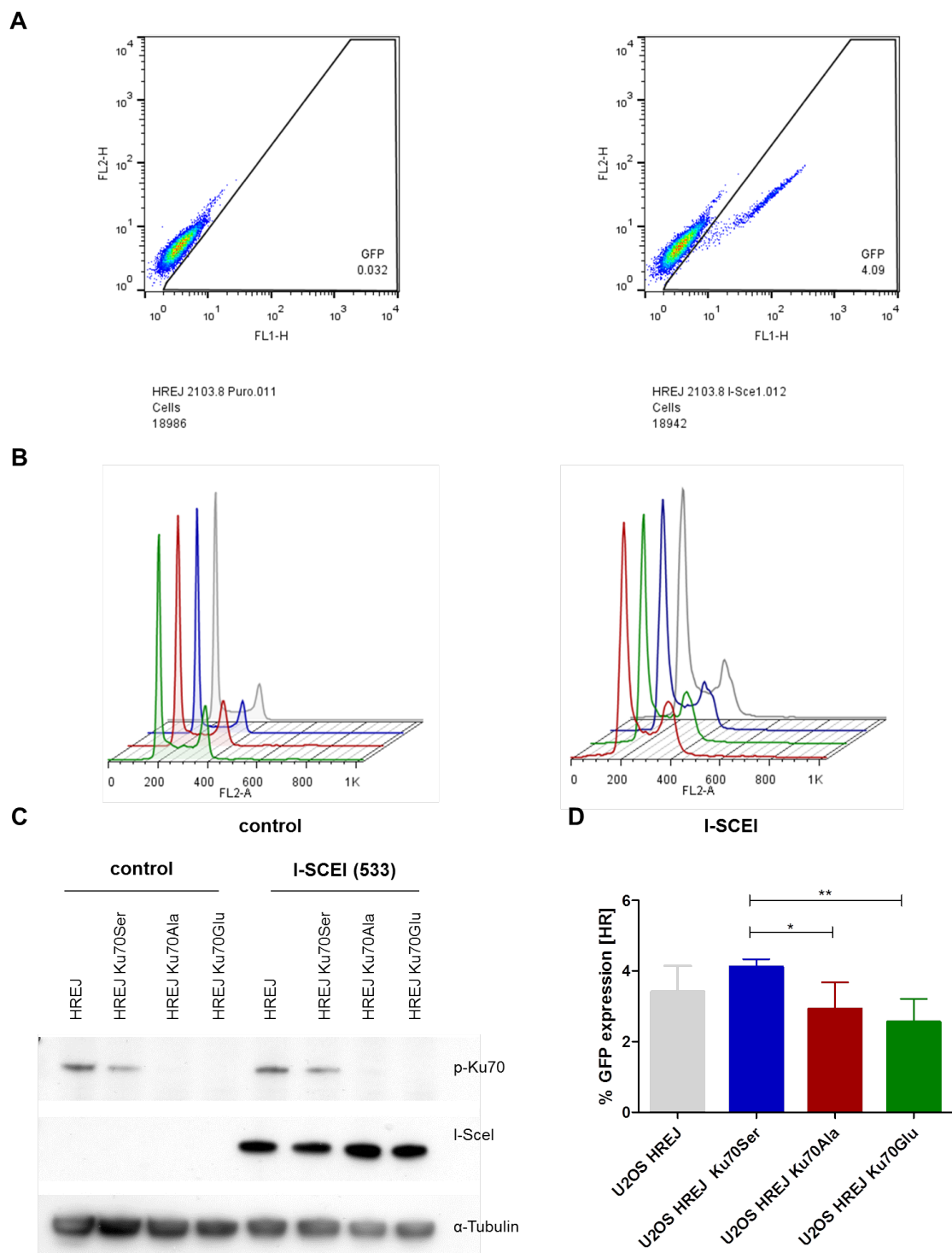


**Figure 4: U2OS HREJ** (A) Representative analysis of GFP-expression in control (left) versus I-SCEI expressing cells (right) by flow cytometry. (B) Cell cycle analysis of control and with I-SCEI transfected U2OS HREJ cell lines. No differences in the cell cycle distribution between the cell lines. grey: U2OS HREJ (non-transfected); blue: U2OS HREJ Ku70Ser; red: U2OS HREJ Ku70Ala; green: U2OS HREJ Ku70Glu. (C) Representative western blot to verify phospho-Ku70 and I-SCEI expression after transfection (72h). (D) Analysis of cell lines. Statistics were performed with Ku70Ser as control column. One-way-Anova;  $n = 6$ ;  $p < 0.01 = *$ ,  $p < 0.001 = **$ .

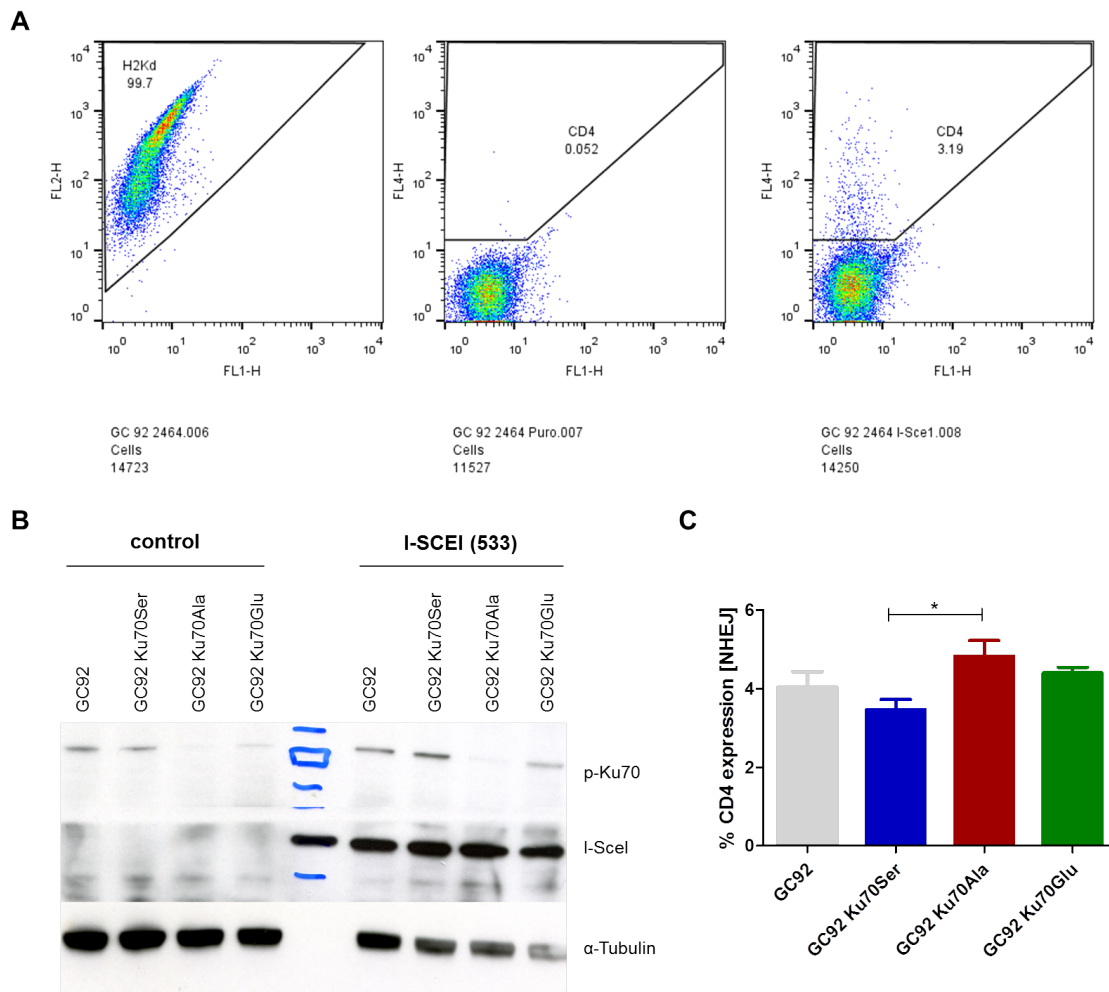


**Figure 5: GC92** (A) Representative analysis of H2Kd expression (left) and CD4-expression in control (middle) versus I-SCEI expressing cells (right) by flow cytometry. (B) Representative western blot to verify phospho-Ku70 and I-SCEI expression after transfection (72h). (C) Analysis of cell lines. One-way-Anova;  $n = 4$ ;  $p < 0.01 = *$ .

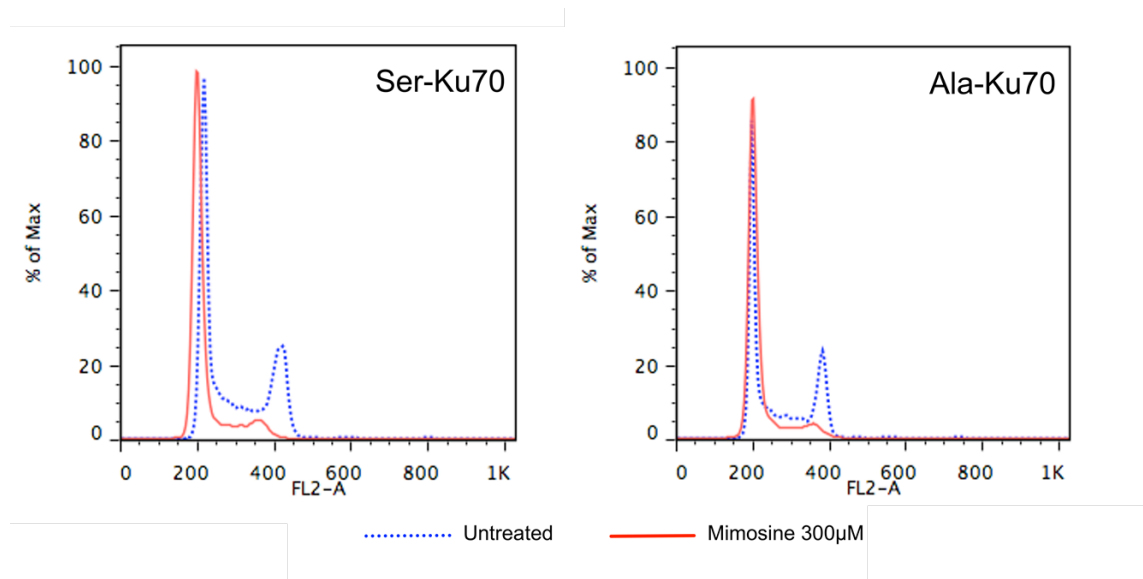


**Figure 6: Synchronization of GC92 cells in G1** Cells were synchronized ON with 300μM of mimosine.

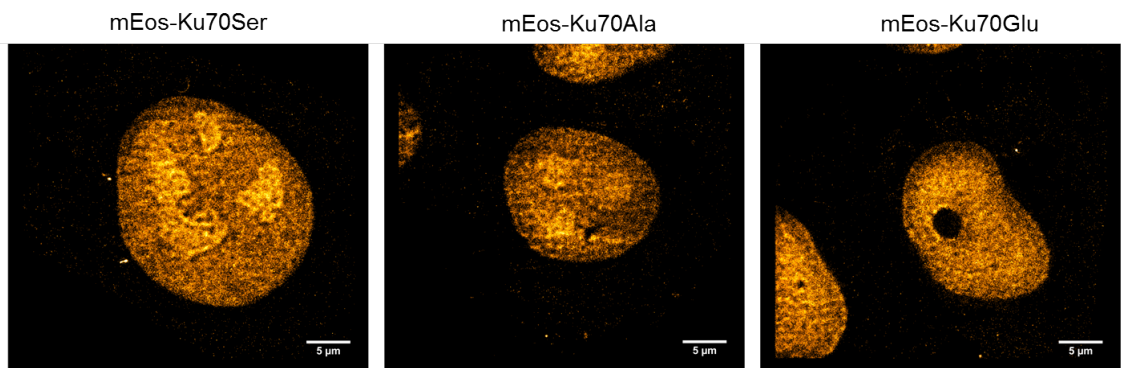


**Figure 7: Nuclear localization** (A) U2OS-mEos-Ku70Ser cells show a clear compartmentalization (B) U2OS-mEos-Ku70Ala cells show compartmentalization (C) U2OS-mEos-Ku70Ser cells show no compartmentalization





## Part VIII

### Appendix C: Article - Dynamics of phospho-S27-S33-Ku70 at DNA DSBs : functional link to genome stability



**“Dynamics of phospho-S27-S33-Ku70 at DNA DSBs : functional link to genome stability”**

Amelie Schellenbauer<sup>1</sup>, Marie-Noelle Guilly<sup>1</sup>, Romain Grall<sup>1</sup>, Romain Le Bars<sup>2</sup>, Denis Biard<sup>3</sup>, Vilma Barroca<sup>4</sup>, Sandrine Morel-Altmeier<sup>1</sup>, Youenn Corre<sup>1</sup>, Lamy Ibrahim<sup>5</sup>, Emilie Rass<sup>6</sup>, Benoit Theze<sup>6</sup>, Josée Guirouilh-Barbat<sup>7</sup>, Pascale Bertrand<sup>6</sup>, Jeroen A.A. Demmers<sup>8</sup>, Bernard S. Lopez<sup>7</sup>, Sylvie Chevillard<sup>1</sup> and Jozo Delic<sup>1\*</sup>

<sup>1</sup>Laboratoire de Cancérologie Expérimentale ; <sup>3</sup>Service d'étude des prions et maladies atypiques (SEPIA), Team Cellular Engineering and Human Syndromes; <sup>4</sup>INSERM, Laboratoire Réparation et Transcription dans les cellules Souches ; <sup>5</sup>Plateforme de Microscopie ; <sup>6</sup>Laboratoire de Réparation et Vieillessement ; Commissariat à l'Energie Atomique et aux Energies Alternatives (CEA), Université Paris-Saclay, DRF, Institut François Jacob, IRCM, 18, Av. du Panorama, 92265 Fontenay aux Roses, \*Université Paris Descartes, 75006 Paris, France

<sup>2</sup>Light Microcopy Facility, Imagerie-Gif, Institute for Integrative Biology of the Cell (I2BC), CEA, CNRS, Univ. Paris-Sud, Université Paris-Saclay, 91198, Gif-sur-Yvette cedex, France

<sup>7</sup>CNRS UMR 8200, Institut de Cancérologie Gustave-Roussy, Université Paris-Saclay, 114 Rue Edouard Vaillant, 94805 Villejuif, France

<sup>8</sup>Proteomics Center, Room Ee-679A | Faculty Building, Erasmus University Medical Center Wytemaweg 80, 3015 CN Rotterdam, The Netherlands

**Abstract**

In mammalian cells the main DNA repair pathways ensuring double-strand breaks (DSBs) repair and genome stability are canonical nonhomologous end-joining (cNHEJ) and homologous recombination (HR). DNA damages induced by irradiation are repaired mainly by cNHEJ that is active throughout the cell cycle with biphasic kinetics. We have recently identified a new form of phospho-S27-S33-Ku70 (pKu70) overexpressed in resistant chronic leukemia B cells with upregulated cNHEJ. Here we report that this form is involved in accelerated dynamics of NHEJ in unsynchronized and G1 arrested cells. Phosphorylatable form is necessary for Ku70 nucleolar localization, for pKu70 efficient timely neddylation-dependent dissociation from the sites of DNA damage. Loss of this form severely compromises genome stability through chromosomal loss/translocation events. Moreover, in an I-SCE1-inducible assay, phosphorylatable Ku70 has been proved to stimulate HR. Together, these data shed new light on cNHEJ regulation and its possible interplay with HR through a “renewed” genome guardian Ku70.

## Introduction

DNA damages generated by exogenous genotoxic stress must be repaired rapidly and accurately to maintain cell integrity and to prevent genome instability and, to avoid subsequent cancer development. Thus, not only cell's DNA repair capacity but also simultaneous repair fidelity should be orchestrated timely at each DNA lesion. To avoid death and to ensure its legitimate survival, cell developed multiple DNA repair systems providing the specificity of DNA damage<sup>1 and ref. within</sup>. DNA DSBs are the most deleterious for cell since only one not- or miss-repaired may be fatal for cell outcome<sup>2-4</sup>. To deal with this kind of damage cell developed the DNA damage response system (DDR) that essentially include damage signaling by three phosphatidylinositol-3-related family kinases ATM, ATR and DNA-PKcs which regulates the activities of proteins involved in non-homologous end joining (NHEJ) and homology-directed recombination (HR)<sup>5-13</sup> and in the engaging cell cycle checkpoints<sup>14</sup>. These last processes are concomitant and inseparable from proper DDR since they impair cell cycle progression with damaged DNA through the DNA synthesis/mitosis (S/G2/M) phase<sup>6,15,16</sup>. One of the main hallmark of cancer cells is a cooperative deregulation of both DDR and cell cycle checkpoints that deserves their clinical targeting<sup>3,5,17-19</sup>. Dogmatically, it is assumed that HR and NHEJ act in a "balanced" cell cycle-dependent competition to efficiently protect cell integrity<sup>9 and ref. within</sup>. Two principal "deciders" helped by auxiliary factors, of the engaged pathway are BRCA1<sup>11,20,21</sup> and 53BP1<sup>22, rev. 23, 24</sup>, initiating HR or cNHEJ, respectively.

Generally considered as accurate, HR relies on a homologous sister chromatid strands as identical DNA template available in late-S/G2 of the cell cycle<sup>rev9, 25</sup>. By contrast, cNHEJ is considered as error-prone as it is active throughout cell cycle. Ku heterodimer is the key regulator of this type of DNA repair process<sup>10,12</sup>. Displaying high DNA end-binding affinity it forms with DNA-PKcs a trimer referred as DNA-PK holoenzyme, initiating DDR cascade leading to cNHEJ fulfillment<sup>26,27</sup>. Structural studies of the Ku-DNA-end complex and Ku-telomeric DNA complex suggested that Ku70 helix DNA-end interaction is specific for NHEJ while Ku80 helix is oriented towards telomeric chromatin; a model that may partly explain telomeric paradox of Ku heterodimer avoiding telomeric fusions<sup>28</sup>. Next step of cNHEJ is DNA-end processing engaging Artemis nuclease, polynucleotide kinase (PNK), DNA polymerases Pol  $\lambda$  and Pol  $\mu$ , Aprataxin and polynucleotide kinase/phosphatase-like factor (APLF), MRN, WRN helicase. The processing step is finally followed by ligation step necessitating DNA ligase IV and XRCC4 as well cofactors XLF (Cernunos) and Paxx<sup>rev.12</sup>. Recruitment and activation of cNHEJ proteins is essentially ensured by the Ku-binding motif<sup>29</sup> and DNA-PKcs kinase activity<sup>rev.30</sup>. Following DNA DSBs, DNA-PKcs phosphorylation (mainly autophosphorylation but also ATM- and/or ATR-dependent phosphorylations), occurs on more than 40 sites and this phosphorylation is for instance the only

phosphorylation regulating the kinetic of cNHEJ<sup>30</sup>. Recently, a cluster phosphorylation of Ku70 at the junction of its pillar and bridge region (putative S and T residues between T298 and S314 in core domain), has been reported to facilitate the dissociation of the Ku heterodimer from DNA ends and to promote HR in S phase<sup>31</sup>. Another way proposed to remove Ku from the sites of initial DNA damage is the neddylation and subsequent ubiquitylation of Ku<sup>32</sup>. Effectively, ubiquitination sites on both subunits of Ku are at origin of the release of Ku only after successful DNA repair. Moreover, this study uncovers downregulation of Ku70 specific protein interactors after inhibition of neddylation. One of these interactors is the AAA+-type ATPase VCP/p97, shown to extract trapped Ku from DNA<sup>33</sup>.

Finally, DNA ends with 5' or 3' overhangs, may proceed through a search of sequence microhomology before ligation resulting in a nucleotides' loss and repair inaccuracy<sup>rev.8,12,34</sup>. Microhomology-directed DNA end-joining may be achieved by cNHEJ but may also be Ku-independent (alternative NHEJ) and as thus, both of them represent new potential mechanisms of genome instability<sup>rev34</sup>. aNHEJ is depending on MRN complex and may be suppressed by the versatile protein WRN (regulating also HR and cNHEJ), through inhibition of Mre11/CtIP-mediated resection and subsequent large DNA deletions<sup>35</sup>. Indeed, of particular importance for genome stability appears to be played by resection-dependent slow kinetics cNHEJ during G1 also sharing initial components of HR. Effectively, this type of end-resection in cNHEJ repair necessitates CtIP/Brca1 interaction and exonuclease Exo1 to be finally achieved by endonuclease Artemis<sup>36</sup> operating in both HR and cNHEJ. This process results also in nucleotides loss and translocation events and as thus, represents a potential source of illegitimate, disordered cancer genome. Hence, depending on the DNA-end configuration at the sites of damage and according to the availability of necessary factors and the cell cycle phase, the step of end processing puts common proteins of different DNA repair pathways into tight dynamic interactions. Their interactions should engage the appropriated pathway to remove DNA DSBs<sup>rev 12 and 34, 35-39</sup>. This concept favors thus the interplay and complementarity between different repair pathways in all phases of cell cycle rather than a competition.

The defects in DNA repair and DDR genes allow cancer cells to develop the resistance to radio- and/or chemo-therapies<sup>rev. 17, 19</sup>. Recently, this resistance has been "revisited" and provided the new anti-cancer strategy to target specifically malignant cells<sup>rev.40, 41</sup>. Hence, the molecular profiling of tumor samples may improve DNA-damaging based therapy and help a development of personalized treatments as well as the identification of drug resistance mechanisms enabling an appropriated modification of first-line treatments<sup>41,42</sup>. Exploring the mechanisms of the resistance of chronic lymphoid leukaemia (CLL) cells to current clinical treatment, we have recently identified a new stress-inducible form of phospho-S27-S33-Ku70 (pKu70)<sup>43</sup> overexpressed in leukemic cells resistant *in vitro* and *in vivo* to DNA damage-induced apoptosis and displaying an upregulated cNHEJ<sup>44,45</sup>. Experimental model of breast cancer cell line with shRNA-controlled repression of

endogenous Ku70 simultaneously with the expression of different forms of exogenous Ku70, allowed us to show that this form confers accelerated DNA repair that may deserve basic mechanism through which leukemic cells escape apoptotic death. Here, we used the same shRNA/cDNA vector's approach on different cancer and non-cancer cell lines to further characterize the function of pKu70. We show that pKu70 co-localizes with  $\gamma$ -H2AX at sites of DNA DSBs and confers rapid repair. Immediately after DNA DSBs induction, S27-S33-Ku70 (ser-Ku70) re-localized from nucleoli to the site of DNA damage and, its dissociation is dependent on phosphorylation/neddylation events that may be crucial in preserving genome stability since alanine-Ku70 form causes chromosomal losses and translocations. Accordingly, DNA damages induced in G1 arrested cells are more rapidly repaired in cells expressing ser-Ku70. Moreover, in cells harboring integrated substrate with unique I-SCE1 restriction enzyme site, ser-Ku70 was shown to stimulate HR opening thus the possibility of a new connection between cNHEJ and HR that deserves further investigations.

## Results

### **pKu70 controls cell growth, promotes clonogenic survival and protect cells from apoptosis.**

Multiple studies have shown that Ku deficiency leads to a growth defect<sup>rev.10,12</sup>. We evaluated the onset of a growth deficiency over several days in untreated and irradiated (2 and 4 Gy) transfected U2OS cells. During untreated conditions no significant effect on growth is observed between the different forms of Ku70 (Fig. 1A). However following irradiation, by the seventh day of culture, cell numbers of ala-Ku70- and glu-Ku70-expressing cells are 37.5% (2Gy), 60% (4Gy) and 25% (2Gy) , 50% (4Gy) lower compared to ser-Ku70-expressing cells, respectively (Fig. 1A).

Ku70 deficiency was shown to induce a sever radiosensitivity phenotype in mouse model<sup>46</sup>. To determine whether the Ku70 mutations interfere with radiosensitivity, a clonogenic assay of the cell lines expressing different forms of Ku70 was assessed. Unexpectedly, the plating efficiency already differed significantly between untreated ser-Ku70 and ala-Ku70Ala or glu-Ku70, respectively. Whereas about 36% of the plated cells formed colonies in the ser-Ku70S group, only 24% or 28% of ala-Ku70 and glu-Ku70 formed colonies (see Figure 1B, a). Nevertheless, following irradiation, cell survival decreased further in the ala-Ku70- and glu-Ku70-expressing cells particularly after 4 and 6 Gy, compared to ser-Ku70 (Fig. 1B, b). At 2Gy, 4Gy and 6Gy, approximately 15%, 1% and 0.03% of ser-Ku70 transfected cells give clonogenic progeny, compared to 13%, 0.5% and 0.015% of ala-Ku70 and 8%, 0.3%, 0.004% of glu-Ku70 cells, respectively. These data suggest that ala-Ku70 and glu-Ku70 have an initial defect in colony formation and that this deficiency is further enhanced by irradiation.

Based on the observations of a downregulated cell growth and enhanced radiosensitivity in the ala-Ku70- and glu-Ku70-expressing cells compared to ser-Ku70, we further evaluated the sensitivity to cell death induction by irradiation stress. Total cell death and apoptosis were

evaluated at day 3 and day 4 following irradiation with a double staining with DiOC6 and propidium iodide (PI) (see Fig.1C). Cell death increased with time and irradiation dose in all cell lines. Initial cell death in untreated conditions varies between 5 to 7% at day 3 and 6 to 7% at day 4 in all cell lines. At day 3 after irradiation, the percentage of cell death is about 7%, 11% and 8.5% (2Gy) and 12%, 18% and 14% (4Gy) in ser-Ku70-, ala-Ku70- and glu-Ku70-expressing cells, respectively. Similarly, at day 4, cell death increases to 12%, 17% and 14% (2Gy) and 19%, 30% and 23% (4Gy) for ser-Ku70-, ala-Ku70- and glu-Ku70-expressing cells, respectively. Similar to the effects obtained with irradiation, treatment with phleomycine increases cell death in all cell lines compared to the non-treated conditions (Fig.1C). As all Ku70 construction interacted similarly with Bax (not shown), we concluded that apoptotic death relive on other mechanisms.

**Ser-Ku70 preferentially localizes in nucleoli, pKu70 co-localizes with  $\gamma$ -H2AX at sites of DNA DSBs and interact with core components of NHEJ complex.** To explore cell localization of Ku70 at the molecular scale we performed PALM (photoactivated localization microscopy) experiments. We have constructed the vectors enabling an expression of photo-convertible molecule mEos2 fused to different forms of Ku70 (phosphorylable form ser-Ku70, unphosphorylable form ala-Ku70 or phosphomimetic glu-Ku70) to characterize the nuclear repartition of different forms of Ku70 in cells under stress-less conditions. Figure 2A show that ser-Ku70 fully filled nucleolar structure and is densly located to few nuclear subregions while glu-Ku70 was excluded from nucleoli showing a homogenous nuclear localization. ala-Ku70 cells exhibits two different pattern : mainly nucleolar with less dense regions or less frequently, empty nucleoli with homogenous nuclear localization (like glu-Ku70). This was also evidenced by eGFP-Ku70 fusion proteins in laser micro-irradiation approach and life cell imaging (see below).

Before evaluating the role of phospho-Ku70 on the DSBs, we have addressed localization following DNA damage induced by phleomycine and by laser micro-irradiation. Thus, two complementary approaches, a chromatin binding assay and immunofluorescence labelling were applied. Both approaches allowed co-localizing phospho-Ku70 to damaged DNA. After DNA damage induction by micro-irradiation (UV 405nm, with 1 $\mu$ g/ml of Hoechst 33342 and exposing cells to 10% of laser intensity during 2 seconds in 5 $\mu$  line in nuclear region (on Nikon N1 inverted microscope), phospho-Ku70 co-localizes with the DNA DSB repair marker  $\gamma$ -H2AX (Fig.2B). In parallel, this co-localization occurs in DNA damage, dose-dependent manner when cells were treated with the DSB inducer phleomycine (Fig.2C, a and b). Next, we assessed co-immunopurification assays to validate that pKu70 forms cNHEJ complex in cells. Fig2D,a shows the interactions of phospho-Ku70 with Ku80, Ligase 4 and PAXX, therefore validating that phospho-Ku70 is the part of the cNHEJ complex required to repair a DNA DSB. However, ala-Ku70 and glu-Ku70 equally interact with Ku80, Ligase 4 and PAXX (see Figure 2D, b). Furthermore, a proteomics approach analyzing immunopurified proteins by anit-phospho-S27-Ku70 or anti-Ku70 (clone N3H10, NeoMarkers, Thermo Scientific) antibodies, in a collaborative work with the Proteomic Center, Rotterdam, revealed no



significant differences between the binding of total Ku70 or phospho-Ku70 to the NHEJ core factors XRCC5 (Ku80), XRCC6 (Ku70), PRKDC (DNA- PKcs), LIG4 (Ligase 4) or XRCC4 (Fig.2E). These data may indicate that phospho-Ku70 is not necessary for the formation and recruitment of cNHEJ factors to the break site, but that it is a part of the cNHEJ-complex, interacting with the key players. The fact that the “core” nucleolar factor nucleophosmin (NPM1) interacts less strongly with pKu70 suggests that phosphorylation occurs most likely at the sites of DNA damage induced by laser irradiation (see below). Nevertheless, this interactome approach indicated other factors (most of them already reported in literature to interact with Ku70), that may be specific interactors of unphosphorylated- or phosphorylated-Ku70 such as UBE2M or N4BP1 enzymes involved in NEDD8- or NEDD4-conjugation, respectively. Some of ubiquitin-conjugating or –ligase E3 enzymes (UBE2G2 and TRIM33) may interact preferentially with pKu70. In parallel, “auxiliary” factors able to affect cNHEJ were also found as interactors of unphosphorylated-(WRN and DNA-Pol $\delta$  subunit 4), or phosphorylated-Ku70 (CAF1, Fig.2E).

**Kinetic of DSBs repair is accelerated in unsynchronized and G1 arrested cells expressing pKu70.** By using  $\gamma$ -H2AX and comet assay, we have previously shown an accelerated kinetic of DNA repair in cells expressing pKu70<sup>43</sup>. Here, we have validated this in unsynchronized U2OS and G1 arrested GC92<sup>47</sup> cell systems. Following 4Gy irradiation  $\gamma$ -H2AX foci were assessed by immunofluorescence (illustrated by Fig. 3A) and quantified (automated counting by CellProfiler software, Fig.3B). Untreated U2OS cells displayed similar amount of  $\gamma$ -H2AX foci in the ser-Ku70- and ala-Ku70A-expressing cell lines (median= 5 foci/cell). 0.5h following irradiation, the amount of  $\gamma$ -H2AX foci reaches its maximum; both cell lines showed a median of 24 foci/ cell. At 4h after irradiation ala-Ku70 cells displayed significantly higher ( $p < 0.001$ ) amount of remaining  $\gamma$ H2AX foci (median= 13; 25%-percentile= 8; 75%- percentile= 22), compared to the ser-Ku70-expressing cells (median= 11; 25%percentile= 7; 75% percentile= 19). Similarly, Western blot analysis of  $\gamma$ -H2AX shows a stronger signal at 4 and 6h after irradiation for ala-Ku70- than ser-Ku70-expressing cells (Fig. 3B).

Intrigued by the fact that resection-dependent cNHEJ in G1 may be at origin for the appearance of chromosomal instability<sup>36</sup>, we synchronized GC92 cells over-night by mimosine (300 $\mu$ M) causing G1 arrest. Synchronization of the cells was measured by flow cytometry showing that over 90% of cells were blocked in G1 after overnight treatment (Fig.3C). One hour after removing mimosine, cells were irradiated at 4Gy and examined for kinetic of  $\gamma$ -H2AX disappearance. As depicted in Fig.3D, E, the ala-Ku70-expressing cells displayed higher level of  $\gamma$ -H2AX foci 2 and 4h, similar to the observations seen in unsynchronized U2OS cells (see Figure 3B). These data thus indicate that rapid repair of DSBs in G1 was conducted by pKu70.

**pKu70 confers more rapid dissociation from the sites of DNA-damage: inhibition of neddylation sustains both pKu70 release and DSBs following micro-irradiation.** Following the demonstration of a delayed resolution of  $\gamma$ -H2AX foci in the mutated form of Ku70, we

have addressed real-time live cell imaging to monitor the dynamic of Ku70 recruitment and release at DSBs. For this purpose we transfected cells with vectors enabling expression of fusion eGFP-Ku70 proteins. DSBs were induced by microirradiation (UV 405nm in presence of Hoechst 33342 1 $\mu$ g/ml), with the same experimental conditions as applied in experiment of phospho-Ku70 co-localization with  $\gamma$ -H2AX (Fig.2B). After microirradiation, cells were followed up to 240 min. and pictures were taken every 10 min (Fig 4A). As could be observed, recruitment kinetics are quite similar in eGFP-ser-Ku70- and ala-Ku70-expressing cells, reaching their maximum between 30 and 50min. Quantified intensities seem to indicate that ala-Ku70 gave the stronger signal on DSBs (i.e. 3.1-fold induction for ala-Ku70, whereas the maximal recruitment is 2.6-fold for ser-Ku70, Fig.4B). Dissociation of eGFP-serKu70 from the DNA damage is much faster and reaches 50% at 150 min. Basal levels for the ser-Ku70-expressing cells were reached between 190 and 200min. In contrast, ala-Ku70 cells reached 50% only after 220min, and did not reached basal levels within the 240 min. These data suggest that the phosphorylation of Ku70 favors Ku70 release from the sites of DNA damage and might thus implicate a faster fulfillment of NHEJ process in these cells, compared to ala-Ku70-expressing cells; these data are in agreement with  $\gamma$ -H2AX -foci (Fig. 3B) and -protein level (see below).

Neddylation has been recently reported an important prerequisite process for ubiquitination and subsequent Ku release from the DNA<sup>32</sup>. Intrigued by the observation that phosphorylation of Ku70 favours its release, we asked whether an inhibition of neddylation with MLN4924 may impair the release of ser-Ku70 from the sites of DNA damage. Figure 4C shows ser-Ku70 and ala-Ku70 dissociation kinetics after cell treatment with MLN4924 at 3  $\mu$ M for 1h prior micro-irradiation. Maximal recruitment of ser-Ku70 (6.4-fold) and ala-Ku70 (6.1-fold) after MLN 4924 treatment are approx. 2-fold higher compared to conditions without MLN 4924. Dissociation of ser-Ku70Ser was severely hampered with only 20-25% of Ku70 dissociated at 240min reaching thus the kinetic of ala-Ku70. These data indicate that neddylation of Ku70 acts downstream of Ku70 phosphorylation to conduct Ku70 release. In parallel,  $\gamma$ -H2AX protein level was sustained in ser-Ku70-expressing cells treated by MLN4924 while it remained the same in cells expressing ala-Ku70 further supporting the necessity of neddylation of pKu70 prior to its release from the DSBs. In agreement with this, proteomic data pointed out NEDD8-conjugating enzyme Ubc12 (UBE2M) and NEDD4-binding protein 1 (N4BP1) as well ubiquitin-conjugating enzyme E2 G2 and ubiquitin-ligase protein TRIM33, as new partners whose affinity may depend on Ku70-phosphorylation status (Fig.2E).

**pKu70 stimulates HR activity in absence of exogenous genotoxic stress.** To further explore how the general role of pKu70 in DNA repair could be in the absence of exogenous genotoxic stress, we have addressed two specifically dedicated cell models, U2OS<sup>48</sup> and GC92 cells<sup>47</sup> containing a single copy of a HR or NHEJ only reporter substrates, respectively. Substrate contain unique I-SCE1 restriction enzyme site enabling thus to measure the efficacy of DNA break repair after I-SCE1 endonuclease expression. 72h after I-SCE1 transfection, cells were probed for GFP, CD4- and H2Kd-expressions by FACS analysis. NHEJ activity was measured

via the expression of CD4 that is induced upon I-SCEI transfection, excision of the internal fragment containing the H2Kd and CD8 genes<sup>47</sup>. H2Kd expression as control was monitored before transfection to be about 97-99% in all cell lines (see Figure 5A and 5B). Equal expression of I-SCEI was verified by Western blot (Fig. 5A, c and 5B, b). As a negative control an empty transfection plasmid was used. Unexpectedly, an elevated CD4 expression was observed in ala-Ku70 rather than in ser-Ku70-expressing cells (Fig.5B,c), suggesting that ala-Ku70 cells exhibit higher NHEJ activity toward enzymatically -induced DSB.

HR activity is measured through the expression of GFP, after a recombination event Fig.5A, a). As for the GC92 cells, equal expression of I-SCEI was evaluated and an empty transfection plasmid was used as negative control (Fig.5A,c). To exclude any cell cycle dependent events, the cycle was evaluated before and after transfection. The cell cycle was similar in all cell lines (Figure5A, b). The percentage of cells expressing GFP was increased in the ser-Ku70-expressing cells as compared to the ala-Ku70-expressing cells. This indicates that ser-Ku70-expressing cells have an elevated activity of HR in stress-less conditions and this was not due to a higher proportion of these cells in S/G2. Thus, these data indicate that the phosphorylation of Ku70 can affect the HR and cNHEJ DNA repair pathways.

**pKu70 promotes genome stability after genotoxic stress.** Following impaired release from DNA-damage sites and sustained DSBs in G1 arrested cells expressing the mutated form of Ku70 as well as an increased chromosomal structural aberrations in U2OS expressing ala-Ku70 (not shown), we addressed multi-FISH to assess whether these events may be associated with the appearance of genome instability. Because U2OS and GC92 cell lines are polyploid inherently harboring multiple chromosomal aberrations we have chosen human mammary epithelial (HME) diploid cell line (kind gift from R. Weinberg lab). This approach allowed us to assess more precisely type of chromosomal aberrations that may indicate both chromosomal translocations and lost. Three recurrent aberrations found in this cell line (involving intrachromosomal exchanges short/long arm Chr.1; and interchromosomal exchanges chr. 18:11 and chr. 22:10), were maintained in ser-Ku70- and ala-Ku70-expressing cells. Intriguingly, ser-Ku70- and ala-Ku70-expressing cells' metaphases displayed both additional new aberration der. 8 (amplification possibly affecting C-MYC gene region). Forty % of ala-Ku70 cells metaphases displayed an additional translocation der(13)t(5;13) not observed in ser-Ku70-expressing cells. After irradiation, (4Gy, 24h), ser-Ku70 exhibited significantly lower rate of translocations than ala-Ku70 cells; mean of 1.95 vs 2.72 translocations/metaphase, respectively. In addition, 11 metaphases among 20 analyzed (55%) in ser-Ku70-expressing cells did not shown any additional translocation after irradiation while only 5/21 metaphases (23.8%) of ala-Ku70-expressing cells were without additional translocation events.

## Discussion

The main hallmark of cancer cells is the genomic instability that paradoxically, ensures their illegitimate survival and tumor maintenance. Deregulations in DNA repair and DDR genes in cancers have prompted the development of new therapeutic approaches attempting to target underlying DNA repair pathways specifically in malignant, preserving healthy, cells. The concept of synthetic lethality, well-illustrated by the use of PARP inhibitors for the cancers with HR repair defect, is the most promising therapeutic strategy depending on the identifications of DDR targets in each (sub)type of cancer, in order to rationally develop the appropriated drug(s)<sup>40-42</sup>. Aggressive subset of chronic lymphoid leukaemia (CLL) is currently incurable. For the resistant cells from this subset, we have reported several lines of evidences which are indicative of deregulated cNHEJ as well that current front-line therapy based on DNA metabolism-impairing agents may not be beneficial for patients as it may favor disease relapse and progression<sup>49-51</sup>. More recently, we have identified in these resistant CLL cells an overexpression of a new form of ser27-ser33-Ku70 (pKu70) that conferred rapid but inaccurate DNA repair in a breast cancer cell line model<sup>43</sup>. We have speculated that this alteration may be a possible underlying mechanism of CLL cell resistance to treatment and the appearance of multiple chromosomal aberrations. Here, we have used the same EBV-based vectors enabling simultaneous inhibition of endogenous Ku70 and an expression of different forms of exogenous Ku70 both, in cancer- and non-cancer-derived cell lines. Experiments were performed mainly on U2OS osteosarcoma cell line because the unique I-Sce1 substrate, allowing assessing of HR activity was done in this cell line<sup>ref48</sup>. By laser micro-irradiation and chromatin binding approaches we first demonstrated pKu70 colocalisation with DNA-damage sites/ $\gamma$ -H2AX (Fig.2B). Next, with the assessment of  $\gamma$ -H2AX foci and protein levels, we have confirmed previously reported data<sup>43</sup> of an accelerated DSBs repair kinetic in cells expressing pKu70 as compared to kinetic in cells expressing ala-Ku70. This was established in unsynchronized U2OS as well in G1-arrested GC92 cells<sup>47</sup> (Fig. 3). Chimeric proteins mEos-Ku70 and eGFP-Ku70 showed that ser-Ku70 is preferentially localized in nucleoli while alanine-form exhibited both nuclear and nucleolar localization. Intriguingly, phosphomimetic Ku70 (glu-Ku70) was excluded from nucleoli and exhibited exclusively nuclear localization (Fig.2A); this latter giving intermediate result between ser-Ku70 and ala-Ku70 in all experiments was abandoned during the course of some kinetic studies. Ser-Ku70 nucleolar localization is in agreement with the proteomic data of pKu70/Ku70 interactome pointing out nucleophosmin and the proteins involved in ribosomal biogenesis as the main partners of Ku70 (Fig.2E and unpublished data). Immediately after micro-irradiation ser-Ku70 and ala-Ku70 delocalized from nucleoli to the sites of DSBs. Similar nucleolar delocalization has already been described for Rad52 involved in HR<sup>52</sup>. Other factors (such as WRN, p97/VCP, ABH2 and TRF2)<sup>53-55</sup>, involved in DNA damage repair have already been localized in nucleoli. Thus, these subnuclear membranes-less structures dealing rDNA and rRNA transcription and processing, respectively, and ribosomal assembly<sup>rev.56</sup>, appeared thus as the essential storage organelles of the factors involved in the maintenance of genome stability<sup>57</sup>.

Real-time kinetics in the laser micro-irradiation approach allowed us to establish accelerated release of pKu70 at the sites of DNA damage as compared to ala-Ku70 (Fig.4A, B). This is also in agreement with the kinetics of  $\gamma$ -H2AX foci/protein levels showing time-dependent decrease in  $\gamma$ -H2AX content (Fig.4D,a). Ubiquitin-like protein NEDD8 and subsequent ubiquitylation have been recently shown to promote the release of Ku and Ku-associated proteins from DSBs following repair<sup>32</sup>. Accordingly, we have treated cells with MLN4924 that specifically inhibits NEDD8 conjugation to Ku heterodimer. This treatment clearly sustained eGFP-ser-Ku70 signal at the sites of DNA damage (Fig.4C) and  $\gamma$ -H2AX content in cells expressing phosphorylatable form of Ku70 with no effect on ala-Ku70 expressing cells (Fig.4D,b). Clearly, Ku70 phosphorylation precedes its dissociation from DNA-damage sites. Early nucleoli emptying following laser microirradiation and delocalization of both, ser-Ku70 and ala-Ku70 suggests that Ku70 phosphorylation occurred at the sites of DNA damage even if the basal level of pKu70 in ser-Ku70 expressing cells was significant without any treatment. Further, phospho-S2056-DNA-PKcs and phospho-S1981-ATM, both were shown to be implicated in Ku70 phosphorylation<sup>43</sup>, co-localize in  $\gamma$ -H2AX foci indicating that its phosphorylation most probably take place at the DSBs sites. Further, an increased early signal in ala-Ku70-expressing cells may indicate that the repair and Ku70 dynamics at DNA-damage sites was slowed-down (i.e. signal at 30min post-irradiation in Fig.4B). Based on these and previously reported data concerning the accuracy of DNA repair<sup>43</sup>, we have next transfected U2OS cells harboring a substrate with a unique I-Sce1 site<sup>48</sup> allowing an assessing of HR activity. In parallel, we have transfected the GC92 human fibroblast cell line harboring unique NHEJ substrate cleavable by the I-Sce1 enzyme<sup>47</sup>. As shown in Fig.5A and B, ser-Ku70 expressing cells stimulated HR upon I-Sce1 induction while, unexpectedly, ala-Ku70-expressing cells exhibited significantly higher NHEJ activity. Chen and coll. reported similar results where cluster phosphorylation of Ku70 stimulates HR in S phase and that the ablating phosphorylation gave rise to the sustained retention of at DSBs with a decrease in HR in S phase<sup>58</sup>. However, in that case this cluster phosphorylation in junction/bridge region of Ku70 modulating DNA end resection and HR, was not required for NHEJ activity. Ser27-ser33-Ku70 phosphorylation appears to control both NHEJ and HR activities opening the possibility that like in DNA-PKcs<sup>rev.10, 59</sup>, Ku70 molecule has several phosphorylation sites with variable effect on NHEJ/HR activities. An increased NHEJ activity observed in GC92 cells expressing ala-Ku70 72h following I-Sce1 induction, in absence of stress conditions, appears in a contradiction with other experiments with irradiations/drugs-induced complex DSBs in the same cell type where ser-Ku70 accelerated NHEJ. Since DNA-end binding activity remained the same for ser-Ku70 and ala-Ku70<sup>43</sup> and since eGFP-ala-Ku70 and eGFP-ser-Ku70 are recruited with similar kinetic to DNA-damage sites, this may suggest that in enzymatically-induced DSBs, there is no need for pKu70 where a repair complex may be slightly different to joint blunt ends without any need of end-processing. Effectively, in absence of stress, phosphorylation of Ku70 by cyclinB1/CDK1 in S-M cell cycle phase disrupted Ku dimer formation and subsequent interaction with the origin of DNA replication<sup>60</sup>. At the end of mitosis and in G1, Ku70 became dephosphorylated allowing replication complex formation illustrating thus a

cell cycle-dependent function of non-phosphorylated Ku70. Upon DNA damage, cyclin A1/CDK2-dependent phosphorylation of Ku70 stimulated DNA repair with an inhibition of apoptosis<sup>61</sup>. Otherwise, if sustained DSBs in cells expressing ala-Ku70 were not completely repaired and when they maintained ala-Ku70, then repeated systemic activation of NHEJ may be explained by the model proposed by E. Rosenberg and coll<sup>62</sup>.

Ser27-ser33-Ku70 phosphorylation seems to be critical in end resection-dependent process in G1<sup>36</sup>. Effectively, G1 arrested GC92 cells expressing ala-Ku70 displayed a significantly higher excess of  $\gamma$ -H2AX foci at 2 and 4 hrs post-irradiation; meaning not only that Ku70 was not released but also that NHEJ repair was not achieved. This may suggest that neddylation/ubiquitylation enzymatic complex make the part of DNA repair process. These results (as well as the observed polyploidy in ala-Ku70-expressing cells starting from day 3 post-irradiation, not shown), prompted us to address genome (in)stability in two subsets of Ku70-expressing cells. While U2OS cells are polyploid cells (up to 80 chromosomes) with high level of chromosomal abnormalities, we used non-cancerous mammary epithelium-derived HME cell line<sup>63</sup>. This cell line immortalized by the hTert activation has quasi-normal diploid karyotype enabling thus a relevant assessment of exogenously-induced chromosomal rearrangements. In a multi-FISH approach, ala-Ku70-expressing HME cells irradiated at 4Gy and following first cell division, displayed high number of chromosomal translocations events (Fig6) indicating thus the essential role of pKu70 in maintaining genome stability. Even in absence of exogenous stress ala-Ku70-expressing cells displayed der(13)t(5;13) translocation that was not observed in ser-Ku70-expressing cells. This finding may be suggestive of the role of pKu70 in endogenous-(replication?)-stress-induced DSBs. These results appears to contradict the results previously published<sup>43</sup> where after an estimation of chromosomal structural aberrations in breast cancer cell line ZR75.1, ser-Ku70-expressing but not ala-Ku70-expressing, cells displayed higher level of chromosomal structural aberrations. This discrepancy deserves now further characterizations but it may be due to the differences/relevance in these two methodologies as well as in cell models (i.e. non-cancer vs cancer cell lines with different origin/defect). Effectively, in case of cancer cell lines, we observed significant differences between irradiation-induced features of breast cancer and osteosarcoma cell lines (no major cell cycle checkpoint activation in U2OS cells while ZR75.1 exhibited late S/G2 arrest; significantly higher number of DSBs in ser-Ku70-expressing ZR75.1 untreated cells while this was not observed in U2OS cells, ect.). More recently, we observed an instability in ala-Ku70 ZR75.1 cells but appearing after several (5) days following irradiation opening the possibility of a delayed appearance of instability. To resolve, at least partly, these at first sight inconsistencies, we started a study of pKu70/Ku70 interactome where anti-Ku70 (clone N3H10) or anti-pKu70<sup>43</sup> antibodies were used to immunopurify the partners preferentially interacting with pKu70. First results obtained with HME and two subsets of CLL cells pointed out already identified partners of Ku70 but also the new cell-type specific candidates (Fig2E and unpublished data). In parallel, mouse KI model expressing human ser-Ku70 or ala-Ku70 has been created. For instance, first results did not reveal a significantly differential radiosensitive phenotype but ala-Ku70-derived

embryonic fibroblasts were defective in growth and underwent high apoptosis rate following irradiation (data not shown). Full characterization of these mice is currently underway.

In summary, this work establishes pKu70 as an active effector of cNHEJ, regulating dynamics of its release from the sites of DNA-damage; a process that proved to be critical in the maintaining genome stability. Stimulating HR activity, Ku70 appears as versatile molecule in directing precise DNA repair across cell cycle phases like its HR-specified homolog BRCA1 which is able to modulate resection-dependent cNHEJ in G1<sup>36,64,rev.65</sup> that may be impaired by pKu70 which, in parallel may favor HR in S/G2.

## Methods

**Cell culture.** The cancer cell lines U2OS (osteosarcoma) have been purchased at the ATCC. The U2OS cell line containing reporter system to measure HR<sup>47</sup> efficiency and human fibroblast cell line GC92 containing a reporter system to measure NHEJ<sup>48</sup> were cultured in Dulbecco's modified Eagle's medium (DMEM GlutaMAX, Life Technologies, Thermo Scientific) supplemented with 10% (v/v) fetal bovine serum, 1x non-essential amino acids (Life Technologies, Thermo Scientific). The non-cancerous mammary epithelium-derived HME cell line was a kind gift from R.A. Weinberg lab (Whitehead Institute for Biomedical Research, MIT). HME cell line was additionally supplemented with insulin, EGF and hydrocortisone (all purchased at Sigma-Aldrich). For GC92 cell arrest in G1, cells were treated by mimosine 300 $\mu$ M (Sigma-Aldrich), over-night followed 2h of mimosine-free cell culture before irradiation.

**Clonogenic assay and apoptosis.** Cells were grown to 70-80% confluency were trypsinized, counted and suspended at cell concentrations of ranging 5 to 40x10<sup>3</sup> cells/mL. Cell suspensions were either non irradiated (0Gy) or irradiated at 2, 4 or 6 Gy. Cells were seeded into 10cm<sup>2</sup> cell dishes and left to grow 14 days. For cell death assessing, cells were seeded in duplicate in 24-well plates at 0.03x10<sup>6</sup> (IR) and 0.02x10<sup>6</sup> (NT) cell density. Approximately 4-6h after seeding, cells were irradiated at 2Gy, 4Gy or treated 1h with 100  $\mu$ M phleomycine (InvivoGen). Cell medium was exchanged immediately after treatment and cells left to grow. At day 3 and 4 cells were trypsinized and cell suspension added to FACS-tubes. After centrifugation, supernatant was removed and cell pellet resuspended in medium containing propidium iodide (1:1000) (Sigma-Aldrich) and DiOC6 (3,3'-Dihexyloxacarbocyanine Iodide) (1:2000) (Thermo Scientific). Data were acquired using a cytometer (FACScalibur, BD Biosciences)

**Ku70 shRNA/cDNA vectors and transfections.** EBV-based vectors were generated as previously described<sup>43</sup> to generate stable cell lines that either express: S27-S33-Ku70, A27-A33-Ku70 or E27-E33-Ku70 (phospho-mimetic). Endogenous Ku70 is repressed using shRNA encoded on the same pEBV-vector (exogenously expressed Ku70 was resistant to shRNA repression). The same vectors were used to generate eGFP-Ku70 (pcDNA-eGFP, Addgene,

UK) and mEos-Ku70 (mEos-2 pcDNA, Addgene, UK), fusion proteins. Cell transfection for all vectors was performed the same day, using the same JetPrime DNA transfection kit (Polyplus,-Transfection SA, France) and antibiotic selection conditions (hygromycine or puromycine). As a control for antibiotic selection, non-transfected cells were antibiotic-treated and cell death was monitored over time by light microscopy. Successful transfection for the different Ku70 mutants was monitored using SDS PAGE and Western Blot analysis. All stably transfected cell lines were frozen and stored in liquid nitrogen. eGFP-Ku70 and mEos-Ku70 expressing cells were freshly transfected before each live cell acquisition. All cell lines were kept under constant antibiotic selection pressure.

**$\gamma$ -Irradiation, laser micro-irradiation and real-time life cell imaging.** Gamma irradiation was performed using the  $\gamma$ -irradiator IBL-637 (Cs137). Dose rate used was 4.96 Gy/min for all experiments. For laser micro-irradiation and life cell imaging experiments, U2OS cells expressing eGFP-Ku70 and mEos2-Ku70 fusion proteins (ser-Ku70Ser, ala-Ku70), were transfected a week before each experiment. To stain the nucleus, Hoescht33342 (Sigma-Aldrich) at 1 $\mu$ g/ml was added 30min before laser irradiation by 405nm laser beam (2 seconds of 10% of laser intensity) in a line of 5 $\mu$  in nuclear region (avoiding nucleoli). Background eGFP-fluorescence intensity was measured before irradiation for each cell. Cells were followed in intervals of 10min up to 240 min after irradiation. Data were acquired using the video-confocal inverted microscope Nikon A1 with integrated chamber assuring 5% CO<sub>2</sub> atmosphere and 37°C temperature. Data analysis was conducted using the NIS Elements software (Nikon). For the cell localization analysis of Ku70, PALM acquisitions were performed with the N-STORM (Nikon) system and a SR Apo TIRF 100x (1.49 numerical aperture) oil objective. Images were taken using a TIRF inverted Nikon Eclipse Ti-E microscope, equipped with a quad band emission filter (450/60-525/50-605/50-730/120, Chroma), and coupled to an EMCCD camera (iXon DU897, Andor). Fixed cells expressing mEos2 constructs were used with a sequential activation at 405nm (Cube laser, 100mW, Coherent) and then excitation at 561 nm (Sapphir laser, 150mW, Coherent). NIS-elements AR software (Nikon, v. 4.30.01) and the STORM analysis module (Nikon) was used to control the system and to perform molecule detection. To prevent axial drift we used the perfect focus system (Nikon), and to correct any lateral or axial drift during the acquisition, we apply the auto-correlation algorithm of the NIS-elements AR software (Nikon, v. 4.30.01). Local density analysis was performed using SR-Tesseler software. The local density of the mEos2 molecules were calculated using Voronoi tessellation and then displayed according to a color scale normalized by the mean molecule density of each nucleus.

**$\gamma$ -H2AX foci/protein levels assessment.** Cells were grown on 8-well cover slides (Millicell EZ Slides, Merck-Millipore) for 2 days until 70-80% confluency. Slides were irradiated at 4Gy and left in the incubator for the indicated time points (0.5h, 4h or 24h). After anti-g-H2AX labeling, data acquisition was performed using a microscope (Zeiss, Imager Z2) as previously described<sup>43</sup>. Data analysis was performed using CellProfiler (version 2.2.0, Carpenter lab,



free-ware). Graphics and statistical analysis was performed with GraphPad Prism Software (Inc. La Jolla, USA). Western blot analysis was performed as described<sup>43</sup>.

**Chromatin binding assay.** Cells were seeded until approx. 70% of confluency. For protein extraction the Pre-extraction (PEB) buffer (PIPES 10mM (pH 7.0), NaCl 100mM, Sucrose 300mM, MgCl 3mM, Triton X-100 0.7%, H<sub>2</sub>O) was prepared on ice. Cells were washed 3 x with PBS w/o Ca<sup>2+</sup>/Mg<sup>2+</sup>, then PEB-R buffer (PEB buffer, RNase A 7%) was incubated for 3 min. The supernatant was collected as Fraction 1. The same procedure was repeated once again, to obtain Fraction 2. After twice PBS washing Laemmli- buffer (2x) (100mM Tris HCl (pH 6.8), 10% SDS, 20% Glycerol, 100mM DTT, 1% bromophenol blue, H<sub>2</sub>O) was added to obtain Fraction 3 (chromatin fraction). DNA was then digested by Benzonase (Merck Millipore). To prepare samples for SDS-PAGE, Laemmli 2x were added to Fraction 1 and 2 and all samples were heated for 5min. at 95°C.

**Anti-pKu70/anti-Ku70 protein immunopurifications.** Proteins from at least 15x10<sup>6</sup> cells were extracted on ice for 1h in hypertonic buffer containing NaF 50mM, NaCl 450mM, HEPES 20mM, EDTA 0.2mM, DTT 0.5mM, Iodoacetamide 5mM, "Complete" cocktail (Roche Diagnostic) inhibitor of phosphatases (100µL extraction buffer per 10<sup>7</sup> cells). Cell lysates were centrifuged at 67.000rpm for 1h, 4°C. 10% Glycerol and β- Mercaptoethanol (1:1250) were added to the supernatant and divided in 3 parts (two parts for immunoprecipitations and one for input control). To equilibrate salt content, equilibration buffer (EQ-buffer) (KCl 10mM, MgCl 10mM, HEPES 20mM, EDTA 2.5mM, DTT 0.5mM, Iodoacetamide 5mM, Complete cocktail 1x, Glycerol 10%,) was added in a ratio of 1:3 and protein dosage was performed (Bradford method). Dynabeads (BE-M01/03, EMD Millipore) ( 1µL per 10µg total protein) were washed with PBS w/o Ca<sup>2+</sup>/Ca<sup>2+</sup> twice and cell lysate was added to the beads. To obtain a total volume of 500µL EQ-buffer was added. Antibodies for Ku70 (NeoMarkers, Thermo-Fisher) and p-Ku70<sup>43</sup> were mixed to the lysate/Dynabeads mixture at a concentration of 1% of the total protein amount, incubated under agitation overnight at 4°C. Supernatants were discarded and beads washed three times in PBS, before adding EQ-buffer. Laemmli-buffer (5x) (0.255M Tris HCl (pH6.8), 50% Glycerol, 5% SDS, 0.05% bromophenol blue, 0.1 M DTT), was added and samples were heated at 95°C for 10 min. Immunoprecipitated proteins were resolved on SDS-PAGE for orbital-based shotgun mass spectrometry according to standardized protocol (Proteomic Center, Rotterdam).

**HR and NHEJ activities.** The NHEJ-HR efficiency was performed as previously described by using transfected (ser-Ku70, ala-Ku70 or glu-Ku70) U2OS<sup>47</sup> and GC92 cell models<sup>48</sup>. These cells contain a single copy of a HR and NHEJ or NHEJ only reporter substrates, respectively, to measure the efficacy of DNA break repair after I-SCE1 endonuclease expression. Briefly, 72h after transfection with a plasmid coding for I-SCE1, cells were probed for GFP, CD4- and H2Kd-expressions by FACS analysis (FACScalibur, BD Biosciences). Data analysis was performed using FlowJo 5.7. NHEJ and HR efficiency is obtained by subtracting the signal of

the control plasmid expressing samples from the I-SCEI expressing samples. H2Kd was used as a control for reporter expression in all transfected cells.

#### **Multi-FISH analysis of chromosomal translocations.**

HME mammary epithelial cells (used also in proteomic approach for the analysis of Ku70 interactome), were used to assess chromosomal anomalies following irradiation. Cells were irradiated at 4Gy and metaphases prepared after 24h. Slides were pre-treated with RNase A (120µL per slide in 2xSSC buffer (AM9763, Thermo Scientific)) during 45min, 37 °C to eliminate RNA. To remove remaining cytoplasm a pretreatment with pepsine (P6887, Sigma Aldrich) was performed. Slides were incubated for 30sec-1min, 37 °C in 0.01M HCl, pH 2; 2µg/mL pepsin. Slides were washed with PBS w/o Ca<sup>2+</sup>/Mg<sup>2+</sup> (2x), then with PBS with Ca<sup>2+</sup>/Mg<sup>2+</sup> for 5min. To fix pepsin treated metaphases, slides were incubated in 1% formaldehyde/ PBS with Ca<sup>2+</sup>/Mg<sup>2+</sup> for 10min. at RT. Slides were washed with PBS w/o Ca<sup>2+</sup>/Mg<sup>2+</sup>, 5min. Dehydration was performed in 3 steps, at 70%, 90% and 100% ethanol at RT for 3min. and left to dry for 2-3min. mFISH probe denaturation and hybridization were performed according to the manufacturer's protocol (24XCyte, D-0125-120-DI, MetaSystems). Metaphases were mounted with Fluoromount-G aqueous (F4680, Sigma Aldrich). Data were acquired using the Zeiss Imager Z2 microscope. Data analysis was performed with ISIS software (Metasystem).

#### Acknowledgements

AS benefited fellowship from French Ministry of Research and Technology (MRT) and CEA. This work was supported by Fondation de France, CEA and EdF.

The present work has benefited from the light microscopy facility of Imagerie-Gif, (<http://www.i2bc.paris-saclay.fr>), member of IBISA (<http://www.ibisa.net>), supported by "France-BioImaging" (ANR-10-INBS-04-01), and the Labex "Saclay Plant Science" (ANR-11-IDEX-0003-02).

#### References

- 1 Chatterjee, N. & Walker, G.C. Mechanisms of DNA damage, Repair and Mutagenesis. *Environ. Mol. Mutagen.* **58**, 235-263 (2017).
- 2 Le Guen, T., Ragu, S., Guirouilh-Barbat, J & Lopez, B.S. Role of the double-strand break repair in the maintenance of genomic stability. *Mol. Cell. Oncology* **2**, 1 e968020 (2015).

- 3 Jeggo P.A., Pearl, L.H. & Carr A. M. DNA repair, genome stability and cancer: a historical perspective. *Nat. Rev. Cancer* **16**, 35-42 (2017).
- 4 So, A., Le Guen, T., Lopez, B.S. & Guirouilh-Barbat, J. Genomic rearrangements induced by unscheduled DNA double strand breaks in somatic mammalian cells. *FEBS J.* **284**, 2342-2344 (2017).
- 5 Riballo, E., et al. A pathway of double-strand break rejoining dependent upon ATM, Artemis, and proteins locating to  $\gamma$ -H2AX foci. *Mol. Cell* **16**, 715-724 (2004).
- 6 Mladenov, E., Magin, S., Soni, A. and Iliakis, G. DNA double-strand-break repair in higher eukaryotes and its role in genomic instability and cancer: Cell cycle and proliferation-dependent regulation. *Semin Cancer Biol.* **37-38**, 51-64 (2016).
- 7 Polo, S.E. & Jackson S.P. Dynamics of DNA damage response proteins at DNA breaks: a focus on protein modifications. *Genes Dev.* **25**, 409-433 (2011).
- 8 Mladenov, E. & Iliakis, G. Induction and repair of DNA double strand breaks: The increasing spectrum of non-homologous end joining pathways. *Mut. Res.* **711**, 61-72 (2011).
- 9 Brandsma, I. & Gent, D.C. Pathway choice in DNA double strand break repair: observation of a balancing act. *Genome Integrity* **3**:9 (2012).
- 10 Davis, A.J. & Chen, D. J. DNA double strand break repair via non-homologous end-joining. *Transl. Cancer Res.* **2**, 130-143 (2013).
- 11 Isono, M., et al. BRCA1 directs the repair pathway to homologous recombination by promoting 53BP1 dephosphorylation. *Cell Rep.* **18**, 520-532.
- 12 Chang, H.H.Y., Pannunzio, N., Adachi, N. & Lieber, M.R. Non-homologous DNA end joining and alternative pathways to double-strand break repair. *Nat. Rev. Mol. Cell. Biol.* **11**, 495-506 (2017).
- 13 Blackford, A.N. & Jackson, S.P. ATM, ATR and DNA-PK: The trinity at the Heart of the DNA damage response. *Mol. Cell* **66**, 801-817 (2017).
- 14 Hartwell, L.H. & Weinert, T.A. Checkpoints: controls that ensure the order of cell cycle events. *Science* **246**, 629-634 (1989).
- 15 Warmerdam, D.O. & Kanaar, R. Dealing with DNA damage: Relationship between checkpoint and repair pathways. *Mut. Res.* **704**, 2-11 (2010).
- 16 Shaltiel, I.A., Krenning, L., Bruinsma, W. & Medema, R.H. The same, only different- DNA damage checkpoints and their reversal throughout the cell cycle. *J. Cell Sci.* **128**, 607-620 (2015).
- 17 Jeggo, P.A. & Löbrich, M. How cancer cells hijack DNA double strand-break repair pathways to gain genomic instability. *Biochem. J.* **471**, 1-11 (2015).
- 18 El-Deiry, W.S. p21(WAF1) mediates cell-cycle inhibition, relevant to cancer suppression and therapy. *Cancer Res.* **76**, 5189-91 (2016).
- 19 Visconti, R., Della Monica, R. & Grieco, D. Cell cycle checkpoint in cancer: a therapeutic targetable double-edged sword. *J. Exp. Clin. Cancer Res.* **27**, 153 (2016).

- 20 Chapman, J.R., Sosick, A.J., Boulton, S.J. & Jackson, S.P. BRCA1-associated exclusion of 53BP1 from DNA damage sites underlies temporal control of DNA repair. *J. Cell Sci.* **125**, 3529-3534 (2012).
- 21 Zhang, H. et al. A cell cycle-dependent BRCA1-UHRF1 cascade regulates DNA double-strand break pathway choice. *Nat. Commun.* **7**, 10201 (2015).
- 22 Chapman, J.R. et al. RIF1 is essential for 53BP1-dependent nonhomologous end joining and suppression of DNA double-strand break resection. *Mol. Cell* **49**, 858-871 (2013).
- 23 Panier, S. & Boulton, S.J. Double-strand break repair: 53BP1 comes into focus. *Nat. Rev. Mol. Cell Biol.* **15**, 7-18 (2014).
- 24 Mackay, D.R. et al. Nup153 and Nup50 promotes recruitment of 53BP1 to DNA repair foci by antagonizing BRCA1-dependent events. *J. Cell Sci.* Advance article (2017).
- 25 Ciccia, A. & Elledge, S.J. The DNA damage response: making it safe to play with knives. *Mol. Cell* **40**, 179-204 (2010).
- 26 Gottlieb, T.M. & Jackson, S.P. The DNA-dependent protein kinase: requirement for DNA ends and association with Ku antigen. *Cell* **72**, 131-142 (1993).
- 27 Walker, J.R., Corpina, R.A. & Goldberg, J. Structure of the Ku heterodimer bound to DNA and its implications for double-strand break repair. *Nature* **412**, 607-614 (2001).
- 28 Ribes-Zamora, A., Mihalek, I., Lichtarge, O. & Bertuch, A.A. Distinct faces of the Ku heterodimer mediate DNA repair and telomeric function. *Nat. Struct. Mol. Biol.* **14**, 301-307 (2007).
- 29 Grundy, G.J. et al. The Ku-binding motif is a conserved module for recruitment and stimulation of non-homologous end-joining proteins. *Nat. Commun.* **7**, 11242 (2016).
- 30 Davis, A.J., Chen, B.P.C & Chen, D.J. DNA-PK: a dynamic enzyme in a versatile DSB repair pathway. *DNA Repair* **17**, 21-29 (2014).
- 31 Lee, K-J. et al. Phosphorylation of Ku dictates DNA double-strand break (DSB) repair pathway choice in S phase. *Nucl. Acids Res.* **44**, 1732-45 (2015).
- 32 Jessica S. Brown, J.S. et al. Neddylation promotes ubiquitylation and release of Ku from DNA-damage sites. *Cell Reports* **11**, 704–714 (2015).
- 33 Van den Boom, J. et al. VCP/p97 extracts sterically trapped Ku70/80 rings from DNA in double-strand break repair. *Mol. Cell* **64**, 189–198 (2016).
- 34 Deriano, L. & Roth, D.B. Modernizing the nonhomologous end-joining repertoire: alternative and classical NHEJ share the stage. *Annu. Rev. Genet.* **47**, 451-73 (2013).
- 35 Shamanna, R.A. et al. WRN regulates pathway choice between classical and alternative non-homologous end joining. *Nat. Commun.* **7**, 13785 (2016).
- 36 Biehs, R. et al. Double –strand break resection occurs during non-homologous end joining in G1 but is distinct from resection during homologous recombination. *Mol. Cell* **65**, 1-14 (2017).

- 37 Goedecke, W. et al. Mre11 and Ku70 interact in somatic cells, but are differentially expressed in early meiosis. *Nature Genet.* **23**, 194-198 (1999).
- 38 Foster, S.S., Balestrini, A. & Petrini, J.H. Functional interplay of the Mre11 nuclease and Ku in the response to replication-associated DNA damage. *Mol. Cell. Biol.* **31**, 4379-89 (2011).
- 39 Barton, O. et al. Polo-like kinase 3 regulates CtIP during DNA double-strand break repair in G1. *J. Cell Biol.* **206**, 877-894.
- 40 Cerrato, A., Morra, F. & Celetti, A. Use of poly ADP-ribose polymerase [PARP] inhibitors in cancer cells bearing DDR defects: the rationale for their inclusion in the clinic. *J. Exp. Clin. Cancer Res.* **35**, 179 (2016).
- 41 Brown, J.S., O’Carrigan, B., Jackson, S.P. & Yap, T.A. Targeting DNA repair in cancer: beyond PARP inhibitors. *Cancer Discovery* **7**,20-37 (2017).
- 42 McDonald, E.R. 3<sup>rd</sup> et al. Project DRIVE : A compendium of cancer dependencies and Synthetic Lethal relationship uncovered by large-scale, deep RNAi screening. *Cell* **170**, 577-592.
- 43 Bouley, J. et al. A new phosphorylated form of Ku70 identified in resistant leukemic cells confers fast but unfaithful DNA repair in cancer cell lines. *Oncotarget* **29**, 27980-8000 (2015).
- 44 Deriano, L. et al. Human chronic lymphocytic leukemia B cells can escape DNA damage-induced apoptosis through the nonhomologous end-joining DNA repair pathway. *Blood* **105**, 4776-83 (2005).
- 45 Deriano, L. Et al. Mutagenicity of non-homologous end joining DNA repair in a resistant subset of human chronic lymphocytic leukaemia B cells. *Br. J. Haematol.* **133**, 520-5 (2006).
- 46 Gu, Y. et al. Growth retardation and leaky SCID phenotype of Ku70-deficient mice. *Immunity* **7**, 653-65 (1997).
- 47 Pierce, A.J., Johnson, R.D., Thompson, L.H. & Jasin, M. XRCC3 promotes homology-directed repair of DNA damage in mammalian cells. *Genes Dev.* **13**,2633–2638 (1999).
- 48 Rass, E. et al. Role of Mre11 in chromosomal nonhomologous end joining in mammalian cells. *Nat. Struct. Mol. Biol.* **16**, 819-24 (2009).
- 49 Brugat T, Nguyen-Khac F, Grelier A, Merle-Béral H, Delic J. Telomere dysfunction-induced foci arise with the onset of telomeric deletions and complex chromosomal aberrations in resistant chronic lymphocytic leukemia cells. *Blood* **116**, 239-49 (2010).
- 50 Brugat, T. et al. Aberrant telomere structure is characteristic of resistant chronic lymphocytic leukaemia cells. *Leukemia* **24**, 246-51 (2010).

- 51 Brugat, T., Nguyen-Khac, F., Merle-Béral, H. & Delic, J. Concomitant telomere shortening, acquisition of multiple chromosomal aberrations and *in vitro* resistance to apoptosis in a single case of progressive CLL. *Leuk Res.* **35**, e37-4 (2011).
- 52 Koike, M., Yutoku, Y. & Koike, A. The C-terminal region of Rad52 is essential for Rad52 nuclear and nucleolar localization, and accumulation at DNA damage sites immediately after irradiation. *Biochem. Biophys. Res. Commun.* **435**,260-6 (2013)
- 53 Partridge, J.J., Lopreiato, J.O. Jr., Latterich, M. & Indig, F.E. DNA damage modulates nucleolar interaction of the Werner protein with the AAA ATPase p97/VCP. *Mol. Biol. Cell.* **14**, 4221-9 (2003).
- 54 Li, P. et al. ABH2 couples regulation of ribosomal DNA transcription with DNA alkylation repair. *Cell Rep.* **4**, 817-829 (2013).
- 55 Zhang, S., Hemmerich, P. & Grosse, F. Nucleolar localization of the human telomeric repeat binding factor 2 (TRF2). *J. Cell Sci.* **117**, 3935-3945 (2004).
- 56 Tsekrekou, M., Stratigi, K. & Chatzinikolaou, G. The nucleolus: In genome maintenance and repair. *Int. J. Mol. Sci.* **18**, 1411 (2017).
- 57 Adelman, G et al. DNA ends alter the molecular composition and localization of Ku multicomponent complexes. *Mol. Cell. Proteomics* **11**, 411-21 (2012).
- 58 Lee, K-J. et al. Phosphorylation of Ku dictates DNA double-strand break (DSB) repair pathway choice in S phase. *Nucleic Acids Res.* **44**, 1732-1745 (2016).
- 59 Jette, N. & Lees-Miller, S.P. The DNA-dependent protein kinase: A multifunctional protein kinase with roles in DNA double strand break repair and mitosis. *Prog. Biophys. Mol. Biol.* **117**, 194-205 (2015).
- 60 Mukherjee, S., Chakraborty, P. & Saha, P. Phosphorylation of Ku70 subunit by cell cycle kinases modulates the replication related function of Ku heterodimer. *Nucleic Acids Res.* **44**, 7755-65 (2016).
- 61 Ji, P. et al. DNA damage response involves modulation of Ku70 and Rb functions by cyclin A1 in leukemia cells. *Int. J. Cancer* **121**, 706-713 (2007).
- 62 Reid, D.A. et al. Organization and dynamic of the nonhomologous end-joining machinery during DNA double-strand break repair. *Proc. Natl. Acad. Sci.* **112**, E2575-84 (2015).
- 63 Elenbaas, B. et al. Human breast cancer cells generated by oncogenic transformation of primary mammary epithelial cells. *Genes Dev.* **15**, 50-65 (2001).
- 64 Barton, O. et al. Polo-like kinase 3 regulates CtIP during DNA double-strand break repair in G1. *J. Cell Biol.* **206**, 877-94 (2014).
- 65 Saha, J. & Davis, A.J. Unsolved mystery: the role of BRCA1 in DNA end-joining. *J. Radiat. Res.* **57**, i18-i24 (2016).

## Figure legends

**Figure1 pKu70 controls cell growth, promotes clonogenic survival and protect cells from apoptosis. (A) Cell growth of Ku70-transfected cell lines up to 7 days after irradiation.** No growth defects are observed in non-treated cells. After 2Gy irradiation a growth defect is noted after 4 days, which propagates until day 7. After 4Gy the growth defect is most pronounced. Whereas ala-Ku70 (red line) and glu-Ku70 (green line) expressing cells remain at constant cell numbers between day 3 and 7, ser-Ku70 (blue line) expressing cells resume cell growth after day7. Data represent total cell numbers. Error bars indicate SEM, n=4. Two-way ANOVA, Bonferroni-Test;  $p < 0.05 = *$ ;  $p < 0.01 = **$ ;  $p < 0.001 = ***$ . **(B) Clonogenic Survival** (Left panel, colon colors assigned as in right panel) Plating efficiency (PE) for the Ku70 mutants. Error bars indicate SEM, n = 4. Two-way ANOVA, Bonferroni-Test;  $p < 0.001 = ***$  (Right panel) Survival fraction of ser-Ku70 (blue line), ala-Ku70 (red line) and glu-Ku70 (green line) cells. PE is standardized to 1 at 0Gy, for each cell line. Data are fit to the linear-quadratic model. Error bars indicate SEM, n = 4. Two-way ANOVA, Bonferroni-Test;  $p < 0.05 = *$ ;  $p < 0.001 = ***$ . **(C) Cell death by apoptosis** (a) A representative plot with 4 quadrants that was used for data analysis. Cells that are alive are DiOC6+/PI-. Loss of MOMP leads to a decrease of DiOC6, apoptotic cells are thus DiOC6-/PI-. Dead cells show a PI positive and DiOC6 negative staining DiOC6+/PI-. (b) Percent of apoptotic and dead cells on day 3 after NT conditions, 2Gy or 4Gy irradiation. (c) Percent of apoptotic and dead cells on day 3 after Phleomycine treatment (1h). (d) Percent of apoptotic and dead cells on day 4 after NT conditions, 2Gy or 4Gy irradiation. (e) Percent of apoptotic and dead cells on day 4 after Phleomycine treatment (1h). Colon colors assigned as in Fig.1B. Data represent percent of apoptotic and dead cells. Error bars indicate SEM, n > 6. Two-way ANOVA, Bonferroni-Test;  $p < 0.05 = *$ ;  $p < 0.01 = **$ ;  $p < 0.001 = ***$ .

## Figure2

**Ser-Ku70 preferentially localizes in nucleoli, co-localizes with  $\gamma$ -H2AX at sites of DNA DSBs and interact with core components of NHEJ complex. (A).** (Upper panel), Cells were transfected with mEos2-ser-Ku70, mEos2-ala-Ku70 or mEos2-glu-Ku70 vectors and 48h after the florescence was examined by photo-activated localization microscopy (PALM). Scale bar =5 $\mu$ . (Lower panel), Local density analysis was also performed on the PALM data to characterize the different patterns of Ku70 nuclear distribution. **(B)** Cells were laser micro-irradiated (as described in Method section). Anti-pKu70 (b, green) and anti- $\gamma$ -H2AX (c, red) immunostaining was performed as described. Hoechst 33342 was used for chromatin-DNA labelling (a), overlay (d). **(C)** (a) Representative Western blot of a chromatin binding assay U2OS cells expressing ser-Ku70 were untreated (NT) or treated with indicated concentrations of DSBs-inducer Phleomycine. Two soluble fractions (F1 and F2) and chromatin fraction (F3, see Methods section) were probed for pKu70, Ku70 and  $\gamma$ -H2AX contents. (b) Quantification of the chromatin binding assay. n = 4. One-way ANOVA,  $p < 0.0001 = ****$ . **(D)** (a) Co- immunoprecipitation shows that pKu70 interacts with Ku80, Ligase

4 and PAXX. (b) Similarly Ku70 mutants show interaction with Ku80, Ligase 4 and PAXX. (E) Whole cell protein extracts of transfected HME cells expressing ser-Ku70 were co-immunoprecipitated, resolved by SDS-PAGE and proteolysed with trypsin. Peptides were analyzed through a Label-free-quantification (LFQ)-approach using an orbitrap-based mass spectroscopy analyzer. Corresponding genes symbolized by grey squares are considered with non-significant differences in their affinity towards Ku70 and/or pKu70 whereas these in red squares are considered as more specific partners of total Ku70 or pKu70.

### Figure3

**Kinetic of DSBs repair is accelerated in unsynchronized and G1 arrested cells expressing pKu70.** (A panel) Representative images of  $\gamma$ -H2AX foci in untreated and irradiated cells (4Gy) at several time points (0.5h, 4h, 24h) were shown. Nuclei are stained with Hoechst 33342 (blue),  $\gamma$ -H2AX with AlexaFlour 488 (green). Scale bar=5 $\mu$ m. (B) Results after automated quantification of  $\gamma$ -H2AX foci (CellProfiler). Cells were scored positive, when at least 3 foci were detected. At least 800 cells per cell line have been evaluated. Graphs represent data as boxplots with median, 1st and 3rd quartile, outliers are shown as dots, n=4. Unpaired t-test,  $p < 0.001 = ***$ . (C) GC92 cells were untreated (dotted blue line) or treated by mimosine (300 $\mu$ M overnight (red line), fixed and the cell cycle verified by flow cytometry. (D)  $\gamma$ -H2AX persistence in G1 after mimosine treatment. Representative images of  $\gamma$ -H2AX foci in ser-Ku70 and ala-Ku70A-expressing cells before (NT) and 2 and 4h after 4Gy-irradiation were shown. (E)  $\gamma$ -H2AX foci were scored as in (B). Graphs represent data as boxplots with median, 1st and 3rd quartile, upper and lower extreme whiskers at 95 and 5 percentiles, outliers are shown as dots, n=2. Unpaired t-test,  $p < 0.001 = **$ . Scale bar: 10  $\mu$ m.

### Figure4

**pKu70 confers more rapid dissociation from the sites of DNA-damage: inhibition of neddylation sustains both pKu70 release and DSBs following micro-irradiation.** Ku70 DNA DSB dissociation kinetics (A) Representative images of dissociation kinetics in GFP-Ku70Ser and GFP-Ku70Ala cells. Pictures depict cells before (NT), shortly after (t0) and at three time points after micro-irradiation (405nm). White arrows point to the damage site. (B) Relative intensity folds change based on the initial fluorescence intensity in NT cells. n=20 (ser-Ku70); n=27 (ala-Ku70). Unpaired t-test,  $p < 0.01 = *$ . Scale bar: 10 $\mu$ M. Western Blot of  $\gamma$ -H2AX after cell treatment with MLN4924 (3 $\mu$ M, 1h) followed by irradiation (4Gy). Actin is used as a loading control.

### Figure5



**Ser-Ku70 stimulates HR activity in absence of exogenous genotoxic stress. (A)** HR activity was measured using the U2OS cell line that expresses the integrated reporter construct pDR-GFP. This cell line was transfected by ser-, ala- or glu-Ku70 vectors as described in Methods section. The reporter is composed of two inactive eGFP genes. The upstream GFP gene is truncated; the gene downstream of the promoter has an integrated I-SCEI cleavage site and is therefore inactive. Upon I-SCEI expression the cleaved GFP gene recombines with the truncated GFP gene on the sister chromatid, resulting in the expression of GFP that was measured by flow cytometry. Results represent values that were calculated as: (I-SCEI-transfection events) - (control- transfection events). n= 6. Unpaired t-test,  $p < 0.01 = *$ . **(B)** NHEJ activity was measured using the human fibroblast cell line GC92 (SV40-transformed) that has the pCOH-CD4 (cohesive ends) reporter construct integrated intrachromosomally.. Upon cleavage by I-SCEI a fragment containing the H2Kd and CD8 genes is excised. Rejoining of the flanking ends by cNHEJ brings the pCMV promoter closer to the CD4 gene, which promotes its expression. The CD4 expression on the cell surface was quantified by flow cytometry. Results represent values that were calculated as: (I-SCEI-transfection events) - (control- transfection events). n= 4. Unpaired t-test,  $p < 0.01 = *$ .

#### Figure6

##### **pKu70 promotes genome stability after genotoxic stress.**

HME cells expressing ser-Ku70 or ala-Ku70 forms were irradiated at 4Gy and 24h after metaphases were probed for chromosomal aberrations by multi-FISH approach. Examples of 4 representative metaphases are shown. (Upper panel, left) untreated (NT) ser-Ku70 cells showing ins(1), ins(8), -10, del(11), der(18)t(11:18), +20, der(22)t(10;22); (Upper panel, right) ala-Ku70 cells showing the same aberrations as in left panel with an additional der(13)t((5;13) translocation. After irradiation (lower panels) only new translocation events (compared to untreated conditions), were taken into account. Other markers of genome instability : dmin (double minute); del (deletion); ace (acentric fragment); C-Frag (chromosomal fragment); mar (marker), are shown.

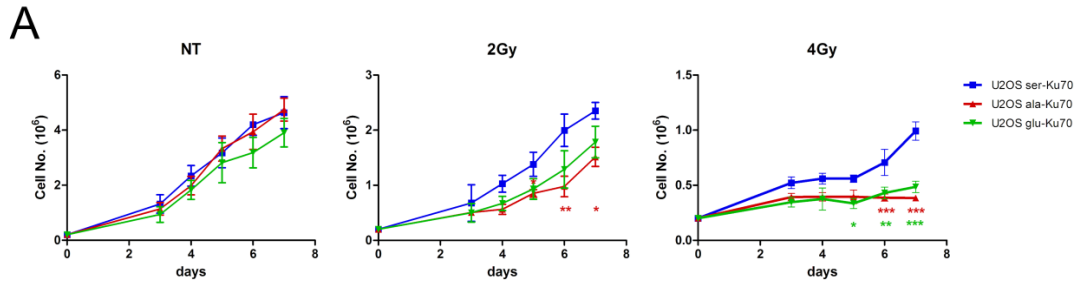


Fig 1 A

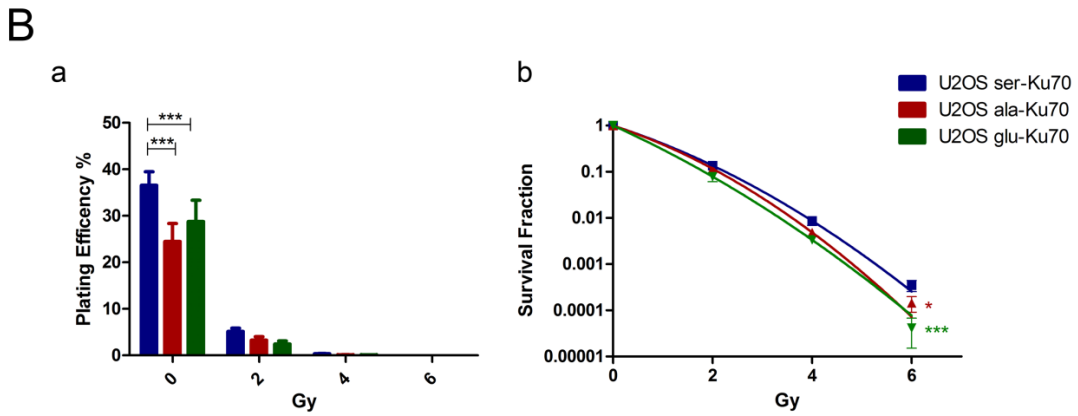


Fig. 1B

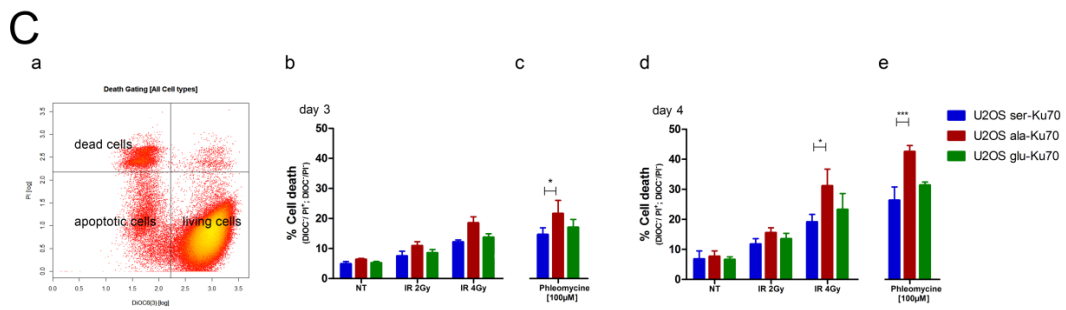


Fig. 1C

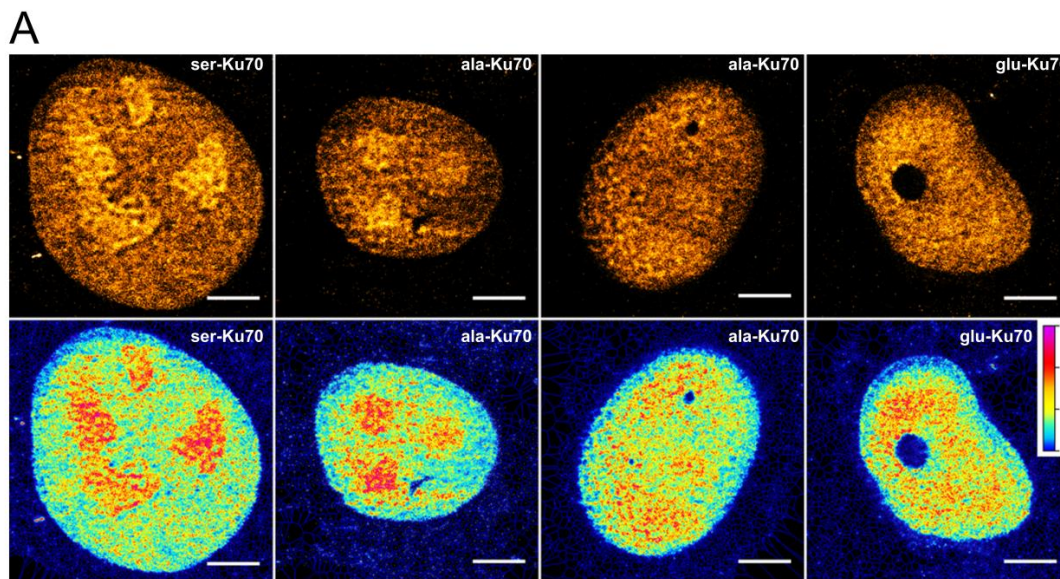


Fig. 2A

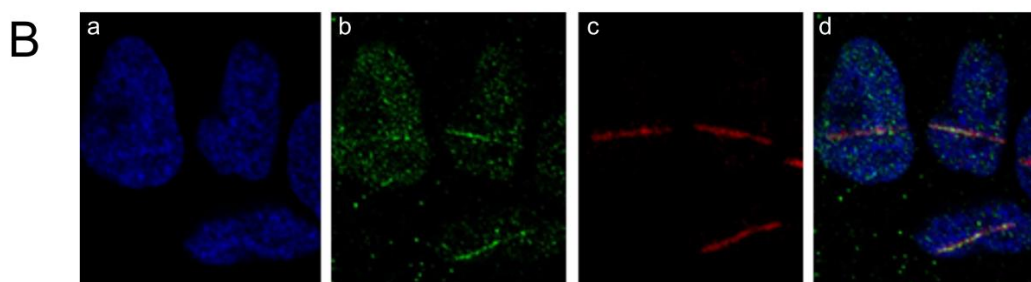


Fig. 2B

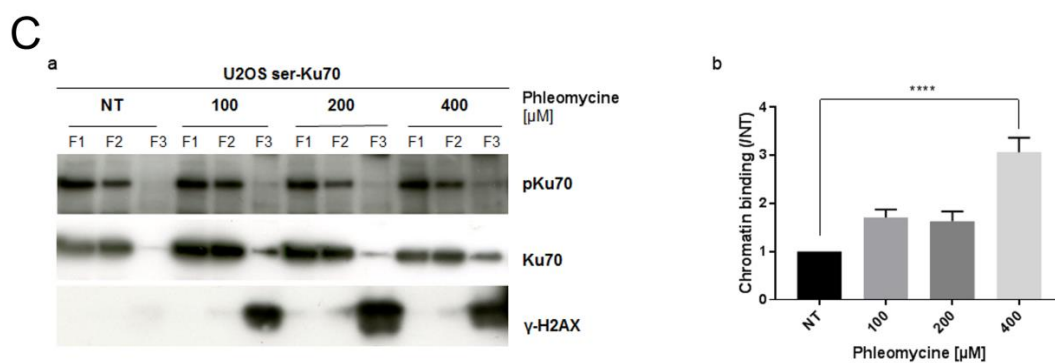


Fig. 2C

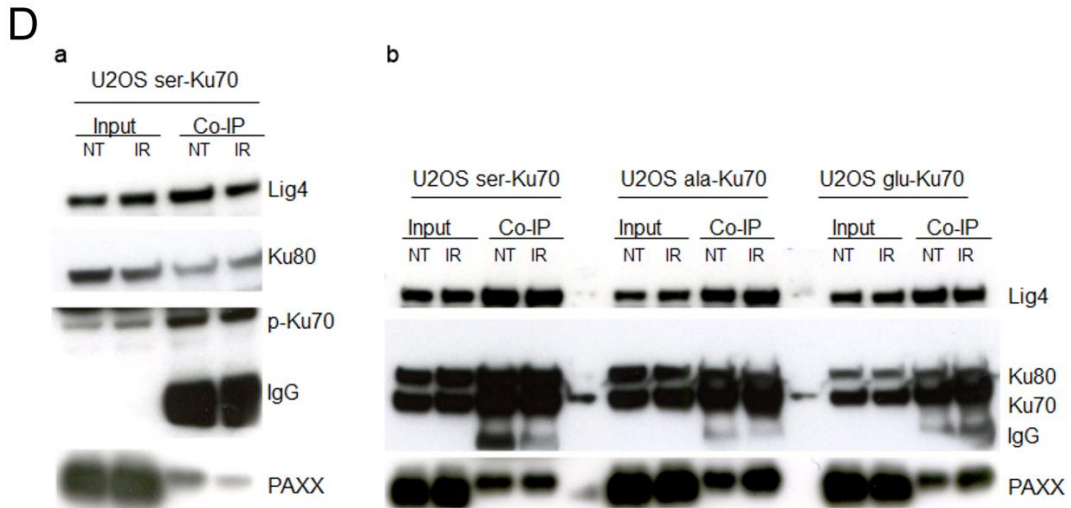


Fig. 2D

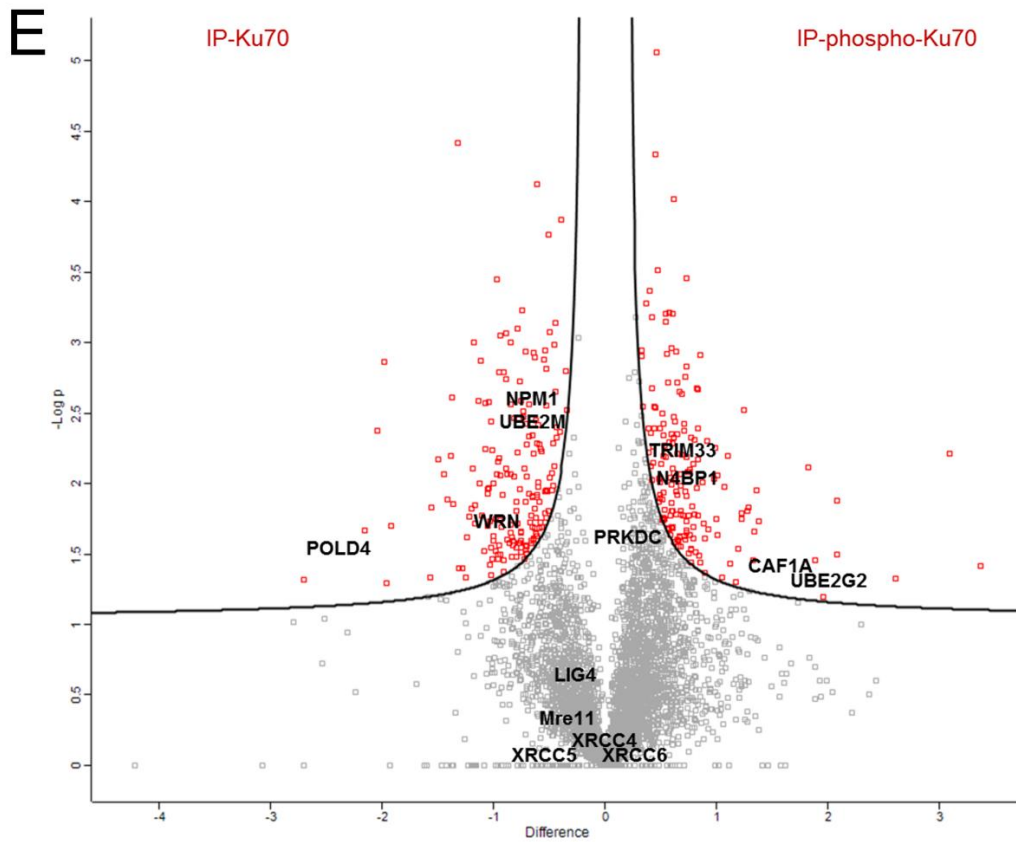


Fig. 2E

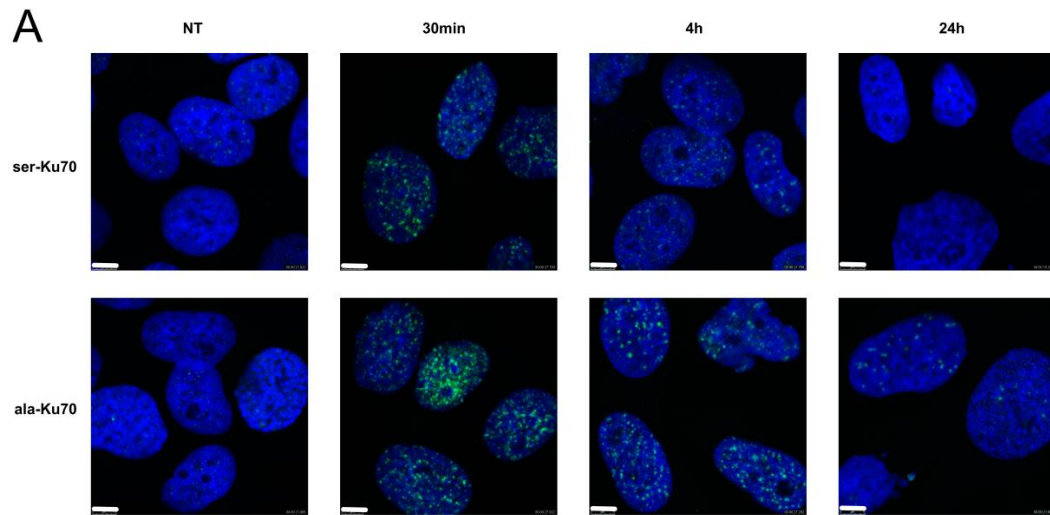


Fig. 3A

B

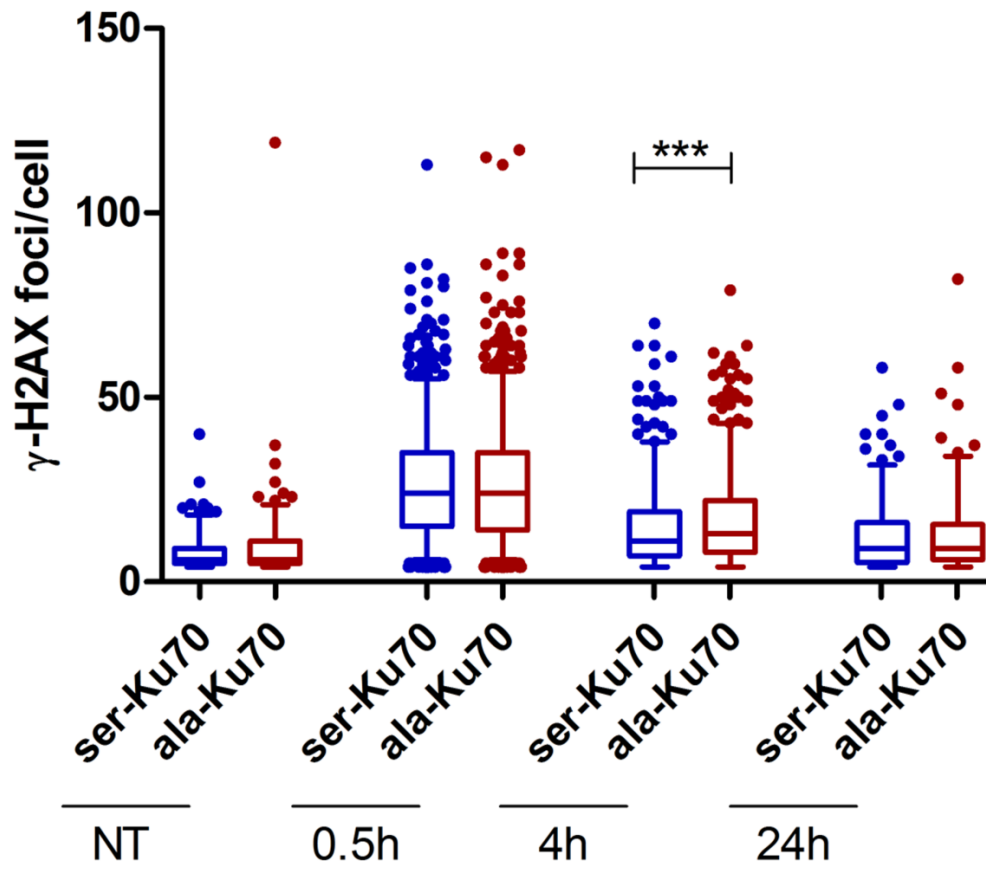


Fig. 3B

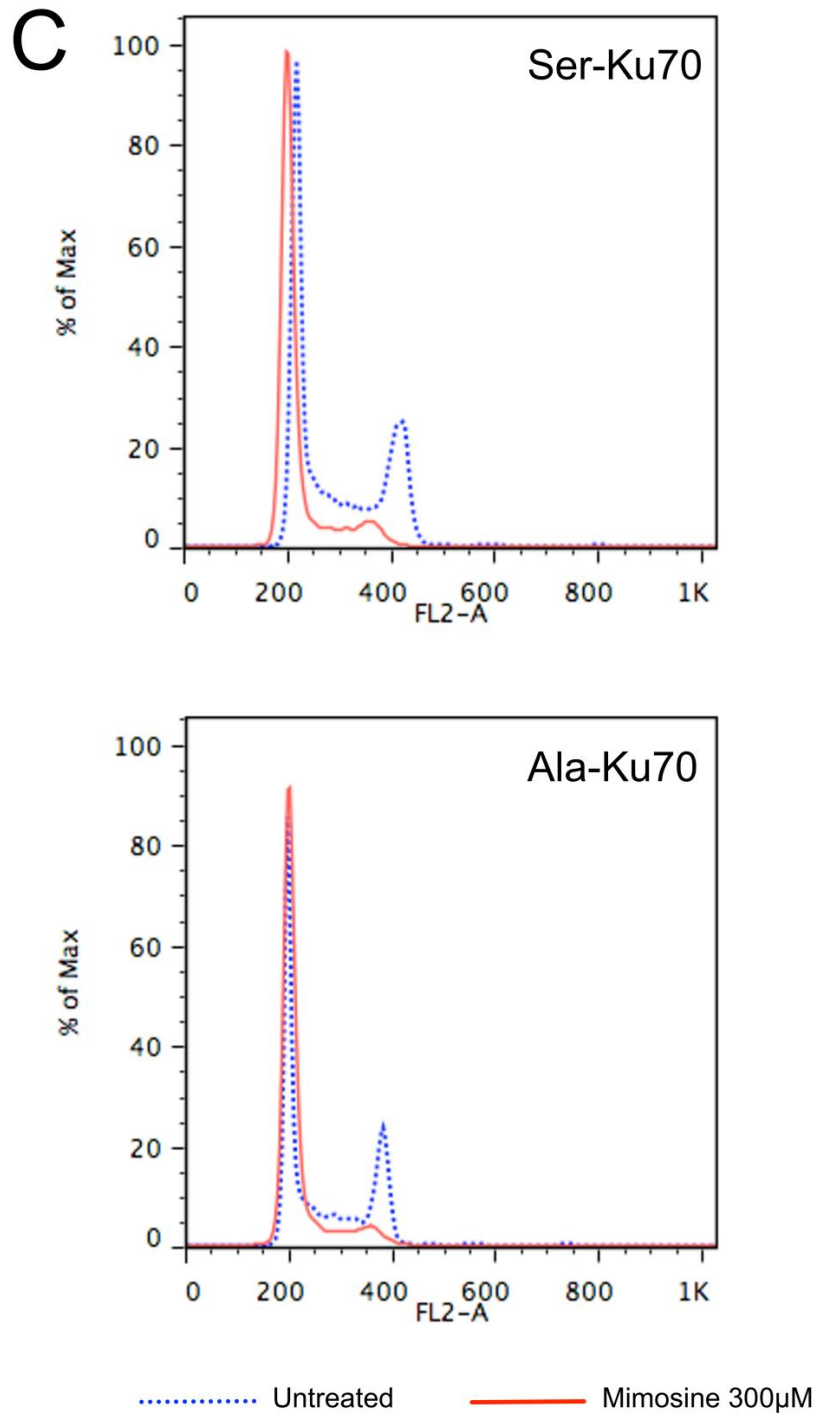


Fig.3C

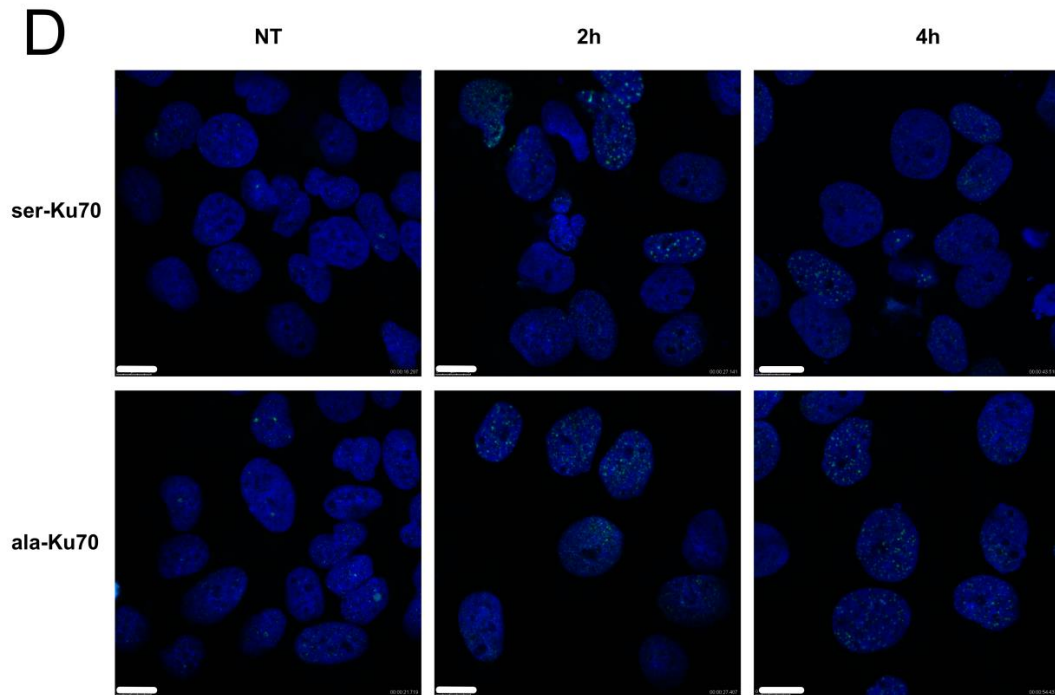


Fig.3D



E

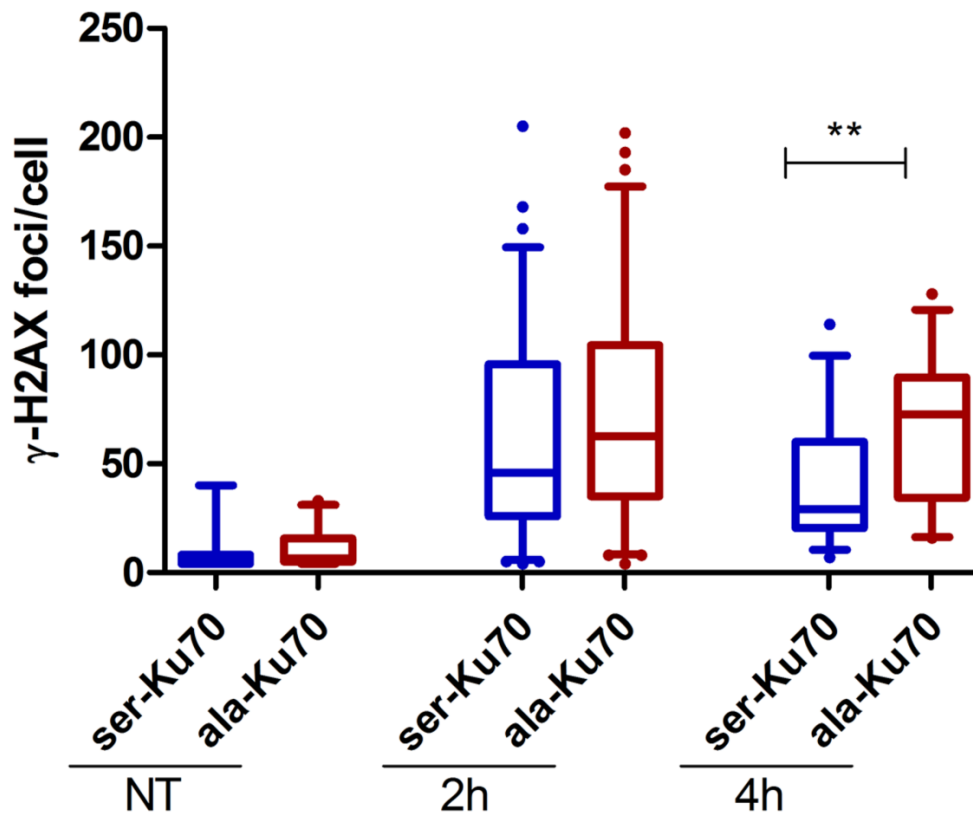


Fig.3E

A

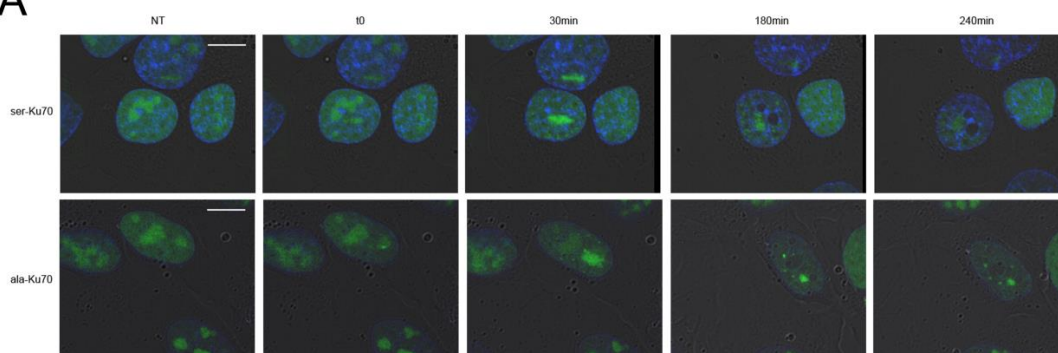


Fig. 4A

B

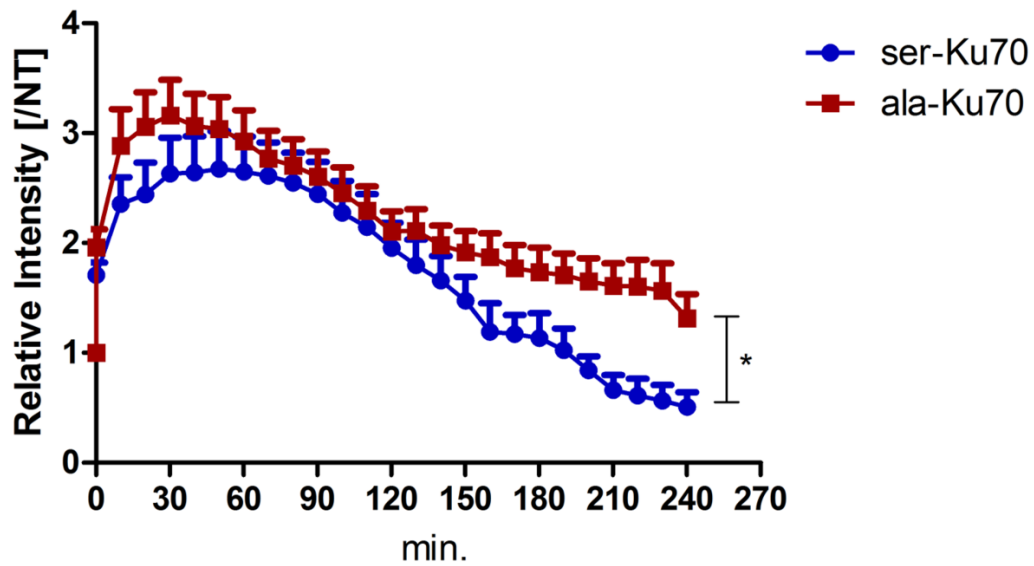


Fig. 4B

C

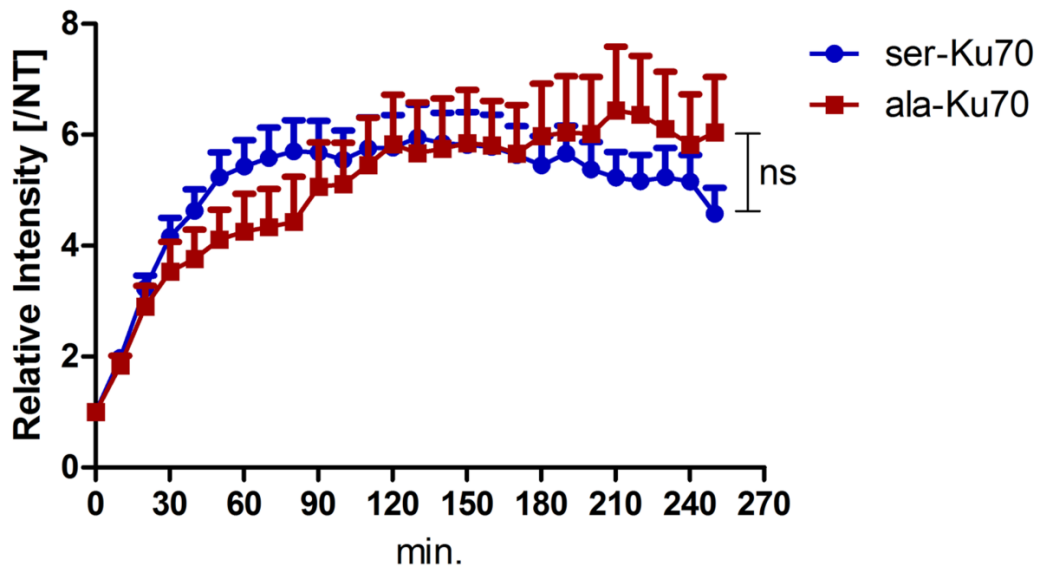


Fig. 4C

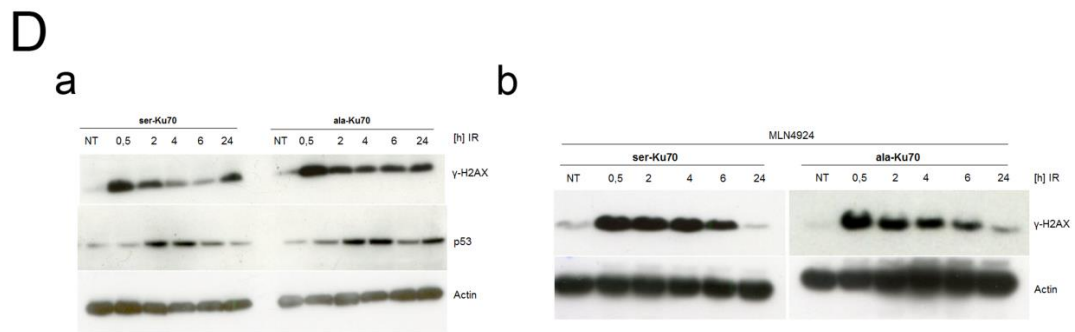


Fig.4D

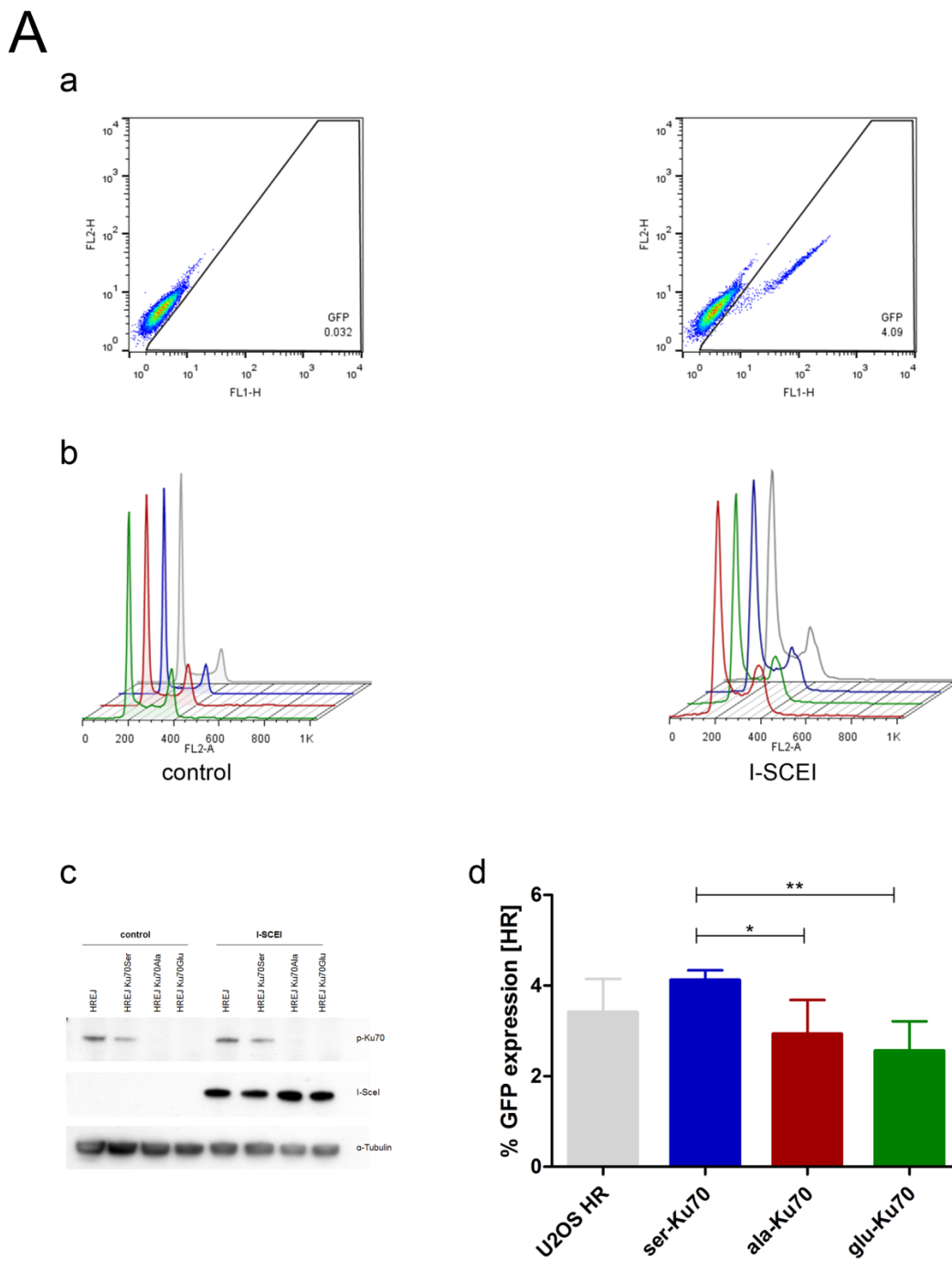


Fig.5A

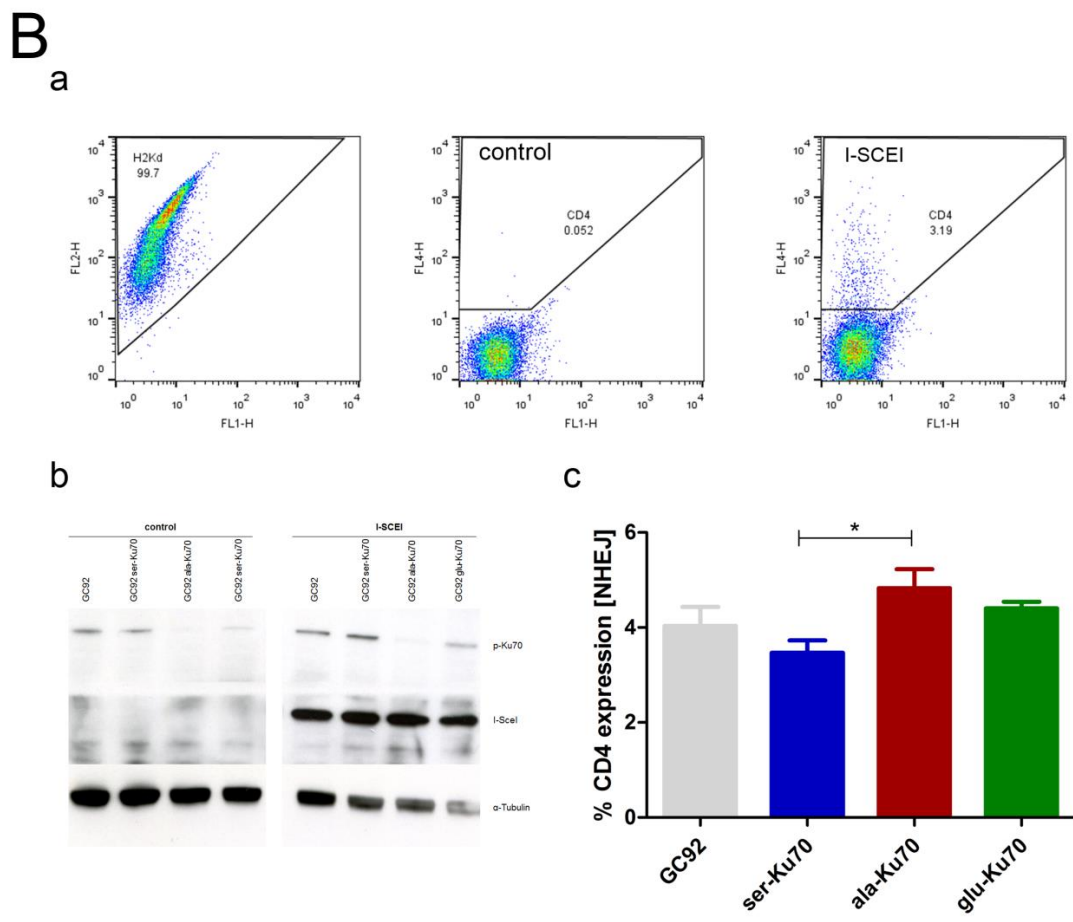


Fig.5B

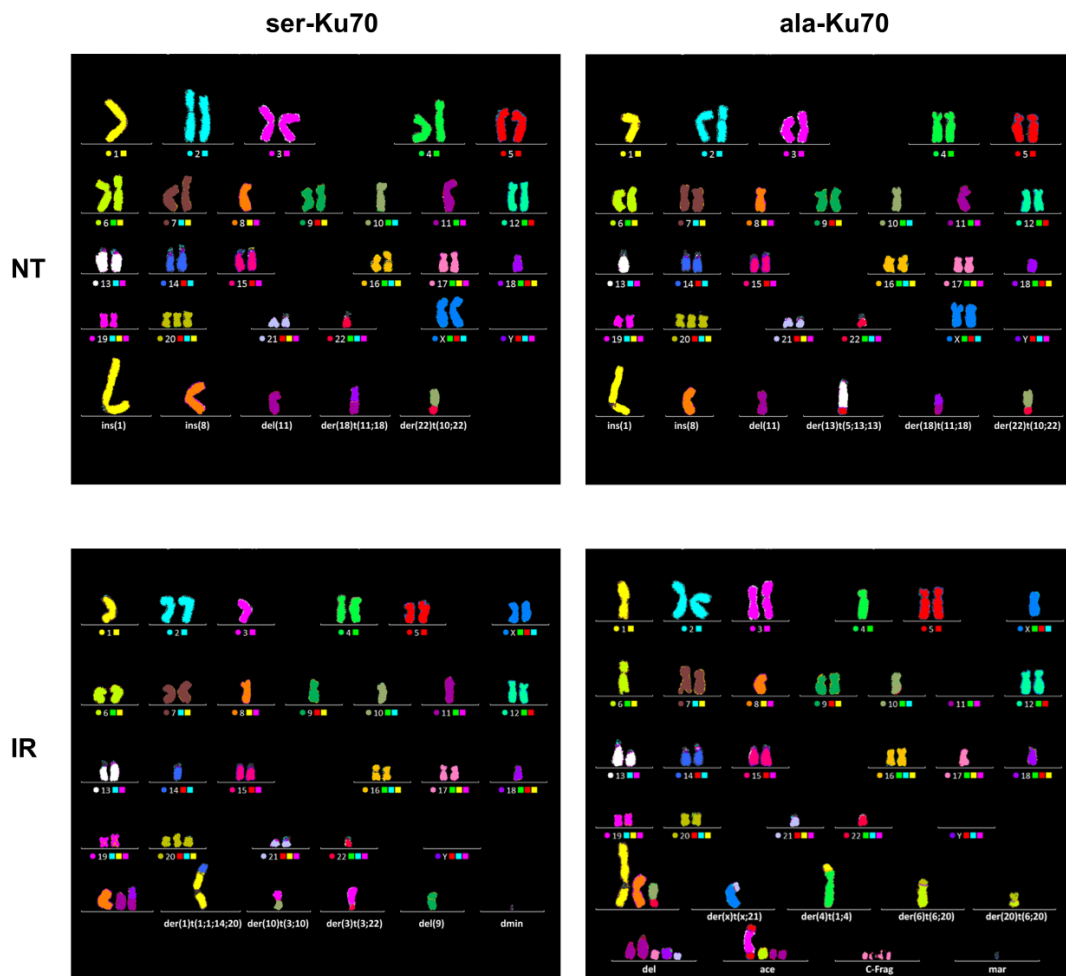


Fig.6

# Bibliography

- [1] Penny A. Jeggo, Laurence H. Pearl, and Antony M. Carr. DNA repair, genome stability and cancer: a historical perspective. *Nature reviews. Cancer*, 16(1):35–42, 2016. ISSN 1474-1768. doi: 10.1038/nrc.2015.4. URL <http://dx.doi.org/10.1038/nrc.2015.4>.
- [2] Errol C Friedberg. A brief history of the DNA repair field. *Cell research*, 18(1):3–7, 2008. ISSN 1748-7838. doi: 10.1038/cr.2007.113. URL <http://www.ncbi.nlm.nih.gov/pubmed/18157159>.
- [3] Douglas Hanahan and Robert A. Weinberg. Hallmarks of cancer: The next generation. *Cell*, 144(5):646–674, 2011. ISSN 00928674. doi: 10.1016/j.cell.2011.02.013. URL <http://dx.doi.org/10.1016/j.cell.2011.02.013>.
- [4] T Tojo, J Kaburaki, M Hayakawa, T Okamoto, M Tomii, and M Homma. Precipitating antibody to a soluble nuclear antigen "Ki" with specificity for systemic lupus erythematosus. *Ryumachi. [Rheumatism]*, 21 Suppl:129–40, jan 1981. ISSN 0300-9157.
- [5] T Mimori, M Akizuki, H Yamagate, S Inada, S Yoshida, and M Homma. Characterization of a High Molecular Weight Acidic Nuclear Protein Recognized by Autoantibodies in Sera from Patients with Polymyositis-Scleroderma Overlap.pdf. *The American Society for Clinical , Inc.*, 68: 611–620, 1981.
- [6] W H Reeves. Use of monoclonal antibodies for the characterization of novel DNA-binding proteins recognized by human autoimmune sera. *The Journal of experimental medicine*, 161(1):18–39, jan 1985. ISSN 0022-1007. URL <http://www.pubmedcentral.nih.gov/articlerender.fcgi?artid=2187551&tool=pmcentrez&rendertype=abstract>.
- [7] Ann-Michele Francoeur, Carol L Peebles, T Gompper, and ENG M. Tan. Identification of Ki (Ku, p70/p80) autoantigens and analysis of anti-Ki autoantibody reactivity. *The Journal of Immunology*, 136(5):1648–1653, 1986.
- [8] Tsuneyo Mimori and John Avery Hardin. Mechanism of Interaction between Ku Protein and DNA\*. *The Journal of biological chemistry*, 261(August 5): 10375–10379, 1986.

- [9] Jessica a Downs and Stephen P Jackson. A means to a DNA end: the many roles of Ku., may 2004. ISSN 1471-0072. URL <http://www.ncbi.nlm.nih.gov/pubmed/15122350>.
- [10] T Mimori, Y Ohosone, N Hama, A Suwa, M Akizuki, M Homma, A J Griffith, and J A Hardin. Isolation and characterization of cDNA encoding the 80-kDa subunit protein of the human autoantigen Ku (p70/p80) recognized by autoantibodies from patients with scleroderma-polymyositis overlap syndrome. *Proceedings of the National Academy of Sciences of the United States of America*, 87(5):1777–81, mar 1990. ISSN 0027-8424. URL <http://www.pubmedcentral.nih.gov/articlerender.fcgi?artid=53566&tool=pmcentrez&rendertype=abstract>.
- [11] W H Reeves and Z M Sthoeger. Molecular cloning of cDNA encoding the p70 (Ku) lupus autoantigen. *The Journal of biological chemistry*, 264(9):5047–52, mar 1989. ISSN 0021-9258. URL <http://www.ncbi.nlm.nih.gov/pubmed/2466842>.
- [12] William S Dynan and Sunghan Yoo. Interaction of Ku protein and DNA-dependent protein kinase catalytic subunit with nucleic acids. *Nucleic Acids Research*, 26(7):1551–1559, 1998.
- [13] David Gell and Stephen P Jackson. Mapping of protein – protein interactions within the DNA-dependent protein kinase complex. *Nucleic acids research*, 27(17):3494–3502, 1999.
- [14] J R Walker, R a Corpina, and J Goldberg. Structure of the Ku heterodimer bound to DNA and its implications for double-strand break repair. *Nature*, 412(6847):607–14, aug 2001. ISSN 0028-0836. doi: 10.1038/35088000. URL <http://www.ncbi.nlm.nih.gov/pubmed/11493912>.
- [15] J J Turchi, K M Henkels, and Y Zhou. Cisplatin-DNA adducts inhibit translocation of the Ku subunits of DNA-PK. *Nucleic acids research*, 28(23):4634–41, 2000. ISSN 1362-4962. URL <http://www.pubmedcentral.nih.gov/articlerender.fcgi?artid=115169&tool=pmcentrez&rendertype=abstract>.
- [16] S Yoo and W S Dynan. Geometry of a complex formed by double strand break repair proteins at a single DNA end: recruitment of DNA-PKcs induces inward translocation of Ku protein. *Nucleic acids research*, 27(24):4679–4686, 1999. ISSN 1362-4962. doi: 10.1093/nar/27.24.4679.
- [17] Boris Kysela, Aidan J. Doherty, Miroslav Chovanec, Thomas Stiff, Simon M. Ameer-Beg, Borivoj Vojnovic, Pierre Marie Girard, and Penny a. Jeggo. Ku stimulation of DNA ligase IV-dependent ligation requires inward movement along the DNA molecule. *Journal of Biological Chemistry*, 278(25):22466–22474, 2003. ISSN 00219258. doi: 10.1074/jbc.M303273200.
- [18] M Yaneva, T Kowalewski, and M.R Lieber. Interaction of DNA-dependent protein kinase with DNA and with Ku- biochemical ans atomic force microscopy studied.pdf. *The EMBO journal*, 16(16):5098–5112, 1997.



- [19] M Falzon, J W Fewell, and E L Kuff. EBP-80, a transcription factor closely resembling the human autoantigen Ku, recognizes single- to double-strand transitions in DNA. *Journal of Biological Chemistry*, 268(14):10546–10552, 1993. ISSN 0021-9258. URL <http://www.ncbi.nlm.nih.gov/pubmed/8486707>.
- [20] Peter R Blier, Andrew J Griffith, Joe Craft, and a Hardin. Binding of Ku Protein to DNA. *journal of Biological Chemistry*, 268(10):7594–7601, 1993. ISSN 0021-9258.
- [21] Richard Harris, Diego Esposito, Andrew Sankar, Joseph D. Maman, John A. Hinks, Laurence H. Pearl, and Paul C. Driscoll. The 3D Solution Structure of the C-terminal Region of Ku86 (Ku86CTR). *Journal of Molecular Biology*, 335(2):573–582, 2004. ISSN 00222836. doi: 10.1016/j.jmb.2003.10.047.
- [22] L. Aravind and Eugene V. Koonin. SAP - A putative DNA-binding motif involved in chromosomal organization. *Trends in Biochemical Sciences*, 25(3):112–114, 2000. ISSN 09680004. doi: 10.1016/S0968-0004(99)01537-6.
- [23] Ziming Zhang, Lingyang Zhu, Donghai Lin, Fanqing Chen, David J. Chen, and Yuan Chen. The Three-dimensional Structure of the C-terminal DNA-binding Domain of Human Ku70. *Journal of Biological Chemistry*, 276(41):38231–38236, 2001. ISSN 00219258. doi: 10.1074/jbc.M105238200.
- [24] Angel Rivera-Calzada, Laura Spagnolo, Laurence H Pearl, and Oscar Llorca. Structural model of full-length human Ku70-Ku80 heterodimer and its recognition of DNA and DNA-PKcs. *EMBO reports*, 8(1):56–62, 2006. ISSN 1469-221X. doi: 7400847[pii]\r10.1038/sj.embor.7400847. URL <http://embor.embopress.org/content/8/1/56.abstract>.
- [25] Ziming Zhang, Weidong Hu, Leticia Cano, Terry D Lee, David J Chen, and Yuan Chen. Solution structure of the C-terminal domain of Ku80 suggests important sites for protein-protein interactions. *Structure (London, England : 1993)*, 12(3):495–502, mar 2004. ISSN 0969-2126. doi: 10.1016/j.str.2004.02.007. URL <http://www.ncbi.nlm.nih.gov/pubmed/15016365>.
- [26] Zhiyong Han, Christine Johnston, Westley H. Reeves, Timothy Carter, James H. Wyche, and Eric A. Hendrickson. Characterization of a Ku86 variant protein that results in altered DNA binding and diminished DNA-dependent protein kinase activity. *Journal of Biological Chemistry*, 271(24):14098–14104, 1996. ISSN 00219258. doi: 10.1074/jbc.271.24.14098.
- [27] C Muller and B Salles. Regulation of DNA-dependent protein kinase activity in leukemic cells. *Oncogene*, 15(19):2343–8, 1997. ISSN 0950-9232. doi: 10.1038/sj.onc.1201402. URL <http://www.ncbi.nlm.nih.gov/pubmed/9393878>.
- [28] B K Singleton, S T Rottinghaus, and G E Taccioli. The C Terminus of Ku80 Activates the DNA-Dependent Protein Kinase Catalytic Subunit. *Molecular and cellular biology*, 19(5):3267–3277, 1999.

- [29] Jacob Falck, Julia Coates, and Stephen P Jackson. Conserved modes of recruitment of ATM , ATR and DNA-PKcs to sites of DNA damage. *Nature*, 434(March):605–611, 2005.
- [30] N J Jones, R Cox, and J Thacker. Six complementation groups for ionizing-radiation sensitivity in Chinese hamster cells. *Mutation Res.*, 193:139–144, 1988.
- [31] J Thacker and R E Wilkinson. The genetic basis of resistance to ionising radiation damage in cultured mammalian cells. *Mutation research*, 254(2): 135–142, 1991. ISSN 09218777.
- [32] P a Jeggo, J Tesmer, and D J Chen. Genetic analysis of ionising radiation sensitive mutants of cultured mammalian cell lines. *Mutation research*, 254 (2):125–33, 1991. ISSN 0027-5107. URL <http://www.ncbi.nlm.nih.gov/pubmed/2002809>.
- [33] Malgorzata Z Zdzienicka. Mammalian mutants defective in the response to ionizing radiation-induced DNA damage. *Mutation research*, 336:203–213, 1995.
- [34] Andrew R. Collins. Mutant rodent cell lines sensitive to ultraviolet light , ionizing radiation and cross-linking agents : a comprehensive survey of genetic and biochemical characteristics. *Mutation Research/DNA Repair*, 293:99–118, 1993.
- [35] L. M. Kemp, S. G. Sedgwick, and P. A. Jeggo. X-ray sensitive mutants of Chinese hamster ovary cells defective in double-strand break rejoining. *Mutation Research DNA Repair Reports*, 132(5-6):189–196, 1984. ISSN 01678817. doi: 10.1016/0167-8817(84)90037-3.
- [36] P A Jeggo and L M Kemp. X-Ray-sensitive mutants of Chinese hamster ovary cell line. Isolation and cross- sensitivity to other DNA damaging agents. *Mutation research*, 112:313–327, 1983.
- [37] P. A. Jeggo. X-ray sensitive mutants of Chinese hamster ovary cell line: radio-sensitivity of DNA synthesis. *Mutation Research DNA Repair Reports*, 145(3):171–176, 1985. ISSN 01678817. doi: 10.1016/0167-8817(85)90024-0.
- [38] PA. Jeggo. Genetic analysis of X-ray-sensitive mutants of the CHO cell line Jeggo. *Mutation Research DNA Repair Reports*, 146:265–270, 1985.
- [39] L. M. Kemp and P. A. Jeggo. Radiation-induced chromosome damage in X-ray-sensitive mutants (xrs) of the Chinese hamster ovary cell line. *Mutation Research DNA Repair Reports*, 166(3):255–263, 1986. ISSN 01678817. doi: 10.1016/0167-8817(86)90025-8.
- [40] B K Singleton, A Priestley, H Steingrimsdottir, D Gell, T Blunt, S P Jackson, A R Lehmann, and P A Jeggo. Molecular and biochemical characterization of xrs mutants defective in Ku80. *Molecular and cellular biology*, 17(3):1264–73, mar 1997. ISSN 0270-7306.

URL <http://www.pubmedcentral.nih.gov/articlerender.fcgi?artid=231851&tool=pmcentrez&rendertype=abstract>.

- [41] Vaughn Smider, W Kimryn Rathmell, Michael R Lieber, and Gilbert Chut. Restoration of X-ray Resistance and V ( D ) J Recombination in Mutant Cells by Ku cDNA. *Science*, 61:13–16, 1994.
- [42] G E Taccioli, T M Gottlieb, T Blunt, A Priestley, J Demengeot, R Mizuta, a R Lehmann, F W Alt, S P Jackson, and P A Jeggo. Ku80: product of the XRCC5 gene and its role in DNA repair and V(D)J recombination. *Science (New York, N.Y.)*, 265(5177):1442–5, sep 1994. ISSN 0036-8075. doi: 10.1126/science.8073286. URL <http://www.ncbi.nlm.nih.gov/pubmed/8073286>.
- [43] A Errami, V Smider, W K Rathmell, D M He, E A Hendrickson, M Z Zdzienicka, and G Chu. Ku86 defines the genetic defect and restores X-ray resistance and V(D)J recombination to complementation group 5 hamster cell mutants. *Molecular and cellular biology*, 16(4):1519–26, apr 1996. ISSN 0270-7306. URL <http://www.pubmedcentral.nih.gov/articlerender.fcgi?artid=231136&tool=pmcentrez&rendertype=abstract>.
- [44] Penny A Jeggo, Guillermo E Taccioli, and Stephen P Jackson. Menage à trois: double strans break repair, V(D)J recombination and DNA-PK. *Bioassays*, 17(11):949–957, 1995.
- [45] Tanya M Gottlieb and P Jackson. The DNA-Dependent Protein Kinase: Requirment for DNA Ends and Association with Ku Antigen. *Cell*, 72: 131–142, 1993.
- [46] Nicholas J Finnie, Tanya M Gottlieb, Tracy Blunt, Penny A Jeggo, and Stephen P Jackson. DNA-dependent protein kinase activity is absent in xrs-6 cells: Implications for site-specific recombination and DNA double-strand break repair. *Proc Natl Acad Sci U S A*, 92(January):320–324, 1995.
- [47] Nicolai V Boubnov, Kathryn T. Hall, Zachary Wills, Sang Eun Lee, Dong Min He, Damien M Benjamin, Cheryl R Pulaskit, Hamid Band, Westley Reeveso, Eric A Hendricksont, and David T Weaver. Complementation of the ionizing radiation sensitivity, DNA end binding, and (V(D)J recombination defects of double-strand break repair mutants by the p86 Ku autoantigen. *Biochemistry*, 92(January):890–894, 1995.
- [48] U Grawunder, M Wilm, X Wu, P Kulesza, T E Wilson, M Mann, and M R Lieber. Activity of DNA ligase IV stimulated by complex formation with XRCC4 protein in mammalian cells. *Nature*, 388(6641):492–5, 1997. ISSN 0028-0836. doi: 10.1038/41358. URL <http://dx.doi.org/10.1038/41358>  
<http://www.ncbi.nlm.nih.gov/pubmed/9242410>.
- [49] S. A. Nick McElhinny, C. M. Snowden, J. McCarville, and D. A. Ramsden. Ku recruits the XRCC4-ligase IV complex to DNA ends. *Molecular and Cellular Biology*, 20(9):2996–3003, 2000.

- ISSN 0270-7306. doi: 10.1128/MCB.20.9.2996-3003.2000. URL <http://www.pubmedcentral.nih.gov/articlerender.fcgi?artid=85565&tool=pmcentrez&rendertype=abstract>.
- [50] Ling Chen, Kelly Trujillo, Patrick Sung, and Alan E. Tomkinson. Interactions of the DNA ligase IV-XRCC4 complex with DNA ends and the DNA-dependent protein kinase. *Journal of Biological Chemistry*, 275(34): 26196–26205, 2000. ISSN 00219258. doi: 10.1074/jbc.M000491200.
- [51] D B Roth, T Lindahl, and M Gellert. How to make ends meet The repair of double-stranded breaks in DNA and the recombination Ku protein , which binds DNA ends , and its associated protein kinase . *Current Biology*, 5(5): 496–499, 1995.
- [52] S Thode, A Schäfer, P Pfeiffer, and W Vielmetter. A novel pathway of DNA end-to-end joining. *Cell*, 60(6):921–8, mar 1990. ISSN 0092-8674. URL <http://www.ncbi.nlm.nih.gov/pubmed/2317864>.
- [53] Nicole Beyert, Susanne Reichenberger, Michael Peters, Markus Hartung, Bernd Göttlich, Wolfgang Goedecke, Walter Vielmetter, and Petra Pfeiffer. Nonhomologous DNA end joining of synthetic hairpin substrates in *Xenopus laevis* egg extracts. *Nucleic Acids Research*, 22(9):1643–1650, 1994. ISSN 03051048. doi: 10.1093/nar/22.9.1643.
- [54] L H Thompson and P a Jeggo. Nomenclature of human genes involved in ionizing radiation sensitivity. *Mutation research*, 337(2):131–4, sep 1995. ISSN 0027-5107. URL <http://www.ncbi.nlm.nih.gov/pubmed/7565861>.
- [55] John Thacker and Małgorzata Z. Zdzienicka. The mammalian XRCC genes: Their roles in DNA repair and genetic stability. *DNA Repair*, 2(6):655–672, 2003. ISSN 15687864. doi: 10.1016/S1568-7864(03)00062-4.
- [56] T Lindahl. Instability and decay of the primary structure of DNA. *Nature*, 363:210–211, 1993.
- [57] Jan H J Hoeijmakers. Genome maintenance for Preventing Cancer. *DNA Repair*, 411:366–374, 2001. ISSN 00280836. doi: 10.1038/35077232.
- [58] Jessica S. Brown, Brent O’Carrigan, Stephen P. Jackson, and Timothy A. Yap. Targeting DNA repair in cancer: Beyond PARP inhibitors. *Cancer Discovery*, 7(1):20–37, 2017. ISSN 21598290. doi: 10.1158/2159-8290.CD-16-0860.
- [59] Keith W Caldecott. Single-strand break repair and genetic disease. *Nature reviews. Genetics*, 9(5):341–55, 2008. ISSN 1471-0064. doi: 10.1038/nrg2346. URL <http://www.pubmedcentral.nih.gov/articlerender.fcgi?artid=2756414&tool=pmcentrez&rendertype=abstract>.
- [60] Stephen Jackson and Jiri Bartek. The DNA-damage response in human biology and disease. *Nature*, 461(7267):1071–1078, 2009. ISSN 1476-4687. doi: 10.1038/nature08467. URL

<http://www.pubmedcentral.nih.gov/articlerender.fcgi?artid=2906700&tool=pmcentrez&rendertype=abstract>.

- [61] Hans E. Krokan and Magnar Bjoras. Base Excision Repair. *Perspectives in Biology*, 5:1–17, 2008. doi: 10.1101/cshperspect.a012583. URL <papers://a0f45058-72ca-4dc9-be03-e459899c7713/Paper/p615>.
- [62] Jurgen A. Marteijn, Hannes Lans, Wim Vermeulen, and Jan H. J. Hoeijmakers. Understanding nucleotide excision repair and its roles in cancer and ageing. *Nature Reviews Molecular Cell Biology*, 15(7):465–481, jun 2014. ISSN 1471-0072. doi: 10.1038/nrm3822. URL <http://www.ncbi.nlm.nih.gov/pubmed/24954209><http://www.nature.com/doifinder/10.1038/nrm3822>.
- [63] H Walden and a J Deans. The Fanconi anemia DNA repair pathway: structural and functional insights into a complex disorder. *Annu Rev Biophys*, 43:257–278, 2014. ISSN 1936-1238. doi: 10.1146/annurev-biophys-051013-022737. URL <http://www.ncbi.nlm.nih.gov/pubmed/24773018><http://www.annualreviews.org/doi/abs/10.1146/annurev-biophys-051013-022737>.
- [64] Sonali Bhattacharjee and Saikat Nandi. Choices have consequences: the nexus between DNA repair pathways and genomic instability in cancer. *Clinical and Translational Medicine*, 5(1):45, 2016. ISSN 2001-1326. doi: 10.1186/s40169-016-0128-z. URL <http://www.ncbi.nlm.nih.gov/pubmed/27921283><http://clintransmed.springeropen.com/articles/10.1186/s40169-016-0128-z>.
- [65] Raphael Ceccaldi, Beatrice Rondinelli, and Alan D. D’Andrea. Repair Pathway Choices and Consequences at the Double-Strand Break. *Trends in Cell Biology*, 26(1):52–64, 2016. ISSN 18793088. doi: 10.1016/j.tcb.2015.07.009. URL <http://dx.doi.org/10.1016/j.tcb.2015.07.009>.
- [66] Ludovic Deriano and David B Roth. Modernizing the nonhomologous end-joining repertoire: alternative and classical NHEJ share the stage. *Annual review of genetics*, 47:433–55, 2013. ISSN 1545-2948. doi: 10.1146/annurev-genet-110711-155540. URL <http://www.ncbi.nlm.nih.gov/pubmed/24050180>.
- [67] Mireille Bétermier, Pascale Bertrand, and Bernard S Lopez. Is non-homologous end-joining really an inherently error-prone process? *PLoS genetics*, 10(1):e1004086, jan 2014. ISSN 1553-7404. doi: 10.1371/journal.pgen.1004086. URL <http://www.pubmedcentral.nih.gov/articlerender.fcgi?artid=3894167&tool=pmcentrez&rendertype=abstract>.
- [68] Ketki Karanam, Ran Kafri, Alexander Loewer, and Galit Lahav. Quantitative Live Cell Imaging Reveals a Gradual Shift between DNA Repair Mechanisms and a Maximal Use of HR in Mid S Phase. *Molecular Cell*, 47(2):320–329, 2012. ISSN 10972765. doi: 10.1016/j.molcel.2012.05.052.

- [69] Emil Mladenov, Simon Magin, Aashish Soni, and George Iliakis. DNA double-strand-break repair in higher eukaryotes and its role in genomic instability and cancer: Cell cycle and proliferation-dependent regulation. *Seminars in Cancer Biology*, 37-38:51–64, jun 2016. ISSN 1044579X. doi: 10.1016/j.semcancer.2016.03.003. URL <http://www.ncbi.nlm.nih.gov/pubmed/27016036><http://linkinghub.elsevier.com/retrieve/pii/S1044579X16300074>.
- [70] Victoria L. Fell and Caroline Schild-Poulter. The Ku heterodimer: Function in DNA repair and beyond. *Mutation Research - Reviews in Mutation Research*, 763:15–29, 2015. ISSN 13882139. doi: 10.1016/j.mrrev.2014.06.002. URL <http://dx.doi.org/10.1016/j.mrrev.2014.06.002>.
- [71] N Adachi, T Ishino, Y Ishii, S Takeda, and H Koyama. DNA ligase IV-deficient cells are more resistant to ionizing radiation in the absence of Ku70: Implications for DNA double-strand break repair. *Proceedings of the National Academy of Sciences*, 98(21):12109–12113, 2001. ISSN 0027-8424. doi: 10.1073/pnas.201271098. URL <http://www.pnas.org/cgi/doi/10.1073/pnas.201271098>.
- [72] A. Kakarougkas and P. A. Jeggo. DNA DSB repair pathway choice: An orchestrated handover mechanism. *British Journal of Radiology*, 87(1035), 2014. ISSN 00071285. doi: 10.1259/bjr.20130685.
- [73] Zhiyong Mao, Michael Bozzella, Andrei Seluanov, and Vera Gorbunova. DNA repair by nonhomologous end joining and homologous recombination during cell cycle in human cells. *Cell Cycle*, 7(18):2902–29, 2008. ISSN 15378276. doi: 10.1016/j.pestbp.2011.02.012. Investigations.
- [74] Agnel Sfeir and Lorraine S. Symington. Microhomology-Mediated End Joining: A Back-up Survival Mechanism or Dedicated Pathway? *Trends in Biochemical Sciences*, 40(11):701–714, 2015. ISSN 13624326. doi: 10.1016/j.tibs.2015.08.006. URL <http://dx.doi.org/10.1016/j.tibs.2015.08.006>.
- [75] Raphael Ceccaldi, Jessica C Liu, Ravindra Amunugama, Ildiko Hajdu, Benjamin Primack, Mark I R Petalcorin, Kevin W O'Connor, Panagiotis A Konstantinopoulos, Stephen J Elledge, Simon J Boulton, Timur Yusufzai, and Alan D D'Andrea. Homologous-recombination-deficient tumours are dependent on Pol $\theta$ -mediated repair. *Nature*, 518(7538):258–62, 2015. ISSN 1476-4687. doi: 10.1038/nature14184. URL <http://www.pubmedcentral.nih.gov/articlerender.fcgi?artid=4415602&tool=pmcentrez&rendertype=abstract>.
- [76] Minli Wang, Weizhong Wu, Wenqi Wu, Bustanur Rosidi, Lihua Zhang, Huichen Wang, and George Iliakis. PARP-1 and Ku compete for repair of DNA double strand breaks by distinct NHEJ pathways. *Nucleic acids research*, 34(21):6170–82, jan 2006. ISSN 1362-4962. doi: 10.1093/nar/gkl840. URL <http://www.pubmedcentral.nih.gov/articlerender.fcgi?artid=1693894&tool=pmcentrez&rendertype=abstract>.

- [77] Pedro A Mateos-Gomez, Fade Gong, Nidhi Nair, Kyle M Miller, Eros Lazzerini-Denchi, and Agnel Sfeir. Mammalian polymerase  $\theta$  promotes alternative NHEJ and suppresses recombination. *Nature*, 518 (7538):254–7, 2015. ISSN 1476-4687. doi: 10.1038/nature14157. URL <http://www.pubmedcentral.nih.gov/articlerender.fcgi?artid=4718306&tool=pmcentrez&rendertype=abstract>.
- [78] Sophie Paillard, Francois Strauss, Institut Jacques Monod, and Place Jussieu. Analysis of the mechanism of interaction of simian Ku protein with DNA. *Nucleic acids research*, 19(20):5619–24, oct 1991. ISSN 0305-1048. URL <http://www.pubmedcentral.nih.gov/articlerender.fcgi?artid=328966&tool=pmcentrez&rendertype=abstract>.
- [79] P.-O. Pierre-Olivier Mari, Bogdan I. Florea, Stephan P. Persengiev, Nicole S. Verkaik, H. T. Bruggenwirth, Mauro Modesti, Giuseppina Giglia-Mari, Karel Bezstarosti, Jeroen A. A. Demmers, Theo M. Luider, Adriaan B. Houtsmuller, Dik C. van Gent, Hennie T Brüggenwirth, Mauro Modesti, Giuseppina Giglia-Mari, Karel Bezstarosti, Jeroen A. A. Demmers, Theo M. Luider, Adriaan B. Houtsmuller, and Dik C. van Gent. Dynamic assembly of end-joining complexes requires interaction between Ku70/80 and XRCC4. *Proceedings of the National Academy of Sciences of the United States of America*, 103(49):18597–18602, 2006. ISSN 0027-8424. doi: 10.1073/pnas.0609061103. URL <http://www.pubmedcentral.nih.gov/articlerender.fcgi?artid=1693708&tool=pmcentrez&rendertype=abstract> <http://www.scopus.com/inward/record.url?eid=2-s2.0-33845484385&partnerID=tZ0tx3y1>.
- [80] Ken-ichi Yano, Keiko Morotomi-Yano, Kyung-Jong Lee, and David J. Chen. Functional significance of the interaction with Ku in DNA double-strand break recognition of XLF. *FEBS*, 585(6):841–846, 2011. ISSN 15378276. doi: 10.1016/j.immuni.2010.12.017. Two-stage.
- [81] T Ochi, A N Blackford, J Coates, S Jhujh, S Mehmood, N Tamura, J Travers, Q Wu, V M Draviam, C V Robinson, T L Blundell, and S P Jackson. DNA repair. PAXX, a paralog of XRCC4 and XLF, interacts with Ku to promote DNA double-strand break repair. *Science*, 347(6218):185–188, 2015. ISSN 1095-9203. doi: 10.1126/science.1261971. URL <http://www.ncbi.nlm.nih.gov/pubmed/25574025>.
- [82] Xiangyu Liu, Zhengping Shao, Wenxia Jiang, Brian J. Lee, and Shan Zha. PAXX promotes KU accumulation at DNA breaks and is essential for end-joining in XLF-deficient mice. *Nature Communications*, 8:13816, 2017. ISSN 2041-1723. doi: 10.1038/ncomms13816. URL <http://www.nature.com/doifinder/10.1038/ncomms13816>.
- [83] Satish K. Tadi, Carine Tellier-Lebègue, Clément Nemoz, Pascal Drevet, Stéphane Audebert, Sunetra Roy, Katheryn Meek, Jean-Baptiste Charbonnier, and Mauro Modesti. PAXX Is an Accessory c-NHEJ Factor that Associates with Ku70 and Has Overlapping Functions with XLF. *Cell Reports*, 17

- (2):541–555, 2016. ISSN 22111247. doi: 10.1016/j.celrep.2016.09.026. URL <http://linkinghub.elsevier.com/retrieve/pii/S2211124716312487>.
- [84] Spencer J Collis, Theodore L DeWeese, Penelope A Jeggo, and Antony R Parker. The life and death of DNA-PK. *Oncogene*, 24(6):949–961, 2005. ISSN 0950-9232. doi: 10.1038/sj.onc.1208332. URL <http://www.nature.com/doifinder/10.1038/sj.onc.1208332>.
- [85] Katherine S Pawelczak, Sara M Bennett, and John J Turchi. Coordination of DNA-PK activation and nuclease processing of DNA termini in NHEJ. *Antioxidants & redox signaling*, 14(12):2531–43, 2011. ISSN 1557-7716. doi: 10.1089/ars.2010.3368. URL <http://www.pubmedcentral.nih.gov/articlerender.fcgi?artid=3096510&tool=pmcentrez&rendertype=abstract>.
- [86] Erik de Vries, Wim van Driel, Wilma G. Bergsma, Annika C. Arnberg, and Peter C. van der Vliet. HeLa nuclear protein recognizing DNA termini and translocating on DNA forming a regular DNA-multimeric protein complex. *Journal of Molecular Biology*, 208(1):65–78, jul 1989. ISSN 00222836. doi: 10.1016/0022-2836(89)90088-0. URL <http://www.sciencedirect.com/science/article/pii/0022283689900880><http://www.ncbi.nlm.nih.gov/pubmed/2769755>.
- [87] Steven A. Roberts and Dale A. Ramsden. Loading of the nonhomologous end joining factor, Ku, on protein-occluded DNA ends. *Journal of Biological Chemistry*, 282(14):10605–10613, 2007. ISSN 00219258. doi: 10.1074/jbc.M611125200.
- [88] Sébastien Britton, Julia Coates, and Stephen P. Jackson. A new method for high-resolution imaging of Ku foci to decipher mechanisms of DNA double-strand break repair. *Journal of Cell Biology*, 202(3):579–595, 2013. ISSN 00219525. doi: 10.1083/jcb.201303073.
- [89] T M Bliss and D P Lane. Ku selectively transfers between DNA molecules with homologous ends. *Journal of Biological Chemistry*, 272(9):5765–5773, 1997. ISSN 00219258. doi: 10.1074/jbc.272.9.5765.
- [90] Dalong Pang, Sunghan Yoo, William S. Dynan, Mira Jung, and Anatoly Dritschilo. Ku Proteins Join DNA Fragments as Shown by Atomic Force Microscopy. *Cancer Research*, 57:1412–1415, 1997.
- [91] Dale A. Ramsden and Martin Geliert. Ku protein stimulates DNA end joining by mammalian DNA ligases: A direct role for Ku in repair of DNA double-strand breaks. *EMBO Journal*, 17(2):609–614, 1998. ISSN 02614189. doi: 10.1093/emboj/17.2.609.
- [92] Evi Soutoglu, Jonas F. Dorn, Kundan Sengupta, Maria Jasin, Andre Nussenzweig, Thomas Ried, Gaudenz Danuser, and Tom Misteli. Positional stability of single double-strand breaks in mammalian cells. *Nature Cell Biology*, 9(6):675–682, 2007. ISSN 1878-5832. doi: 10.3816/CLM.2009.n.003.Novel.



- [93] Sara N. Andres, Alexandra Vergnes, Dejan Ristic, Claire Wyman, Mauro Modesti, and Murray Junop. A human XRCC4-XLF complex bridges DNA. *Nucleic Acids Research*, 40(4):1868–1878, 2012. ISSN 03051048. doi: 10.1093/nar/gks022.
- [94] Virginie Ropars, Pascal Drevet, Pierre Legrand, Sonia Bacconnais, Jeremy Amram, Guilhem Faure, José a Márquez, Olivier Piétrement, Raphaël Guerois, Isabelle Callebaut, Eric Le Cam, Patrick Revy, Jean-Pierre de Villartay, and Jean-Baptiste Charbonnier. Structural characterization of filaments formed by human Xrcc4-Cernunnos/XLF complex involved in non-homologous DNA end-joining. *Proceedings of the National Academy of Sciences of the United States of America*, 108(31):12663–12668, 2011. ISSN 0027-8424. doi: 10.1073/pnas.1100758108.
- [95] Dylan A. Reid, Sarah Keegan, Alejandra Leo-Macias, Go Watanabe, Natasha T. Strande, Howard H. Chang, Betul Akgol Oksuz, David Fenyo, Michael R. Lieber, Dale A. Ramsden, and Eli Rothenberg. Organization and dynamics of the nonhomologous end-joining machinery during DNA double-strand break repair. *Proceedings of the National Academy of Sciences*, 112(20):E2575–E2584, 2015. ISSN 0027-8424. doi: 10.1073/pnas.1420115112. URL <http://www.pnas.org/content/112/20/E2575>. long{ }5Cn<http://www.pnas.org/lookup/doi/10.1073/pnas.1420115112>{ }5Cn<http://www.scopus.com/inward/record.url?eid=2-s2.0-84929465548&partnerID=tZ0tx3y1>.
- [96] Lisa G. DeFazio, Rachel M. Stansel, Jack D. Griffith, and Gilbert Chu. Synapsis of DNA ends by DNA-dependent protein kinase. *EMBO Journal*, 21(12):3192–3200, 2002. ISSN 02614189. doi: 10.1093/emboj/cdf299.
- [97] Dennis Merkle, Wesley D. Block, Yaping Yu, Susan P. Lees-Miller, and David T. Cramb. Analysis of DNA-Dependent Protein Kinase-Mediated DNA End Joining by Two-Photon Fluorescence Cross-Correlation Spectroscopy. *Biochemistry*, 45(13):4164–4172, apr 2006. ISSN 0006-2960. doi: 10.1021/bi0524060. URL <http://pubs.acs.org/doi/abs/10.1021/bi0524060>.
- [98] Thomas Graham, Johannes C Walter, and Joseph J Loparo. Two-Stage Synapsis of DNA Ends during Non-homologous End Joining. *Molecular Cell*, 61(6):850–858, 2016. ISSN 10972765. doi: 10.1016/j.molcel.2016.02.010. URL <http://www.sciencedirect.com/science/article/pii/S1097276516000940>{ }5Cn<http://linkinghub.elsevier.com/retrieve/pii/S1097276516000940>.
- [99] Brandi L Mahaney, Katheryn Meek, and Susan P Lees-Miller. Repair of ionizing radiation-induced DNA double-strand breaks by non-homologous end-joining. *The Biochemical journal*, 417(3):639–50, feb 2009. ISSN 1470-8728. doi: 10.1042/BJ20080413. URL <http://www.pubmedcentral.nih.gov/articlerender.fcgi?artid=2975036&tool=pmcentrez&rendertype=abstract>.

- [100] Howard H. Y. Chang, Go Watanabe, Christina A. Gerodimos, Takashi Ochi, Tom L. Blundell, Stephen P. Jackson, and Michael R. Lieber. Different DNA End Configurations Dictate Which NHEJ Components are Most Important for Joining Efficiency. *Journal of Biological Chemistry*, 291(47):jbc.M116.752329, 2016. ISSN 0021-9258. doi: 10.1074/jbc.M116.752329. URL <http://www.jbc.org/lookup/doi/10.1074/jbc.M116.752329>.
- [101] Sean Rooney, Frederick W Alt, David Lombard, Scott Whitlow, Mark Eckersdorff, James Fleming, Sebastian Fugmann, David O Ferguson, David G Schatz, and JoAnn Sekiguchi. Defective DNA repair and increased genomic instability in Artemis-deficient murine cells. *The Journal of experimental medicine*, 197(5):553–65, 2003. ISSN 0022-1007. doi: 10.1084/jem.20021891. URL <http://www.pubmedcentral.nih.gov/articlerender.fcgi?artid=2193825&tool=pmcentrez&rendertype=abstract>.
- [102] Despina Moshous, Isabelle Callebaut, Régina De Chasseval, Barbara Corneo, Marina Cavazzana-Calvo, Françoise Le Deist, Ilhan Tezcan, Ozden Sanal, Yves Bertrand, Noel Philippe, Alain Fischer, and Jean Pierre De Villartay. Artemis, a novel DNA double-strand break repair/V(D)J recombination protein, is mutated in human severe combined immune deficiency. *Cell*, 105(2):177–186, 2001. ISSN 00928674. doi: 10.1016/S0092-8674(01)00309-9.
- [103] Wenxia Jiang, Jennifer L. Crowe, Xiangyu Liu, Satoshi Nakajima, Yunyue Wang, Chen Li, Brian J. Lee, Richard L. Dubois, Chao Liu, Xiaochun Yu, Li Lan, and Shan Zha. Differential phosphorylation of DNA-PKcs regulates the interplay between end-processing and end-ligation during nonhomologous end-joining. *Molecular Cell*, 58(1):172–185, 2015. ISSN 10974164. doi: 10.1016/j.molcel.2015.02.024. URL <http://dx.doi.org/10.1016/j.molcel.2015.02.024>.
- [104] Kiran N Mahajan, Stephanie a Nick McElhinny, Beverly S Mitchell, and Dale a Ramsden. Association of DNA polymerase mu (pol mu) with Ku and ligase IV: role for pol mu in end-joining double-strand break repair. *Molecular and cellular biology*, 22(14):5194–202, 2002. ISSN 0270-7306. doi: 10.1128/MCB.22.14.5194. URL <http://www.ncbi.nlm.nih.gov/pubmed/12077346> <http://www.pubmedcentral.nih.gov/articlerender.fcgi?artid=PMC139779>.
- [105] Yunmei Ma, Haihui Lu, Brigitte Tippin, Myron F. Goodman, Noriko Shimazaki, Osamu Koiwai, Chih L. Hsieh, Klaus Schwarz, and Michael R. Lieber. A biochemically defined system for mammalian nonhomologous DNA end joining. *Molecular Cell*, 16(5):701–713, 2004. ISSN 10972765. doi: 10.1016/j.molcel.2004.11.017.
- [106] Michal Hammel, Yaping Yu, Sarvan Kumar Radhakrishnan, Chirayu Chokshi, Miaw-Sheue Tsai, Yoshihiro Matsumoto, Monica Kuzdovich, Soumya G Remesh, Shujuan Fang, Alan E Tomkinson, Susan P Lees-Miller, and John A Tainer. An Intrinsically Disordered APLF Links Ku, DNA-PKcs and XRCC4-DNA Ligase IV in an Extended Flexible Non-Homologous End

- Joining Complex. *Jbc*, 291(3):1–36, 2016. ISSN 0021-9258. doi: 10.1074/jbc.M116.751867. URL <http://www.jbc.org/lookup/doi/10.1074/jbc.M116.751867>.
- [107] Gabrielle J Grundy, Stuart L Rulten, Raquel Arribas-Bosacoma, Kathryn Davidson, Zuzanna Kozik, Antony Oliver, Laurence H. Pearl, and Keith W Caldecott. The Ku-binding motif is a conserved module for recruitment and stimulation of non-homologous end-joining proteins. *Nature Communications*, 7:1–7, 2016. ISSN 0032-3896. doi: 10.1038/pj.2016.37. URL <http://www.nature.com/doi/10.1038/pj.2016.37>.
- [108] Parimal Karmakar, Carey M. Snowden, Dale A. Ramsden, and Vilhelm A. Bohr. Ku heterodimer binds to both ends of the Werner protein and functional interaction occurs at the Werner N-terminus. *Nucleic Acids Research*, 30(16):3583–91, 2002. ISSN 1362-4962. doi: doi:10.1093/nar/gkf482.
- [109] Steven a Roberts, Natasha Strande, Martin D Burkhalter, Christina Strom, Jody M Havener, Paul Hasty, and Dale a Ramsden. Ku is a 5'-dRP/AP lyase that excises nucleotide damage near broken ends. *Nature*, 464(7292):1214–7, apr 2010. ISSN 1476-4687. doi: 10.1038/nature08926. URL <http://www.pubmedcentral.nih.gov/articlerender.fcgi?artid=2859099&tool=pmcentrez&rendertype=abstract>.
- [110] Natasha Strande, Steven a Roberts, Sehyun Oh, Eric a Hendrickson, and Dale a Ramsden. Specificity of the dRP/AP lyase of Ku promotes nonhomologous end joining (NHEJ) fidelity at damaged ends. *The Journal of biological chemistry*, 287(17):13686–93, apr 2012. ISSN 1083-351X. doi: 10.1074/jbc.M111.329730. URL <http://www.pubmedcentral.nih.gov/articlerender.fcgi?artid=3340204&tool=pmcentrez&rendertype=abstract>.
- [111] Dylan A. Reid, Michael P. Conlin, Yandong Yin, Howard H. Chang, Go Watanabe, Michael R. Lieber, Dale A. Ramsden, and Eli Rothenberg. Bridging of double-stranded breaks by the nonhomologous end-joining ligation complex is modulated by DNA end chemistry. *Nucleic Acids Research*, pages 1–15, 2016. ISSN 0305-1048. doi: 10.1093/nar/gkw1002. URL [http://fdslive.oup.com/www.oup.com/pdf/production\\_in\\_progress.pdf?%5Cnhttp://www.ncbi.nlm.nih.gov/pubmed/27899565](http://fdslive.oup.com/www.oup.com/pdf/production_in_progress.pdf?%5Cnhttp://www.ncbi.nlm.nih.gov/pubmed/27899565).
- [112] K M Frank, N E Sharpless, Y Gao, J M Sekiguchi, D O Ferguson, C Zhu, J P Manis, J Horner, R A DePinho, and F W Alt. DNA ligase IV deficiency in mice leads to defective neurogenesis and embryonic lethality via the p53 pathway. *Molecular Cell*, 5(6):993–1002, 2000. ISSN 1097-2765. doi: S1097-2765(00)80264-6[pil]. URL [http://www.ncbi.nlm.nih.gov/pubmed/10911993%5Cnhttp://ac.els-cdn.com/S1097276500802646/1-s2.0-S1097276500802646-main.pdf?\\_tid=c805c4f6-590c-11e2-ba69-00000aab0f01&acdnat=1357592400\\_abfc8eac0b4928f6ad95b91df3045f13](http://www.ncbi.nlm.nih.gov/pubmed/10911993%5Cnhttp://ac.els-cdn.com/S1097276500802646/1-s2.0-S1097276500802646-main.pdf?_tid=c805c4f6-590c-11e2-ba69-00000aab0f01&acdnat=1357592400_abfc8eac0b4928f6ad95b91df3045f13).

- [113] Deborah E. Barnes, Gordon Stamp, Ian Rosewell, Angela Denzel, and Tomas Lindahl. Targeted disruption of the gene encoding DNA ligase IV leads to lethality in embryonic mice. *Current Biology*, 8(25):1395–1398, 1998. ISSN 09609822. doi: 10.1016/S0960-9822(98)00021-9.
- [114] E. Riballo, S. E. Critchlow, S. H. Teo, A. J. Doherty, A. Priestley, B. Broughton, B. Kysela, H. Beamish, N. Plowman, C. F. Arlett, A. R. Lehmann, S. P. Jackson, and P. A. Jeggo. Identification of a defect in DNA ligase IV in a radiosensitive leukaemia patient. *Current Biology*, 9(13):699–702, 1999. ISSN 09609822. doi: 10.1016/S0960-9822(99)80311-X.
- [115] Mark O’Driscoll, Karen M. Cerosaletti, Pierre M. Girard, Yan Dai, Markus Stumm, Boris Kysela, Betsy Hirsch, Andrew Gennery, Susan E. Palmer, Jörg Seidel, Richard A. Gatti, Raymonda Varon, Marjorie A. Oettinger, Heidemarie Neitzel, Penny A. Jeggo, and Patrick Concannon. DNA ligase IV mutations identified in patients exhibiting developmental delay and immunodeficiency. *Molecular Cell*, 8(6):1175–1185, 2001. ISSN 10972765. doi: 10.1016/S1097-2765(01)00408-7.
- [116] Dietke Buck, Despina Moshous, Régina de Chasseval, Yunmei Ma, Françoise le Deist, Marina Cavazzana-Calvo, Alain Fischer, Jean Laurent Casanova, Michael R. Lieber, and Jean Pierre de Villartay. Severe combined immunodeficiency and microcephaly in siblings with hypomorphic mutations in DNA ligase IV. *European Journal of Immunology*, 36(1):224–235, 2006. ISSN 00142980. doi: 10.1002/eji.200535401.
- [117] T D Stamato, R Weinstein, A Giaccia, and L Mackenzie. Isolation of cell cycle-dependent gamma ray-sensitive Chinese hamster ovary cell. *Somatic cell genetics*, 9(2):165–73, mar 1983. ISSN 0098-0366. URL <http://www.ncbi.nlm.nih.gov/pubmed/6836453>.
- [118] Yu Gang Wang, Chinonye Nnakwe, William S. Lane, Mauro Modesti, and Karen M. Frank. Phosphorylation and regulation of DNA ligase IV stability by DNA-dependent protein kinase. *Journal of Biological Chemistry*, 279(36):37282–37290, 2004. ISSN 00219258. doi: 10.1074/jbc.M401217200.
- [119] Peter Ahnesorg, Philippa Smith, and Stephen P. Jackson. XLF interacts with the XRCC4-DNA Ligase IV complex to promote DNA nonhomologous end-joining. *Cell*, 124(2):301–313, 2006. ISSN 00928674. doi: 10.1016/j.cell.2005.12.031.
- [120] Dietke Buck, Laurent Malivert, Régina De Chasseval, Anne Barraud, Marie Claude Fondanèche, Ozden Sanal, Alessandro Plebani, Jean Louis Stéphan, Markus Hufnagel, Françoise Le Deist, Alain Fischer, Anne Durandy, Jean Pierre De Villartay, and Patrick Revy. Cernunnos, a novel nonhomologous end-joining factor, is mutated in human immunodeficiency with microcephaly. *Cell*, 124(2):287–299, 2006. ISSN 00928674. doi: 10.1016/j.cell.2005.12.030.

- [121] Chun J Tsai, Sunny a Kim, and Gilbert Chu. Cernunnos/XLF promotes the ligation of mismatched and noncohesive DNA ends. *Proceedings of the National Academy of Sciences of the United States of America*, 104(19):7851–6, 2007. ISSN 0027-8424. doi: 10.1073/pnas.0702620104. URL <http://www.ncbi.nlm.nih.gov/pubmed/17470781><http://www.pubmedcentral.nih.gov/articlerender.fcgi?artid=PMC1859989>.
- [122] Sunetra Roy, Abinadabe J. de Melo, Yao Xu, Satish K. Tadi, Aurélie Négrel, Eric Hendrickson, Mauro Modesti, and Katheryn Meek. XRCC4/XLF Interaction Is Variably Required for DNA Repair and Is Not Required for Ligase IV Stimulation. *Molecular and Cellular Biology*, 35(17):3017–3028, 2015. ISSN 0270-7306. doi: 10.1128/MCB.01503-14. URL <http://mcb.asm.org/lookup/doi/10.1128/MCB.01503-14>.
- [123] A Craxton, J Somers, D Munnur, R Jukes-Jones, K Cain, and M Malewicz. XLS (c9orf142) is a new component of mammalian DNA double-stranded break repair. *Cell death and differentiation*, 22(6):890–7, 2015. ISSN 1476-5403. doi: 10.1038/cdd.2015.22. URL <http://www.pubmedcentral.nih.gov/articlerender.fcgi?artid=4423191&tool=pmcentrez&rendertype=abstract><http://www.scopus.com/inward/record.url?eid=2-s2.0-84939946728&partnerID=tZ0tx3y1>.
- [124] Mengtan Xing, Mingrui Yang, Wei Huo, Feng Feng, Leizhen Wei, Wenxia Jiang, Shaokai Ning, Zhenxin Yan, Wen Li, Qingsong Wang, Mei Hou, Chunxia Dong, Rong Guo, Ge Gao, Jianguo Ji, Shan Zha, Li Lan, Huanhuan Liang, and Dongyi Xu. Interactome analysis identifies a new paralogue of XRCC4 in non-homologous end joining DNA repair pathway. *Nature Communications*, 6:6233, 2015. ISSN 2041-1723. doi: 10.1038/ncomms7233. URL <http://dx.doi.org/10.1038/ncomms7233>.
- [125] Lisa Postow, Cristina Ghenoiu, Eileen M. Woo, Andrew N. Krutchinsky, Brian T. Chait, and Hironori Funabiki. Ku80 removal from DNA through double strand break-induced ubiquitylation. *Journal of Cell Biology*, 182(3):467–479, 2008. ISSN 00219525. doi: 10.1083/jcb.200802146.
- [126] Birthe B Kragelund, Eric Weterings, Rasmus Hartmann-Petersen, and Guido Keijzers. The Ku70/80 ring in Non-Homologous End-Joining: easy to slip on, hard to remove. *Frontiers in bioscience (Landmark edition)*, 21:514–27, 2016. ISSN 1093-4715. URL <http://www.ncbi.nlm.nih.gov/pubmed/26709791>.
- [127] Lisa Postow and Hironori Funabiki. An SCF complex containing Fbxl12 mediates DNA damage-induced Ku80 ubiquitylation. *Cell Cycle*, 12(4):587–595, 2013. ISSN 15384101. doi: 10.4161/cc.23408.
- [128] Jessica S. Brown, Natalia Lukashchuk, Matylda Sczaniecka-Clift, S??bastien Britton, Carlos le Sage, Patrick Calsou, Petra Beli, Yaron Galanty, and Stephen P. Jackson. Neddylation Promotes Ubiquitylation and Release of Ku from DNA-Damage Sites. *Cell Reports*, 11(5):704–714, 2015. ISSN 22111247. doi: 10.1016/j.celrep.2015.03.058.

- [129] Johannes van den Boom, Markus Wolf, Lena Weimann, Nina Schulze, Fanghua Li, Farnusch Kaschani, Anne Riemer, Christian Zierhut, Markus Kaiser, George Iliakis, Hironori Funabiki, and Hemmo Meyer. VCP/p97 Extracts Sterically Trapped Ku70/80 Rings from DNA in Double-Strand Break Repair. *Molecular Cell*, 64(1):189–198, 2016. ISSN 10972765. doi: 10.1016/j.molcel.2016.08.037. URL <http://linkinghub.elsevier.com/retrieve/pii/S1097276516305160>.
- [130] Lin Feng and Junjie Chen. The E3 ligase RNF8 regulates KU80 removal and NHEJ repair. *Nature Structural & Molecular Biology*, 19(2):201–206, 2014. ISSN 15378276. doi: 10.1016/j.immuni.2010.12.017. Two-stage.
- [131] J. Lehman, D. Hoelz, and J J. Turchi. DNA-dependent conformational changes in the Ku heterodimer. *Biochemistry*, 47(15):4359–4368, 2008. ISSN 1878-5832. doi: 10.3816/CLM.2009.n.003.Novel.
- [132] Jeffrey R Skaar, Julia K Pagan, and Michele Pagano. Mechanisms and function of substrate recruitment by F-box proteins. *Nature reviews. Molecular cell biology*, 14(6):369–81, 2013. ISSN 1471-0080. doi: 10.1038/nrm3582. URL <http://dx.doi.org/10.1038/nrm3582>.
- [133] Elena B Kabotyanski, Larissa Gomelsky, Jung-ok Han, Thomas D Stamato, and David B Roth. Double-strand break repair in Ku86- and. *Nuclear medicine communications*, 26(23):27–31, 1998.
- [134] Elke Feldmann, Viola Schmiemann, Wolfgang Goedecke, Susanne Reichenberger, and Petra Pfeiffer. DNA double strand break in cell free extracts from Ku80-deficient cells implications for Ku serving as an alignment factor in non-homologous DNA end joining. *Nucleic acids research*, 28(13):2585–2596, 2000.
- [135] Julianne Smith, Enriqueta Riballo, Boris Kysela, Celine Baldeyron, Kostas Manolis, Christel Masson, Michael R. Lieber, Dora Papadopoulo, and Penny Jeggo. Impact of DNA ligase IV on the fidelity of end joining in human cells. *Nucleic Acids Research*, 31(8):2157–2167, 2003. ISSN 03051048. doi: 10.1093/nar/gkg317.
- [136] Michael J Diflippantonio, Jie Zhu, Hua Tang Chen, Eric Meffre, Michel C Nussenzweig, Edward E. Max, Thomas Ried, and André Nussenzweig. DNA repair protein Ku80 suppresses chromosomal aberrations and malignant transformation. *Nature*, 404:510–514, 2000. doi: 10.1007/s40778-014-0003-z. Genome.
- [137] G C Li, H Ouyang, X Li, H Nagasawa, J B Little, D J Chen, C C Ling, Z Fuks, and C Cordon-Cardo. Ku70: a candidate tumor suppressor gene for murine T cell lymphoma. *Molecular cell*, 2(1):1–8, jul 1998. ISSN 1097-2765. URL <http://www.ncbi.nlm.nih.gov/pubmed/9702186>.
- [138] a Nussenzweig, K Sokol, P Burgman, L Li, and G C Li. Hypersensitivity of Ku80-deficient cell lines and mice to DNA damage: the effects of ionizing

- radiation on growth, survival, and development. *Proceedings of the National Academy of Sciences of the United States of America*, 94(25):13588–13593, 1997. ISSN 0027-8424. doi: 10.1073/pnas.94.25.13588.
- [139] Maria Jasin and Rodney Rothstein. Repair of Strand Breaks by Homologous Recombination. *Cold Spring Harbor Perspectives in Biology*, 5:1–18, 2013.
- [140] Wolf-Dietrich Heyer, Kirk T Ehmsen, and Jie Liu. Regulation of homologous recombination in eukaryotes. *Annual review of genetics*, 44:113–39, 2010. ISSN 1545-2948. doi: 10.1146/annurev-genet-051710-150955. URL <http://www.ncbi.nlm.nih.gov/pubmed/20690856>`{%}5Cnhttp://www.pubmedcentral.nih.gov/articlerender.fcgi?artid=PMC4114321`.
- [141] J Ross Chapman, Martin R G Taylor, and Simon J Boulton. Playing the end game: DNA double-strand break repair pathway choice., aug 2012. ISSN 1097-4164. URL <http://www.ncbi.nlm.nih.gov/pubmed/22920291>.
- [142] George Iliakis, Tamara Murmann, and Aashish Soni. Alternative end-joining repair pathways are the ultimate backup for abrogated classical non-homologous end-joining and homologous recombination repair: Implications for the formation of chromosome translocations. *Mutation Research - Genetic Toxicology and Environmental Mutagenesis*, 793:166–175, 2015. ISSN 18793592. doi: 10.1016/j.mrgentox.2015.07.001. URL <http://dx.doi.org/10.1016/j.mrgentox.2015.07.001>.
- [143] Catherine T Yan, Cristian Boboila, Ellen Kris Souza, Sonia Franco, Thomas R Hickernell, Michael Murphy, Sunil Gumaste, Mark Geyer, Ali A Zarrin, John P Manis, Klaus Rajewsky, and Frederick W Alt. IgH class switching and translocations use a robust non-classical end-joining pathway. *Nature*, 449(7161):478–82, 2007. ISSN 1476-4687. doi: 10.1038/nature06020. URL <http://www.ncbi.nlm.nih.gov/pubmed/17713479>.
- [144] Deniz Simsek, Erika Brunet, Sunnie Yan Wai Wong, Sachin Katyal, Yankun Gao, Peter J. McKinnon, Jacqueline Lou, Lei Zhang, James Li, Edward J. Rebar, Philip D. Gregory, Michael C. Holmes, and Maria Jasin. DNA ligase III promotes alternative nonhomologous end-joining during chromosomal translocation formation. *PLoS Genetics*, 7(6):1–11, 2011. ISSN 15537390. doi: 10.1371/journal.pgen.1002080.
- [145] Deniz Simsek and Maria Jasin. Alternative end-joining is suppressed by the canonical NHEJ component Xrcc4/ligase IV during chromosomal translocation formation. *Nat Struct Mol Biol*, 17(4):410–416, 2010. ISSN 08966273. doi: 10.1038/nsmb.1773. URL <http://dx.doi.org/10.1038/nsmb.1773>.
- [146] Simon J Boulton and Stephen P Jackson. *Saccharomyces cerevisiae* Ku70 potentiates pathways DNA repair. *EMBO Journal*, 15(18):5093–5103, 1996.
- [147] Feng Liang and Maria Jasin. Ku80-deficient cells exhibit excess degradation of extrachromosomal DNA. *Journal of Biological Chemistry*, 271(24):14405–14411, 1996. ISSN 00219258. doi: 10.1074/jbc.271.24.14405.

- [148] Lan N Truong, Yongjiang Li, Linda Z Shi, Patty Yi-Hwa Hwang, Jing He, Hailong Wang, Niema Razavian, Michael W Berns, and Xiaohua Wu. Microhomology-mediated End Joining and Homologous Recombination share the initial end resection step to repair DNA double-strand breaks in mammalian cells. *Proceedings of the National Academy of Sciences of the United States of America*, 110(19):7720–5, 2013. ISSN 1091-6490. doi: 10.1073/pnas.1213431110. URL <http://www.pubmedcentral.nih.gov/articlerender.fcgi?artid=3651503&tool=pmcentrez&rendertype=abstract>.
- [149] Yu Zhang and Maria Jasin. An essential role for CtIP in chromosomal translocation formation through an alternative end-joining pathway. *Nature structural & molecular biology*, 18(1):80–4, 2011. ISSN 1545-9985. doi: 10.1038/nsmb.1940. URL <http://www.scopus.com/inward/record.url?eid=2-s2.0-78650995499&partnerID=tZ0tx3y1>.
- [150] Julie Della-Maria, Yi Zhou, Miaw Sheue Tsai, Jeff Kuhnlein, James P. Carney, Tanya T. Paull, and Alan E. Tomkinson. Human Mre11/human Rad50/Nbs1 and DNA ligase IIIalpha/XRCC1 protein complexes act together in an alternative nonhomologous end joining pathway. *Journal of Biological Chemistry*, 286(39):33845–33853, 2011. ISSN 00219258. doi: 10.1074/jbc.M111.274159.
- [151] Marc Audebert, Bernard Salles, and Patrick Calsou. Involvement of poly(ADP-ribose) polymerase-1 and XRCC1/DNA ligase III in an alternative route for DNA double-strand breaks rejoining. *Journal of Biological Chemistry*, 279(53):55117–55126, 2004. ISSN 00219258. doi: 10.1074/jbc.M404524200.
- [152] Isabelle Robert, Françoise Dantzer, and Bernardo Reina-San-Martin. Parp1 facilitates alternative NHEJ, whereas Parp2 suppresses IgH/c-myc translocations during immunoglobulin class switch recombination. *The Journal of experimental medicine*, 206(5):1047–1056, 2009. ISSN 00221007. doi: 10.1084/jem.20082468.
- [153] Jia-Lin Ma, Eun Mi Kim, James E Haber, and Sang Eun Lee. Yeast Mre11 and Rad1 Proteins Define a Ku-Independent Mechanism To Repair Double-Strand Breaks Lacking Overlapping End Sequences. *Molecular and Cellular Biology*, 23(23):8820–8828, 2003. ISSN 0270-7306. doi: 10.1128/MCB.23.23.8820-8828.2003.
- [154] Nicole Bennardo, Anita Cheng, Nick Huang, and Jeremy M. Stark. Alternative-NHEJ is a mechanistically distinct pathway of mammalian chromosome break repair. *PLoS Genetics*, 4(6), 2008. ISSN 15537390. doi: 10.1371/journal.pgen.1000110.
- [155] Sze Ham Chan, Amy Marie Yu, and Mitch McVey. Dual roles for DNA polymerase theta in alternative end-joining repair of double-strand breaks in *Drosophila*. *PLoS Genetics*, 6(7):1–16, 2010. ISSN 15537390. doi: 10.1371/journal.pgen.1001005.



- [156] Amy Marie Yu and Mitch McVey. Synthesis-dependent microhomology-mediated end joining accounts for multiple types of repair junctions. *Nucleic Acids Research*, 38(17):5706–5717, 2010. ISSN 13624962. doi: 10.1093/nar/gkq379.
- [157] Hailong Wang and Xingzhi Xu. Microhomology-mediated end joining: new players join the team. *Cell & Bioscience*, 7(1):6, 2017. ISSN 2045-3701. doi: 10.1186/s13578-017-0136-8. URL <http://cellandbioscience.biomedcentral.com/articles/10.1186/s13578-017-0136-8>.
- [158] Tatiana Kent, Gurushankar Chandamouly, Shane Micheal McDevitt, Ahmet Y. Ozdemir, and Richard T. Pomerantz. Mechanism of Microhomology-Mediated End-Joining Promoted by Human DNA Polymerase Theta. *Nature structural & molecular biology*, 22(3):230–237, 2015. ISSN 1527-5418. doi: 10.1001/jamasurg.2014.1086.Feasibility.
- [159] Huichen Wang, Bustanur Rosidi, Ronel Perrault, Minli Wang, Lihua Zhang, Frank Windhofer, and George Iliakis. DNA Ligase III as a Candidate Component of Backup Pathways of Nonhomologous End Joining DNA Ligase III as a Candidate Component of Backup Pathways of Nonhomologous End Joining. *Cancer Research*, 65(10):4020–4030, 2005. ISSN 0008-5472. doi: 10.1158/0008-5472.CAN-04-3055.
- [160] Barbara Corneo, Rebecca L Wendland, Ludovic Deriano, Xiaoping Cui, Isaac a Klein, Serre-Yu Wong, Suzzette Arnal, Abigail J Holub, Geoffrey R Weller, Bette a Pancake, Sundeep Shah, Vicky L Brandt, Katheryn Meek, and David B Roth. Rag mutations reveal robust alternative end joining. *Nature*, 449(7161):483–486, 2007. ISSN 0028-0836. doi: 10.1038/nature06168.
- [161] Mieun Lee-Theilen, Allysia J Matthews, Dierdre Kelly, Simin Zheng, and Jayanta Chaudhuri. CtIP promotes microhomology-mediated alternative end joining during class-switch recombination. *Nature Structural & Molecular Biology*, 18(1):75–79, 2011. ISSN 1545-9993. doi: 10.1038/nsmb.1942. URL <http://dx.doi.org/10.1038/nsmb.1942>{%}5Cnpapers3://publication/doi/10.1038/nsmb.1942.
- [162] Raghavendra A. Shamanna, Huiming Lu, Jessica K. de Freitas, Jane Tian, Deborah L. Croteau, and Vilhelm A. Bohr. WRN regulates pathway choice between classical and alternative non-homologous end joining. *Nature communications*, 7(May):13785, 2016. ISSN 2041-1723. doi: 10.1038/ncomms13785. URL <http://www.nature.com/doiifinder/10.1038/ncomms13785>{%}5Cn<http://www.ncbi.nlm.nih.gov/pubmed/27922005>.
- [163] David M. Weinstock, Erika Brunet, and Maria Jasin. Formation of NHEJ-derived reciprocal chromosomal translocations does not require Ku70. *Nature Cell Biology*, 9(8):978–981, 2007. ISSN 09652140. doi: 10.1097/OPX.0b013e3182540562.The.
- [164] Hind Ghezraoui, Marion Piganeau, Benjamin Renouf, Jean-Baptiste Renaud, Annahita Sallmyr, Brian Ruis, Sehyun Oh, Alan E Tomkinson, Eric A

- Hendrickson, Carine Giovannangeli, Maria Jasin, and Erika Brunet. Chromosomal Translocations in Human Cells Are Generated by Canonical Non-homologous End-Joining. *Molecular Cell*, 55(6):829–842, 2014. ISSN 1097-2765. doi: 10.1016/j.molcel.2014.08.002. URL <http://dx.doi.org/10.1016/j.molcel.2014.08.002>.
- [165] Ronja Biehs, Monika Steinlage, Olivia Barton, Szilvia Juhasz, Julia Kunzel, Julian Spies, Atsushi Shibata, Penny Jeggo, and Markus Löbrich. DNA double-strand break resection occurs during non-homologous end-joining in G1 but is distinct to resection during homologous recombination in G2. *Molecular Cell*, 65:671–684, 2017. ISSN 10972765. doi: 10.1016/j.molcel.2016.12.016.
- [166] Andreas Kakarougkas, Amani Ismail, Yoko Katsuki, Raimundo Freire, Atsushi Shibata, and Penny A. Jeggo. Co-operation of BRCA1 and POH1 relieves the barriers posed by 53BP1 and RAP80 to resection. *Nucleic Acids Research*, 41(22):10298–10311, 2013. ISSN 03051048. doi: 10.1093/nar/gkt802.
- [167] Yi Zhou, Pierre Caron, Gaëlle Legube, and Tanya T. Paull. Quantitation of DNA double-strand break resection intermediates in human cells. *Nucleic Acids Research*, 42(3):1–11, 2014. ISSN 03051048. doi: 10.1093/nar/gkt1309.
- [168] Lorraine S. Symington and Jean Gautier. Double-Strand Break End Resection and Repair Pathway Choice. *Annual Review of Genetics*, 45(1):247–271, 2011. ISSN 0066-4197. doi: 10.1146/annurev-genet-110410-132435.
- [169] Pablo Huertas. DNA resection in eukaryotes: deciding how to fix the break. *Nature structural & molecular biology*, 17(1):11–16, 2010. ISSN 1545-9993. doi: 10.1038/nsmb.1710. URL <http://dx.doi.org/10.1038/nsmb.1710>.
- [170] Nicole Hustedt and Daniel Durocher. The control of DNA repair by the cell cycle. *Nat Cell Biol*, 19(1):1–9, 2017. ISSN 1465-7392. doi: 10.1038/ncb3452. URL <http://dx.doi.org/10.1038/ncb3452>. URL <http://10.0.4.14/ncb3452>.
- [171] Valerie Garcia, Sarah E L Phelps, Stephen Gray, and Matthew J Neale. Bidirectional resection of DNA double-strand breaks by Mre11 and Exo1. *Nature*, 479(7372):241–244, 2012. doi: 10.1038/nature10515.Bidirectional.
- [172] Pauline Chanut, Sébastien Britton, Julia Coates, Stephen P. Jackson, and Patrick Calsou. Coordinated nuclease activities counteract Ku at single-ended DNA double-strand breaks. *Nature Communications*, 7:12889, 2016. ISSN 2041-1723. doi: 10.1038/ncomms12889. URL <http://www.nature.com/doifinder/10.1038/ncomms12889>.
- [173] Pablo Huertas and Stephen P Jackson. Human CtIP mediates cell cycle control of DNA end resection and double strand break repair. *The Journal of biological chemistry*, 284(14):9558–9565, 2009. ISSN 0021-9258. doi: 10.1074/jbc.M808906200.

- [174] Alessandro A. Sartori, Claudia Lukas, Julia Coates, Martin Mistrik, Shuang Fu, Jiri Bartek, Richard Baer, Jiri Lukas, and Stephen P. Jackson. Human CtIP promotes DNA end resection. *Nature*, 450(7169):509–514, 2007. ISSN 0028-0836. doi: 10.1038/nature06337.
- [175] Maximina H Yun and Kevin Hiom. CtIP-BRCA1 modulates the choice of DNA double-strand break repair pathway throughout the cell cycle. *Nature*, 459(7245):460–463, 2009. doi: 10.1038/nature07955.CtIP-BRCA1.
- [176] L. Chen, C. J. Nievera, A. Y.-L. Lee, and X. Wu. Cell Cycle-dependent Complex Formation of BRCA1.CtIP.MRN Is Important for DNA Double-strand Break Repair. *Journal of Biological Chemistry*, 283(12):7713–7720, 2008. ISSN 0021-9258. doi: 10.1074/jbc.M710245200. URL <http://www.jbc.org/cgi/doi/10.1074/jbc.M710245200>.
- [177] Anne Bothmer, Davide F Robbiani, Niklas Feldhahn, Anna Gazumyan, Andre Nussenzweig, and Michel C Nussenzweig. 53BP1 regulates DNA resection and the choice between classical and alternative end joining during class switch recombination. *The Journal of experimental medicine*, 207(4):855–65, 2010. ISSN 1540-9538. doi: 10.1084/jem.20100244. URL <http://jem.rupress.org/cgi/content/long/207/4/855>.
- [178] James M. Daley and Patrick Sung. RIF1 in DNA Break Repair Pathway Choice. *Molecular Cell*, 49(5):840–841, 2013. ISSN 10972765. doi: 10.1016/j.molcel.2013.02.019. URL <http://dx.doi.org/10.1016/j.molcel.2013.02.019>.
- [179] J. Ross Chapman, Patricia Barral, Jean Baptiste Vannier, Valérie Borel, Martin Steger, Antonia Tomas-Loba, Alessandro A. Sartori, Ian R. Adams, Facundo D. Batista, and Simon J. Boulton. RIF1 Is Essential for 53BP1-Dependent Nonhomologous End Joining and Suppression of DNA Double-Strand Break Resection. *Molecular Cell*, 49(5):858–871, 2013. ISSN 10972765. doi: 10.1016/j.molcel.2013.01.002.
- [180] Michela Di Virgilio, Elsa Callen, Arito Yamane, Wenzhu Zhang, Mila Jankovic, Alexander D Gitlin, Niklas Feldhahn, Wolfgang Resch, Thiago Y Oliveira, Brian T Chait, André Nussenzweig, Rafael Casellas, Davide F Robbiani, and Michel C Nussenzweig. Rif1 prevents resection of DNA breaks and promotes immunoglobulin class switching. *Science (New York, N.Y.)*, 339(6120):711–5, 2013. ISSN 1095-9203. doi: 10.1126/science.1230624. URL <http://www.pubmedcentral.nih.gov/articlerender.fcgi?artid=3815530&tool=pmcentrez&rendertype=abstract>.
- [181] Cristina Escribano-Díaz, Alexandre Orthwein, Amélie Fradet-Turcotte, Mengtan Xing, Jordan T F Young, Ján Tkáč, Michael A. Cook, Adam P. Rosebrock, Meagan Munro, Marella D. Canny, Dongyi Xu, and Daniel Durocher. A Cell Cycle-Dependent Regulatory Circuit Composed of 53BP1-RIF1 and BRCA1-CtIP Controls DNA Repair Pathway Choice. *Molecular Cell*, 49(5):872–883, 2013. ISSN 10972765. doi: 10.1016/j.molcel.2013.01.001.

- [182] Michal Zimmermann and Titia De Lange. 53BP1 : pro choice in DNA repair. *Trends in Cell Biology*, 24(2):108–117, 2014. ISSN 0962-8924. doi: 10.1016/j.tcb.2013.09.003. URL <http://dx.doi.org/10.1016/j.tcb.2013.09.003>.
- [183] Michal Zimmermann, Francisca Lottersberger, and Sara B Buonomo. 53BP1 Regulates DSB Repair Using Rif1 to Control 5' End Resection. *Science*, 339(6120):700–704, 2013.
- [184] Xiaoping Cui, Yaping Yu, Shikha Gupta, Young-moon Cho, Susan P Lees-miller, and Katheryn Meek. Autophosphorylation of DNA-Dependent Protein Kinase Regulates DNA End Processing and May Also Alter Double-Strand Break Repair Pathway Choice Autophosphorylation of DNA-Dependent Protein Kinase Regulates DNA End Processing and May Also Alter Double-Strand. *Molecular and cellular biology*, 25(24):10842–10852, 2005. doi: 10.1128/MCB.25.24.10842.
- [185] Jessica A Neal, Van Dang, Pauline Douglas, Marc S Wold, Susan P Lees-Miller, and Katheryn Meek. Inhibition of homologous recombination by DNA-dependent protein kinase requires kinase activity, is titratable, and is modulated by autophosphorylation. *Molecular and cellular biology*, 31(8):1719–33, 2011. ISSN 1098-5549. doi: 10.1128/MCB.01298-10. URL <http://mcb.asm.org.ezproxy.library.tufts.edu/content/31/8/1719.full{#}T1>.
- [186] Yi Zhou and Tanya T. Paull. DNA-dependent protein kinase regulates DNA end resection in concert with Mre11-Rad50-Nbs1 (MRN) and Ataxia Telangiectasia-mutated (ATM). *Journal of Biological Chemistry*, 288(52):37112–37125, 2013. ISSN 00219258. doi: 10.1074/jbc.M113.514398.
- [187] Yi Zhou, Ji-Hoon Lee, Wenxia Jiang, Jennie L. Crowe, Shan Zha, and Tanya T. Paull. Regulation of the DNA Damage Response by DNA-PKcs Inhibitory Phosphorylation of ATM. *Molecular Cell*, 65(1):91–104, 2016. ISSN 10972765. doi: 10.1016/j.molcel.2016.11.004. URL <http://www.ncbi.nlm.nih.gov/pubmed/27939942{ }0Ahttp://linkinghub.elsevier.com/retrieve/pii/S1097276516307122>.
- [188] Andrea J Hartlerode, Mary J Morgan, Yipin Wu, Jeffrey Buis, and David O Ferguson. Recruitment and activation of the ATM kinase in the absence of DNA-damage sensors. *Nature structural & molecular biology*, 22(9):736–43, 2015. ISSN 1545-9985. doi: 10.1038/nsmb.3072. URL <http://dx.doi.org/10.1038/nsmb.3072{ }5Cnhttp://www.nature.com/doifinder/10.1038/nsmb.3072{ }5Cnhttp://www.ncbi.nlm.nih.gov/pubmed/26280532{ }5Cnhttp://www.pubmedcentral.nih.gov/articlerender.fcgi?artid=PMC4560612>.
- [189] Yu Zhang, Melissa L Hefferin, Ling Chen, Eun Yong Shim, Hui-Min Tseng, Youngho Kwon, Patrick Sung, Sang Eun Lee, and Alan E Tomkinson. Role of Dnl4-Lif1 in nonhomologous end-joining repair complex assembly and suppression of homologous recombination. *Nature structural & molecular*

- biology*, 14(7):639–46, 2007. ISSN 1545-9993. doi: 10.1038/nsmb1261. URL <http://dx.doi.org/10.1038/nsmb1261>.
- [190] Sang Eun Lee, J. Kent Moore, Allyson Holmes, Keiko Umezu, Richard D. Kolodner, and James E. Haber. Saccharomyces and Ku70, Mre11/Rad50, and RPA Proteins Regulate Adaptation to G2 / M Arrest after DNA Damage. *Cell*, 94(3):399–409, 1998. ISSN 00928674. doi: 10.1016/S0092-8674(00)81482-8.
- [191] Eun Yong Shim, Woo-hyun Chung, Matthew L Nicolette, Yu Zhang, Melody Davis, Zhu Zhu, Tanya T Paull, Grzegorz Ira, and Sang Eun Lee. Saccharomyces cerevisiae Mre11/Rad50/Xrs2 and Ku proteins regulate association of Exo1 and Dna2 with DNA breaks. *The EMBO Journal*, 29(19):3370–3380, 2010. ISSN 0261-4189. doi: 10.1038/emboj.2010.219. URL <http://dx.doi.org/10.1038/emboj.2010.219>.
- [192] Dongliang Wu, Leana M Topper, and Thomas E Wilson. Recruitment and Dissociation of Nonhomologous End Joining Proteins at a DNA Double-Strand Break in Saccharomyces cerevisiae. *Genetics*, 178:1237–1249, 2008. doi: 10.1534/genetics.107.083535.
- [193] Eleni P Mimitou and Lorraine S Symington. Ku prevents Exo1 and Sgs1-dependent resection of DNA ends in the absence of a functional MRX complex or Sae2. *The EMBO journal*, 29(19):3358–69, 2010. ISSN 1460-2075. doi: 10.1038/emboj.2010.193. URL <http://dx.doi.org/10.1038/emboj.2010.193>  
<http://www.ncbi.nlm.nih.gov/pubmed/20729809>  
<http://www.pubmedcentral.nih.gov/articlerender.fcgi?artid=PMC2957202>.
- [194] Jingxin Sun, Kyung Jong Lee, Anthony J. Davis, and David J. Chen. Human Ku70/80 protein blocks exonuclease 1-mediated DNA resection in the presence of human Mre11 or Mre11/Rad50 protein complex. *Journal of Biological Chemistry*, 287(7):4936–4945, 2012. ISSN 00219258. doi: 10.1074/jbc.M111.306167.
- [195] Zhengping Shao, Anthony J. Davis, Kazi R. Fattah, Sairei So, Jingxin Sun, Kyung Jong Lee, Lynn Harrison, Jun Yang, and David J. Chen. Persistently bound Ku at DNA ends attenuates DNA end resection and homologous recombination. *DNA Repair*, 11(3):310–316, 2012. ISSN 15687864. doi: 10.1016/j.dnarep.2011.12.007. URL <http://dx.doi.org/10.1016/j.dnarep.2011.12.007>.
- [196] Kyung-jong Lee, Janapriya Saha, Jingxin Sun, Kazi R Fattah, Shu-chi Wang, Burkhard Jakob, Linfeng Chi, Shih-ya Wang, Gisela Taucher-scholz, Anthony J Davis, and David J Chen. Phosphorylation of Ku dictates DNA double-strand break ( DSB ) repair pathway choice in S phase. *Nucleic Acids Research*, pages 1–14, 2015. ISSN 1362-4962. doi: 10.1093/nar/gkv1499.

- [197] Ismail Hassan Ismail, Jean-Philippe Gagné, Marie-Michelle Genois, Hilmar Strickfaden, Darin McDonald, Zhizhong Xu, Guy G Poirier, Jean-Yves Masson, and Michael J Hendzel. The RNF138 E3 ligase displaces Ku to promote DNA end resection and regulate DNA repair pathway choice. *Nature cell biology*, 17(11):1446–57, 2015. ISSN 1476-4679. doi: 10.1038/ncb3259. URL <http://www.ncbi.nlm.nih.gov/pubmed/26502055>.
- [198] Christine K. Schmidt, Yaron Galanty, Matylda Sczaniecka-Clift, Julia Coates, Satpal Jhujh, Mukerrem Demir, Matthew Cornwell, Petra Beli, and Stephen P. Jackson. Systematic E2 screening reveals a UBE2D–RNF138–CtIP axis promoting DNA repair. *Nature Cell Biology*, 17(11):1458–1470, 2015. ISSN 1465-7392. doi: 10.1038/ncb3260. URL <http://www.nature.com/doifinder/10.1038/ncb3260>.
- [199] T Clouaire and G Legube. DNA double strand break repair pathway choice: a chromatin based decision? *Nucleus (Austin, Tex.)*, 6(2):107–13, 2015. ISSN 1949-1042. doi: 10.1080/19491034.2015.1010946. URL <http://www.ncbi.nlm.nih.gov/pubmed/25675367>.
- [200] Farjana Fattah, Eu Han Lee, Natalie Weisensel, Yongbao Wang, Natalie Lichter, and Eric A Hendrickson. Ku Regulates the Non-Homologous End Joining Pathway Choice of DNA Double-Strand Break Repair in Human Somatic Cells. *PLoS Genetics*, 6(2):1–14, 2010. doi: 10.1371/journal.pgen.1000855.
- [201] P Pace, G Mosedale, MR Hodkinson, IV Rosado, M Sivasubramaniam, and K Patel. Ku70 corrupts DNA Repair in the Absence of the Fanconi Anemia Pathway. *Science*, 329(July):219–224, 2010.
- [202] Steven S Foster, Alessia Balestrini, John H J Petrini, and Foster E T Al. Functional Interplay of the Mre11 Nuclease and Ku in the Response to Replication-Associated DNA Damage. *Molecular and cellular biology*, 31(21):4379–4389, 2011. doi: 10.1128/MCB.05854-11.
- [203] Qiao Cheng, Nadia Barboule, Philippe Frit, Dennis Gomez, Oriane Bombarde, Bettina Couderc, Guo Sheng Ren, Bernard Salles, and Patrick Calso. Ku counteracts mobilization of PARP1 and MRN in chromatin damaged with DNA double-strand breaks. *Nucleic Acids Research*, 39(22):9605–9619, 2011. ISSN 03051048. doi: 10.1093/nar/gkr656.
- [204] Yasuo Ariumi, Mitsuko Masutani, Terry D Copeland, Tuneyo Mimori, Takashi Sugimura, Kunitada Shimotohno, Kunihiro Ueda, Masakazu Hatanaka, and Makoto Noda. Suppression of the poly ( ADP-ribose ) polymerase activity by DNA-dependent protein kinase in vitro. *Oncogene*, 18: 4616–4625, 1999.
- [205] Wael Y Mansour, K Borgmann, C Petersen, Ekkehard Dikomey, and Jochen Dahm-daphi. The absence of Ku but not defects in classical non-homologous

- end-joining is required to trigger PARP1-dependent end-joining. *DNA Repair*, 12(12):1134–1142, 2013. ISSN 1568-7864. doi: 10.1016/j.dnarep.2013.10.005. URL <http://dx.doi.org/10.1016/j.dnarep.2013.10.005>.
- [206] Stephen J. Elledge and Bin-Bing S. Zhou. The DNA damage response: putting checkpoints in perspective. *Nature*, 408(6811):433–439, nov 2000. ISSN 00280836. doi: 10.1038/35044005. URL <http://www.nature.com/doifinder/10.1038/35044005>.
- [207] Alyson K Freeman and Alvaro Na Monteiro. Phosphatases in the cellular response to DNA damage. *Cell communication and signaling : CCS*, 8(1):27, 2010. ISSN 1478-811X. doi: 10.1186/1478-811X-8-27. URL <http://www.ncbi.nlm.nih.gov/pubmed/20860841><http://www.pubmedcentral.nih.gov/articlerender.fcgi?artid=PMC2954851>.
- [208] A Maréchal and L Zou. DNA Damage Sensing by the ATM and ATR kinases. *Perspectives in Biology*, 5:1–18, 2013.
- [209] Shuhei Matsuoka, Bryan A Ballif, Agata Smogorzewska, E Robert Mcdonald Iii, Kristen E Hurov, Ji Luo, Corey E Bakalarski, Zhenming Zhao, Nicole Solimini, Yaniv Lerenthal, Yosef Shiloh, Steven P Gygi, and Stephen J Elledge. ATM and ATR Substrate Analysis Reveals Extensive Protein Networks Responsive to DNA Damage. *Science*, 316(May), 2007.
- [210] Yosef Shiloh and Yael Ziv. The ATM protein kinase: regulating the cellular response to genotoxic stress, and more. *Nature Publishing Group*, 14(4): 197–210, 2013. ISSN 1471-0072. doi: 10.1038/nrm3546. URL <http://dx.doi.org/10.1038/nrm3546>.
- [211] Ji-Hoon Lee and Tanya T. Paull. ATM Activation by DNA Double-Strand Breaks Through the Mre11-Rad50-Nbs1 Complex. *Science*, 308(5721), 2005. URL <http://science.sciencemag.org/content/308/5721/551.long>.
- [212] Ji-Hoon Lee and Tanya T. Paull. Direct Activation of the ATM Protein Kinase by the Mre11/Rad50/Nbs1 Complex. *Science*, 304(5667), 2004. URL <http://science.sciencemag.org/content/304/5667/93.long>.
- [213] Emmy P Rogakou, Chye Boon, Christophe Redon, and William M Bonner. Megabase Chromatin Domains Involved in DNA Double-Strand Breaks In Vivo. *The Journal of cell biology*, 146:905–915, 1999.
- [214] Emmy P Rogakou, Duane R Pilch, Ann H Orr, Vessela S Ivanova, and William M Bonner. DNA Double-stranded Breaks Induce Histone H2AX Phosphorylation on Serine 139 \*. *The Journal of biological chemistry*, 10: 5858–5868, 1998.
- [215] Yingli Sun, Xiaofeng Jiang, Shujuan Chen, Norvin Fernandes, and Brendan D Price. A role for the Tip60 histone acetyltransferase in the acetylation and activation of ATM. *Proceedings of the National Academy of Sciences of the United States of America*, 102(37):

- 13182–7, sep 2005. ISSN 0027-8424. doi: 10.1073/pnas.0504211102. URL <http://www.ncbi.nlm.nih.gov/pubmed/16141325><http://www.pubmedcentral.nih.gov/articlerender.fcgi?artid=PMC1197271>.
- [216] Yingli Sun, Ye Xu, Kanaklata Roy, and Brendan D Price. DNA damage-induced acetylation of lysine 3016 of ATM activates ATM kinase activity. *Molecular and cellular biology*, 27(24):8502–9, dec 2007. ISSN 1098-5549. doi: 10.1128/MCB.01382-07. URL <http://www.ncbi.nlm.nih.gov/pubmed/17923702><http://www.pubmedcentral.nih.gov/articlerender.fcgi?artid=PMC2169409>.
- [217] Sergei V Kozlov, Mark E Graham, Cheng Peng, Philip Chen, Phillip J Robinson, and Martin F Lavin. Involvement of novel autophosphorylation sites in ATM activation. *The EMBO journal*, 25(15):3504–3514, 2006. ISSN 0261-4189. doi: 10.1038/sj.emboj.7601231.
- [218] Christopher J. Bakkenist and Michael B. Kastan. DNA damage activates ATM through intermolecular autophosphorylation and dimer dissociation. *Nature*, 421(6922):499–506, jan 2003. ISSN 0028-0836. doi: 10.1038/nature01368. URL <http://www.nature.com/doifinder/10.1038/nature01368>.
- [219] S Banin, L Moyal, S Shieh, Y Taya, C W Anderson, L Chessa, N I Smorodinsky, C Prives, Y Reiss, Y Shiloh, Y Ziv, A. J. Levine, M. Lavin, Y. Shiloh, Y. Shiloh, C. Barlow, Y. Xu, D. Baltimore, S. E. Morgan, M. B. Kastan, K. Savitsky, K. Savitsky, M. F. Hoekstra, K. O. Hartley, E. J. Brown, G. J. Brunn, G. J. Brunn, T.-A. Lin, Y. Ziv, S. Gilad, S. Gilad, M. T. Ui, T. Okada, K. Hazeki, O. Hazeki, M. P. Wymann, J. D. Siliciano, S.-Y. Shieh, M. Ikeda, Y. Taya, C. Prives, D. Watters, M. Kitagawa, L. J. Ko, N. D. Lakin, K. D. Brown, K. S. Keegan, M. Jung, M. Fiscella, J. Momand, G. P. Zambetti, D. C. Olson, D. George, A. J. Levine, J. D. Oliner, Y. Haupt, R. Maya, A. Kazaz, and M. Oren. Enhanced phosphorylation of p53 by ATM in response to DNA damage. *Science (New York, N.Y.)*, 281(5383):1674–7, 1998. ISSN 0036-8075. doi: 10.1126/science.281.5383.1674. URL <http://www.ncbi.nlm.nih.gov/pubmed/9733514>.
- [220] Nicholas D Lakin, Byron C Hann, and Stephen P Jackson. The ataxia-telangiectasia related protein ATR mediates DNA-dependent phosphorylation of p53. *Oncogene*, 18(27):3989–95, 1999. ISSN 0950-9232. doi: 10.1038/sj.onc.1202973. URL <http://www.ncbi.nlm.nih.gov/pubmed/10435622>.
- [221] Yi-Hung Ou, Pei-Han Chung, Te-Ping Sun, and Sheau-Yann Shieh. p53 C-terminal phosphorylation by CHK1 and CHK2 participates in the regulation of DNA-damage-induced C-terminal acetylation. *Molecular biology of the cell*, 16(4):1684–95, apr 2005. ISSN 1059-1524. doi: 10.1091/mbc.E04-08-0689. URL <http://www.ncbi.nlm.nih.gov/pubmed/15659650><http://www.pubmedcentral.nih.gov/articlerender.fcgi?artid=PMC1073652>.



- [222] Nozomi Tomimatsu, Candice G T Tahimic, Akihiro Otsuki, Sandeep Burma, Akiko Fukuhara, Kenzo Sato, Goshi Shiota, Mitsuo Oshimura, David J Chen, and Akihiro Kurimasa. Ku70/80 modulates ATM and ATR signaling pathways in response to DNA double strand breaks. *The Journal of biological chemistry*, 282(14):10138–45, apr 2007. ISSN 0021-9258. doi: 10.1074/jbc.M611880200. URL <http://www.ncbi.nlm.nih.gov/pubmed/17272272>.
- [223] Xiang-Yang Zhou, Xiang Wang, Hongyan Wang, David J Chen, Gloria C Li, George Iliakis, and Ya Wang. Ku affects the ATM-dependent S phase checkpoint following ionizing radiation. *Oncogene*, 21(41):6377–81, 2002. ISSN 0950-9232. doi: 10.1038/sj.onc.1205782. URL <http://www.ncbi.nlm.nih.gov/pubmed/12214278>.
- [224] Victoria L Fell and Caroline Schild-Poulter. Ku Regulates Signaling to DNA Damage Response Pathways through the Ku70 von Willebrand A domain. *Molecular and cellular biology*, pages 76–87, 2011.
- [225] Victoria L Fell, Stephanie R Rogers, Amelia S Aitken, Sarah M Hoffer, and Caroline Schild-Poulter. Ku70 phosphorylation mediates Aurora B inhibition and activation of the DNA damage response. *Scientific reports*, 6:1–17, 2016. ISSN 2045-2322. doi: 10.1038/srep37194. URL <http://dx.doi.org/10.1038/srep37194>.
- [226] R H Medema and L Macurek. Checkpoint control and cancer. *Oncogene*, 31(21):2601–13, 2012. ISSN 1476-5594. doi: 10.1038/onc.2011.451. URL <http://www.scopus.com/inward/record.url?eid=2-s2.0-84861526824&partnerID=tZ0tx3y1>.
- [227] Jonathon Pines. Cubism and the cell cycle: the many faces of the APC/C. *Nature reviews. Molecular cell biology*, 12(7):427–438, 2011. ISSN 1471-0072. doi: 10.1038/nrm3132. URL <http://dx.doi.org/10.1038/nrm3132>.
- [228] George Iliakis, Ya Wang, Jun Guan, and Huichen Wang. DNA damage checkpoint control in cells exposed to ionizing radiation. *Oncogene*, 22:5834–5847, 2003. ISSN 0950-9232. doi: 10.1038/sj.onc.1206682.
- [229] Jiri Bartek and Jiri Lukas. Pathways governing G1 / S transition and their response to DNA damage. *FEBS Letters* 490, 490:117–122, 2001.
- [230] Indra A Shaltiel, Lenno Krenning, Wytse Bruinsma, and René H Medema. The same, only different - DNA damage checkpoints and their reversal throughout the cell cycle. *Journal of cell science*, 128(4):607–20, 2015. ISSN 1477-9137. doi: 10.1242/jcs.163766. URL <http://jcs.biologists.org/content/128/4/607.abstract>.
- [231] René H Medema and Libor Macurek. Checkpoint recovery in cells: how a molecular understanding can help in the fight against cancer. *F1000 biology reports*, 3:10, 2011. ISSN 1757-594X. doi: 10.3410/B3-10. URL <http://www.ncbi.nlm.nih.gov/pubmed/21655336><http://www.pubmedcentral.nih.gov/articlerender.fcgi?artid=PMC3100786>.

- [232] Xiongbin Lu, Thuy-Ai Nguyen, Sung-Hwan Moon, Yolanda Darlington, Matthias Sommer, and Lawrence A Donehower. The type 2C phosphatase Wip1: an oncogenic regulator of tumor suppressor and DNA damage response pathways. *Cancer metastasis reviews*, 27(2): 123–35, jun 2008. ISSN 0167-7659. doi: 10.1007/s10555-008-9127-x. URL <http://www.ncbi.nlm.nih.gov/pubmed/18265945><http://www.pubmedcentral.nih.gov/articlerender.fcgi?artid=PMC2362138>.
- [233] Xiang Wang, Gloria C Li, George Iliakis, and Ya Wang. Ku Affects the CHK1-dependent G 2 Checkpoint after Ionizing Radiation 1. *Cancer Res.*, 62:6031–6034, 2002.
- [234] E. Rampakakis, D. Di Paola, and M. Zannis-Hadjopoulos. Ku is involved in cell growth, DNA replication and G1-S transition. *Journal of Cell Science*, 121(5):590–600, 2008. ISSN 0021-9533. doi: 10.1242/jcs.021352. URL <http://jcs.biologists.org/cgi/doi/10.1242/jcs.021352>.
- [235] Ping Ji, Nicole Bäumer, Taijun Yin, Sven Diederichs, Feng Zhang, Carmela Beger, Karl Welte, Simone Fulda, Wolfgang E. Berdel, Hubert Serve, and Carsten Müller-Tidow. DNA damage response involves modulation of Ku70 and Rb functions by cyclin A1 in leukemia cells. *International Journal of Cancer*, 121(4):706–713, 2007. ISSN 00207136. doi: 10.1002/ijc.22634.
- [236] Soumita Mukherjee, Prabal Chakraborty, and Partha Saha. Phosphorylation of Ku70 subunit by cell cycle kinases modulates the replication related function of Ku heterodimer. *Nucleic Acids Research*, pages 1–11, 2016. ISSN 0305-1048. doi: 10.1093/nar/gkw622. URL <http://nar.oxfordjournals.org/lookup/doi/10.1093/nar/gkw622>.
- [237] L. Hayflick and P.S. Moorhead. The serial cultivation of human diploid cell strains. *Experimental Cell Research*, 25(3):585–621, 1961. ISSN 00144827. doi: 10.1016/0014-4827(61)90192-6. URL <http://www.sciencedirect.com/science/article/pii/0014482761901926>.
- [238] Fabrizio d’Adda di Fagagna. Living on a break: cellular senescence as a DNA-damage response. *Nature reviews. Cancer*, 8(7):512–522, 2008. ISSN 1474-175X. doi: 10.1038/nrc2440.
- [239] Judith Campisi and Fabrizio d’Adda di Fagagna. Cellular senescence: when bad things happen to good cells., sep 2007. ISSN 1471-0080. URL <http://www.ncbi.nlm.nih.gov/pubmed/17667954>.
- [240] David A. Gewirtz, Shawn E. Holt, and Lynne W. Elmore. Accelerated senescence: An emerging role in tumor cell response to chemotherapy and radiation. *Biochemical Pharmacology*, 76(8):947–957, 2008. ISSN 00062952. doi: 10.1016/j.bcp.2008.06.024.
- [241] Rebecca J Sabin and Rhona M Anderson. Cellular Senescence - its role in cancer and the response to ionizing radiation. *Genome integrity*, 2(1):7, 2011. ISSN 2041-9414. doi: 10.1186/2041-9414-2-7.

- URL <http://www.pubmedcentral.nih.gov/articlerender.fcgi?artid=3169443&tool=pmcentrez&rendertype=abstract>.
- [242] Daniel Munoz-Espin and Manuel Serrano. Cellular senescence: from physiology to pathology. *Nature reviews. Molecular cell biology*, 15(7):482–496, 2014. ISSN 1471-0080 (Electronic). doi: 10.1038/nrm3823.
- [243] Agata Smogorzewska and Titia de Lange. Different telomere damage signaling pathways in human and mouse cells. *The EMBO Journal*, 21(16):4338–4348, 2002. ISSN 14602075. doi: 10.1093/emboj/cdf433. URL <http://emboj.embopress.org/cgi/doi/10.1093/emboj/cdf433>.
- [244] Jerry W. Shay, Olivia M. Pereira-Smith, and Woodring E. Wright. A role for both RB and p53 in the regulation of human cellular senescence. *Experimental Cell Research*, 196(1):33–39, 1991. ISSN 00144827. doi: 10.1016/0014-4827(91)90453-2.
- [245] Y Gu, K J Seidl, G a Rathbun, C Zhu, J P Manis, N van der Stoep, L Davidson, H L Cheng, J M Sekiguchi, K Frank, P Stanhope-Baker, M S Schlissel, D B Roth, and F W Alt. Growth retardation and leaky SCID phenotype of Ku70-deficient mice., nov 1997. ISSN 1074-7613. URL <http://www.ncbi.nlm.nih.gov/pubmed/9390689>.
- [246] André Nussenzweig, Changhu Chen, Vera da Costa Soares, Mercedes Sanchez, Karen Sokol, Michel C. Nussenzweig, and Gloria C. Li. Requirement for Ku80 in growth and immunoglobulin V(D)J recombination, 1996. ISSN 0028-0836. URL <http://www.nature.com/doi/10.1038/382551a0>.
- [247] D.-S. Lim, H. Vogel, D. M. Willerford, A. T. Sands, K. A. Platt, and P. Hasty. Analysis of ku80-Mutant Mice and Cells with Deficient Levels of p53. *Molecular and Cellular Biology*, 20(11):3772–3780, 2000. ISSN 0270-7306. doi: 10.1128/MCB.20.11.3772-3780.2000. URL <http://mcb.asm.org/cgi/doi/10.1128/MCB.20.11.3772-3780.2000>.
- [248] H. Vogel, D.-S. Lim, G. Karsenty, M. Finegold, and P. Hasty. Deletion of Ku86 causes early onset of senescence in mice. *Proceedings of the National Academy of Sciences*, 96(19):10770–10775, 1999. ISSN 0027-8424. doi: 10.1073/pnas.96.19.10770. URL <http://www.pnas.org/cgi/doi/10.1073/pnas.96.19.10770>.
- [249] A V Gudkov and E A Komarova. The role of p53 in determining sensitivity to radiotherapy. *Nature reviews. Cancer*, 3(2):117–129, 2003. ISSN 1474175X. doi: 10.1038/nrc992. URL <http://www.ncbi.nlm.nih.gov/pubmed/12563311>.
- [250] Igor B. Roninson, Eugenia V. Broude, and Bey-Dih Chang. If not apoptosis, then what? Treatment-induced senescence and mitotic catastrophe in tumor cells. *Drug Resistance Updates*, 4(5):303–313, 2001. ISSN 13687646. doi: 10.1054/drup.2001.0213. URL <http://www.drupjournal.com/article/S1368764601902134/fulltext>.

- [251] S. Elmore. Apoptosis: A Review of programmed Cell Death. *Toxicol Pathol.*, 35(4):495–516, 2007. ISSN 09652140. doi: 10.1097/OPX.0b013e3182540562. The.
- [252] Sonja Matt and Thomas G. Hofmann. The DNA damage-induced cell death response: a roadmap to kill cancer cells. *Cellular and Molecular Life Sciences*, 73(15):2829–2850, 2016. ISSN 14209071. doi: 10.1007/s00018-016-2130-4.
- [253] Bruce. Alberts, John. Wilson, and Tim. Hunt. *Molecular biology of the cell*. Garland Science, 2008. ISBN 9780815341116. URL <http://www.garlandscience.com/product/isbn/0815341059>.
- [254] Wynand P Roos, Adam D Thomas, and Bernd Kaina. DNA damage and the balance between survival and death in cancer biology. *Nature reviews. Cancer*, 16(1):20–33, 2015. ISSN 1474-1768. doi: 10.1038/nrc.2015.2. URL [http://www.nature.com/nrc/journal/v16/n1/full/nrc.2015.2.html?WT.ec\\_{\\_}id=NRC-201601{&}spMailingID=50322112{&}spUserID=MTc1NDg1MTA1ODkwSO{&}spJobID=823506265{&}spReportId=ODIzNTA2MjY1S0](http://www.nature.com/nrc/journal/v16/n1/full/nrc.2015.2.html?WT.ec_{_}id=NRC-201601{&}spMailingID=50322112{&}spUserID=MTc1NDg1MTA1ODkwSO{&}spJobID=823506265{&}spReportId=ODIzNTA2MjY1S0).
- [255] Michael A. Sheard. Ionizing radiation as a response-enhancing agent for CD95-mediated apoptosis. *International Journal of Cancer*, 96(4):213–220, 2001. ISSN 00207136. doi: 10.1002/ijc.1020.
- [256] Carsten Scaffidi, Simone Fulda, Anu Srinivasan, Claudia Friesen, Feng Li, Kevin J Tomaselli, Klaus-michael Debatin, Peter H Krammer, and Marcus E Peter. Two CD95 ( APO-1 / Fas ) signaling pathways. *EMBO Journal*, 17(6):1675–1687, 1998.
- [257] Patrick Maier, Linda Hartmann, Frederik Wenz, and Carsten Herskind. Cellular pathways in response to ionizing radiation and their targetability for tumor radiosensitization. *International Journal of Molecular Sciences*, 17(1), 2016. ISSN 14220067. doi: 10.3390/ijms17010102.
- [258] Wynand P. Roos and Bernd Kaina. DNA damage-induced cell death: From specific DNA lesions to the DNA damage response and apoptosis. *Cancer Letters*, 332(2):237–248, 2013. ISSN 03043835. doi: 10.1016/j.canlet.2012.01.007. URL <http://dx.doi.org/10.1016/j.canlet.2012.01.007>.
- [259] Honglin Li, Hong Zhu, Chi-Jie Xu, and Junying Yuan. Cleavage of BID by Caspase 8 Mediates the Mitochondrial Damage in the Fas Pathway of Apoptosis. *Cell*, 94:491–501, 1998. ISSN 00928674. doi: 10.1016/S0092-8674(00)81590-1.
- [260] S Fulda and K-M Debatin. Extrinsic versus intrinsic apoptosis pathways in anticancer chemotherapy. *Oncogene*, 25:4798–4811, 2006. ISSN 0950-9232. doi: 10.1038/sj.onc.1209608.

- [261] Mingan Shi, Carolyn J. Vivian, Kyung Jong Lee, Chunmin Ge, Keiko Morotomi-Yano, Claudia Manzl, Florian Bock, Shigeo Sato, Chieri Tomomori-Sato, Ruihong Zhu, Jeffrey S. Haug, Selene K. Swanson, Michael P. Washburn, David J. Chen, Benjamin P C Chen, Andreas Villunger, Laurence Florens, and Chunying Du. DNA-PKcs-PIDDosome: A Nuclear Caspase-2-Activating Complex with Role in G2/M Checkpoint Maintenance. *Cell*, 136(3):508–520, 2009. ISSN 00928674. doi: 10.1016/j.cell.2008.12.021. URL <http://dx.doi.org/10.1016/j.cell.2008.12.021>.
- [262] Sharad Kumar. Caspase 2 in apoptosis, the DNA damage response and tumour suppression: enigma no more? *Nature reviews. Cancer*, 9(12):897–903, 2009. ISSN 1474-175X. doi: 10.1038/nrc2745.
- [263] M Olsson, J Forsberg, and B Zhivotovsky. Caspase-2: the reinvented enzyme. *Oncogene*, 34(15):1877–1882, 2014. ISSN 1476-5594. doi: 10.1038/onc.2014.139. URL <http://www.ncbi.nlm.nih.gov/pubmed/24882576>.
- [264] L Dorstyn, J Puccini, C H Wilson, S Shalini, M Nicola, S Moore, and S Kumar. Caspase-2 deficiency promotes aberrant DNA-damage response and genetic instability. *Cell Death and Differentiation*, 19(8):1411–1411, 2012. ISSN 1350-9047. doi: 10.1038/cdd.2012.76. URL <http://dx.doi.org/10.1038/cdd.2012.36>.
- [265] Avigail D Amsel, Moran Rathaus, Noam Kronman, and Haim Y Cohen. Regulation of the proapoptotic factor Bax by Ku70-dependent deubiquitylation. *Proceedings of the National Academy of Sciences of the United States of America*, 105(13):5117–22, 2008. ISSN 1091-6490. doi: 10.1073/pnas.0706700105. URL <http://www.scopus.com/inward/record.url?eid=2-s2.0-42449160125&partnerID=tZ0tx3y1>.
- [266] Moran Rathaus, Batya Lerrer, and Haim Y. Cohen. DeubiKuitylation: A novel DUB enzymatic activity for the DNA repair protein, Ku70. *Cell Cycle*, 8(12):1843–1852, 2009. ISSN 15384101. doi: 8864[pii].
- [267] Jia Liu, Janice R. Naegele, and Stanley L. Lin. The DNA-PK Catalytic Subunit Regulates Bax-mediated Excitotoxic Cell Death by Ku70 Phosphorylation. *Brain Research*, 1296(860):164–175, 2009. doi: 10.1016/j.brainres.2009.07.101.The.
- [268] C Subramanian, A W Opipari Jr., X Bian, V P Castle, and R P Kwok. Ku70 acetylation mediates neuroblastoma cell death induced by histone deacetylase inhibitors. *Proc Natl Acad Sci U S A*, 102(13):4842–4847, 2005. doi: 0408351102[pii]\r10.1073/pnas.0408351102. URL <http://www.ncbi.nlm.nih.gov/pubmed/15778293>.
- [269] Chitra Subramanian, Jason a Jarzembowski, Anthony W Opipari, Valerie P Castle, and Roland Ps Kwok. HDAC6 Deacetylates Ku70 and Regulates Ku70-Bax Binding in Neuroblastoma. *Neoplasia (New York, N.Y.)*, 13(8):

- 726–734, 2011. ISSN 1476-5586. doi: 10.1593/neo.11558. URL <http://dx.doi.org/10.1593/neo.11558>.
- [270] V Gama, J A Gomez, L D Mayo, M W Jackson, D Danielpour, K Song, A L Haas, M J Laughlin, and S Matsuyama. Hdm2 is a ubiquitin ligase of Ku70-Akt promotes cell survival by inhibiting Hdm2-dependent Ku70 destabilization. *Cell death and differentiation*, 16(5):758–69, 2009. ISSN 1476-5403. doi: 10.1038/cdd.2009.6. URL <http://www.scopus.com/inward/record.url?eid=2-s2.0-67349258111&partnerID=tZ0tx3y1>.
- [271] Suparna Mazumder, Dragos Plesca, Michael Kinter, and Alexandru Almasan. Interaction of a cyclin E fragment with Ku70 regulates Bax-mediated apoptosis. *Molecular and cellular biology*, 27(9):3511–20, may 2007. ISSN 0270-7306. doi: 10.1128/MCB.01448-06. URL <http://www.pubmedcentral.nih.gov/articlerender.fcgi?artid=1899959&tool=pmcentrez&rendertype=abstract>.
- [272] Chin-Rang Yang, Konstantin Leskov, Kelly Hosley-Eberlein, Tracy Criswell, John J Pink, Timothy J Kinsella, and David A Boothman. Nuclear clusterin/XIP8, an x-ray-induced Ku70-binding protein that signals cell death. *PNAS*, 97(11):5907–5912, 2000.
- [273] H Vakifahmetoglu, M Olsson, and B Zhivotovsky. Death through a tragedy: mitotic catastrophe. *Cell death and differentiation*, 15(7):1153–62, 2008. ISSN 1350-9047. doi: 10.1038/cdd.2008.47. URL <http://www.ncbi.nlm.nih.gov/pubmed/18404154>.
- [274] Ilio Vitale, Lorenzo Galluzzi, Maria Castedo, and Guido Kroemer. Mitotic catastrophe: a mechanism for avoiding genomic instability. *Nature Reviews Molecular Cell Biology*, 12(6):385–392, 2011. ISSN 1471-0072. doi: 10.1038/nrm3115. URL <http://www.ncbi.nlm.nih.gov/pubmed/21527953>.
- [275] Maria Castedo, Jean-Luc Perfettini, Thomas Roumier, Karine Andreau, Rene Medema, and Guido Kroemer. Cell death by mitotic catastrophe: a molecular definition. *Oncogene*, 23(16):2825–37, 2004. ISSN 0950-9232. doi: 10.1038/sj.onc.1207528. URL <http://www.nature.com/onc/journal/v23/n16/pdf/1207528a.pdf> <http://www.ncbi.nlm.nih.gov/pubmed/15077146>.
- [276] Aristides G. Eliopoulos, Sophia Havaki, and Vassilis G. Gorgoulis. DNA Damage Response and Autophagy: A Meaningful Partnership. *Frontiers in Genetics*, 7(November):1–13, 2016. ISSN 1664-8021. doi: 10.3389/fgene.2016.00204. URL <http://journal.frontiersin.org/article/10.3389/fgene.2016.00204/full>.
- [277] Graeme Hewitt and Viktor I Korolchuk. Repair, Reuse, Recycle: The Expanding Role of Autophagy in Genome Maintenance. *Trends in cell biology*, 0(0):529–535, 2016. ISSN 1879-3088. doi: 10.1016/j.tcb.2016.11.011. URL <http://www.ncbi.nlm.nih.gov/pubmed/28011061>.

- [278] H Rodriguez-Rocha, Aracely-Garcia-Garcia, M I Panayiotidis, and R Franco. DNA damage and autophagy. *Mutat Res*, 711(1-2):158–166, 2011. ISSN 15378276. doi: 10.1016/j.immuni.2010.12.017.Two-stage.
- [279] D Gozuacik and A Kimchi. Autophagy as a cell death and tumor suppressor mechanism. *Oncogene*, 23(16):2891–2906, 2004. ISSN 0950-9232. doi: 10.1038/sj.onc.1207521. URL <http://www.ncbi.nlm.nih.gov/pubmed/15077152>.
- [280] Kenneth Murphy, Paul Travers, Mark Walport, and Charles Janeway. *Janeway's Immunobiology*. Garland Science, New York, 8th edition, 2012.
- [281] Jean-Pierre de Villartay. Congenital defects in V(D)J recombination. *British Medical Bulletin*, 114(1):157–167, 2015. ISSN 0007-1420. doi: 10.1093/bmb/ldv020. URL <https://academic.oup.com/bmb/article-lookup/doi/10.1093/bmb/ldv020>.
- [282] Gayle S. Bosma, R. Philip Custer, and Melvin J. Bosma. A severe combined immunodeficiency mutation in the mouse. *Nature*, 301(10 February):527–530, 1983.
- [283] G.M. Fulop and R.A. Phillips. The scid mutation in mice causes a general defect in DNA repair. *Nature*, 347(4 October):479–482, 1990.
- [284] Guillermo E Taccioli, Gary Rathbun, Eugene Oltz, Thomas Stamato, Penny A Jeggo, and Frederick W Alt. Impairment of V ( D ) J Recombination in Double-Strand Break Repair Mutants. *Science*, 260:207–210, 1993.
- [285] David G. Schatz and Patrick C. Swanson. V(D)J Recombination: Mechanisms of Initiation. *Annual Review of Genetics*, 45(1):167–202, 2011. ISSN 0066-4197. doi: 10.1146/annurev-genet-110410-132552. URL <http://www.annualreviews.org/doi/10.1146/annurev-genet-110410-132552>.
- [286] Molly A. Bogue, Chiyu Wang, Chengming Zhu, and David B. Roth. V(D)J recombination in Ku86-deficient mice: Distinct effects on coding, signal, and hybrid joint formation. *Immunity*, 7(1):37–47, 1997. ISSN 10747613. doi: 10.1016/S1074-7613(00)80508-7.
- [287] M M Purugganan, S Shah, J F Kearney, and D B Roth. Ku80 is required for addition of N nucleotides to V(D)J recombination junctions by terminal deoxynucleotidyl transferase. *Nucleic acids research*, 29(7):1638–1646, 2001. ISSN 1362-4962.
- [288] P Soulas-Sprauel, P Rivera-Munoz, L Malivert, G Le Guyader, V Abramowski, P Revy, and J-P de Villartay. V(D)J and immunoglobulin class switch recombinations: a paradigm to study the regulation of DNA end-joining. *Oncogene*, 26(56):7780–7791, 2007. ISSN 0950-9232. doi: 10.1038/sj.onc.1210875. URL <http://www.nature.com/doi/10.1038/sj.onc.1210875>.

- [289] Lisa Woodbine, Andrew R. Gennery, and Penny A. Jeggo. The clinical impact of deficiency in DNA non-homologous end-joining. *DNA Repair*, 17:9–20, 2014. ISSN 15687856. doi: 10.1016/j.dnarep.2014.04.002. URL <http://dx.doi.org/10.1016/j.dnarep.2014.02.011>.
- [290] Yijie Gao, Yi Sun, Karen M Frank, Pieter Dikkes, Yuko Fujiwara, Katherine J Seidl, Joann M Sekiguchi, Gary A Rathbun, Wojciech Swat, Jiyang Wang, Roderick T Bronson, Barbara A Malynn, Margaret Bryans, Chengming Zhu, Jayanta Chaudhuri, Laurie Davidson, Roger Ferrini, Thomas Stamato, Stuart H Orkin, Michael E Greenberg, and Frederick W Alt. A Critical Role for DNA End-Joining Proteins in Both Lymphogenesis and Neurogenesis. *Cell*, 95(December 23):891–902, 1998.
- [291] K M Frank, J M Sekiguchi, K J Seidl, W Swat, G a Rathbun, H L Cheng, L Davidson, L Kangaloo, and F W Alt. Late embryonic lethality and impaired V(D)J recombination in mice lacking DNA ligase IV. *Nature*, 396 (January):173–177, 1998. ISSN 0028-0836. doi: 10.1038/24172.
- [292] C Zhu, M A Bogue, D S Lim, P Hasty, and D B Roth. Ku86-deficient mice exhibit severe combined immunodeficiency and defective processing of V(D)J recombination intermediates. *Cell*, 86(3):379–89, aug 1996. ISSN 0092-8674. URL <http://www.ncbi.nlm.nih.gov/pubmed/8756720>.
- [293] H Ouyang, A Nussenzweig, A Kurimasa, V C Soares, X Li, C Cordon-Cardo, Wh Li, N Cheong, M Nussenzweig, G Iliakis, D J Chen, and G C Li. Ku70 is required for DNA repair but not for T cell antigen receptor gene recombination In vivo. *J Exp.Med*, 186(0022-1007 (Print)):921–929, 1997.
- [294] Y Gu, S Jin, Y Gao, D T Weaver, and F W Alt. Ku70-deficient embryonic stem cells have increased ionizing radiosensitivity, defective DNA end-binding activity, and inability to support V(D)J recombination. *Proceedings of the National Academy of Sciences of the United States of America*, 94(15):8076–81, jul 1997. ISSN 0027-8424. URL <http://www.pubmedcentral.nih.gov/articlerender.fcgi?artid=21559&tool=pmcentrez&rendertype=abstract>.
- [295] Michael R. Lieber, Joanne E. Hesse, Susanna Lewis, Gayle C. Bosma, Naomi Rosenberg, Kiyoshi Mizuuchi, Melvin J. Bosma, and Martin Gellert. The defect in murine severe combined immune deficiency: Joining of signal sequences but not coding segments in V(D)J recombination. *Cell*, 55(1):7–16, 1988. ISSN 00928674. doi: 10.1016/0092-8674(88)90004-9.
- [296] Barbara A. Malynn, T. Keith Blackwell, Gabrielle M. Fulop, Gary A. Rathbun, Andrew J W Furley, Pierre Ferrier, L. Bruce Heinke, Robert A. Phillips, George D. Yancopoulos, and Frederick W. Alt. The scid defect affects the final step of the immunoglobulin VDJ recombinaase mechanism. *Cell*, 54(4): 453–460, 1988. ISSN 00928674. doi: 10.1016/0092-8674(88)90066-9.
- [297] T Blunt, N J Finnie, G E Taccioli, G C Smith, J Demengeot, T M Gottlieb, R Mizuta, a J Varghese, F W Alt, and P a Jeggo. Defective DNA-dependent



- protein kinase activity is linked to V(D)J recombination and DNA repair defects associated with the murine scid mutation. *Cell*, 80(5):813–823, 1995. ISSN 00928674. doi: 10.1016/0092-8674(95)90360-7.
- [298] T Blunt, D Gell, M Fox, G E Taccioli, A R Lehmann, S P Jackson, and P A Jeggo. Identification of a nonsense mutation in the carboxyl-terminal region of DNA-dependent protein kinase catalytic subunit in the scid mouse. *Proc Natl Acad Sci U S A*, 93(19):10285–10290, 1996. URL <http://www.ncbi.nlm.nih.gov/entrez/query.fcgi?cmd=Retrieve{&}db=PubMed{&}dopt=Citation{&}list{&}uids=8816792>.
- [299] N Nicolas, D Moshous, M Cavazzana-Calvo, D Papadopoulo, R de Chasseval, F Le Deist, a Fischer, and J P de Villartay. A human severe combined immunodeficiency (SCID) condition with increased sensitivity to ionizing radiations and impaired V(D)J rearrangements defines a new DNA recombination/repair deficiency. *The Journal of experimental medicine*, 188(4):627–634, 1998. ISSN 0022-1007. doi: 10.1084/jem.188.4.627.
- [300] Cédric Touvrey, Chrystelle Couedel, Pauline Soulas, Rachel Couderc, Maria Jasin, Jean Pierre de Villartay, Patrice N. Marche, Evelyne Jouvin-Marche, and Serge M. Candéias. Distinct effects of DNA-PKcs and Artemis inactivation on signal joint formation in vivo. *Molecular Immunology*, 45(12):3383–3391, 2008. ISSN 01615890. doi: 10.1016/j.molimm.2008.04.004.
- [301] S Lewis, A Gifford, and D Baltimore. DNA elements are asymmetrically joined during the site-specific recombination of kappa immunoglobulin genes. *Science (New York, N.Y.)*, 228(4700):677–85, 1985. ISSN 0036-8075. URL <http://www.ncbi.nlm.nih.gov/pubmed/3158075>.
- [302] Gang Li, Frederick W. Alt, Hwei Ling Cheng, James W. Brush, Peter H. Goff, Mike M. Murphy, Sonia Franco, Yu Zhang, and Shan Zha. Lymphocyte-Specific Compensation for XLF/Cernunnos End-Joining Functions in V(D)J Recombination. *Molecular Cell*, 31(5):631–640, 2008. ISSN 10972765. doi: 10.1016/j.molcel.2008.07.017.
- [303] Gabriella Vera, Paola Rivera-munoz, Vincent Abramowski, Laurent Malivert, Annick Lim, and Christine Bole-feysot. Cernunnos Deficiency Reduces Thymocyte Life Span and Alters the T Cell Repertoire in Mice and Humans. *Molecular and Cellular Biology*, 33(4):701–711, 2013. doi: 10.1128/MCB.01057-12.
- [304] Shan Zha, Chunguang Guo, Cristian Boboila, Valentyn Oksenysh, Hwei-ling Cheng, Yu Zhang, and Duane R Wesemann. ATM damage response and XLF repair factor are functionally redundant in joining DNA breaks. *Nature*, 469(7329):250–254, 2011. ISSN 0028-0836. doi: 10.1038/nature09604. URL <http://dx.doi.org/10.1038/nature09604>.
- [305] Chloé Lescale, Vincent Abramowski, Marie Bedora-Faure, Valentine Murigneux, Gabriella Vera, David B. Roth, Patrick Revy, Jean-Pierre de Villartay, and Ludovic Deriano. RAG2 and XLF/Cernunnos interplay reveals

- a novel role for the RAG complex in DNA repair. *Nature Communications*, 7:10529, 2016. ISSN 00219258. doi: 10.1038/ncomms10529. URL <http://www.nature.com/doifinder/10.1038/ncomms10529>.
- [306] Vipul Kumar, Frederick W. Alt, and Richard L. Frock. PAXX and XLF DNA repair factors are functionally redundant in joining DNA breaks in a G1-arrested progenitor B-cell line. *Proceedings of the National Academy of Sciences*, 113(38):10619–10624, 2016. ISSN 0027-8424. doi: 10.1073/pnas.1611882113. URL <http://www.pnas.org/lookup/doi/10.1073/pnas.1611882113>.
- [307] C Lescale, H Lenden Hasse, A N Blackford, G Balmus, J Bianchi, W Yu, L Bacoccina, A Jarade, C Clouin, R Sivapalan, B Reina-San-Martin, S P Jackson, and L Deriano. Specific Roles of XRCC4 Paralogs PAXX and XLF during V ( D ) J Recombination. *Cell Repo*, 16(September 13):2967–2979, 2016. ISSN 22111247. doi: 10.1016/j.celrep.2016.08.069.
- [308] N Tuteja, R Tuteja, A Ochem, P Taneja, N W Huang, A Simoncsits, S Susic, K Rahman, L Marusic, J Q Chen, J W Zhang, S G Wang, S Pongor, and A Falaschi. Human DNA Helicase-Ii - a Novel DNA Unwinding Enzyme Identified as the Ku Autoantigen. *Embo Journal*, 13(20):4991–5001, 1994.
- [309] Alexander E Ochem, Doris Skopac, Mario Costa, Thierry Rabilloud, and Laurent Vuillard. Functional Properties of the Separate Subunits of Human DNA Helicase II / Ku Autoantigen. *Biochemistry*, 272(47):29919 –29926, 1997.
- [310] Diamanto Matheos, Marcia T. Ruiz, Gerald B. Price, and Maria Zannis-Hadjopoulos. Ku antigen, an origin-specific binding protein that associates with replication proteins, is required for mammalian DNA replication. *Biochimica et Biophysica Acta - Gene Structure and Expression*, 1578(1-3): 59–72, 2002. ISSN 01674781. doi: 10.1016/S0167-4781(02)00497-9.
- [311] Xianming Mo and William S Dynan. Subnuclear Localization of Ku Protein : Functional Association with RNA Polymerase II Elongation Sites. *Molecular and cellular biology*, 22(22):8088–8099, 2002. doi: 10.1128/MCB.22.22.8088.
- [312] Robin L Woodard, Kyung-jong Lee, Juren Huang, and William S Dynan. Distinct Roles for Ku Protein in Transcriptional Reinitiation and DNA Repair \*. *The Journal of biological chemistry*, 276(18):15423–15433, 2001. doi: 10.1074/jbc.M010752200.
- [313] Anne Kuhn, Tanya M Gottlieb, Stephen P Jackson, and G Ingrid. DNA-dependent protein kinase: a potent inhibitor of transcription by RNA polymerase I. *Genes & Development*, 9:193–203, 1995.
- [314] J a Downs and S P Jackson. Involvement of DNA end-binding protein Ku in Ty element retrotransposition. *Molecular and cellular biology*, 19(9):6260–6268, 1999. ISSN 0270-7306.

- [315] Ling Li, Jennifer M. Olvera, Kristine E. Yoder, Richard S. Mitchell, Scott L. Butler, Michael Lieber, Sandra L. Martin, and Frederic D. Bushman. Role of the non-homologous DNA end joining pathway in the early steps of retroviral infection. *EMBO Journal*, 20(12):3272–3281, 2001. ISSN 02614189. doi: 10.1093/emboj/20.12.3272.
- [316] R Daniel, R A Katz, and A M Skalka. A role for DNA-PK in retroviral DNA integration. *Science (New York, N. Y.)*, 284(5414):644–647, 1999. ISSN 00368075. doi: 10.1126/science.284.5414.644.
- [317] M T Ruiz, D Matheos, G B Price, and M Zannis-Hadjopoulos. OBA/Ku86: DNA binding specificity and involvement in mammalian DNA replication. *Molecular biology of the cell*, 10(3):567–80, 1999. ISSN 1059-1524. URL <http://www.pubmedcentral.nih.gov/articlerender.fcgi?artid=25188&tool=pmcentrez&rendertype=abstract>.
- [318] O Novac, D Matheos, F D Araujo, G B Price, and M Zannis-Hadjopoulos. In vivo association of Ku with mammalian origins of DNA replication. *Molecular biology of the cell*, 12(11):3386–3401, 2001. ISSN 1059-1524. URL <http://eutils.ncbi.nlm.nih.gov/entrez/eutils/elink.fcgi?dbfrom=pubmed&id=11694575&retmode=ref&cmd=prlinks%5Cpapers2://publication/uuid/94309D72-F8C2-4313-99D6-05EDD74856DE>.
- [319] Sahar Sibani, Gerald B. Price, and Maria Zannis-Hadjopoulos. Ku80 binds to human replication origins prior to the assembly of the ORC complex. *Biochemistry*, 44(21):7885–7896, 2005. ISSN 00062960. doi: 10.1021/bi047327n.
- [320] Eros Lazzerini-Denchi and Agnel Sfeir. Stop pulling my strings — what telomeres taught us about the DNA damage response. *Nature Reviews Molecular Cell Biology*, 17(6):364–378, 2016. ISSN 1471-0072. doi: 10.1038/nrm.2016.43. URL <http://www.nature.com/doifinder/10.1038/nrm.2016.43>.
- [321] Giulia B. Celli, Eros Lazzerini Denchi, and Titia de Lange. Ku70 stimulates fusion of dysfunctional telomeres yet protects chromosome ends from homologous recombination. *Nature Cell Biology*, 8(8):855–890, 2006. ISSN 1465-7392. doi: 10.1038/ncb1444. URL <http://www.nature.com/doifinder/10.1038/ncb1444>.
- [322] H.-L. Hsu, D. Gilley, E. H. Blackburn, and D. J. Chen. Ku is associated with the telomere in mammals. *Proceedings of the National Academy of Sciences*, 96(22):12454–12458, 1999. ISSN 0027-8424. doi: 10.1073/pnas.96.22.12454. URL <http://www.pnas.org/cgi/doi/10.1073/pnas.96.22.12454>.
- [323] Y. Wang, G. Ghosh, and E. A. Hendrickson. Ku86 represses lethal telomere deletion events in human somatic cells. *Proceedings of the National Academy of Sciences*, 106(30):12430–12435, 2009. ISSN 0027-8424. doi: 10.1073/pnas.0903362106. URL <http://www.pnas.org/cgi/doi/10.1073/pnas.0903362106>.

- [324] Sandra M Indiviglio and Alison a Bertuch. Ku's essential role in keeping telomeres intact. *Proceedings of the National Academy of Sciences of the United States of America*, 106(30):12217–12218, 2009. ISSN 0027-8424. doi: 10.1073/pnas.0906427106.
- [325] Kyungjae Myung, Goutam Ghosh, Farjana J Fattah, Gang Li, Haeyoung Kim, Amalia Dutia, Evgenia Pak, Stephanie Smith, and Eric A Hendrickson. Regulation of telomere length and suppression of genomic instability in human somatic cells by Ku86. *Mol Cell Biol*, 24(11):5050–5059, 2004. ISSN 0270-7306. doi: 10.1128/MCB.24.11.5050.
- [326] Isabel Jaco, Purificación Muñoz, and María A. Blasco. Role of human Ku86 in telomere length maintenance and telomere capping. *Cancer Research*, 64(20):7271–7278, 2004. ISSN 00085472. doi: 10.1158/0008-5472.CAN-04-1381.
- [327] A. Sfeir and T. de Lange. Removal of Shelterin Reveals the Telomere End-Protection Problem. *Science*, 336(6081):593–597, 2012. ISSN 0036-8075. doi: 10.1126/science.1218498. URL <http://www.sciencemag.org/cgi/doi/10.1126/science.1218498>.
- [328] Albert Ribes-Zamora, Sandra M. Indiviglio, Ivana Mihalek, Christopher L. Williams, and Alison A. Bertuch. TRF2 Interaction with Ku Heterotrimerization Interface Gives Insight into c-NHEJ Prevention at Human Telomeres. *Cell Reports*, 5(1):194–206, 2013. ISSN 22111247. doi: 10.1016/j.celrep.2013.08.040. URL <http://dx.doi.org/10.1016/j.celrep.2013.08.040>.
- [329] T Mimori, J a Hardin, and J a Steitz. Characterization of the DNA-binding protein antigen Ku recognized by autoantibodies from patients with rheumatic disorders. *Journal of Biological Chemistry*, 261(5):2274–2278, 1986. ISSN 0021-9258. URL <http://www.ncbi.nlm.nih.gov/pubmed/3511059>.
- [330] Tsuneyo Mimori. Clinical Significance of Anti-Ku Autoantibodies -A Serologic Marker of Overlap Syndrome? *Internal Medicine*, 41(12):1096–1098, 2002. ISSN 0918-2918. doi: 10.2169/internalmedicine.41.1096.
- [331] J. Chan, M. Lerman, B. Prabhakar, O. Isozaki, P. Santisteban, R. Kuppers, E. Oates, A. Notkins, and L. Kohn. Cloning and characterisation of a cDNA that encodes a 70 kDA novel human thyroid autoantigen. *Journal of Biological Chemistry*, 264(7):3651–4, 1989.
- [332] Bellur S Prabhakar, Graham P Allaway, Javaraiah Srinivasappa, and Abner Louis Notkins. Cell Surface Expression of the 70-kD Component of Ku , a DNA-binding Nuclear Autoantigen. *The Journal of clinical investigation*, 86(1989):1301–1305, 1990.
- [333] Sylvie Monferran, Jenny Paupert, Stéphanie Dauvillier, Bernard Salles, and Catherine Muller. The membrane form of the DNA repair protein Ku interacts at the cell surface with metalloproteinase 9. *The EMBO journal*,

- 23(19):3758–68, oct 2004. ISSN 0261-4189. doi: 10.1038/sj.emboj.7600403. URL <http://www.pubmedcentral.nih.gov/articlerender.fcgi?artid=522801&tool=pmcentrez&rendertype=abstract>.
- [334] Catherine Muller, Jenny Paupert, Sylvie Monferran, and Bernard Salles. The Double Life of the Ku Protein. *Cell Cycle*, 4(3):438–441, 2005.
- [335] M. Mahler, A. Swart, J. Wu, M. Szmyrka-Kaczmarek, J.-L. Senecal, Y. Troyanov, J. G. Hanly, and M. J. Fritzler. Clinical and serological associations of autoantibodies to the Ku70/Ku80 heterodimer determined by a novel chemiluminescent immunoassay. *Lupus*, 25(8):889–896, 2016. ISSN 0961-2033. doi: 10.1177/0961203316640918. URL <http://lup.sagepub.com/cgi/doi/10.1177/0961203316640918>.
- [336] C. Belizna, D. Henrion, A. Beucher, C. Lavigne, A. Ghaali, and H. Lévesque. Anti-Ku antibodies: Clinical, genetic and diagnostic insights. *Autoimmunity Reviews*, 9(10):691–694, 2010. ISSN 15689972. doi: 10.1016/j.autrev.2010.05.020. URL <http://dx.doi.org/10.1016/j.autrev.2010.05.020>.
- [337] K K Khanna and S P Jackson. DNA double-strand breaks: signaling, repair and the cancer connection. *Nature genetics*, 27(3):247–54, 2001. ISSN 1061-4036. doi: 10.1038/85798. URL <http://www.ncbi.nlm.nih.gov/pubmed/11242102>.
- [338] Han Li, Hannes Vogel, Valerie B Holcomb, Yansong Gu, and Paul Hasty. Deletion of Ku70, Ku80, or both causes early aging without substantially increased cancer. *Molecular and cellular biology*, 27(23):8205–14, 2007. ISSN 1098-5549. doi: 10.1128/MCB.00785-07. URL <http://www.scopus.com/inward/record.url?eid=2-s2.0-36849088515&partnerID=tZ0tx3y1>.
- [339] Zarir E. Karanjawala, Ulf Grawunder, Chih Lin Hsieh, and Michael R. Lieber. The nonhomologous DNA end joining pathway is important for chromosome stability in primary fibroblasts. *Current Biology*, 9(24):1501–1504, 1999. ISSN 09609822. doi: 10.1016/S0960-9822(00)80123-2.
- [340] Fabrizio D’Adda di Fagagna, M. Prakash Hande, Wei Min Tong, David Roth, Peter M. Lansdorp, Zhao Qi Wang, and Stephen P. Jackson. Effects of DNA nonhomologous end-joining factors on telomere length and chromosomal stability in mammalian cells. *Current Biology*, 11(15):1192–1196, 2001. ISSN 09609822. doi: 10.1016/S0960-9822(01)00328-1.
- [341] Wei-min Tong, Ulrich Cortes, M Prakash Hande, Bassem R Haddad, and Zhao-qi Wang. Synergistic Role of Ku80 and Poly ( ADP-ribose ) Polymerase in Suppressing Chromosomal Aberrations and Liver Cancer Formation Synergistic Role of Ku80 and Poly ( ADP-ribose ) Polymerase in Suppressing. *Cancer research*, 62:6990–6996, 2002.
- [342] Yu-Tzu Tai, Klaus Podar, Stine-Kathrein Kraeft, Fengfei Wang, Gloria Young, Boris Lin, Deepak Gupta, Lan Bo Chen, and Kenneth C Anderson. Translocation of Ku86/Ku70 to the multiple myeloma cell membrane:

- functional implications. *Experimental hematology*, 30(3):212–20, mar 2002. ISSN 0301-472X. URL <http://www.ncbi.nlm.nih.gov/pubmed/11882358>.
- [343] I. S. Ayene, Lance P. Ford, and Cameron J. Koch. Ku protein targeting by Ku70 small interfering RNA enhances human cancer cell response to topoisomerase II inhibitor and radiation. *Molecular Cancer Therapeutics*, 4(4):529–536, 2005. ISSN 1535-7163. doi: 10.1158/1535-7163.MCT-04-0130. URL <http://mct.aacrjournals.org/cgi/doi/10.1158/1535-7163.MCT-04-0130>.
- [344] A Klein, O Miera, O Bauer, S Golfier, and F Schriever. Chemosensitivity of B cell chronic lymphocytic leukemia and correlated expression of proteins regulating apoptosis, cell cycle and DNA repair. *Leukemia : official journal of the Leukemia Society of America, Leukemia Research Fund, U.K.*, 14(1):40–46, 2000. ISSN 08876924. doi: 10.1038/sj.leu.2401636.
- [345] S Pucci, P Mazzairelli, C Rabitti, M Giai, M Gallucci, G Flammia, a Alcini, V Altomare, and V M Fazio. Tumor specific modulation of KU70/80 DNA binding activity in breast and bladder human tumor biopsies. *Oncogene*, 20(6):739–747, 2001. ISSN 0950-9232. doi: 10.1038/sj.onc.1204148.
- [346] P. Mazzairelli, P. Parrella, D. Seripa, E. Signori, G. Perrone, C. Rabitti, D. Borzomati, A. Gabbrielli, M.G. Matera, C. Gravina, M. Caricato, M.L. Poeta, M. Rinaldi, S. Valeri, R. Coppola, and V.M. Fazio. DNA end binding activity and Ku70/80 heterodimer expression in human colorectal tumor. *World Journal of Gastroenterology*, 11(42):6694–6700, 2005. ISSN 10079327.
- [347] P Parrella, P Mazzairelli, E Signori, G Perrone, G F Marangi, C Rabitti, M Delfino, M Prencipe, A P Gallo, M Rinaldi, G Fabbrocini, S Delfino, P Persichetti, and V M Fazio. Expression and heterodimer-binding activity of Ku70 and Ku80 in human non-melanoma skin cancer. *Journal of Clinical Pathology*, 59(11):1181–1185, 2006. ISSN 0021-9746. doi: 10.1136/jcp.2005.031088. URL <http://jcp.bmj.com/cgi/doi/10.1136/jcp.2005.031088>.
- [348] Yasuhiro Komuro, Toshiaki Watanabe, Yoshio Hosoi, Yoshihisa Matsumoto, Keiichi Nakagawa, Nelson Tsuno, Shinsuke Kazama, Joji Kitayama, Norio Suzuki, and Hirokazu Nagawa. The expression pattern of Ku correlates with tumor radiosensitivity and disease free survival in patients with rectal carcinoma. *Cancer*, 95(6):1199–1205, 2002. ISSN 0008543X. doi: 10.1002/cncr.10807.
- [349] Yuanfang Lu, Jingyan Gao, and Yuanming Lu. Downregulated Ku70 and ATM associated to poor prognosis in colorectal cancer among Chinese patients. *OncoTargets and Therapy*, 7:1955–1961, 2014. ISSN 11786930. doi: 10.2147/OTT.S67814.
- [350] C.-M. Wendtner, Peter Dreger, Michael Gregor, Richard Greil, Wolfgang Ulrich Knauf, Johannes Schetelig, Michael Steurer, and Stephan Stilgenbauer. Chronic Lymphocytic Leukemia Guideline. *Onkopedia Guidelines*, page 16, 2012.

- [351] A. Redaelli, B.L. Laskin, J.M. Stephens, M.F. Botteman, and C.L. Pashos. The clinical and epidemiological burden of chronic lymphocytic leukaemia. *European Journal of Cancer Care*, 13(3):279–287, jul 2004. ISSN 0961-5423. doi: 10.1111/j.1365-2354.2004.00489.x. URL <http://www.ncbi.nlm.nih.gov/pubmed/15196232><http://doi.wiley.com/10.1111/j.1365-2354.2004.00489.x>.
- [352] Chadi Nabhan, Briseis Aschebrook-Kilfoy, Brian C.-H. Chiu, Sonali M. Smith, Tait D. Shanafelt, Andrew M. Evens, and Neil E. Kay. The impact of race, ethnicity, age and sex on clinical outcome in chronic lymphocytic leukemia: a comprehensive Surveillance, Epidemiology, and End Results analysis in the modern era. *Leukemia & Lymphoma*, 55(12):2778–2784, 2014. ISSN 1042-8194. doi: 10.3109/10428194.2014.898758. URL <http://www.tandfonline.com/doi/full/10.3109/10428194.2014.898758>.
- [353] Thomas J. Kipps, Freda K. Stevenson, Catherine J. Wu, Carlo M. Croce, Graham Packham, William G. Wierda, Susan O’Brien, John Gribben, and Kanti Rai. Chronic lymphocytic leukaemia. *Nature Reviews Disease Primers*, 3:1–21, 2017. ISSN 2056-676X. doi: 10.1038/nrdp.2017.8. URL <http://www.nature.com/articles/nrdp20178>.
- [354] Cancer Research UK. Survival — Chronic lymphocytic leukaemia (CLL) —, 2017. URL <http://www.cancerresearchuk.org/about-cancer/chronic-lymphocytic-leukaemia-ctl/survival>.
- [355] Michael Hallek, Bruce D Cheson, Daniel Catovsky, Federico Caligaris-cappio, Guillaume Dighiero, and Hartmut Do. Guidelines for the diagnosis and treatment of chronic lymphocytic leukemia : a report from the International Workshop on Chronic Lymphocytic Leukemia updating the National Cancer Institute – Working Group 1996 guidelines. *Blood*, 111(12):5446–5456, 2008. ISSN 00064971. doi: 10.1182/blood-2007-06-093906.The.
- [356] Thorsten Zenz, Barbara Eichhorst, Raymonde Busch, Tina Denzel, Sonja Häbe, Dirk Winkler, Andreas Bühler, Jennifer Edelmann, Manuela Bergmann, Georg Hopfinger, Manfred Hensel, Michael Hallek, Hartmut Döhner, and Stephan Stilgenbauer. TP53 mutation and survival in chronic lymphocytic leukemia. *Journal of Clinical Oncology*, 28(29):4473–4479, 2010. ISSN 0732183X. doi: 10.1200/JCO.2009.27.8762.
- [357] Belinda Austen, Anna Skowronska, Claire Baker, Judith E. Powell, Anne Gardiner, David Oscier, Aneela Majid, Martin Dyer, Reiner Siebert, A. Malcolm Taylor, Paul A. Moss, and Tatjana Stankovic. Mutation status of the residual ATM allele is an important determinant of the cellular response to chemotherapy and survival in patients with chronic lymphocytic leukemia containing an 11q deletion. *Journal of Clinical Oncology*, 25(34):5448–5457, 2007. ISSN 0732183X. doi: 10.1200/JCO.2007.11.2649.
- [358] J Delic, M Morange, and H Magdelenat. Ubiquitin pathway involvement in human lymphocyte gamma- irradiation-induced apoptosis. *Mol. Cell Biol.*, 13(8):4875–4883, 1993. ISSN 02707306.

- [359] Peggy Masdehors, Satoshi Omura, H el ene Merle-Beral, Frank Mentz, Jean Marc Cosset, Jeanine Dumont, Henri Magdel enat, and Jozo Delic. Increased sensitivity of CLL-derived lymphocytes to apoptotic death activation by the proteasome-specific inhibitor lactacystin. *British Journal of Haematology*, 105(3):752–757, 1999. ISSN 00071048. doi: 10.1046/j.1365-2141.1999.01388.x.
- [360] J Delic, P Masdehors, S Omura, J M Cosset, J Dumont, J L Binet, and H Magdel enat. The proteasome inhibitor lactacystin induces apoptosis and sensitizes chemo- and radioresistant human chronic lymphocytic leukaemia lymphocytes to TNF-alpha-initiated apoptosis. *British journal of cancer*, 77(7):1103–7, 1998. ISSN 0007-0920. URL <http://www.pubmedcentral.nih.gov/articlerender.fcgi?artid=2150120&tool=pmcentrez&rendertype=abstract>.
- [361] Ludovic Deriano, Olivier Guipaud, Jacques-louis Binet, Michelle Ricoul, Gaby Potocki-veronese, Vincent Favaudon, Zofia Maciorowski, Catherine Muller, Bernard Salles, Laure Sabatier, Jozo Delic, and Nonhomologous Nhej Dna. Human chronic lymphocytic leukemia B cells can escape DNA damage – induced apoptosis through the nonhomologous end-joining DNA repair pathway. *Blood*, 105(12):4776–4784, 2005. doi: 10.1182/blood-2004-07-2888. Supported.
- [362] Jozo Delic, Jean-Brice Marteau, Karim Maloum, Florence Nguyen-Khac, Fr ed eric Davi, Zahia Azgui, V eronique Leblond, and Jacques-louis Binet. DNA Damage Response / Signaling and Genome ( In ) Stability as the New Reliable Biological Parameters Defining Clinical Feature of CLL. In Dr. Pablo Opezzo, editor, *Chronic lymphocytic leukemia*, chapter 4, pages 63–94. InTech, 2012.
- [363] Lesley Ann Sutton and Richard Rosenquist. Deciphering the molecular landscape in chronic lymphocytic leukemia: Time frame of disease evolution. *Haematologica*, 100(1):7–16, 2014. ISSN 15928721. doi: 10.3324/haematol.2014.115923.
- [364] L Deriano. *Apoptose et stabilit e de l’ADN dans la Leuc emie Lympho ide Chronique-B : Implication du syst eme de r eparation des cassures double brin de l’ADN par recombinaison non homologue*. PhD thesis, Universit e Paris Descartes, 2005.
- [365] R Blaise, P Masdehors, A Laug e, D Stoppa-Lyonnet, C Alapetite, H Merle-B eral, J L Binet, S Omura, H Magdel enat, L Sabatier, and J Delic. Chromosomal DNA and p53 stability, ubiquitin system and apoptosis in B-CLL lymphocytes. *Leukemia & lymphoma*, 42(6):1173–1180, 2001. ISSN 1042-8194. doi: 10.3109/10428190109097742.
- [366] R. Blaise, C. Alapetite, P. Masdehors, H. Merle-Beral, C. Roulin, J. Delic, and L. Sabatier. High levels of chromosome aberrations correlate with



- impaired in vitro radiation-induced apoptosis and DNA repair in human B-chronic lymphocytic leukaemia cells. *International Journal of Radiation Biology*, 78(8):671–679, 2002. ISSN 0955-3002. doi: 10.1080/09553000110120364. URL <http://www.tandfonline.com/doi/full/10.1080/09553000110120364>.
- [367] Ludovic Deriano, Hélène Merle-Béral, Olivier Guipaud, Laure Sabatier, and Jozo Delic. Mutagenicity of non-homologous end joining DNA repair in a resistant subset of human chronic lymphocytic leukaemia B cells. *British journal of haematology*, 133(5):520–5, jun 2006. ISSN 0007-1048. doi: 10.1111/j.1365-2141.2006.06071.x. URL <http://www.ncbi.nlm.nih.gov/pubmed/16681639>.
- [368] Thibaut Brugat, Florence Nguyen-Khac, Aurore Grelier, Hélène Merle-Béral, and Jozo Delic. Telomere dysfunction-induced foci arise with the onset of telomeric deletions and complex chromosomal aberrations in resistant chronic lymphocytic leukemia cells. *Blood*, 116(2):239–49, jul 2010. ISSN 1528-0020. doi: 10.1182/blood-2009-12-257618. URL <http://www.ncbi.nlm.nih.gov/pubmed/20424183>.
- [369] Julien Bouley, Lina Saad, Romain Grall, Amelie Schellenbauer, Denis Biard, Bernard Salles, Karim Maloum, Hélène Merle-béral, Sylvie Chevillard, and Jozo Delic. A new phosphorylated form of Ku70 identified in resistant leukemic cells confers fast but unfaithful DNA repair in cancer cell lines. *Oncotarget*, 6(29):27980–28000, 2015.
- [370] C Oberle and C Blattner. Regulation of the DNA Damage Response to DSBs by Post-Translational Modifications. *Current genomics*, 11(3):184–198, 2010. ISSN 13892029. doi: 10.2174/138920210791110979.
- [371] PhosphoSite. PhosphoSite-Ku70, 2017. URL <http://www.phosphosite.org/proteinAction.action?id=2075&showAllSites=true>.
- [372] M Yaneva and H Busch. A 10S particle released from deoxyribonuclease-sensitive regions of HeLa cell nuclei contains the 86-kilodalton-70-kilodalton protein complex. *Biochemistry*, 25(18):5057–5063, 1986. ISSN 00062960. URL [http://www.ncbi.nlm.nih.gov/entrez/query.fcgi?cmd=Retrieve&db=PubMed&dopt=Citation&list\\_uids=3768331](http://www.ncbi.nlm.nih.gov/entrez/query.fcgi?cmd=Retrieve&db=PubMed&dopt=Citation&list_uids=3768331).
- [373] N V Boubnov and D T Weaver. scid cells are deficient in Ku and replication protein A phosphorylation by the DNA-dependent protein kinase . These include : scid Cells Are Deficient in Ku and Replication Protein A Phosphorylation by the DNA-Dependent Protein Kinase. *Molecular and Cellular Biology*, 15(10):5700–5706, 1995.
- [374] Shengfang Jin and David T Weaver. Double-strand break repair by Ku70 requires heterodimerization with Ku80 and DNA binding functions. *The EMBO journal*, 16(22):6874–6885, 1997.

- [375] Doug W Chan, Ruiqiong Ye, Christian J Veillette, and Susan P Lees-miller. DNA-Dependent Protein Kinase Phosphorylation Sites in Ku 70 / 80 Heterodimer. *Biochemistry*, 38:1819–1828, 1999.
- [376] Mariko Morii, Sho Kubota, Takuya Honda, Ryuzaburo Yuki, Takao Morinaga, Takahisa Kuga, Takeshi Tomonaga, Naoto Yamaguchi, and Noritaka Yamaguchi. Src acts as an effector for Ku70-dependent suppression of apoptosis through phosphorylation of Ku70 at Tyr-530. *Journal of Biological Chemistry*, 292(5):1648–1665, 2017. ISSN 1083351X. doi: 10.1074/jbc.M116.753202.
- [377] Emilie Rass, Anastazja Grabarz, Isabelle Plo, Jean Gautier, Pascale Bertrand, and Bernard S Lopez. Role of Mre11 in chromosomal nonhomologous end joining in mammalian cells. *Nature structural & molecular biology*, 16(8):819–824, 2009. ISSN 1545-9993. doi: 10.1038/nsmb.1641. URL <http://dx.doi.org/10.1038/nsmb.1641>.
- [378] B. Elenbaas, Lisa Spirio, Frederick Koerner, Mark D. Fleming, Drazen B. Zimonjic, Joana Liu Donaher, Nicholas C. Popescu, William C Hahn, and Robert A. Weinberg. Human breast cancer cells generated by oncogenic transformation of primary mammary epithelial cells. *Genes & Development*, 15(1):50–65, jan 2001. ISSN 08909369. doi: 10.1101/gad.828901. URL <http://www.genesdev.org/cgi/doi/10.1101/gad.828901>.
- [379] Denis Biard. *Diplôme National d'HABILITATION A DIRIGER DES RECHERCHES de l'Université Paris-Sud 11*. PhD thesis, Université Paris Sud - Paris XI, 2008.
- [380] G. Li, C. Nelsen, and E. A. Hendrickson. Ku86 is essential in human somatic cells. *Proceedings of the National Academy of Sciences*, 99(2):832–837, 2002. ISSN 0027-8424. doi: 10.1073/pnas.022649699. URL <http://www.pnas.org/cgi/doi/10.1073/pnas.022649699>.
- [381] PA. Jeggo. Studies on mammalian mutants defective in rejoining double-strand breaks in DNA. *Mutation research*, 239(1):1–16, 1990.
- [382] S. Omori, Y. Takiguchi, A. Suda, T. Sugimoto, H. Miyazawa, N. Tanabe, K. Tatsumi, H. Kimura, P E Pardington, F Chen, D J Chen, and T. Kuriyama. Suppression of a DNA double-strand break repair gene, Ku70, increases radio- and chemosensitivity in a human lung carcinoma cell line. *DNA Repair (Amst)*, 1(4):299–310, 2002. doi: S156878640200006X[pil]. URL <http://www.ncbi.nlm.nih.gov/entrez/query.fcgi?cmd=Retrieve{&}db=PubMed{&}dopt=Citation{&}list{&}uids=12509248{&}5Cnhttp://www.ncbi.nlm.nih.gov/pubmed/12509248>.
- [383] Kazi R. Fattah, Brian L. Ruis, and Eric A. Hendrickson. Mutations to Ku reveal differences in human somatic cell lines. *DNA Repair*, 7(5):762–774, 2008. ISSN 15687864. doi: 10.1016/j.dnarep.2008.02.008.

- [384] Zeng Fu Shang, Bo Huang, Qin Zhi Xu, Shi Meng Zhang, Rong Fan, Xiao Dan Liu, Yu Wang, and Ping Kun Zhou. Inactivation of DNA-dependent protein kinase leads to spindle disruption and mitotic catastrophe with attenuated checkpoint protein 2 phosphorylation in response to DNA damage. *Cancer Research*, 70(9):3657–3666, 2010. ISSN 00085472. doi: 10.1158/0008-5472.CAN-09-3362.
- [385] Noah Dephoure, Kathleen L Gould, Steven P Gygi, and Douglas R Kellogg. Mapping and analysis of phosphorylation sites: a quick guide for cell biologists., mar 2013. ISSN 1939-4586. URL <http://www.pubmedcentral.nih.gov/articlerender.fcgi?artid=3583658&tool=pmcentrez&rendertype=abstract>.
- [386] L. M. Ogawa, S. J. Baserga, C. Agaton, C. A. Szigartyo, B. Amini, E. Andersen, A. C. Andersson, P. Angelidou, A. Asplund, C. Asplund, L. Berglund, K. Bergstrom, H. Brumer, D. Cerjan, M. Ekstrom, A. Elobeid, C. Eriksson, L. Fagerberg, R. Falk, J. Fall, M. Forsberg, M. G. Bjorklund, K. Gumbel, A. Halimi, I. Hallin, C. Hamsten, M. Hansson, M. Hedhammar, G. Hercules, C. Kampf, K. Larsson, M. Lindskog, W. Lodewyckx, J. Lund, J. Lundberg, K. Magnusson, E. Malm, P. Nilsson, J. Odling, P. Oksvold, I. Olsson, E. Oster, J. Ottosson, L. Paavilainen, A. Persson, R. Rimini, J. Rockberg, M. Runeson, A. Sivertsson, A. Skollermo, J. Steen, M. Stenvall, F. Sterky, S. Stromberg, M. Sundberg, H. Tegel, S. Tourle, E. Wahlund, A. Walden, J. Wan, H. Wernerus, J. Westberg, K. Wester, U. Wrethagen, L. L. Xu, S. Hober, and F. Ponten. Crosstalk between the nucleolus and the DNA damage response. *Mol. BioSyst.*, 13(3):443–455, feb 2017. ISSN 1742-206X. doi: 10.1039/C6MB00740F. URL <http://xlink.rsc.org/?DOI=C6MB00740F>.
- [387] D W Chan and S P Lees-Miller. The DNA-dependent protein kinase is inactivated by autophosphorylation of the catalytic subunit. *The Journal of biological chemistry*, 271(15):8936–41, apr 1996. ISSN 0021-9258. URL <http://www.ncbi.nlm.nih.gov/pubmed/8621537>.
- [388] Ayeong So, Tangui Le Guen, Bernard S. Lopez, and Josee Guirouilh-Barbat. Genomic rearrangements induced by unscheduled DNA double strand breaks in somatic mammalian cells. *FEBS Journal*, 284:1–21, 2017. ISSN 17424658. doi: 10.1111/febs.14053.
- [389] H Li, Y J Choi, M A Hanes, T Marple, H Vogel, and P Hasty. Deleting Ku70 is milder than deleting Ku80 in p53-mutant mice and cells. *Oncogene*, 28(16):1875–1878, 2009. ISSN 0950-9232. doi: 10.1038/onc.2009.57. URL <http://www.nature.com/doifinder/10.1038/onc.2009.57>.
- [390] Anthony J. Davis, Benjamin P C Chen, and David J. Chen. DNA-PK: A dynamic enzyme in a versatile DSB repair pathway. *DNA Repair*, 17(214): 21–29, 2014. ISSN 15687856. doi: 10.1016/j.dnarep.2014.02.020.
- [391] Tracey Dobbs, John A. Tainer, and Susan P. Lees-Miller. A structural model for regulation of NHEJ by DNA-PKcs autophosphorylation. *DNA Repair*, 9(12):1307–1314, 2010. ISSN 15378276. doi: 10.1038/jid.2014.371.

- [392] A T Blunt, D N A Ends, Howard H Y Chang, Go Watanabe, and Michael R Lieber. Unifying the DNA End-processing Roles of the Artemis Nuclease. *The Journal of biological chemistry*, 290(40):24036–24050, 2015. doi: 10.1074/jbc.M115.680900.
- [393] Mauro Modesti, Joanne E Hesse, and Martin Gellert. DNA binding of Xrcc4 protein is associated with V ( D ) J recombination but not with stimulation of DNA ligase IV activity. *The EMBO journal*, 18(7):2008–2018, 1999.
- [394] Yaping Yu, Wei Wang, Qi Ding, Ruiqiong Ye, Dawn Chen, Dennis Merkle, David Schriemer, Katheryn Meek, and Susan P. Lees-Miller. DNA-PK phosphorylation sites in XRCC4 are not required for survival after radiation or for V(D)J recombination. *DNA Repair*, 2(11):1239–1252, 2003. ISSN 15687864. doi: 10.1016/S1568-7864(03)00143-5.
- [395] Mukesh Kumar Sharma, Shoji Imamichi, Mikoto Fukuchi, Mahadeo Samarth, Masanori Tomita, and Yoshihisa Matsumoto. In cellulo phosphorylation of XRCC4 Ser320 by DNA-PK induced by DNA damage. *Journal of Radiation Research*, 57(2):115–120, 2016. doi: 10.1093/jrr/rrv086.
- [396] Amy L Cherry, Timothy J Nott, Geoffrey Kelly, Stuart L Rulten, Keith W Caldecott, and Stephen J Smerdon. Versatility in phospho-dependent molecular recognition of the XRCC1 and XRCC4 DNA-damage scaffolds by aprataxin-family FHA domains. *DNA Repair*, 35:116–125, 2015. ISSN 1568-7864. doi: 10.1016/j.dnarep.2015.10.002. URL <http://dx.doi.org/10.1016/j.dnarep.2015.10.002>.
- [397] Natasha Iles, Stuart Rulten, Sherif F El-khamisy, Keith W Caldecott, and M O L C E L L B Iol. APLF ( C2orf13 ) Is a Novel Human Protein Involved in the Cellular Response to Chromosomal DNA Strand Breaks. *Molecular and Cellular Biology*, 27(10):3793–3803, 2007. doi: 10.1128/MCB.02269-06.
- [398] Christine Anne Koch, Roger Agyei, Sarah Galicia, Pavel Metalnikov, O Donnell, Andrei Starostine, and Daniel Durocher. Xrcc4 physically links DNA end processing by polynucleotide kinase to DNA ligation by DNA ligase IV. *The EMBO Journal*, 23(19):3874–3885, 2004. doi: 10.1038/sj.emboj.7600375.
- [399] Pengda Liu, Wenjian Gan, Ralph Scully, Wenyi Wei, Non-homologous End-joining D N A Repair, Pengda Liu, Wenjian Gan, Chunguang Guo, Anyong Xie, Daming Gao, Jianping Guo, and Jinfang Zhang. Akt-Mediated Phosphorylation of XLF Impairs Non- Article Akt-Mediated Phosphorylation of XLF Impairs. *Molecular Cell*, 57(4):648–661, 2015. ISSN 1097-2765. doi: 10.1016/j.molcel.2015.01.005. URL <http://dx.doi.org/10.1016/j.molcel.2015.01.005>.
- [400] Abinadabe J De Melo, Davide Normanno, Katheryn Meek, Mauro Modesti, Aix-marseille Universite, Molecular Genetics, East Lansing, United

- States, Diagnostic Investigation, East Lansing, and United States. Mutational phospho-mimicry reveals a regulatory role for the XRCC4 and XLF C-terminal tails in modulating DNA bridging during classical non-homologous end joining. *eLife*, 4(1):1–28, 2017. doi: 10.7554/eLife.22900.
- [401] Pauline Douglas, Shikha Gupta, Nick Morrice, Katheryn Meek, and Susan P Lees-Miller. DNA-PK-dependent phosphorylation of Ku70/80 is not required for non-homologous end joining. *DNA repair*, 4(9):1006–18, aug 2005. ISSN 1568-7864. doi: 10.1016/j.dnarep.2005.05.003. URL <http://www.ncbi.nlm.nih.gov/pubmed/15941674>.
- [402] Felix Dietlein and H. Christian Reinhardt. Molecular pathways: Exploiting tumor-specific molecular defects in DNA repair pathways for precision cancer therapy. *Clinical Cancer Research*, 20(23):5882–5887, 2014. ISSN 15573265. doi: 10.1158/1078-0432.CCR-14-1165.
- [403] Gero Knittel, Paul Liedgens, and Hans C. Reinhardt. Targeting ATM-deficient CLL through interference with DNA repair pathways. *Frontiers in Genetics*, 6(JUN):1–9, 2015. ISSN 16648021. doi: 10.3389/fgene.2015.00207.
- [404] J. Setton, R.S. Bindra, and S.N. Powell. Chapter 9 – DNA double-strand repair by nonhomologous end joining and its clinical relevance. In *DNA Repair in Cancer Therapy*, pages 277–302. Academic Press, 2016. ISBN 9780128035825. doi: 10.1016/B978-0-12-803582-5.00009-7. URL <http://www.sciencedirect.com/science/article/pii/B9780128035825000097>.
- [405] Josée Guirouilh-Barbat, Camille Gelot, Anyong Xie, Elodie Dardillac, Ralph Scully, and Bernard S. Lopez. 53BP1 Protects against CtIP-Dependent Capture of Ectopic Chromosomal Sequences at the Junction of Distant Double-Strand Breaks. *PLoS genetics*, 12(10):e1006230, 2016. ISSN 15537404. doi: 10.1371/journal.pgen.1006230.